

**Metabolic engineering strategies for biomanufacturing
of chemicals using *Yarrowia lipolytica* and
*Escherichia coli***

by

Teshager Bitew Kefale

A thesis

presented to the University of Waterloo

in fulfillment of the

thesis requirement for the degree of

Doctor of Philosophy

in

Biology

Waterloo, Ontario, Canada, 2024

© Teshager Bitew Kefale 2024

Examining Committee Membership

The following served on the Examining Committee for this thesis. The decision of the Examining Committee is by majority vote.

External Examiner: Dr. Rebecca Shapiro
Associate Professor, Department of Molecular and Cellular Biology
University of Guelph

Internal-External Examiner: Dr. Subha Kalyanamoorthy
Assistant Professor, Department of Chemistry
University of Waterloo

Supervisor: Dr. Trevor Charles
Professor, Department of Biology
University of Waterloo

Internal Member: Dr. Moira Glerum
Professor, Department of Biology
University of Waterloo

Internal Member: Dr. Bernard Duncker
Professor, Department of Biology
University of Waterloo

Author's Declaration

I hereby declare that I am the sole author of this thesis. This is a true copy of the thesis, including any required final revisions, as accepted by my examiners.

I understand that my thesis may be made electronically available to the public.

Abstract

This dissertation advances metabolic engineering by optimizing the genetic and metabolic capabilities of *Yarrowia lipolytica* and *Escherichia coli* to enhance their applications in biotechnology. It focuses on improving *Y. lipolytica*'s mannitol and amino acids production by varying fermentation temperatures and employing techniques like shake flask fermentation, HPLC, and NMR. Notably, mannitol production was enhanced through targeted modifications of *FBP1* gene at elevated temperatures. RNAseq analyses highlighted shifts in metabolic pathways under thermal stress, markedly in lipid, sugar and amino acids metabolism. Additionally, a dual-gRNA CRISPR-Cas9 system was integrated within the pCRISPRYL2 plasmid, noticeably improving genetic editing precision by overcoming the constraints of the non-homologous end joining (NHEJ) pathway. Furthermore, the study pioneered a Cell-Free Metabolic Engineering (CFME) strategy to synthesize 5-Aminolevulinic Acid (5-ALA) utilizing optimized enzymatic reactions and operational conditions, presenting a scalable and eco-friendly alternative to conventional whole-cell systems. In parallel, engineered *E. coli* demonstrated robust heme production capabilities in both whole-cell and cell-free systems. Heme derivatives, including valuable pigments like biliverdin, Phycocyanobilin (PCB) and Phycoerythrobilin (PEB) were also produced at a 1L bioreactor scale utilizing *E. coli* engineered with unexplored enzymes. Overall, this work not only expands the scope of metabolic engineering but also sets a foundational work for future innovations in biomanufacturing.

Keywords: Metabolic Engineering, *Yarrowia lipolytica*, *E. coli*, Fermentation temperature, CRISPR-Cas9 System, Cell-Free Metabolic Engineering, 5-Aminolevulinic Acid, RNAseq, Heme, Biliverdin and Phycocyanobilin and Phycoerythrobilin.

Acknowledgements

This journey towards my doctoral degree has been a monumental chapter in my life, marked by challenges, research findings, and invaluable learning experiences. It would have been impossible without the support, guidance, and encouragement from many remarkable individuals. I am deeply grateful to each of you for your contributions to my personal and academic growth.

Firstly, I owe a debt of gratitude to my supervisor, Dr. Trevor Charles. Your unwavering support and insightful discussions throughout my PhD study have been the backbone of my academic success. You gave me the freedom to explore my passions, both within and outside of academia, which has been a source of immense growth and learning for me. You inspired me to think innovatively, to venture into the entrepreneurial world, and to extend the impact of my lab work beyond traditional boundaries. Thank you for being a source of inspiration.

My supervisory committee members, Dr. Moira Glerum and Bernard Duncker, your contributions have been key in shaping my research. Dr. Glerum, your guidance and sense of humor made every interaction enjoyable and insightful. I am grateful for the opportunity to experiment with our CRISPR course module in your lab, using the *PIC2* gene. Dr. Bernard, your guidance and insightful discussions have significantly contributed to my academic development.

A heartfelt thanks to Dr. Laura and Dr. Bob Lemieux. Laura, your guidance and support have been indispensable throughout my dissertation work and in my ventures beyond academia. Your mentorship, particularly in allowing me to be involved in the development of the CRISPR module for the BIOL432 course, not only improved my teaching skills but also made a lasting impact on the students. To both of you, thank you for being a family I could always turn to.

Dr. Kirsten Müller, Dr. Mungo Marsden, Dr. Shawn Wettig, and April Wettig, your support and kindness have been instrumental in my journey. April, your endless patience in addressing my

questions, even the trivial ones, and your prompt resolution of any issues I encountered have been pivotal in ensuring the smooth progression of my academic endeavors.

To the founding team of Biofect Innovations—Dr. Ralph Christian Delos Santos, Dr. Louis Lo, and John Abousawan—working alongside such brilliant minds has been an honor and a privilege. Our team's hard work and dedication have been instrumental in bringing our company to this stage, and I am confident in our continued success.

My Lab mate and a good friend, Dragan, your support and friendship have truly made this academic journey memorable. Your presence has brought laughter and comfort during challenging times, turning our work into a fulfilling adventure. I'm immensely grateful. I also extend my heartfelt thanks to Kerrin for her invaluable assistance with bioinformatics analysis, which has greatly enriched our research. Additionally, a special appreciation to Alex for his expertise in NMR analysis, which has been pivotal to our success.

To my family—my late father Bitew, mother Ababa, sister Zed, brother Kiber, wife Emebet, and my daughter Maya—your love, support, and sacrifices have been the foundation of my dreams. My late father, your inspiration and love for education have been my guiding stars, and I dedicate this achievement to your memory. Ababa, your love and sacrifices have shaped who I am today. Zed and Kiber, your support has been my rock. Emebet, your companionship, care, and love have been my strength. And Maya, you have brought immeasurable joy and light into my life.

This journey has been filled with challenges and triumphs, and each one of you has played a crucial role in making this achievement possible. Your presence in my life, whether in person or in spirit, has been a source of strength and inspiration. Thank you for being a part of my story and for contributing to this significant milestone in my life.

Dedication

To my late father, Bitew Kefale, whose wisdom and values forever inspire me, and to my daughter, Maya Teshager, the light of my life. This work honors a cherished past and looks towards a hopeful future.

Table of Contents

Examining Committee Membership	ii
Author's Declaration.....	iii
Abstract.....	iv
Acknowledgements.....	v
Dedication.....	vii
List of Figures.....	xvi
List of Tables.....	xviii
List of Abbreviations.....	xix
List of Symbols.....	xxiii
Chapter 1.....	1
Introduction.....	1
1.1 Organization of the dissertation	7
Chapter 2.....	8
Literature Review.....	8
2.1 <i>Yarrowia lipolytica</i>	8
2.2 Lipid metabolism: the center of <i>Y. lipolytica</i> 's metabolic engineering	9
2.3 Synthetic biology tools for <i>Y. lipolytica</i>	12
2.3.1 Expression vectors.....	12
2.3.2 Promoters.....	14

2.3.3 Terminators.....	17
2.3.4 CRISPR gene editing tools for <i>Y. lipolytica</i>	17
2.4 Products derived from metabolically engineered <i>Y. lipolytica</i>	21
2.4.1 Biofuels.....	21
2.4.2 Biochemicals	22
2.4.3 Proteins and enzymes	23
2.4.4 Lipids and oils	24
2.4.5 Specialty chemicals	25
2.5 Challenges in metabolic engineering of <i>Y. lipolytica</i>	26
2.6 Mannitol	27
2.6.1 Natural sources of mannitol.....	28
2.6.2 Chemical synthesis of mannitol.....	29
2.6.3 Biological production of mannitol.....	30
2.6.4 Mannitol production using <i>Y. lipolytica</i>	31
2.6.5 Extraction and purification	33
2.7 5-aminolevulinic acid.....	34
2.7.1 Uses and synthesis pathways.....	34

2.7.2 Manipulation of porphobilinogen synthase	35
2.8 Heme importance and production	36
2.8.1 Metabolic pathways involved in heme production.....	37
2.8.2 Metabolic engineering strategies for enhanced heme production	39
2.9 Heme derivatives.....	41
2.9.1 Biliverdin synthesis: heme oxygenases	43
2.9.2 PCB and PEB synthesis: Ferredoxin-dependent bilin reductases (FDBRs).....	44
2.9.3 Advancements and challenges in biliverdin synthesis	45
2.9.4 Advances and challenges in phycocyanobilin biosynthesis	47
2.9.5 Advances and challenges in phycoerythrobilin biosynthesis	48
2.9.6 Promising applications of biliverdin, PCB, and PEB.....	49
2.10 Cell free metabolic engineering (CFME).....	50
2.10.1 Advantages of CFME over whole-cell metabolic engineering (WCME)	52
2.10.2 Challenges and limitations of CFME	53
Chapter 3.....	54
A temperature switch: an efficient strategy to turn on <i>Y. lipolytica</i> 's mannitol and amino acids production	54

3.1 Introduction	54
3.2 Materials and methods	58
3.2.1 Chemicals and Enzymes.....	58
3.2.2 Strains and culture maintenance	58
3.2.3 Transformation of <i>E. coli</i> and <i>Y. lipolytica</i>	59
3.2.4 Plasmid isolation protocol	60
3.2.5 PCR amplification and PCR and gel clean-ups	61
3.2.6 Plasmid construction.....	62
3.2.7 Shake flask fermentation	63
3.2.8 Analytical methods: HPLC and NMR.....	64
3.2.9 Spectrophotometric sulfo-phospho-vanillin (SPV) lipid quantification.....	65
3.2.10 RNA extraction.....	66
3.2.11 Differential expression analysis.....	67
3.2.12 Gene Ontology (GO) enrichment analysis	67
3.2.13 Data visualization	68
3.3 Results	69
3.3.1 <i>Y. lipolytica</i> growth: a temperature and feedstock analysis.....	69

3.3.2	<i>Y. lipolytica</i> 's metabolic responses to temperature variations	72
3.3.3	Temperature-induced pyruvate and its derivative production with <i>Y. lipolytica</i> ...	75
3.3.4	Enhanced mannitol production using <i>Y. lipolytica</i> at elevated temperatures	77
3.3.5	Modification of <i>FBPI</i> and its role in mannitol production	80
3.3.6	Transcriptional responses of <i>Y. lipolytica</i> to elevated temperatures	83
3.4	Discussion	94
3.4.1	<i>Y. lipolytica</i> growth: a temperature and feedstock analysis.....	94
3.4.2	<i>Y. lipolytica</i> 's metabolic responses to temperature variations	97
3.4.3	Temperature-induced pyruvate and its derivative production with <i>Y. lipolytica</i> .	101
3.4.4	Enhanced mannitol production using <i>Y. lipolytica</i> at elevated temperatures	104
Chapter 4	111
Development of a dual gRNA CRISPR tool kit for manipulation of <i>Y. lipolytica</i>		111
4.1	Introduction	111
4.2	Materials and methods	114
4.2.1	Chemicals and enzymes.....	114
4.2.2	Strains	114
4.2.3	Media and culture conditions	115

4.2.4 gRNA design and plasmid construction	116
4.2.5 Colony PCR, plasmid extraction and PCR conditions	121
4.2.6 Transformation of <i>E. coli</i> and <i>Y. lipolytica</i>	122
4.2.7 Data Analysis.....	123
4.3 Results	124
4.3.1 Development of the Poh1 strain	124
4.3.2 Development of a Dual gRNA CRISPR Tool for <i>Y. lipolytica</i>	126
4.4 Discussion	130
Chapter 5	133
Optimizing 5-aminolevulinic acid production via cell-free metabolic engineering (CFME).....	133
5.1 Introduction	133
5.2 Materials and methods	137
5.2.1 Strains and plasmids	137
5.2.2 Shake flask cultivation.....	138
5.2.3 Cell lysis and extract preparation	138
5.2.4 Reaction setup for 5-ALA production	139
5.2.5 Quantification of 5-ALA	140

5.3 Results	141
5.3.1 Production of 5-ALA through CFME	141
5.3.2 Effect of temperature on 5-ALA synthesis.....	144
5.3.3 Effect of glycine concentration on 5-ALA synthesis	146
5.3.4 Scalability of cell-free 5-ALA synthesis	147
5.4 Discussion	150
Chapter 6.....	157
Production of heme and heme derived pigments using engineered <i>E. coli</i>	157
6.1 Introduction	157
6.2 Materials and methods	161
6.2.1 Chemicals and enzymes.....	161
6.2.2 Bacterial strains and plasmids	161
6.2.3 Media and cultivation conditions	165
6.2.4 PCR amplification and plasmid isolation protocols	167
6.2.5 Transformation of <i>E. coli</i>	168
6.2.6 Cell lysis and extract preparation	169
6.2.7 Reaction setup for heme production.....	169

6.2.8 Heme and heme-derivatives extraction	170
6.2.9 Analytical method for simultaneous separation and quantification of heme, biliverdin and PCB	170
6.3 Result.....	172
6.3.1 Efficient HPLC method for simultaneous separation of heme, biliverdin and PCB	172
6.3.2 Heme production with engineered <i>E. coli</i> and cell free metabolic engineering ...	174
6.3.3 Biliverdin PCB and PEB production with engineered <i>E. coli</i>	180
6.4 Discussion	187
Chapter 7.....	192
Conclusions and future directions.....	192
7.1 Conclusions	192
7.2 Future directions.....	195
References.....	202
Appendices.....	233
Appendix 1.	233
Appendix 2.	234

List of Figures

Figure 2.1 Key metabolic pathways in <i>Y. lipolytica</i> ..	11
Figure 3.1 Detailed evaluation of the influence of varying temperatures on <i>Y. lipolytica</i> growth across distinct feedstocks.....	71
Figure 3.2 Temperature-dependent variations in metabolite production and lipid accumulation in <i>Y. lipolytica</i> ..	74
Figure 3.3 Variation in organic and amino acid production in <i>Y. lipolytica</i> under varying temperature conditions.....	76
Figure 3.4 Temporal profile of mannitol production and glycerol consumption by <i>Y. lipolytica</i> in shake-flask experiments.....	79
Figure 3.5 Comprehensive analysis of the effects of <i>FBP1</i> gene manipulation on mannitol synthesis in <i>Y. lipolytica</i> ..	82
Figure 3.6 Comprehensive analysis of differentially expressed genes at elevated temperatures..	90
Figure 3.7 Detailed analysis of <i>Y. lipolytica</i> metabolic pathways and transporters in response to varied temperature conditions.....	92
Figure 4.1 Detailed map of the parent pCRISPRy1 vector designed for <i>Y. lipolytica</i> gene editing.....	117
Figure 4.2 Po1h strain development from Po1g..	125

Figure 4.3 Dual gRNAs based gene edition system for <i>Y. lipolytica</i> using pCRISPRYL2 vector.	127
Figure 4.4 Gene editing efficiencies using pCRISPRYL2 vector.	128
Figure 5.1 5-ALA synthesis via CFME.....	142
Figure 5.2 Effect of temperature of reaction on CFME based 5-ALA production.....	144
Figure 5.3 Effect of glycine concentration on CFME based 5-ALA production.....	146
Figure 5.4 Scalability of CFME based 5-ALA production.....	148
Figure 6.1 Simultaneous separation of heme and bilins with reverse phase HPLC.....	174
Figure 6.2 C4 and C5 heme biosynthesis pathways.....	176
Figure 6.3 Heme production with engineered <i>E. coli</i>	177
Figure 6.4 Heme production via cell free metabolic engineering.....	179
Figure 6.5 Structure of heme derivatives and their biosynthesis pathways.	181
Figure 6.6 Biliverdin synthesis using engineered <i>E. coli</i>	184
Figure 6.7 Phycocyanobilin (PCB) synthesis using engineered <i>E. coli</i>	185
Figure 6.8 Phycoerythrobilin (PEB) synthesis using engineered <i>E. coli</i>	186

List of Tables

Table 4.1 Primers used for developing a dual gRNA expression plasmid pCRISPRYL2.....	118
Table 4.2 Guide RNA expressed with pCRISPRYL2 and their target genes.	119
Table 4.3 Plasmids used in this study.	120
Table 5.1 Comparison of whole cell and cell free metabolic engineering efficiency.....	143
Table 6.1 List of primers used for exploring heme and its derivatives production.....	163
Table 6.2 List of plasmids used for exploring heme and its derivatives production.....	164
Table 6.3 Enzymes screened to produce biliverdin, PCB and PEB and their sources.....	182

List of Abbreviations

Abbreviation	Description
5-ALA	5-Aminolevulinic Acid
5-FOA	5-Fluoroorotic Acid
ACC1	Acetyl-CoA Carboxylase
ACL	ATP Citrate Lyase
ACS	Acetyl-CoA Synthetase
ALAD	5-ALA Dehydratase
ALAS	5-Aminolevulinate Synthase
AmpR	Ampicillin Resistance
ARS/CEN	Autonomously Replicating Sequence/Centromere
ATCC	American Type Culture Collection
ATP	Adenosine Triphosphate
CEN	Centromere
CFME	Cell-Free Metabolic Engineering
CoA	Coenzyme A
ColE1	ColE1 Origin of Replication
CPO	Coproporphyrinogen Oxidase
CRISPR	Clustered Regularly Interspaced Short Palindromic Repeats
CRISPRi	CRISPR interference
CYC	Cytochrome C
D2O	Deuterium Oxide

DCW	Dry Cell Weight
DE	Differential Expression
DE	Differential Expression
DGA1	Diacylglycerol Acyltransferase
DMAB	4-Dimethylaminobenzaldehyde
DMSO	Dimethyl Sulfoxide
DNA	Deoxyribonucleic Acid
DSS	4,4-Dimethyl-4-silapentane-1-sulfonic acid
DtxR	Diphtheria Toxin Repressor
FAA	5-Fluoroanthranilic Acid
FAS	Fatty Acid Synthase
FBP1	Fructose-1,6-bisphosphatase
FDBR	Ferredoxin-Dependent Bilin Reductase
FDR	False Discovery Rate
GO	Gene Ontology
GRAS	Generally Recognized As Safe
gRNA	Guide RNA
HO	Heme Oxygenase
HO2582	Heme Oxygenase from <i>Pseudomonas putida</i> KT2440
HPLC	High-Pressure Liquid Chromatography
HR	Homologous Recombination
IDT	Integrated DNA Technologies
Indels	Insertions or Deletions

IPTG	Isopropyl β -D-1-thiogalactopyranoside
LB	Lysogeny Broth
LDH	Lactate Dehydrogenase
LEU2	Leucine 2
MFE1	Multifunctional Enzyme
MPC1	Mitochondrial Pyruvate Carrier 1
MPC2	Mitochondrial Pyruvate Carrier 2
NEB	New England Biolabs
NHEJ	Non-Homologous End Joining
NIR	Near-Infrared
NMR	Nuclear Magnetic Resonance
OD600	Optical Density at 600 nm
PBG	Porphobilinogen
PBGD	Porphobilinogen Deaminase
PCA	Principal Component Analysis
PCB	Phycocyanobilin
PCR	Polymerase Chain Reaction
PcyA	Phycocyanobilin:ferredoxin oxidoreductase
PDA1	Pyruvate Dehydrogenase E1 Component Alpha Chain
PDB1	Pyruvate Dehydrogenase E1 Component Beta Chain
PDH	Pyruvate Dehydrogenase
PEB	Phycoerythrobilin
PebS	Phycoerythrobilin synthase

PEX10	Peroxisome Biogenesis Factor 10
Pol III	RNA Polymerase III
POX1	Acyl-Coenzyme A Oxidase
PUFAs	Polyunsaturated Fatty Acids
PYC1	Pyruvate Carboxylase 1
RBS	Ribosomal Binding Site
RNAseq	RNA sequencing
ROS	Reactive Oxygen Species
SD	Synthetic Defined medium
SPV	Sulfo-Phospho-Vanillin
TAG	Triacylglycerides
TB	Terrific Broth
TCA	Tricarboxylic Acid
TFA	Trifluoroacetic Acid
TRC	Toronto Research Chemicals
TRP1	Tryptophan 1 Gene
UAS	Upstream Activating Sequences
URA	Uracil
vvm	Volume of Air per Volume of Culture per Minute
WCME	Whole-Cell Metabolic Engineering
WT	Wild Type (control strain)
YNB	Yeast Nitrogen Base medium
YPD	Yeast Extract Peptone Dextrose

List of Symbols

Symbol	Description
%	Percent
<	Less Than
>	Greater Than
°C	Degrees Celsius
μL	Microliter
μM	Micromolar
±	Plus/Minus
bp	Base Pairs
g/g	Grams per Gram
g/L	Grams per Liter
h	Hours
mg/L	Milligrams per Liter
mL	Milliliter
mM	Millimolar
nm	Nanometer
pH	Potential of Hydrogen (pH Scale)
rpm	Revolutions per Minute

Chapter 1

Introduction

Metabolic engineering, an important field in shaping advancements across various industries such as pharmaceuticals, biofuels, and agriculture, involves the strategic modification of an organism's metabolic pathways to achieve specific objectives. It plays a crucial role in enhancing the production of desired compounds and pioneering new metabolic pathways for the synthesis of novel molecules. This field has seen rapid growth, propelled by deeper insights into metabolic pathways and advancements in genetic engineering, making it a key contributor to sustainable solutions across diverse sectors (Nielsen, 2001; Stephanopoulos, 1999). The effectiveness of metabolic engineering largely depends on the careful selection of a suitable microbial host. Factors such as the host's genetic makeup, growth characteristics, and substrate utilization are vital in determining the efficiency of the engineered pathways. Additionally, the host's compatibility with downstream processes and scalability potential is fundamental, ensuring that theoretical models are effectively translated into practical applications with wide-ranging industry implications (Nielsen, 2001; Nurwono et al., 2023; Stephanopoulos, 1999).

Yarrowia lipolytica and *Escherichia coli* have emerged as prominent organisms in metabolic engineering, distinguished by their exceptional metabolic adaptability and robustness to genetic manipulations. Their prominence in the field is not merely a consequence of their physiological traits but also stems from their proven track record in facilitating a range of biotechnological breakthroughs. These microorganisms serve as versatile platforms, enabling the exploration and exploitation of diverse metabolic pathways. This versatility is particularly valuable in the context of producing novel bio-based products and in optimizing existing biosynthetic routes for efficiency and yield. Their contribution to metabolic engineering extends beyond the laboratory, translating

into tangible advancements in sectors such as pharmaceuticals, biofuels, and environmental sustainability. Opting for these organisms as microbial hosts in metabolic engineering initiatives is a strategic decision crucial for successful outcomes (Nurwono et al., 2023; Park and Ledesma-Amaro, 2023; Pontrelli et al., 2018; Yang et al., 2020; Zhu and Jackson, 2015). The rationale for choosing these hosts in my dissertation work emanates from these key attributes. Their adaptability and responsiveness to genetic modifications make them ideal candidates for my metabolic engineering goals, offering a reliable foundation for innovative and efficient biotechnological solutions.

Y. lipolytica, renowned for its metabolic efficiency, particularly in the tricarboxylic acid (TCA) cycle, stands out as a prime candidate for biomanufacturing diverse compounds (Park and Ledesma-Amaro, 2023; Zhu and Jackson, 2015). Its status as a Generally Recognized As Safe (GRAS) organism boosts its appeal in the food and pharmaceutical industries. Moreover, its ability to utilize varied feedstocks and excel in high-density fermentation highlights its suitability for large-scale applications, making it an invaluable asset in biotechnological advancements (Park and Ledesma-Amaro, 2023; Zhu and Jackson, 2015). These properties have catalyzed the development of specific molecular tools for this yeast. Its fully sequenced genome has enhanced our genetic insights, while CRISPR-Cas9 technology has revolutionized its genome editing, enabling more targeted and effective genetic modifications (Gao et al., 2018; Holkenbrink et al., 2018; Larroude et al., 2020; Schwartz et al., 2019; Schwartz et al., 2017a; Schwartz et al., 2017b; Schwartz et al., 2016). Despite these advancements, there's a continuous need for enhancing synthetic biology tools for *Y. lipolytica*, including more expression plasmids, stronger promoters, and an expanded repertoire of CRISPR-based techniques. This dissertation introduces a dual gRNA CRISPR system, advancing the capabilities of existing methodologies.

In terms of metabolic capabilities, beyond its established role in lipid production, *Y. lipolytica* demonstrates remarkable versatility in synthesizing a wide array of chemicals. This includes the production of citric acid (Cavallo et al., 2017; Papanikolaou et al., 2002b), bio-based polymers (Lajus et al., 2020; Rigouin et al., 2019), amino acids (Larroude et al., 2021), and sugar alcohols (Egermeier et al., 2017; Jagtap et al., 2021; Tomaszewska et al., 2012). Among these, the production of mannitol is gaining increased attention in biotechnology due to its unique physicochemical properties and growing demand. Mannitol's crystalline structure and moisture resistance make it invaluable in various sectors, including pharmaceuticals, food, and cosmetics. Its use in enhancing pharmaceutical formulations and as a dental-friendly sugar substitute underscores its multifaceted applications in both industrial and healthcare contexts (Abbasi et al., 2021; Bilal et al., 2021).

Mannitol production has traditionally relied on the chemical hydrogenation of D-glucose and D-fructose, a process limited by its need for highly purified substrates and environmental concerns (Makkee et al., 1985). Seeking sustainable alternatives, the industry is increasingly turning towards biological methods like biomanufacturing with *Y. lipolytica*. This yeast offers an eco-friendly solution, promising to address both environmental and efficiency challenges in mannitol production (Abbasi et al., 2021; Bilal et al., 2021). Pioneering research into *Y. lipolytica*'s mannitol synthesis, particularly focusing on pH-dependent mechanisms, underscores the profound effect of environmental factors on metabolic efficiency (Egermeier et al., 2017). However, the role of temperature in this process remains underexplored, presenting an opportunity to refine production methods for better sustainability and cost-effectiveness. Understanding these thermal impacts could further enhance *Y. lipolytica*'s role in metabolic engineering, enabling more tailored production of various biochemicals, including amino acids, and broadening its application in

industrial and pharmaceutical sectors. Therefore, this dissertation work also introduces efficient bioprocess strategies that leverage fermentation temperature for the efficient co-production of mannitol and amino acids.

E. coli, with its well-understood genetic framework and metabolic versatility, is a key player in biotechnology, excelling in various fermentation environments. Its genome's tractability (Pontrelli et al., 2018), coupled with the integration of CRISPR technology, has significantly streamlined genetic modifications, enhancing its role in producing diverse biochemicals (Hashemi, 2020; Wu et al., 2017). This capability was demonstrated by the production of 5-aminolevulinic acid (5-ALA), a compound with critical roles in medical, agricultural, and cosmetic applications (Kang et al., 2011; Miscevic et al., 2021; Pu et al., 2023; Ting and Ng, 2023). 5-ALA production using *E. coli* circumvents the drawbacks of traditional chemical synthesis, such as unwanted by-products and environmental impacts, offering a more sustainable and effective alternative. This method enhances yield and purity to meet the increasing demand for 5-ALA, particularly for its role in advanced medical therapies like photodynamic therapy and photodiagnosis, representing a major bioproduction milestone that combines ecological sustainability with economic viability (Jiang et al., 2022; Kang et al., 2017).

The scientific community and industry are also increasingly leveraging *E. coli* for the biosynthesis of essential tetrapyrroles like heme, biliverdin, phycocyanobilin (PCB), and phycoerythrobilin (PEB), each with distinct applications (Choi et al., 2022; Ge et al., 2018; Geng et al., 2022; Stiefelmaier et al., 2018; Takemoto and Chen, 2017). Heme, crucial for oxygen transport in hemoglobin, is being employed to provide plant-based meat alternatives with authentic meat-like qualities (Ko et al., 2021). Biliverdin, recognized for its anti-inflammatory and antioxidant properties, is emerging in medical circles for therapeutic applications and drug

development (Bai et al., 2015; Baylor and Butler, 2019; Overhaus et al., 2006; Tian et al., 2017). PCB and PEB, derivatives from cyanobacteria and algae, are valued for their unique optical characteristics, serving in the food and cosmetics industry and in advanced technological applications like near-infrared (NIR) imaging and sensors (Ge et al., 2018; Rodriguez et al., 2016; Wang et al., 2019). Amidst a growing preference for natural over synthetic dyes, these tetrapyrroles are seeing an upsurge in demand. Traditional extraction methods, however, struggle with low yield, high cost, and environmental concerns (Bermejo Román et al., 2002). This dissertation elaborates on how our approach, utilizing *E. coli* as a microbial host and employing novel enzymes previously unexplored with this organism, provides a sustainable and efficient solution for biomanufacturing these natural pigments, demonstrating *E. coli's* transformative potential in sustainable production practices.

E. coli's capability for producing 5-ALA and other essential tetrapyrroles, such as heme, biliverdin, PCB, and PEB through whole-cell metabolic engineering (WCME), is well established. However, WCME is often hindered by challenges like cofactor imbalances and feedback inhibition, affecting the efficiency of biosynthetic pathways shared with 5-ALA. The inefficiencies in traditional extraction and purification methods further exacerbate production costs for these compounds (Rather et al., 2022). This has motivated the exploration of alternative approaches like cell-free metabolic engineering (CFME), an underutilized yet promising strategy. CFME offers the potential to bypass cellular constraints, providing greater control over reaction environments. This could lead to substantial improvements in yield and efficiency in the manufacturing of 5-ALA and tetrapyrroles, heralding a transformative shift in biomanufacturing practices (Garcia et al., 2021; Lim and Kim, 2019; Rasor et al., 2021). In this dissertation, we investigate CFME's potential for synthesizing 5-ALA and heme, representing novel applications of this technique in

bioproduction. We report on our unique approach and findings, contributing to the pioneering use of CFME in the synthesis of these important biochemicals.

This dissertation advances metabolic engineering by exploring how *Y. lipolytica* and *E. coli* efficiently produce vital biochemicals. It offers new insights into their capabilities and industrial applications, highlighting their potential in biotechnology. Chapter 3 discusses the metabolic resilience of *Y. lipolytica*, presenting an exhaustive analysis of its response to thermal stress with a particular emphasis on the biosynthesis of mannitol and amino acids. It incorporates a detailed transcriptional study to illustrate the profound impact of fermentation temperature fluctuations on the organism's growth and metabolic network. Advancing to Chapter 4, the dissertation introduces a dual-gRNA CRISPR system developed for gene editing of *Y. lipolytica*, demonstrating an advancement in genome editing precision. The focus then transitions to *E. coli* in Chapter 5, which discusses the design and refinement of a cell-free metabolic engineering approach for efficient synthesis of 5-ALA. Chapter 6 expands the exploration to include *E. coli*'s capacity to biosynthesize natural colorants, such as heme, biliverdin, PCB, and PEB, employing both whole-cell and novel cell-free engineering methods, particularly for heme synthesis. Chapter 7 integrates these findings, providing conclusions and recommending future directions to enhance the biochemical synthesis capabilities of *Y. lipolytica* and *E. coli*, as explored in Chapters 3 to 6. It outlines strategies to refine metabolic pathways and improve biomanufacturing efficiencies, setting the stage for innovative applications in metabolic engineering. Collectively, this dissertation synthesizes these multifaceted studies into a cohesive narrative, showcasing the transformative potential of these microorganisms to optimize biomanufacturing processes and advance the frontiers of metabolic engineering research.

1.1 Organization of the dissertation

Chapter 2: Literature Review

Chapter 3: A temperature switch: an efficient strategy to turn on *Y. lipolytica*'s mannitol and amino acids production. Transcriptional changes induced by elevated fermentation temperatures in *Y. lipolytica* will also be presented.

Chapter 4: Development of a dual gRNA CRISPR tool for manipulation of *Y. lipolytica*

Chapter 5: Optimizing 5-aminolevulinic acid production via cell-free metabolic engineering (CFME)

Chapter 6: Production of heme and heme derived pigments using engineered *E. coli*

Chapter 7: Conclusions and future directions

Chapter 2

Literature Review

2.1 *Yarrowia lipolytica*

Selecting an appropriate host organism is a crucial strategic consideration within the metabolic engineering field. Conventional host organisms are well studied and offer certain advantages, yet non-conventional hosts such as the yeast *Y. lipolytica* are emerging as promising alternatives (Liu et al., 2015; Park and Ledesma-Amaro, 2023; Zhu and Jackson, 2015). *Y. lipolytica* belongs to the Ascomycota phylum and the Dipodascaceae family and naturally thrives in lipid-rich conditions (Fickers et al., 2005; Liu et al., 2015). Its metabolic flexibility and a unique lipid biosynthesis pathway, especially its ATP citrate lyase reaction, have been the focus of extensive biotechnological research for the past seventy years. These distinctive features provide exciting avenues for the biosynthesis of a variety of fine chemicals, challenging traditional models (Fickers et al., 2005; Liu et al., 2015; Park and Ledesma-Amaro, 2023; Zhu and Jackson, 2015).

Y. lipolytica's genetic structure is notably complex. It possesses a large genome with six nuclear chromosomes and an extra mitochondrial chromosome, larger than that of the well-known *S. cerevisiae*. Despite its 20.5 Mb size, the gene density is just 46.3%, a stark contrast to the 70.3% in *S. cerevisiae* (Dujon et al., 2004). The whole genome sequences of *Y. lipolytica* strains such as CLIB122, W29, and PO1f are accessible in public repositories, allowing for an in-depth analysis of their genetic composition and comparative studies with other yeasts. This accessibility, combined with technological breakthroughs like the CRISPR/Cas9 gene-editing system (Gao et al., 2016; Holkenbrink et al., 2018; Schwartz et al., 2017a; Schwartz et al., 2016), has significantly

accelerated the genetic manipulation of *Y. lipolytica*, paving the way for its role in industrial biotechnology and synthetic biology applications.

In terms of growth, *Y. lipolytica* is an obligate aerobic yeast with a growth optimum at moderate temperatures, specifically between 25 to 30°C (Madzak, 2021). This yeast can also grow across a wide range of pH levels (Madzak, 2021), demonstrating a significant adaptability to varying environmental conditions. It can assimilate diverse carbon sources, including common hydrophilic substrates like glucose, glycerol, acetate and fructose, as well as hydrophobic molecules and industrial byproducts, such as crude glycerol (Fickers et al., 2005; Liu et al., 2015; Madzak, 2021). The flexibility of *Y. lipolytica* extends to its nitrogen metabolism, which can process both inorganic and organic forms efficiently (Brabender et al., 2018). The capacity to utilize a broad array of substrates indicates *Y. lipolytica*'s potential for application in various biotechnological sectors.

The following sections will delve deeper into the metabolic engineering of *Y. lipolytica*, offering a detailed analysis of its various aspects. We will examine the yeast's metabolic pathways, with a particular focus on lipid metabolism. Additionally, we will review the array of synthetic biology tools specifically developed for use with this yeast. The discussion will also cover the wide range of products that can be derived from *Y. lipolytica*, its potential industrial applications, and the challenges encountered in these processes.

2.2 Lipid metabolism: the center of *Y. lipolytica*'s metabolic engineering

Y. lipolytica's rising prominence in biotechnological research is primarily attributed to its remarkable ability to synthesize triacylglycerides (TAG) *de novo*. The specialized pathways dedicated to the production and maintenance of a high pool of acetyl-CoA are the foundation of *Y.*

lipolytica's metabolic architecture, essential for the efficient synthesis of TAG (Liu et al., 2015; Park and Ledesma-Amaro, 2023; Zhu and Jackson, 2015). As illustrated in Figure 2.1, acetyl-CoA is an essential precursor for generating both the intermediates of the tricarboxylic acid (TCA) cycle and various lipids. The yeast's metabolic plasticity is also marked by a significant glycolytic flux mediated by the enzyme pyruvate dehydrogenase (PDH). In addition, *Y. lipolytica* has evolved an effective mechanism for acetyl-CoA transport, the citrate-malate antiport system, which shuttles this molecule between the mitochondrial and cytosolic compartments. The performance of this transport system is modulated by the interplay between nitrogen sources and the metabolites of the citric acid (TCA) cycle, which subsequently influences lipid synthesis. These innate metabolic traits have evolved to make *Y. lipolytica* a leading organism for diverse biotechnological applications (Liu et al., 2015; Park and Ledesma-Amaro, 2023; Zhu and Jackson, 2015).

The synthesis of fatty acids (FA) primarily occurs in the cytosol of *Y. lipolytica*, initiating with acetyl-CoA. This starting molecule is generated by a few enzymes, including acetyl-CoA synthetase (ACS), the pyruvate dehydrogenase complex (PDH), and ATP citrate lyase (ACL), with the latter enzyme's presence being a distinctive feature of oleaginous yeasts. Following its production, acetyl-CoA is transformed into malonyl-CoA by acetyl-CoA carboxylase (Acc1). The process culminates with the fatty acid synthase (FAS) enzyme, which synthesizes acyl-CoA by sequentially adding two-carbon units derived from acetyl-CoA and malonyl-CoA (Liu et al., 2015; Park and Ledesma-Amaro, 2023; Zhu and Jackson, 2015). This comprehensive pathway is depicted in Figure 2.1.

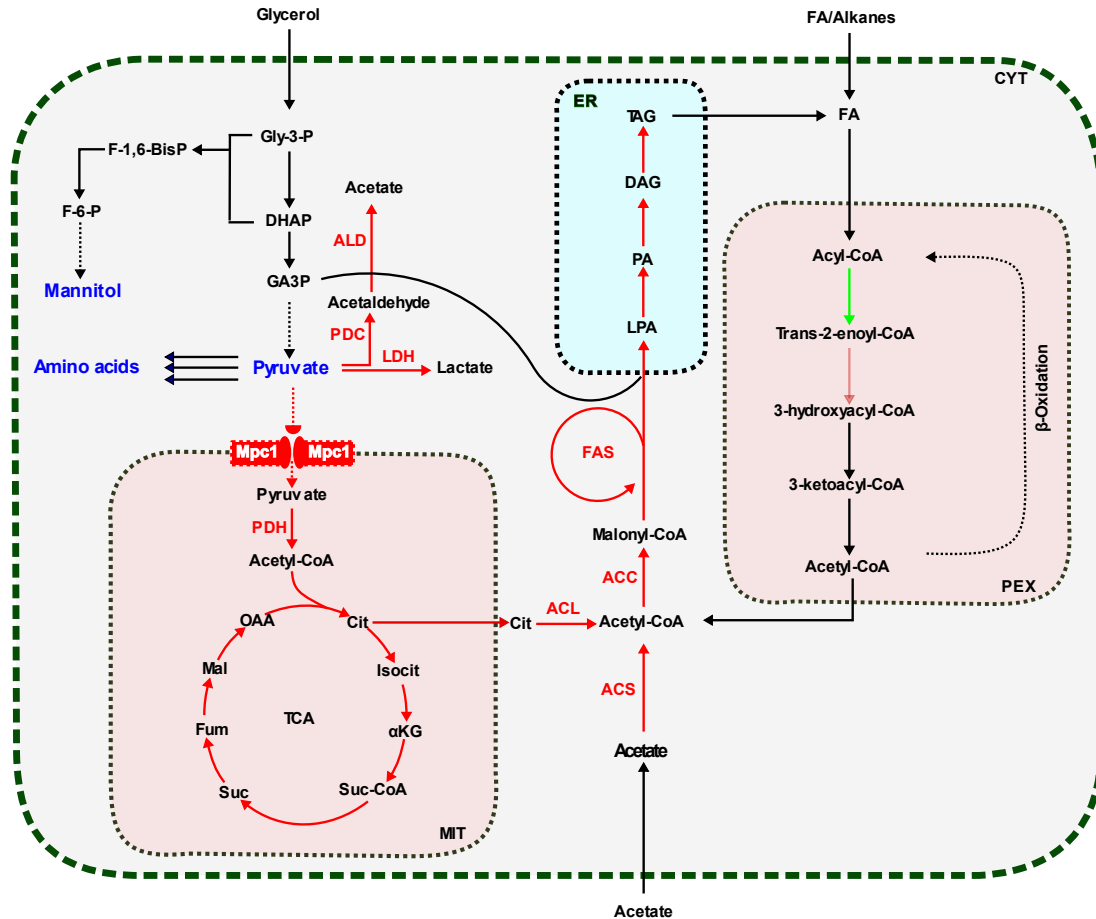


Figure 2.1 Key metabolic pathways in *Y. lipolytica*. This schematic illustrates the central metabolic routes, highlighting the citrate-malate antiport system for acetyl-CoA transport, the enzymatic steps involved in fatty acid synthesis, and the integration of TCA cycle metabolites.

Y. lipolytica is equipped with metabolic pathways capable of generating a wide array of lipid types, ranging from saturated and unsaturated fatty acids to more complex lipids such as phospholipids and sterols. This capability to produce diverse lipid profiles is particularly valuable to industries focused on specific lipid applications, like the manufacturing of omega-3 and omega-6 polyunsaturated fatty acids (PUFAs) used in functional foods and nutraceuticals (Park and Ledesma-Amaro, 2023; Xie et al., 2015). Moreover, *Y. lipolytica* possesses a highly efficient beta-

oxidation pathway, a critical process for lipid degradation. In this process, fatty acid molecules are systematically broken down into two-carbon units through a cyclical series of reactions. Key enzymes involved in this cycle, including acyl-CoA oxidase and 3-ketoacyl-CoA thiolase, are crucial for ensuring effective lipid catabolism. The presence and efficiency of these enzymes highlight *Y. lipolytica's* metabolic plasticity (Fickers et al., 2005).

2.3 Synthetic biology tools for *Y. lipolytica*

2.3.1 Expression vectors

Episomal vectors are pivotal in the genetic engineering of *Y. lipolytica*, facilitating the manipulation of this yeast's genome. These vectors, which closely resemble mini-chromosomes and exist in limited numbers within cells, utilize an ARS/CEN sequence for replication (Fournier et al., 1993). Despite the risk of these vectors being lost during cell division, which could impede heterologous protein production, their utility is particularly evident in applications requiring transient expression. Episomal vectors are preferred in CRISPR gene editing and the Cre-lox system for their ease of recycling (Madzak, 2018). The efficiency of these vectors was significantly advanced through engineering the centromeric region of *Y. lipolytica* by adding different promoters upstream, thereby controlling its function and enhancing its utility. This modification led to an 80% increase in plasmid copy number and gene expression, with a dynamic range expansion of nearly 2.7-fold, independent of the promoter or gene used in the expression cassette (Liu et al., 2014). The pYL15 vector also developed, demonstrating remarkable flexibility and functioning as either a centromeric replicative vector or an integrative one, depending on its form upon transformation (Bredeweg et al., 2017). Furthermore, innovatively addressing the reliance of episomal vectors on chromosomal replication systems, a mitochondrial DNA sequence, mtORI,

was identified within *Y. lipolytica* that autonomously replicates circular plasmids. This 516-base-pair sequence fosters enhanced protein expression and genetic stability, propelling the capabilities of synthetic biology and cementing *Y. lipolytica's* role as a microbial cell factory (Cui et al., 2021a). This discovery offers a new horizon in the genetic engineering of unconventional yeasts, presenting a stable and efficient system for episomal vectors to operate independently from the chromosomal replication machinery.

Integrative vectors are essential tools in the genetic engineering of *Y. lipolytica*, enabling the insertion of genes into specific loci within the genome, thus matching the stability of the organism's native genes. These vectors typically exploit regions of homology to target gene integration. The application of strains with integrated docking platforms, such as pBR322 and zeta, further increases this specificity. The pBR-based mono-integrative vectors, including pINA1296, pINA1269 and pINA1269, demonstrate an advanced vector design by targeting the pBR322 docking sites in Po1e or Po1g strains (Madzak et al., 2000), and are commercialized through the YLEX kit. In contrast, zeta-element-based vectors represent a divergent approach, providing additional genomic integration sites and broadening the scope for genetic manipulation within the species (Nicaud et al., 2002). Recently, the EasyCloneYALI genetic toolbox, leveraging CRISPR/Cas9 technology, facilitates marker-free genomic editing, boasting an integration and deletion efficiency of over 80% with non-replicating DNA fragments, thus enhancing metabolic pathway engineering through its comprehensive suite of gene expression vectors (Holkenbrink et al., 2018). The YaliBrick platform, enhancing the genetic engineering toolkit, allows for the efficient cloning of multigene pathways, enabling the rapid and balanced assembly of complex gene networks, as illustrated by the synthesis of the violacein pathway. The integration of CRISPR-Cas9 into the YaliBrick system further increases genomic editing precision, enabling

precise indel mutations and targeted gene deletions (Wong et al., 2017; Wong et al., 2019). The collective integration of these technologies has solidified *Y. lipolytica* as a leading platform for biotechnological applications.

2.3.2 Promoters

Promoters are essential due to their pivotal role in initiating transcription. These specific DNA sequences, positioned upstream of genes, are composed of elements such as upstream activating sequences (UAS), proximal promoter sequences, and TATA boxes, which collectively orchestrate the timing and intensity of gene expression (Nicaud et al., 2002). The diverse promoters in *Y. lipolytica* provide a flexible toolkit for genetic engineering, each with unique attributes.

Constitutive promoters, for instance, ensure steady gene expression levels, crucial for consistent metabolic engineering (Blazeck et al., 2011). The pGAP promoter is particularly noted for its reliable expression in *Y. lipolytica* (Nicaud, 2012), while the pTEF promoter, sourced from the translation elongation factor 1 alpha gene, is commended for its stable performance (Madzak et al., 2000; Nicaud, 2012). Inducible promoters are an important component of *Y. lipolytica*'s metabolic engineering. They exist in different forms, designed to activate gene expression in response to specific environmental stimuli. Among them, the XPR2 promoter (pXPR2) stands out for its effectiveness; however, its complex activation requirements have limited its industrial utility (Madzak, 2018; Madzak et al., 2000). Despite these challenges, extensive research, and modification of the XPR2 promoter have enhanced its inducibility and practicality. Techniques to improve its application include tweaking its regulatory components and refining the conditions under which it is induced (Madzak, 2018; Madzak et al., 2000). Recent innovations have also uncovered copper-inducible promoters like PMT-2 and PMT-6, whose inducibility rivals that of

potent constitutive promoters such as TEF (Xiong and Chen, 2020). Furthermore, the development of promoters like pEYK1 and pUAS/URS(POX2) has introduced unique inducible traits (Shabbir Hussain et al., 2017; Trassaert et al., 2017). Notably, a novel light-regulated expression system was added to the inducible promoter repertoire recently (Zhang et al., 2021). Additionally, *Y. lipolytica* features inducible promoters that react to various carbon sources—such as pG3P, pICL1, pPOT1, pPOX1, pPOX2, and pPOX5—allowing for finely-tuned gene expression control, a key advantage in the field of metabolic engineering (Juretzek et al., 2000). This rich array of inducible promoters equips researchers with the tools to orchestrate gene expression more precisely, enhancing the yeast's utility in industrial processes.

Hybrid promoters are significantly boosting gene expression beyond what native promoters can achieve for *Y. lipolytica* (Zeng et al., 2018). The hp4d hybrid promoter demonstrates this advancement. It was created by fusing UAS1XPR2 elements with a basic LEU2 promoter, resulting in marked enhancements in expression and inducibility (Madzak et al., 2000). This innovative blend of UAS tandem elements with core promoters has led to the development of robust chimeric promoters such as hp1d, hp2d, hp3d, and hp4d, with their effectiveness increasing with the addition of UAS1XPR2 fragments. Among them, hp4d stands out as the strongest, widely applied in expressing heterologous genes (Madzak et al., 2000). Progressing from this, the construction of synthetic promoter libraries, like the UAS1XPR2-LEU and UAS1XPR2(8/16)-TEF libraries marks a further advancement (Blazeck et al., 2011). The UAS1XPR2-LEU library merges 1 to 32 repeats of UAS1XPR2 upstream of the LEU2 promoter, while the UAS1XPR2(8/16)-TEF library incorporates 8 or 16 copies of UAS1XPR2 into the TEF promoter. These libraries have generated a spectrum of hybrid promoters with a range of activities, some displaying up to eight times the efficiency of the strongest natural promoters in *Y. lipolytica*

(Blazeck et al., 2011). Thus, hybrid promoters are pivotal in expanding the capabilities of *Y. lipolytica* for industrial and biotechnological applications, offering tailor-made gene expression levels that cater to diverse metabolic engineering needs.

The development of hybrid promoters for *Y. lipolytica* has continued to advance with researchers recently having taken a modular approach to create promoters with enhanced or precisely controlled activity. Their extensive research has uncovered robust native promoters such as H3, ACBP, and TMAL, which show exceptional strength in glycerol-based media, especially when linked to the reporter gene mCherry, highlighting pH3's superior potency. Building on this, they engineered novel hybrid promoters by merging Upstream Activating Sequence 1B (UAS1B8) with minimal promoters from H3 (260) or TMAL (250). These new hybrids outperformed the well-established UAS1B8-TEF1(136) promoter (Georgiadis et al., 2023), marking a significant stride in promoter engineering. Such continuous innovations are crucial for enhancing *Y. lipolytica*'s versatility in various biotechnological applications, pushing the boundaries of what can be achieved with this organism's gene expression system.

Incorporating introns into *Y. lipolytica*'s promoter engineering strategies has proven to be advantageous as well. These non-coding DNA sequences, once thought to be mere spacers, are now recognized as powerful tools for intensifying gene expression. Introns have been strategically incorporated into promoter sequences to generate significant increases in activity (Hong et al., 2012; Tai and Stephanopoulos, 2013). For instance, the integration of a 113 bp intron segment into the TEF promoter led to an impressive 17-fold increase in expression compared to the original promoter (Tai and Stephanopoulos, 2013). Further validating the powerful role of introns in enhancing gene expression, the pFBA1 promoter, when augmented with native introns, has been demonstrated to enhance activity fivefold compared to its intron-less counterpart (Hong et al.,

2012). These findings collectively reinforce the notion that intron-mediated enhancement is a versatile and effective strategy for improving promoter efficiency, offering a promising pathway for the development of highly efficient gene expression systems within this industrially valuable yeast.

2.3.3 Terminators

Terminators are key regulators of gene expression in *Y. lipolytica*, as they modulate mRNA stability and lifespan (Geisberg et al., 2014). Native terminators from genes such as TEF1, XPR2, LIP2, and POX2 are traditionally employed to manage the expression of introduced genes (Markham and Alper, 2018). The CYC1t terminator, initially characterized in *S. cerevisiae*, has also been successfully repurposed in *Y. lipolytica*, signifying its effective cross-species application (Mumberg et al., 1995). Progress in synthetic biology has produced a suite of short synthetic terminators tailored for *S. cerevisiae*, which, when applied to *Y. lipolytica*, have shown promising results. Specifically, synthetic terminators like Tsynth2, Tsynth7, Tsynth8, Tsynth10, Tsynth22, and Tsynth27 have markedly enhanced gene expression, with some even surpassing the CYC1t terminator's efficiency by up to 60% (Curran et al., 2015). This evidences that while the attention in yeast molecular biology is often on promoters, the potential of terminators, particularly synthetic variants, is substantial and deserves greater recognition for their role in genetic expression systems.

2.3.4 CRISPR gene editing tools for *Y. lipolytica*

The introduction of CRISPR gene editing tools has been a game-changer in the field of metabolic engineering, propelling forward the potential for targeted genetic modifications. Originating from

bacterial immune systems, CRISPR technology has been refined to allow for precise edits to the genetic makeup of various organisms, unlocking new possibilities for strain development that were once considered unattainable. At the heart of this cutting-edge technology is the Cas9 protein, a nuclease that, when partnered with a guide RNA, can locate, and bind to specific DNA sequences within the cell nucleus. This complex then makes a strategic cut in the DNA strand, triggering the cell's natural repair processes (Nishida and Kondo, 2021). Depending on the circumstances, the cell may employ Non-Homologous End Joining (NHEJ), which can lead to insertions or deletions, or, if a donor sequence is provided, it may use homology-directed repair. The latter pathway is especially valuable to scientists aiming for precise genetic insertions, as it allows for the integration of new DNA with exceptional accuracy (Nishida and Kondo, 2021).

The CRISPR-Cas9 system has significantly transformed the genetic engineering of *Y. lipolytica*, a yeast that poses unique challenges unlike the more amenable *S. cerevisiae*. The creation of a single-plasmid CRISPR-Cas9 Toolkit marked a substantial progression, streamlining the simultaneous delivery of Cas9 protein and guide RNA into the cell. This innovation has been effectively employed to elevate lipid production by targeting genes in the lipid metabolism pathway, such as DGA1 and GPD1 (Gao et al., 2016). Simultaneously, a pioneering method was developed that integrates native RNA polymerase III (Pol III) promoters with tRNA genes, exploiting the yeast's intrinsic tRNA processing to synthesize mature sgRNAs. This strategy facilitated the precise elimination of genes using a multiplexed sgRNA approach, considerably widening the metabolic engineering potential of *Y. lipolytica* (Schwartz et al., 2016). These two groundbreaking efforts represent the initial exploration into CRISPR-based gene editing in *Y. lipolytica*.

The utilization of the CRISPR-Cas9 gene editing system further expanded the potential for genetic manipulation in *Y. lipolytica*. The introduction of YaliBricks marked a key advancement, simplifying the assembly of multi-gene pathways to align with BioBrick standards, thereby enabling the rapid construction of complex genetic systems like the violacein biosynthetic pathway (Wong et al., 2017). Although YaliBricks tends to induce minor frameshift mutations, it represents a significant step forward in genetic engineering efficiency. In response to the challenges posed by YaliBricks, a novel dual cleavage strategy using paired sgRNAs was developed, facilitating more predictable gene knockouts. This method primarily employs perfect nonhomologous end-joining for DNA repair and has proven to be twice as effective as traditional homology recombination in tests conducted on six genes. Not only does this dual cleavage technique refine the gene knockout process, but it also enhances the accuracy of targeted gene integration, thereby expanding the potential for genetic engineering in *Y. lipolytica* (Gao et al., 2018). Concurrently, the EasyCloneYALI genetic toolbox was developed specifically for *Y. lipolytica*. This toolbox stands out for its precise genome editing capabilities, particularly its capacity for marker-free integration (Holkenbrink et al., 2018), further pushing the boundaries of what can be achieved in the genetic engineering of this yeast species.

Building on these significant developments in *Y. lipolytica* genetic engineering, 2018 marked another milestone with the introduction of the CRISPR interference (CRISPRi) system., a revolutionary tool enabling precise and reversible gene silencing (Schwartz et al., 2017a; Schwartz and Wheeldon, 2018). This innovation broadened the understanding of gene function and emerged as a cost-effective and efficient alternative to conventional gene knockout techniques. The CRISPRi system's unique feature is its multiplexed approach, which allows for the simultaneous repression of multiple genes, thereby overcoming technical limitations previously encountered in

genetic manipulation. Additionally, the system's design enhances the organism's genetic editing accuracy by suppressing the error-prone nonhomologous end-joining pathway (Schwartz et al., 2017a). This shift towards the more accurate homologous recombination pathway for DNA modifications represents a significant step forward in genetic engineering practices of *Y. lipolytica*.

The year 2020 witnessed substantial advancements in the application of the CRISPR-Cas9 system to *Y. lipolytica*. These developments were driven using predictive tools for analyzing secondary RNA structures, leading to refined tRNA-sgRNA fusion designs that notably improved the system's efficiency, particularly in targeting previously challenging chromosomal locations (Abdel-Mawgoud and Stephanopoulos, 2020). Concurrently, addressing the limitations of homologous recombination for genome integration, a novel homology-independent genome editing tool was introduced. Characterized by optimized Cas9 cleavage efficiency, this tool achieved impressive integration efficiencies, reaching up to 55% post-G1 phase synchronization, offering an efficient alternative to traditional HR-dependent methods in *Y. lipolytica* (Cui et al., 2021b).

Moving beyond specific technical improvements, the application of the CRISPR-Cas9 system in *Y. lipolytica* has undergone a broader evolutionary shift, fueled by the integration of computational biology and experimental genetics. A prime example of this is the development of DeepGuide, an innovative deep learning algorithm that illustrates the powerful impact of merging machine learning with CRISPR technology (Baisya et al., 2022). This convergence signifies a major evolution in genetic engineering, highlighting the importance of blending computational analysis with traditional genetic methods. Such integration has become crucial in advancing the capabilities and applications of the field.

Despite the significant potential of the CRISPR-Cas9 system in *Y. lipolytica*, challenges like off-target effects remain. Addressing these issues, the incorporation of machine learning tools, particularly DeepGuide, shows promise in enhancing precision. As synthetic biology progresses, combining computational techniques with genetic experimentation is key to fully exploiting the CRISPR-Cas9 system's potential. This approach is essential for driving forward innovation and reaching new scientific and practical milestones.

2.4 Products derived from metabolically engineered *Y. lipolytica*

2.4.1 Biofuels

Y. lipolytica is gaining recognition as a leading organism in biofuel production, capitalizing on its impressive metabolic capabilities. Notably, its ability to accumulate lipids up to 20% of its dry weight positions it as an ideal candidate for biofuel development (Beopoulos et al., 2011). This yeast's potential in biofuel production primarily stems from its remarkable lipid biosynthesis capabilities, which have been significantly boosted through metabolic engineering. The overexpression of key genes involved in lipid metabolism has led to increased lipid storage and the production of unsaturated fatty acids (Tai and Stephanopoulos, 2013). Further enhancing its potential, the CRISPR/Cas9 technique has been adapted to optimize lipid production pathways and reduce competing metabolic activities (Darvishi et al., 2017; Spagnuolo et al., 2019). Optimal growth conditions, such as nitrogen-limited environments and suitable carbon-to-nitrogen ratios, have been instrumental in augmenting lipid accumulation (Papanikolaou et al., 2002a). Recent studies have also focused on improving cellular oxidative stress defense pathways in *Y. lipolytica*. These efforts have successfully synchronized cell growth with lipid production, improved cell

fitness, and achieved industrially relevant lipid levels in controlled bioreactors, thereby enhancing the yeast's potential in sustainable biofuel production (Xu et al., 2017).

Y. lipolytica's versatility extends to the production of a diverse range of biofuels. It is integral to biodiesel production through the transesterification of microbial lipids (Beopoulos et al., 2009). The yeast also contributes to bio-jet fuel production by generating branched and aromatic hydrocarbons aligned with aviation fuel standards (Li et al., 2020). It shows promise in butanol production, offering superior fuel properties compared to ethanol (Yu et al., 2018). Furthermore, *Y. lipolytica* is also pivotal in developing drop-in biofuels like farnesene and squalene, serving as direct diesel replacements (Blazeck et al., 2014).

2.4.2 Biochemicals

Y. lipolytica has expanded its traditional role in biofuel, fat, and oil production to become a pivotal organism in the sustainable synthesis of diverse biochemicals. This transition offers a greener alternative to conventional petrochemical methods. It has shown remarkable capability in producing citric acid, a key ingredient in the food, pharmaceutical, and cosmetics industries (Cavallo et al., 2017; Gao et al., 2022a; Papanikolaou et al., 2002b). This is achieved not just through its ability to ferment various sugars but also via strategic metabolic engineering, specifically the overexpression of tricarboxylic acid cycle genes, leading to increased citric acid production (Tan et al., 2016). Further demonstrating its versatility, *Y. lipolytica* is adept at producing polyols, such as a low-calorie sweetener synthesized through glycerol fermentation, and mannitol (Gao et al., 2022a; Tomaszewska et al., 2012), a versatile sugar alcohol with wide-ranging applications.

It is also recognized as an efficient source of ω -hydroxy fatty acids, which are crucial for polymer manufacturing (Park et al., 2023; Wang et al., 2022). Additionally, its ability to synthesize aromatic compounds such as phenylpropanoids enhances its role in the production of flavorings, fragrances, and medicinal products (Gu et al., 2020). This diverse range of biochemical production positions *Y. lipolytica* as a sustainable alternative to traditional petrochemical methods, aligning with environmentally friendly practices. Leveraging its varied metabolic attributes and utilizing advanced genetic engineering techniques, *Y. lipolytica* is increasingly recognized as a preferred microbial host for the eco-friendly production of diverse biochemicals.

2.4.3 Proteins and enzymes

Y. lipolytica is rapidly emerging as a leading microbial platform for protein production owing to its sophisticated protein expression system and post-translational modification capabilities. This makes it particularly effective for producing a wide array of proteins, both native and heterologous (Madzak, 2015). A key feature of *Y. lipolytica* is its ability to secrete proteins directly into the culture medium, significantly simplifying the purification process (Madzak, 2015; Nicaud et al., 2002). Utilizing this yeast, researchers have successfully produced various enzymes, including lipases, proteases, phytases, and an array of recombinant proteins. These enzymes have been applied across diverse sectors such as food, pharmaceuticals, and bioenergy, demonstrating the yeast's versatility and industrial relevance.

Among these, lipases have garnered significant research interest due to their critical role in triglyceride hydrolysis and wide-ranging industrial applications (da Silva et al., 2023). To boost lipase production, *Y. lipolytica* has been genetically modified, involving both the enhancement of its native lipase genes and the introduction of lipase genes from other organisms (Madzak, 2015).

Particularly noteworthy within this yeast are two lipases, Lipase YL (Lip2p) and Lipase X. Lipase YL has gained prominence in biodiesel production, excelling in esterification and transesterification processes. Conversely, Lipase X is valued in the food industry for its unique properties that enhance the flavor of dairy products, highlighting its diverse utility (Brígida et al., 2014).

2.4.4 Lipids and oils

Y. lipolytica has emerged as a key source for lipids and oils, especially omega-3 fatty acids, which are recognized for their wide-ranging health benefits, including improvements in heart health and cognitive function. This yeast has been instrumental in synthesizing two primary omega-3 fatty acids: eicosapentaenoic acid (EPA) and docosahexaenoic acid (DHA). The production of EPA in *Y. lipolytica* was achieved by introducing desaturase and elongase genes, demonstrating the potential of microbial-based fatty acid production (Xue et al., 2013). Similarly, DHA production involved using genes from marine organisms, providing a sustainable alternative to traditional marine-derived DHA (Gemperlein et al., 2019). Additionally, *Y. lipolytica* has been used to produce other omega-3 variants, including stearidonic acid (SDA), alpha-linolenic acid (ALA), and docosapentaenoic acid (DPA), further demonstrating its versatility and utility (Xie et al., 2015).

Y. lipolytica's success in Omega-3 fatty acid synthesis has laid the groundwork for its application in producing specialty oils with compositions identical to specific plant-derived lipids. Demonstrating this capability, *Y. lipolytica* was used to produce a lipid profile similar to cocoa butter, indicating its commercial potential and offering a sustainable alternative amid concerns about cocoa supply and deforestation (Papanikolaou et al., 2003). *Y. lipolytica* is also proving to

be an asset in the production of Medium Chain Fatty Acids (MCFAs), which are increasingly sought after for their dietary benefits and their use in cosmetics and personal care products (Sarria et al., 2017). Through the redirection of its metabolic pathways, *Y. lipolytica* has been successful in synthesizing specific MCFAs, notably C8 and C10 fatty acids (Wang et al., 2022). Building on this achievement, researchers have also managed to produce lauric acid (C12), an MCFA prized for its antimicrobial properties and widespread use in products like soaps (Wang et al., 2022). Furthermore, recent research efforts have expanded *Y. lipolytica*'s capabilities to include the production of caprylic acid (C8) and caproic acid (C6). These acids are not only valued for their antimicrobial properties but also for their potential role in weight management (Wang et al., 2022). Such advancements in producing a range of MCFAs underscore the growing importance and versatility of *Y. lipolytica* in the field of MCFA production.

2.4.5 Specialty chemicals

Linalool, a terpene alcohol known for its unique aroma, is highly sought-after in the fragrance industry. It is a common component of various essential oils, and its synthesis has garnered considerable interest. *Y. lipolytica*, with its flexible metabolic pathways, is an excellent candidate for linalool production. By specifically altering its metabolic routes, this yeast can produce linalool efficiently and in significant amounts (Cao et al., 2017). Similarly, utilizing a targeted approach in metabolic engineering, *Y. lipolytica* has been effectively used to synthesize β -carotene, an essential precursor to vitamin A (Larroude et al., 2018). These achievements highlight *Y. lipolytica*'s capacity to produce complex compounds like linalool and β -carotene, demonstrating its crucial role in serving various industrial needs.

In the field of sustainable materials, *Y. lipolytica* has been explored for its ability to produce eco-friendly biopolymers like polyhydroxyalkanoates (PHAs), offering a greener alternative to traditional plastics (Gao et al., 2015). Additionally, its capability in producing specialty chemicals is evident in its synthesis of Gamma Decalactone (Braga and Belo, 2015), a compound with a peach-like scent essential in the flavor and fragrance industry, and Itaconic Acid (Blazeck et al., 2015), an important bio-based building block, further expanding its industrial relevance. These developments collectively demonstrate *Y. lipolytica's* growing role as a versatile and valuable organism in various biotechnological sectors.

2.5 Challenges in metabolic engineering of *Y. lipolytica*

While the biotechnological potential of *Y. lipolytica* is significant, fully harnessing its capabilities presents distinct challenges. A key issue is the lack of well-defined genetic tools specifically designed for this non-conventional yeast. Techniques like CRISPR/Cas9, for instance, are less efficient in *Y. lipolytica* compared to their performance in more established organisms like *S. cerevisiae* (Abdel-Mawgoud and Stephanopoulos, 2020; Schwartz et al., 2017a; Schwartz and Wheeldon, 2018; Wong et al., 2019), highlighting the need for yeast-specific genetic tool development. Additionally, the metabolic flexibility of *Y. lipolytica*, though advantageous, can pose obstacles. Efforts to increase lipid production, for example, may inadvertently boost citric acid levels due to metabolic pathway interferences (Beopoulos et al., 2009). Moreover, the yeast's ability to produce various lipids requires precise tailoring of its metabolic pathways, often involving modifications across multiple genes, complicating the engineering process (Qiao et al., 2015). Despite these challenges, the prospects of *Y. lipolytica* in biotechnology are promising,

necessitating continued research and innovative approaches to fully exploit this versatile yeast's potential.

2.6 Mannitol

Mannitol, a sugar alcohol also known as a polyol, is widely used across various industries due to its unique physicochemical properties. Its non-hygroscopic nature and resistance to human metabolism make it particularly valuable in the pharmaceutical and food sectors. Historically, mannitol was derived from the manna tree, *Fraxinus ornus*, with the crystalline substance it produces, known as "manna," giving mannitol its name. It was prized in ancient civilizations for both its sweetness and medicinal benefits. In the pharmaceutical industry, mannitol is utilized for its therapeutic qualities, notably as an osmotic diuretic to treat conditions like increased intracranial pressure and cerebral edema. It is also recognized for its stabilizing role in freeze-dried drug formulations. In the food industry, mannitol is valued for its sweet taste, with roughly half the caloric content of sucrose and a cooling effect upon dissolution, making it a popular choice in confections, chewing gums, and low-calorie snacks (Godswill, 2017; Shawkat et al., 2012; Song and Vieille, 2009).

The increasing demand for mannitol during the 19th and 20th centuries, particularly driven by the expanding pharmaceutical industry, highlighted the necessity for more efficient production methods. By the mid-20th century, there was a significant shift towards chemical synthesis in mannitol production, diminishing the dependence on natural sources. This shift was primarily driven by advancements in organic chemistry, which equipped researchers with the tools to modify mannitol at the molecular level. The industrial revolution further amplified this demand, spurring

the move towards mass production of mannitol to meet growing market needs (Song and Vieille, 2009).

The renewed interest in biotechnological methods for mannitol production aligns with the current emphasis on sustainability and green initiatives. Modern research is increasingly focused on microbial fermentation, a process that utilizes microorganisms to produce mannitol in an environmentally friendly manner (Song and Vieille, 2009). The evolution of mannitol manufacturing is a compelling example of how scientific research, technological advancements, and industry needs intersect. The insights gained from its historical development are shaping ongoing research and production methods, as well as the future applications of mannitol. The subsequent sections will cover deeper into biotechnological approaches for mannitol production, compare them with chemical methods, and conclude with a discussion on the latest advancements and potential future innovations in this field.

2.6.1 Natural sources of mannitol

Mannitol naturally occurs in diverse environments and plays crucial roles in plants, such as osmoregulation and carbon storage (Stoop et al., 1996). Historically, the manna tree, *Fraxinus ornus*, was a primary source, with its dried sap yielding crystalline mannitol, used for various purposes in ancient societies (Godswill, 2017; Shawkat et al., 2012; Song and Vieille, 2009). In addition, fruits like olives, strawberries, and celery also contain mannitol, contributing to their taste and texture (Yao et al., 2014). In the marine environment, brown algae species like *Fucus* and *Laminaria* produce mannitol as a byproduct of photosynthesis. This mannitol serves to maintain osmotic balance and acts as a reserve carbohydrate, utilized metabolically under certain conditions (Reed et al., 1985).

In the microbial world, fungi from the *Penicillium* and *Aspergillus* families produce mannitol as a response to environmental challenges such as dryness and oxidative stress. The rapid growth and scalability of microbial cultures make fungal mannitol production a promising avenue for sustainable production, drawing attention from the scientific community (Song and Vieille, 2009). The widespread occurrence of mannitol in nature demonstrates its critical role in the survival and function of various organisms. The ongoing search for environmentally friendly mannitol sources benefits from these natural reservoirs, guiding research and industry towards efficient extraction and production methods.

2.6.2 Chemical synthesis of mannitol

The growing demand for large-scale, consistent mannitol production led to the development of chemical synthesis methods, providing an efficient alternative to conventional natural extraction. This chemical approach, capable of producing mannitol in large quantities, has become indispensable in various industries (Dai et al., 2017). Central to this method is the hydrogenation of fructose, typically using metal catalysts such as nickel and ruthenium. When executed under precise temperature and pressure conditions, this process effectively converts fructose into mannitol. Subsequently, crystallization methods are employed to refine the produced mannitol, ensuring its purity and suitability for industrial use (Dai et al., 2017).

Chemical synthesis of mannitol, while effective, faces significant challenges. The reliance on metal catalysts in the process has raised environmental concerns and questions about the sustainable sourcing of these metals. Additionally, the dependence on fructose as the primary raw material makes this method susceptible to fluctuations in agricultural production and market trends, emphasizing the need for a stable and high-quality source of fructose (Dai et al., 2017;

Song and Vieille, 2009). In response to these issues, the field of green chemistry is gaining momentum, focusing on developing environmentally friendly mannitol synthesis methods. These new techniques aim to reduce harmful inputs and waste, aligning with broader sustainability objectives (Dai et al., 2017; Song and Vieille, 2009). As the mannitol production landscape continues to develop, the emphasis is on achieving a balance between production efficiency, product quality, and environmental stewardship. The biological production of mannitol has recently gained attention as an eco-friendly alternative to chemical methods. This approach, aligning with green chemistry principles, utilizes the metabolic abilities of specific microorganisms for more sustainable production.

2.6.3 Biological production of mannitol

The biological production of mannitol has recently gained attention as an eco-friendly alternative to chemical methods. This approach, aligning with green chemistry principles, utilizes the metabolic abilities of specific microorganisms for more sustainable production. Central to this method is microbial fermentation, involving a range of microorganisms, from bacteria to fungi, that have been optimized for mannitol production (Dai et al., 2017; Song and Vieille, 2009). Notably, the bacterium *Lactobacillus intermedius* is recognized for its efficient mannitol synthesis, particularly from fructose (Martínez-Miranda et al., 2022; Saha and Nakamura, 2003). In yeasts, *Candida magnoliae* is known for its robust metabolism and ability to produce mannitol (Savergave et al., 2013; Song et al., 2002). Additionally, enzymatic processes represent a promising direction. Early research indicates that enzymes like mannitol dehydrogenase can convert fructose to mannitol with high precision, pointing towards potential future scalability (Slatner et al., 1998). These biological strategies offer exciting prospects for sustainable mannitol production.

While the biological production of mannitol presents a promising sustainable alternative, perfecting this method comes with its own set of challenges. Key issues include optimizing fermentation conditions and achieving consistently high yields, which are active areas of research (Savergave et al., 2013; Song et al., 2002). In essence, the biological approach to mannitol production embodies a synergy of scientific innovation and practical application. Ongoing research is expected to refine these methods further, positioning biological production as a leading approach to meet global mannitol demands in an environmentally responsible manner.

2.6.4 Mannitol production using *Y. lipolytica*

Y. lipolytica has become a notable microbial host for mannitol biosynthesis, especially when utilizing glycerol, a byproduct of biofuel production, as a substrate. Achieving optimal mannitol production with this yeast requires precise adjustment of cultivation conditions. In 2012, Tomaszewska, Rywińska, and their team investigated the use of crude glycerol for producing mannitol and other polyols. Their study tested nine *Y. lipolytica* strains, identifying A UV'1, A-15, and Wratislavia K1 as the most effective mannitol producers in buffered shake-flask cultures. Notably, Wratislavia K1 achieved erythritol concentrations up to 80 g/L, with a yield of 0.49 g/g, while A UV'1 and A-15 produced mannitol concentrations as high as 27.6 g/L. They also found that adding NaCl improved erythritol but negatively impacted mannitol production, emphasizing the need for a balanced medium composition (Tomaszewska et al., 2012). Advancing this research, Juszczuk, Rywińska, and collaborators examined 21 *Y. lipolytica* strains in 2023 for their mannitol-producing capabilities. Strains S2, S3, and S4 were particularly promising. Using an improved fed-batch culture method, they achieved mannitol concentrations of 78.5 g/L, significantly surpassing

the results from 2012 and illustrating the progression in production techniques (Juszczak et al., 2023).

Additionally, researchers have been exploring the impact of pH on mannitol production, revealing insights into the relationship between cultivation conditions and product yields. Egermeier and their group in 2017 also observed pH-dependent variations in polyol production. In bioreactor experiments, they noted that at a pH of 3.5 and after 48 hours of cultivation, 15 out of 20 strains transformed glycerol into polyols. Notably, strain DSM 1345 achieved mannitol concentrations of up to 11 g/L. This strain, which initially showed minimal production in shake flask experiments, exhibited significant mannitol production in the controlled environment of a bioreactor. This research highlighted the critical importance of media composition and the use of controlled environments, like bioreactors, for effective strain characterization and fermentation processes. While their study encompassed both erythritol and mannitol, it reinforced the pivotal role of pH in directing desired metabolic pathways (Egermeier et al., 2017). Complementing these findings, in 2022, Gao, Wang, and their team investigated the concurrent production of mannitol and citric acid using glucose and glycerol. Their findings showed that a slightly acidic environment, particularly at a pH of 3.5, significantly increased mannitol production, reaching concentrations of 37.1 ± 1.5 g/L in a corn stover-based medium (Gao et al., 2022b). This study highlighted *Y. lipolytica's* adaptability and the potential of integrated biorefining processes.

These studies collectively highlight *Y. lipolytica's* potential for efficient mannitol production, particularly when using glycerol as the substrate. The key to optimizing mannitol yield lies in carefully adjusting various factors, including pH, medium composition, and the operational specifics of bioreactors. This precision in cultivation conditions is crucial for maximizing mannitol output with *Y. lipolytica*.

2.6.5 Extraction and purification

The extraction and refining of mannitol, particularly for use in the pharmaceutical and food industries where high purity is crucial, involve complex processes. Achieving the required purity levels necessitates multiple refining stages, whether mannitol is synthesized chemically or extracted from natural sources (Ghoreishi and Shahrestani, 2009; Savergave et al., 2013; Song et al., 2002). Typically, mannitol is extracted from plants or seaweeds using solvents, with water being the preferred solvent due to its polarity and safety. However, this method initially dissolves not only mannitol but also other solutes, necessitating further purification steps (Ghoreishi and Shahrestani, 2009). Crystallization is a key technique in purifying mannitol. By carefully controlling parameters such as temperature and solute concentration, mannitol can be induced to crystallize, leaving impurities in the solvent phase. This method is recommended for scalability and effectiveness as well as achieving high purity levels (Weymarn et al., 2003).

Mannitol produced through microbial fermentation presents distinct challenges, primarily due to the variety of fermentation by-products. To address this, researchers have explored ultrafiltration, a process that utilizes membrane technology with specific pore sizes to separate substances based on molecular size. This method has been considered for isolating mannitol from fermentation mixtures (Saha, 2003). This technique has been successful in attaining high purity levels for mannitol from microbial sources. However, it's crucial to acknowledge that this advanced purification method can contribute to higher overall production costs of mannitol. Consequently, the selection of a purification technique should balance the specific purity requirements against the cost-effectiveness of the process, ensuring the most efficient approach for mannitol production.

2.7 5-aminolevulinic acid

2.7.1 Uses and synthesis pathways

5-Aminolevulinic acid (5-ALA) is a non-proteinogenic amino acid essential in the tetrapyrrole biosynthesis pathway, crucial for many biological processes. It plays a significant role in cellular metabolism and heme synthesis, underscoring its biological importance (Jiang et al., 2022; Kang et al., 2017). Beyond its cellular roles, 5-ALA is recognized for its therapeutic versatility, particularly in photodynamic therapy within the medical field (Gold and Goldman, 2004). In agriculture, it is valued as an effective plant growth enhancer (Rhaman et al., 2021), demonstrating its wide commercial utility. Additionally, recent advancements highlight 5-ALA's potential in neurology, notably in improving brain tumor visualization during surgeries (Ferraro et al., 2016). These diverse applications emphasize the multifaceted significance of 5-ALA across various sectors.

The increasing demand for 5-Aminolevulinic acid (5-ALA) across various sectors has led to microbial synthesis emerging as a preferred production method. This approach is favored over traditional chemical methods, which often involve environmentally harmful reagents. Microbial synthesis offers environmental sustainability and scalability, making it an efficient and viable alternative (Kang et al., 2017).

5-ALA synthesis involves two primary metabolic pathways: the C4 and C5 pathways. The C5 pathway is common in eubacteria, archaeobacteria, algae, and plants. It begins with the glutamylation of tRNA for L-glutamic acid, leading to L-glutamyl-tRNA(Glu), which is then converted into L-glutamate 1-semialdehyde, and finally to 5-ALA. This transformation involves enzymes like glutamyl-tRNA synthetase, glutamyl-tRNA reductase, and glutamate-1-semialdehyde aminotransferase (Jiang et al., 2022; Kang et al., 2017; Miscovic et al., 2021). In

contrast, the C4 pathway, also known as the Shemin pathway, is found in animals and fungi and involves the condensation of succinyl-coenzyme A (CoA) and glycine, catalyzed by the ALA synthetase enzyme. This pathway is used by the bacterium *Rhodobacter sphaeroides* for industrial production of 5-ALA. The choice and optimization of these pathways are crucial for enhancing the yield and purity of 5-ALA in microbial production. A thorough understanding of these pathways and their enzymatic mechanisms is key to improving 5-ALA synthesis (Jiang et al., 2022; Kang et al., 2017; Miscevic et al., 2021).

2.7.2 Manipulation of porphobilinogen synthase

In the pursuit of augmented 5-aminolevulinic acid (5-ALA) production, a key strategy involves overexpressing the *hemA* gene, responsible for the rate-limiting step in its biosynthesis. Concurrently, efforts have been directed towards mitigating competing metabolic pathways. A critical approach in this regard is the genetic modulation of the *hemB* gene, which plays a pivotal role in the heme synthesis pathway. The application of CRISPRi technology to suppress *hemB* activity in *E. coli* has demonstrated significant promise, leading to an increase in 5-ALA synthesis by up to 493.1% (Su et al., 2019). Furthermore, a comprehensive strategy combining *hemB* repression with the integration of the C4 pathway into *E. coli*'s metabolism, as explored by Miscevic et al. (2021), yielded remarkable results. This approach, coupled with process optimizations, successfully achieved a 5-ALA titer of 6.93 g/L from glycerol. These multifaceted approaches underscore the efficacy of integrating genetic engineering with bioprocessing techniques to enhance 5-ALA production significantly.

2.8 Heme importance and production

Heme, a crucial iron-containing molecule, is fundamental in a myriad of biological and industrial applications. In biological systems, its primary functions include essential roles in oxygen transport and storage, and as a catalyst in various enzymatic reactions crucial for cellular metabolism. Heme forms a core part of hemoglobin and myoglobin, proteins vital for oxygen transport and storage in vertebrates. Additionally, it functions as a prosthetic group in numerous enzymes, playing a key role in facilitating redox reactions (Choi et al., 2022; Frankenberg et al., 2003). This multifaceted role of heme demonstrates its importance across different biological contexts.

Heme's therapeutic applications in medicine are diverse. It is particularly effective in treating hemoglobinopathies, disorders characterized by abnormal hemoglobin structure. Additionally, heme is integral in therapies for porphyria, conditions arising from defects in heme biosynthesis (Di Pierro and Granata, 2020; Fontanellas et al., 2016). In the food industry, heme has garnered attention for its use in plant-based meats. Its ability to replicate the flavor and appearance of meat is appealing to consumers looking for plant-based options without sacrificing taste. This application has grown in popularity, fueled by increasing global interest in sustainable and ethical food choices (Ko et al., 2021; Su et al., 2023). Heme's versatility in both medical and food applications illustrates its broad potential and increasing relevance in various sectors.

Traditionally, heme production has relied heavily on extraction from natural sources like animal blood. While effective, this method is increasingly scrutinized for sustainability issues, as it necessitates intensive farming practices that are resource-intensive and contribute to environmental degradation. Additionally, the scalability and consistency of yields from these natural sources can be variable, making it challenging to meet the growing global demand for heme

(Ko et al., 2021; Su et al., 2023). Considering these challenges, there has been a significant shift towards biomanufacturing methods. Microbial factories have become a preferred alternative for sustainable and efficient heme production. These biomanufacturing approaches utilize genetically engineered microbes to synthesize heme in controlled environments, which guarantees consistent quality and yield. Moreover, they are more aligned with global sustainability objectives, as they significantly reduce the environmental footprint associated with traditional heme production methods (Choi et al., 2022; Ko et al., 2021; Su et al., 2023; Yang et al., 2023). This shift towards microbial biomanufacturing marks a crucial step in addressing the environmental and scalability issues associated with conventional heme production.

The transition to biomanufacturing, particularly for heme production, is promising but comes with significant challenges. Ensuring the safety of these products, especially in food and medicine, is crucial. Regulatory bodies enforce strict standards to guarantee that products are safe for consumer use (Tyndall et al., 2022). There is ongoing research into the long-term effects of heme consumption, especially in plant-based meats (Tyndall et al., 2022). This shift also has considerable economic implications. Moving from traditional extraction to microbial factories can transform industries, requiring new skills and creating opportunities in biomanufacturing (Tyndall et al., 2022). However, it challenges traditional farming, highlighting the need for thoughtful economic planning and support for those impacted.

2.8.1 Metabolic pathways involved in heme production

Heme biosynthesis, a multi-step process occurring within the mitochondria and cytosol of eukaryotic cells, starts with the condensation of succinyl-CoA and glycine. This reaction is catalyzed by 5-aminolevulinic acid synthase (ALAS). The product, 5-aminolevulinic acid (5-ALA),

is then converted to porphobilinogen (PBG) by 5-ALA dehydratase (ALAD). PBG is polymerized into hydroxymethylbilane by porphobilinogen deaminase (PBGD). This linear tetrapyrrole is transformed into uroporphyrinogen III, a cyclic compound, by uroporphyrinogen III synthase. Uroporphyrinogen III undergoes several modifications to become coproporphyrinogen III, which is transported to the mitochondria. Here, it is oxidized to protoporphyrinogen IX by coproporphyrinogen oxidase (CPO), then converted to protoporphyrin IX. The final step in heme production is the insertion of an iron ion into the protoporphyrin ring by ferrochelatase, resulting in the formation of heme (Ajioka et al., 2006; Ishchuk et al., 2022; Su et al., 2023). In bacteria, heme synthesis predominantly occurs through the C-5 pathway, which differs from the C-4 pathway seen in eukaryotes right from its first step. This bacterial pathway involves transforming glutamate into 5-aminolevulinic acid (5-ALA) via a three-enzyme process: glutamyl-tRNA synthetase, glutamyl-tRNA reductase, and glutamate-1-semialdehyde-2,1-aminomutase. This pathway was reported to be more energy-efficient, giving bacteria a metabolic edge. Moreover, certain bacteria can alternate between the C-4 and C-5 pathways in response to environmental changes, indicating the versatility of microbial heme biosynthesis (Choi et al., 2022; Dailey et al., 2017; Su et al., 2023; Yang et al., 2023).

Heme biosynthesis regulation significantly differs between the C-4 pathway in eukaryotes and the C-5 pathway in bacteria, reflecting their distinct organisms and environmental conditions. In eukaryotic cells, the C-4 pathway's regulation is stringent, primarily focusing on the first and rate-limiting enzyme, 5-aminolevulinate synthase (ALAS). Expression of ALAS and its activity are influenced by a complex interplay of transcriptional, post-transcriptional, and post-translational mechanisms, sensitive to factors like cellular heme levels and oxidative stress (Ajioka et al., 2006; Ishchuk et al., 2022; Su et al., 2023). Conversely, the C-5 pathway in bacteria is

adapted for prokaryotic life. This pathway's regulation, especially the second step catalyzed by glutamyl-tRNA reductase, responds to the bacterial cell's heme needs. Heme feedback inhibition controls the synthesis of 5-ALA, aligning heme production with cellular demand and conserving resources. Additionally, some bacteria demonstrate remarkable adaptability in heme biosynthesis, capable of switching between the C-4 and C-5 pathways based on environmental conditions (Choi et al., 2022; Dailey et al., 2017; Su et al., 2023; Yang et al., 2023). This flexibility further illustrates the adaptive nature of heme biosynthesis regulation in bacteria.

2.8.2 Metabolic engineering strategies for enhanced heme production

Recent advances in metabolic engineering have significantly enhanced heme production in various organisms, employing a combination of genetic modifications and bioprocess optimization. A notable example by Ko et al. (2021) involves engineering *C. glutamicum*. Their comprehensive approach integrated dual precursor pathways based on thermodynamic principles, overexpressed genes in an unconventional downstream pathway, and included the gene for the transcriptional regulator DtxR. This strategy also involved overexpressing potential heme exporters, knocking out genes associated with heme-binding proteins, altering the cell wall, and reducing intermediate uroporphyrinogen III levels. These multifaceted modifications resulted in markedly increased heme secretion. When this optimized strain of *C. glutamicum* was subjected to fed-batch fermentation, it produced a heme titer of 309.18 ± 16.43 mg/L. This performance translates to a productivity rate of 6.44 mg/L/h and a yield on glucose of 0.61 mmol/mol, demonstrating the strain's efficiency as a cell factory for animal-free heme production.

Zhao et al. (2018) significantly advanced heme production in *E. coli*, shifting from intracellular to secretory production via the C5 pathway in engineered strains. Their method

included key gene knockouts (*ldhA*, *pta*, and *yfeX*, a suspected heme-degrading enzyme) and resulted in a total heme production of 7.88 mg/L, with 1.26 mg/L being extracellular, in flask cultivation. Further enhancement through overexpression of the heme exporter CcmABC led these strains to secrete up to 151.4 mg/L of heme in fed-batch fermentations using glucose and L-glutamate media. Building on these results, Choi et al. (2022) focused on refining the fermentation process of the *E. coli* strain HAEM7. They explored various bioprocess parameters like carbon source selection, iron concentration, pH control, and optimization of induction points, achieving a heme concentration of 1.03 g/L and a productivity rate of 21.5 mg/L/h. Concurrently, Geng, Ge et al. (2022) developed recombinant *E. coli* strains for heme production by combining metabolic and membrane engineering. They optimized genes in the heme synthesis pathway, removed transport genes for heme precursors, and enhanced extracellular transport pathways. Their EJM- Δ CyoE-pCD-AL strain achieved 28.20 ± 0.77 mg/L of heme production in fed-batch fermentation in a 3-L fermenter (Geng et al., 2022). These developments underscore the potential of *E. coli* as a versatile platform for heme production. The diversity in engineering and optimization strategies employed by researchers demonstrates the significant improvements in production capabilities, contributing to sustainable and efficient production practices in microbial heme production.

In an innovative study, Ishchuk et al. (2022) utilized the yeast *S. cerevisiae* and a genome-scale metabolic model (GEM), Yeast8, to identify key fluxes impacting heme synthesis. Their in-silico simulations pinpointed 76 genes that, when deleted or overexpressed, resulted in a threefold increase in heme production. Notably, this enhancement wasn't limited to genes directly involved in heme biosynthesis. It also included genes linked to various metabolic pathways, such as glycolysis, pyruvate metabolism, iron-sulfur (Fe-S) cluster formation, and the metabolism of glycine and succinyl-coenzyme A (CoA). These comprehensive genetic modifications led to the

development of a yeast strain with an impressive 70-fold increase in intracellular heme levels, demonstrating the potential of integrated genomic and metabolic approaches in optimizing heme production.

In 2023, Yang et al. implemented a modular engineering strategy on *Bacillus subtilis* to enhance heme biosynthesis via the C5 pathway. Their approach included strategic gene knockouts and overexpression, improvements in the Urogen III synthesis pathway, and specific adjustments in the downstream synthesis pathway. This set of comprehensive genetic and process modifications led to a significant increase in heme production, achieving a yield of 248.26 ± 6.97 mg/L in a 10 L fermenter during fed-batch fermentation (Yang et al., 2023). This study highlights the effectiveness of targeted and integrated approaches in optimizing microbial pathways for increased heme production.

These research studies collectively show that significant progress in heme production across various host organisms has been achieved through a blend of metabolic engineering, bioprocess optimization, and membrane engineering. Each study contributes valuable insights, highlighting the potential of engineered microorganisms as effective platforms for heme production. This marks a substantial step forward in developing sustainable and efficient production processes in the field, demonstrating the power of combining different scientific and technological approaches.

2.9 Heme derivatives

Heme derivatives encompass a variety of linear tetrapyrrole pigments, collectively referred to as bilins, which are products of heme catabolism. The production of these bilins is mediated by the remarkable enzymatic activities of heme oxygenases (HOs) and ferredoxin-dependent bilin reductases (FDBR) (Kumar and Bandyopadhyay, 2005; Takemoto et al., 2019). While they share

structural similarities, bilins exhibit a vast range of biological functions and have diverse applications. In human physiology, the catabolic breakdown of heme plays a vital role. This process not only aids in recycling iron, a critical component for numerous cellular functions, but also ensures the regulation of intracellular free heme concentrations, keeping them below a crucial threshold of 1 μM (Kumar and Bandyopadhyay, 2005; Sassa, 2004). Crossing this threshold has the potential to trigger oxidative reactions, leading to the production of reactive oxygen species (ROS). These ROS can be detrimental, posing a threat to cellular health and integrity (Frankenberg-Dinkel, 2004; Mysliwa-Kurdziel and Solymosi, 2017).

Pathogenic bacteria have ingeniously adapted the heme degradation pathway for their own benefit. They efficiently extract iron from their host while neutralizing the potential toxicity of internalized heme, exemplifying their impressive ability to adapt for survival (Anzaldi and Skaar, 2010). Conversely, photosynthetic organisms such as plants, algae, and cyanobacteria use the products of heme catabolism differently. They primarily produce biliverdin IX α , which then becomes a precursor for various light-sensitive and light-harvesting tetrapyrroles (Mysliwa-Kurdziel and Solymosi, 2017).

The world of bacteria has revealed a vast array of bilins, each with unique characteristics and potential applications. This group includes well-known derivatives such as biliverdin, mesobiliverdin, mycobilin, staphylobilin, anaeroblin, phycocyanobilin (PCB) and phycoerythrobilin (PEB). Particularly, the vibrant pigments of biliverdin, PCB, and PEB have attracted substantial interest for their applications in therapeutics, diagnostics, and the food industry, presenting significant economic and research opportunities (Celis and DuBois, 2019; Lyles and Eichenbaum, 2018).

Biliverdin occurs in four distinct isomeric forms, each resulting from the cleavage of a specific methane bridge in the parent heme molecule. Among these isomers, biliverdin IX α is not only the most common in nature but also holds the unique capacity to transform into other valuable derivatives like PCB and PEB (Ó'carra and Colleran, 1970). In this context, when we refer to 'biliverdin' within this dissertation, we are predominantly addressing biliverdin IX α , given our research interests in harnessing its potential.

2.9.1 Biliverdin synthesis: heme oxygenases

Biliverdin production, a green tetrapyrrolic pigment, is tightly regulated by the enzymatic breakdown of heme via heme oxygenase. Heme oxygenases, found in various organisms, are key in the specific cleavage of methane bridges in heme at α , β , γ , and δ positions, a process influenced by their regiospecificity (Ó'carra and Colleran, 1970). These enzymes are widespread, and research has revealed notable similarities between prokaryotic and mammalian heme oxygenases. For example, the prokaryotic heme oxygenase HmuO from *Corynebacterium diphtheriae* bears significant resemblance to mammalian HO1 (Schmitt, 1997). This similarity extends to other organisms as well, with studies on HO1 from *Synechocystis spp.* PCC 6803 and HemO from *Neisseria meningitides* showing structural and mechanistic similarities to mammalian HO1 (Cornejo et al., 1998; Zhu et al., 2000). This highlights the evolutionary conservation and functional importance of heme oxygenases across different species.

These early-identified bacterial heme oxygenases (HOs) that closely resemble mammalian ones were classified as canonical heme oxygenases, which generates biliverdin IX α (Wilks and Heinzl, 2014). However, the discovery of IsdG and IsdI in *Staphylococcus aureus aureus* (Celis and DuBois, 2019; Skaar et al., 2004) and MhuD in *Mycobacterium tuberculosis* (Celis and

DuBois, 2019; Nambu et al., 2013) introduced a new class of HOs. These are termed non-canonical heme oxygenases due to their distinct structure and novel mechanism for heme pyrrole ring cleavage. While most HOs in both classes operate in an oxygen-dependent manner, ChuW from *Escherichia coli* O157:H7 is an exception, catalyzing its reaction without oxygen to produce anaeroblin (LaMattina et al., 2016). Canonical heme oxygenases engage in a complex process involving three successive oxygenation steps, culminating in the production of biliverdins, CO, Fe²⁺, and 3H₂O. This process requires the concerted action of Ferredoxin-NADPH Reductase, NADPH, and Ferredoxin (Celis and DuBois, 2019; Frankenberg-Dinkel, 2004; Takemoto et al., 2019; Wilks and Heinzl, 2014). This delineation between the canonical and non-canonical classes highlights the diversity and complexity of bacterial heme oxygenase enzymes.

2.9.2 PCB and PEB synthesis: Ferredoxin-dependent bilin reductases (FDBRs)

Ferredoxin-dependent bilin reductases (FDBRs) are key enzymes in the transformation of biliverdin into phycobilins, known as 'algal biles'. These are unique bilins acting as photosynthetic accessory pigments in several cyanobacteria and eukaryotic algae group (Mysliwa-Kurdziel and Solymosi, 2017). FDBRs use biliverdin IX α to produce colored pigments crucial for light-harvesting or sensing in plants, algae, and cyanobacteria (Mysliwa-Kurdziel and Solymosi, 2017). To date, several FDBRs have been identified and are generally categorized into two functional groups based on their electron transfer capability during the reaction (Busch et al., 2011; Mysliwa-Kurdziel and Solymosi, 2017). The first group can catalyze a two-electron reduction, while the second consists of FDBRs that perform a four-electron reduction of biliverdin. For instance, the cyanobacterial enzyme PcyA reduces biliverdin to phycocyanobilin (PCB) via a four-electron transfer. Similarly, phycoerythrobilin (PEB) synthase, PebS, identified in cyanophages, also

executes a four-electron transfer but in two steps, resulting in PEB through a 15, 16-dihydrobiliverdin intermediate. In cyanobacteria, this reaction is facilitated by two separate enzymes: PebA and PebB, each transferring two electrons to biliverdin to ultimately produce PEB. This process highlights the complexity and variety within the FDBR enzyme family and their role in pigment synthesis.

2.9.3 Advancements and challenges in biliverdin synthesis

The traditional method for producing biliverdin involved converting bilirubin extracted from mammalian bile. This process used 2,3-dichloro-5,6-dicyanobenzoquinone in dimethyl sulphoxide under carefully controlled acidic conditions (McDonagh and Palma, 1980). However, this method had significant drawbacks. Chromatographic analyses, such as high-pressure liquid chromatography (HPLC) and thin-layer chromatography, revealed a mixed product composition, with only a 38% yield of biliverdin IX α (McDonagh, 2005). Given the pharmaceutical industry's stringent purity standards, this raised concerns about its suitability for medical applications. In search of better production methods, researchers explored extracting biliverdin directly from salmon bile. This approach achieved a higher yield of 49.5mg/100ml of biliverdin IX α at a 95.3% purity level (Ding and Xu, 2002). However, the feasibility of scaling this method has been debated, especially considering the ethical and practical implications of needing to sacrifice 50 salmon for each extraction. This ongoing debate points to the need for more sustainable and ethical production methods for biliverdin, especially for pharmaceutical uses.

In response to the limitations of these traditional methods, the scientific community has pivoted to bio-based production using microbial cell factories for biliverdin synthesis. *Candida albicans*, when supplemented with 1g/L of hemoglobin, showed promise in biliverdin production

(Pendrak and Roberts, 2013). However, the cost of hemoglobin supplementation raises concerns about the method's scalability and economic feasibility. A significant breakthrough was achieved with the engineering of *E. coli* to express cyanobacterial HO1, leading to a consistent yield of 23.5mg/L of biliverdin IX α in fed-batch fermentation, marking a major advancement in microbial-based synthesis (Chen et al., 2012). The field saw further progress with the introduction of *hema* from *Rhodobacter sphaeroides* into *E. coli*, expanding the range of microbial strategies (Takemoto and Chen, 2017). Another notable development involved engineering *Corynebacterium glutamicum*, which achieved biliverdin production levels of 68.74 ± 4.97 mg/L in 5L fed-batch fermentations (Seok et al., 2019). However, the method's requirement for 200-500 μ g/L biotin supplementation brings its economic feasibility into question for industrial-scale production. These advancements illustrate the potential of microbial cell factories in biliverdin synthesis, although the economic implications of the required supplements remain a concern for large-scale application.

These advances in biliverdin production indicate that, while significant progress has been made, there is still a substantial need for improvement. Current methods, though innovative, confront complex challenges in terms of yield, purity, and cost-effectiveness. The scientific community stands at the beginning of major breakthroughs, poised to leverage advanced techniques in metabolic engineering, synthetic biology, and computational modeling to revolutionize biliverdin production. As research in this field intensifies, there is an increasing sense of optimism about enhancing biliverdin production.

2.9.4 Advances and challenges in phycocyanobilin biosynthesis

PCB is predominantly found in cyanobacteria and certain types of algae, emerging from the breakdown of phycocyanin. The *Arthrospira* genus, commonly known as *Spirulina*, is a primary natural source of PCB (Mysliwa-Kurdziel and Solymosi, 2017; Sonani et al., 2016). However, extracting PCB from *Spirulina* presents significant challenges. The cyanobacterium's complex cell wall structure and the presence of contaminants often result in low PCB yields, complicating the extraction process and inflating costs (Mysliwa-Kurdziel and Solymosi, 2017). To enhance PCB production, various cultivation methods, including photoautotrophic, mixotrophic, and heterotrophic techniques have been examined (Sonani et al., 2016). Despite these efforts, there is a notable lack of metabolic engineering applications for these native PCB producers. This deficiency could largely be due to the complexities associated with manipulating *Spirulina*. These include challenges like the presence of multiple light-harvesting pigments and a scarcity of sophisticated molecular tools for genetic manipulation. This situation suggests the need for advanced techniques and strategies to effectively harness and optimize PCB production from natural sources like *Spirulina*.

In the search for alternative production methods, *E. coli* has shown promise as a heterologous host for PCB biosynthesis. A landmark achievement was the successful integration of the entire PCB biosynthesis pathway from *Synechocystis* sp. PCC6803 into *E. coli* (Mukougawa et al., 2006; Tooley et al., 2001). These initial reports did not specify yields. Subsequent work achieved a PCB yield of approximately 0.3 mg/L with over 95% purity in *E. coli* engineered with cyanobacterial HO1 and PcyA, enhanced by adding 1 mM 5-ALA (Ge et al., 2013). This same team later boosted PCB production to 6.64 mg/L (Ge et al., 2018), the highest yield reported so far. Meanwhile, mammalian cells have also been engineered to produce PCB, albeit in lower titers of 2 μ M (Müller

et al., 2013) and 2.5 μM (Uda et al., 2017), by introducing PcyA and HO1 from *Synechocystis sp.* PCC6803. While these are pioneering efforts in PCB production using heterologous hosts, the reported yields are currently too low for industrial-scale production. This underscores the need for further metabolic engineering to enhance PCB yields significantly.

2.9.5 Advances and challenges in phycoerythrobilin biosynthesis

Efficient production of PEB faces significant challenges, including isolating it from other algal pigments and its sensitivity to environmental factors like light and oxygen, necessitating creative stabilization methods. Traditional PEB extraction is laborious, typically involving boiling red algal cells in methanol and subsequent liquid chromatography purification (Cornejo et al., 1992). Current research is focused on developing innovative purification techniques, such as advanced chromatographic methods, and engineering microbial strains for enhanced PEB production. Notably, two pioneering studies achieved PEB synthesis in *E. coli*: one using HO1, PebA, and PebB from cyanobacteria (Mukougawa et al., 2006), and the other employing HO1 from cyanobacteria with PebS from cyanophages, reaching a yield of 5.02 mg/L in a 2L batch bioreactor by supplementing 1 mM glutamate and 1 mM 5-ALA (Stiefelmaier et al., 2018). While there have been substantial strides in the microbial production of PEB, the path ahead is still challenging. The yield remains below what is needed for large-scale industrial use. The field urgently requires innovative metabolic engineering and the exploration of alternative microbial hosts to fully exploit the production potential of this valuable pigment.

2.9.6 Promising applications of biliverdin, PCB, and PEB

Biliverdin offers a wide array of therapeutic potentials. Its formidable antioxidant characteristics, along with its established biosafety profile, have catapulted it to prominence in medical research. Numerous studies highlighted its antiviral efficacy, showcasing promise in combating diverse viral diseases agents (Gutiérrez-Grobe et al., 2016; Lehmann et al., 2010; Zhu et al., 2010). Additionally, a sequence of clinical trials has validated its capacity to alleviate lung graft injuries, indicating its viable application in transplant medicine (Kosaka et al., 2013; Sugimoto et al., 2012; Tian et al., 2017; Wang et al., 2010; Zhou et al., 2011). In oncology, biliverdin has emerged as a diagnostic and therapeutic nanoagent, with initial investigations pointing towards its potential in targeted cancer treatments (Xing et al., 2019). Furthermore, its anti-inflammatory properties are being utilized to treat chronic inflammatory diseases, providing a glimmer of hope for patients with conditions such as rheumatoid arthritis and inflammatory bowel disease (Bai et al., 2015; Baylor and Butler, 2019; Overhaus et al., 2006; Tian et al., 2017).

Apart from its direct therapeutic applications, the role of biliverdin as a precursor in the synthesis of PCB and PEB is pivotal. These compounds, with their broad applications in the medical, cosmetic, and food industries, have escalated the demand for biliverdin to new heights (Mysliwa-Kurdziel and Solymosi, 2017). The exploration of biliverdin's near-infrared (NIR) absorption capabilities has unlocked new possibilities in medical imaging, with researchers optimistic about its application in real-time tumor tracking and other in vivo imaging techniques (Filonov et al., 2011; Piatkevich et al., 2013; Shcherbakova et al., 2015; Shcherbakova and Verkhusha, 2013).

PCB is making waves in the colorant industry. As consumer awareness regarding the environmental and health implications of synthetic dyes grows, PCB emerges as a sustainable and

safe alternative. Endorsed by the FDA (Stanic-Vucinic et al., 2018), PCB's use has proliferated across various consumable products (Chakdar and Pabbi, 2016). In addition to its application in food, the cosmetic industry is rapidly adopting PCB, utilizing it in an array of products from lipsticks to eyeshadows, as they shift towards natural and safe ingredients (Eriksen, 2013; Joshi et al., 2018; Morone et al., 2019; Mourelle et al., 2017). In the medical field, research is ongoing into PCB's potential therapeutic properties, particularly its antioxidant capabilities (McCarty, 2007; McCarty et al., 2010; Pentón-Rol et al., 2016; Zheng et al., 2012). It is also under optimization for fluorescence labelling and optoacoustic imaging (Ge et al., 2018; Rodriguez et al., 2016; Wang et al., 2019).

Similarly, phycoerythrobilin (PEB) is establishing its place in the natural colorant market. Its rich pink color is highly desired in the food industry, particularly in products targeting the health-conscious demographic. The cosmetic industry, ever-evolving and in search of innovative ingredients, has started to incorporate PEB into their premium product lines (Chakdar and Pabbi, 2016; Mysliwa-Kurdziel and Solymosi, 2017). Furthermore, in medical settings, PEB is being explored for advanced imaging techniques, especially in fluorescence labeling, with encouraging early findings (Ge et al., 2018; Rodriguez et al., 2016; Wang et al., 2019).

2.10 Cell free metabolic engineering (CFME)

Cell-Free Metabolic Engineering (CFME) is a groundbreaking approach in metabolic engineering that circumvents the traditional limitations of cellular structures. This method utilizes cell lysates, which, free from intact cellular membranes, facilitate the efficient coordination of complex enzymatic processes and metabolic pathways (Garcia et al., 2021; Lim and Kim, 2019; Rasor et al., 2021). The concept of CFME can be traced back to the late 1950s and early 1960s, when

researchers first used cell-free systems to deconstruct the complexities of synthesizing proteins (Hoagland, 1960; Nirenberg and Matthaei, 1961), lipids (Dils and Popják, 1962; Tietz, 1961), and hemoglobin (Schweet et al., 1958), laying the groundwork for future innovations. Over the past decades, bolstered by rapid advancements in molecular biology, biotechnology, and systems biology, CFME has evolved into a sophisticated and adaptable tool. It allows for the exploration of metabolic pathways without the typical constraints of living cells, such as energy requirements for cell maintenance, competition from other metabolic pathways, and product toxicity (Garcia et al., 2021; Lim and Kim, 2019; Rasor et al., 2021). This development marks a significant leap forward in the ability to study and manipulate metabolic pathways.

In recent years, the popularity of CFME has surged, primarily due to its versatility and ability to synthesize a wide range of high-value compounds, including pharmaceuticals and biofuels (Garcia et al., 2021; Grubbe et al., 2020; Lim and Kim, 2019; Rasor et al., 2021). This growing interest is further bolstered by CFME's suitability for rapid prototyping and iterative optimization, which are often challenging in living systems. Moreover, CFME enables real-time monitoring and control of biochemical reactions, providing a level of precision in metabolic engineering that is unprecedented (Garcia et al., 2021; Grubbe et al., 2020; Lim and Kim, 2019; Rasor et al., 2021). As global demand for sustainable and efficient production of bio-based chemicals and therapeutics increases, CFME emerges as a particularly promising platform. Its potential to significantly influence the future of metabolic engineering and synthetic biology is well recognized (Lim and Kim, 2019; Rasor et al., 2021). This advancement positions CFME at the forefront of innovation in the field.

2.10.1 Advantages of CFME over whole-cell metabolic engineering (WCME)

CFME has revolutionized the field of metabolic engineering, offering a plethora of advantages that challenge the capabilities of traditional whole-cell metabolic engineering (WCME). Central to CFME's growing appeal is its ability for rapid prototyping, a stark contrast to the often slow and complex processes seen in WCME, involving cellular transformation and growth phases. This approach allows for quick assembly and evaluation of metabolic pathways, significantly expediting research (Koch et al., 2018; Moore et al., 2017). CFME also operates outside the typical cellular environment, offering unrestricted access to enzymes and metabolic pathways and bypassing the toxicity issues that some compounds pose to living cells. This aspect facilitates smoother experimentation and analysis. Additionally, the *in vitro* nature of CFME grants researchers unprecedented control over reaction conditions like pH, temperature, and substrate concentration, enabling precise optimization for maximum yield and effective handling of sensitive compounds (Carlson et al., 2012; Grubbe et al., 2020; Lim and Kim, 2019; Rasor et al., 2021; Wilding et al., 2018). Beyond rapid prototyping and precision, CFME excels in reproducibility and customization. The flexibility of CFME systems allows researchers to tailor reaction environments to specific needs, such as selecting specific enzymes or eliminating inhibitory components, broadening the scope of metabolic engineering (Carlson et al., 2012; Rasor et al., 2021; Wilding et al., 2018). Overall, CFME, with its array of benefits, is poised to redefine the future of metabolic engineering, establishing itself as an invaluable tool in contemporary metabolic research and applications.

2.10.2 Challenges and limitations of CFME

While CFME offers groundbreaking potential in metabolic engineering, it faces several inherent challenges. Scalability is a primary concern; while CFME is efficient in the lab, expanding these processes to industrial levels introduces significant complexities. Finding the right balance between productivity, yield, and efficiency in this upscaling is a focus of current research (Claassens et al., 2019; Liu et al., 2023; Perez et al., 2016; Rasor et al., 2021; Wilding et al., 2018). Another critical issue is the stability of CFME systems. Without cellular protection, they are vulnerable to enzymatic degradation, impacting their long-term stability. Developing advanced stabilization techniques to enhance shelf-life and robustness is therefore essential (Garcia et al., 2021; Liu et al., 2023; Rasor et al., 2021; Wilding et al., 2018). Additionally, the economic aspects, especially the costs of high-quality cell-free extracts and specialized reagents, present considerable challenges. These costs need careful management to ensure CFME's commercial viability and broader adoption (Garcia et al., 2021; Liu et al., 2023; Rasor et al., 2021; Wilding et al., 2018). Therefore, to fully realize CFME's potential and integrate it successfully into the biotechnological landscape, a collaborative approach involving research, technological innovation, and strategic planning is critical.

Chapter 3

A temperature switch: an efficient strategy to turn on *Y. lipolytica*'s mannitol and amino acids production

3.1 Introduction

Y. lipolytica, a non-conventional yeast, has garnered considerable prominence in the field of metabolic engineering owing to its unique metabolic capabilities and robustness in biomanufacturing high-value compounds biomanufacturing (Park and Ledesma-Amaro, 2023; Zhu and Jackson, 2015). Its versatility is exemplified by its ability to efficiently utilize a wide array of substrates, including glucose, acetate, glycerol, and lipids, positioning it as an invaluable asset in industrial applications (Park and Ledesma-Amaro, 2023; Zhu and Jackson, 2015). Recognized as a Generally Recognized As Safe (GRAS) organism, *Y. lipolytica* is particularly suitable for use in food and pharmaceutical industries. The yeast's intrinsic metabolic pathways are well-suited for producing lipids (Blazeck et al., 2014; Qiao et al., 2015; Zeng et al., 2018), organic acids (Cavallo et al., 2017; Papanikolaou et al., 2002b), and polyols (Egermeier et al., 2017; Jagtap et al., 2021; Tomaszewska et al., 2012), enhancing its desirability as a host for metabolic engineering (Turner & Patel, 2018). Additionally, its genetic malleability facilitates the optimization of these pathways (Gao et al., 2018; Holkenbrink et al., 2018; Larroude et al., 2020; Schwartz et al., 2019; Schwartz et al., 2017a; Schwartz et al., 2017b; Schwartz et al., 2016), thereby improving the yield and variety of producible compounds. These characteristics not only highlights its potential for the efficient production of biochemicals and biofuels but also demonstrates its role in waste valorization and the creation of renewable bioresources.

Environmental factors, particularly pH and temperature, play crucial roles in the growth and metabolism of *Y. lipolytica*. This adaptability is evident across different pH levels, where *Y. lipolytica* demonstrates enhanced mannitol synthesis under lower pH conditions (Egermeier et al., 2017). Understanding the metabolic flexibility of this yeast to pH fluctuation is vital for optimizing bioprocesses, as this factor directly influences the yield and quality of the desired products. Temperature, another key environmental factor, not only affects *Y. lipolytica*'s growth rate but also significantly impacts its metabolic pathways (Hackenschmidt et al., 2019). The yeast typically thrives within a temperature range of 25-30°C (Madzak, 2021), yet its response to elevated temperatures, especially concerning different feedstocks and overall metabolic output, remains insufficiently explored. Moreover, there is a noticeable gap in detailed transcriptional profiling to elucidate how temperature variations affect metabolic pathways, particularly those involved in mannitol and amino acid production. Addressing these gaps is essential for harnessing *Y. lipolytica*'s full biotechnological potential.

Therefore, this dissertation chapter focuses on bridging research gaps concerning the effects of elevated temperatures on *Y. lipolytica*'s growth and metabolism. Central to the study is assessing how increased temperatures impact the yeast's growth dynamics when using various feedstocks, aiming to provide a comprehensive understanding of its metabolic adaptability under thermal stress. Investigating how elevated temperatures affect metabolite synthesis and lipid content is crucial, as these insights will shed light on the thermal modulation of metabolic pathways, a key factor in optimizing industrial bioprocesses. Additionally, the study will explore the specific impact of higher cultivation temperatures on *Y. lipolytica*'s production of mannitol and amino acids. This aspect is particularly important for enhancing the yeast's utility in biomanufacturing applications, where efficient and economically viable production processes are paramount.

Understanding these temperature-induced metabolic shifts will contribute significantly to the advancement of biotechnological applications involving *Y. lipolytica*.

Furthermore, this dissertation aims to strategically enhance mannitol production in *Y. lipolytica* by genetically manipulating its mannitol synthesis pathway, particularly under elevated temperature conditions. Targeted genetic modifications are expected to significantly increase the efficiency and cost-effectiveness of bioproduction processes using this yeast. Additionally, the study encompasses detailed transcriptional profiling to elucidate the metabolic pathway shifts resulting from temperature variations. This in-depth analysis is crucial for a deeper understanding of *Y. lipolytica*'s molecular response to thermal stress, providing valuable insights for both current and future applications in metabolic engineering and industrial bioprocessing. By advancing our knowledge of *Y. lipolytica*'s metabolic dynamics under different temperature conditions, this research will not only contribute to optimizing bioproduction processes but also pave the way for future innovations in biotechnological industries.

Hypothesis and objectives of this chapter:

Hypothesis: Subjecting *Y. lipolytica* to elevated cultivation temperatures is hypothesized to result in notable changes in its growth dynamics and metabolic response. These changes are expected to be influenced by the type of feedstock used, suggesting a link between substrate and the yeast's adaptive mechanisms under thermal stress. Higher temperatures are anticipated to significantly enhance the production of mannitol and amino acids and cause variations in lipid content. These metabolic alterations are likely to be accompanied by distinct transcriptional shifts, indicative of *Y. lipolytica*'s adaptation to the changed temperature conditions. Moreover, it is hypothesized that specifically targeting and manipulating the mannitol synthesis pathway at elevated temperatures

will lead to an increased production of mannitol. The study aims to thoroughly map and understand these metabolic and transcriptional changes through comprehensive transcriptional profiling, providing new insights into how *Y. lipolytica*'s metabolic pathways are affected by temperature variations.

Objectives:

1. Assess the impact of elevated temperatures on *Y. lipolytica*'s growth characteristics when utilizing a variety of feedstocks, including glucose, acetate, glycerol, and soybean oil.
2. Investigate the metabolic flexibility of *Y. lipolytica* under conditions of elevated temperature, focusing on its capacity to modify metabolic pathways in response to thermal stress.
3. Examine the changes in the synthesis of key metabolites and alterations in lipid content in *Y. lipolytica* when exposed to higher temperatures, to understand the metabolic shifts induced by thermal variations.
4. Analyze the specific effects of increased cultivation temperatures on the metabolic production of mannitol and amino acids in *Y. lipolytica*.
5. Engineer the mannitol synthesis pathway in *Y. lipolytica* to further augment mannitol production, particularly under conditions of elevated temperature, thereby improving the overall efficiency of the biosynthesis process.
6. Conduct a detailed transcriptional profiling of *Y. lipolytica* under varied temperature conditions to map and understand the temperature-mediated shifts in metabolic pathways, with a focus on linking these changes to observed alterations in metabolite production.

3.2 Materials and methods

3.2.1 Chemicals and Enzymes

Chemicals used in this study were obtained from Sigma-Aldrich unless otherwise stated. Phusion™ High-Fidelity DNA Polymerase, the Quick Ligation™ Kit and NEBuilder® HiFi DNA Assembly Master Mix were purchased from New England Biolabs (NEB, Canada). Plasmid mini-preps were performed using the EZ-10 Spin Column Plasmid DNA Miniprep Kit (Biobasics, Canada). PCR and gel clean-ups were performed using the QIAquick PCR & Gel Cleanup Kit (Qiagen). Oligonucleotides and guide RNA were purchased from either IDTDNA.

3.2.2 Strains and culture maintenance

Pog1 strain of *Y. lipolytica*, a derived from wild-type strain W29 (ATCC 20460) was acquired from Yeastern Biotech. This strain underwent a series of genetic modifications from the original strain W29 and characterized by its genotype as *MatA*, *leu2-270*, *ura3-302::URA3*, *xpr2-332*, *axp-2*. The W29 strain was chosen due to its well-documented genetic background and its amenability to genetic manipulation. Over the years, W29 has been the subject of numerous studies, making it a reliable reference point for our experiments. Additionally, its genome has been fully sequenced, providing a comprehensive genetic map that aids in the design and verification of CRISPR targets. Plasmid propagation was performed using *E. coli* HI-Control™ 10G chemically competent cells (Lucigen; WI).

For the initial cultivation of *Y. lipolytica* strains, the Yeast Extract Peptone Dextrose (YPD) medium was employed, which comprises 1% yeast extract, 2% peptone, and 2% dextrose. Synthetic Defined (SD) medium, containing 0.67% yeast nitrogen base without amino acids and

2% dextrose, was utilized for the selection and maintenance of transformants. For the selection of *LEU2* transformants, the Yeast Nitrogen Base (YNB) medium was used, which is devoid of Lucine and contains 0.67% yeast nitrogen base, 2% dextrose, and appropriate drop-out supplements. Additionally, the Lysogeny Broth (LB) medium, containing 1% tryptone, 0.5% yeast extract, and 1% NaCl, was employed for cultivating *E. coli* strains that harbored the CRISPR plasmids. To prepare solid media, agar was incorporated at a concentration of 2%. For the selection of transformants, the media were supplemented with the appropriate antibiotics for *E. coli* at the recommended concentrations. All media were adjusted to a pH of 6.5, either with HCl or NaOH, and sterility was maintained by autoclaving the media at 121°C for 20 minutes.

Regarding culture conditions, unless described, *Y. lipolytica* cultures were typically maintained at 30°C with an agitation rate of 200 rpm to ensure optimal growth and aeration. The inoculum was prepared by inoculating a single colony of *Y. lipolytica* from a freshly streaked plate into 5 mL of YPD medium, which was then grown overnight. This pre-culture served as the basis to inoculate larger volumes for subsequent experiments.

3.2.3 Transformation of *E. coli* and *Y. lipolytica*

The transformation of *E. coli* was carried out using *E. coli* HI-Control™ 10G chemically competent cells. The process began by mixing a small quantity of plasmid DNA (1-5 ng) with 50 µl of competent cells in a chilled microcentrifuge tube. This mixture was then incubated on ice for 30 minutes. After this period, the tube underwent a heat shock treatment in a 42°C water bath for precisely 45 seconds, followed by immediate cooling on ice for 2 minutes. Next, 950 µl of pre-warmed LB medium was added to the mixture, and the cells were incubated at 37°C with continuous shaking at 280 rpm for 1 hour. This step facilitated recovery and expression of the

antibiotic resistance marker. Finally, the transformed cells were spread onto LB agar plates containing the appropriate antibiotic and incubated overnight at 37°C to promote colony growth.

The transformation of *Y. lipolytica* was conducted using the Fast Yeast Transformation™ kit from G-Biosciences. Mid-log phase *Y. lipolytica* cells were first harvested and washed using the kit's wash buffer. The cells were then resuspended in the kit's transformation buffer, to which 1 µg of the desired plasmid DNA and the provided carrier DNA were added. This mixture was incubated at room temperature for 20 minutes. Subsequently, the Fast Yeast Transformation Reagent™ from the kit was introduced to the mixture, which was then incubated for an additional 20 minutes at room temperature. Following this, the cells underwent a 40-minute heat shock at 42°C. Post heat shock, the cells were centrifuged, and the resultant pellet was resuspended in YPD medium for a recovery period of 2 hours at 30°C with gentle shaking. The final step involved plating the transformed *Y. lipolytica* cells onto selective media and incubating them at 30°C. Colonies typically appeared within 2-3 days.

3.2.4 Plasmid isolation protocol

Plasmid DNA was extracted from bacterial cultures using the EZ-10 Spin Column Plasmid DNA Miniprep Kit (Biobasics, Canada) according to the manufacturer's instructions. Briefly, a single *E. coli* colony harboring the target plasmid was cultured overnight in 5 mL LB broth with the appropriate antibiotic at 37°C, with shaking. Post incubation, cells were centrifuged and resuspended in Resuspension Buffer (Solution I), followed by lysis using Lysis Buffer (Solution II), and neutralization with Neutralization Buffer (Solution III). The lysate was then centrifuged, and the supernatant carefully transferred to an EZ-10 spin column for purification. After washing the column twice with Wash Buffer, the plasmid DNA was eluted with Elution Buffer or sterile

distilled water. The eluted DNA was stored at -20°C for long-term usage or at 4°C for immediate use, and its quality and quantity were assessed using Nanodrop.

3.2.5 PCR amplification and PCR and gel clean-ups

For PCR amplification, the Phusion™ High-Fidelity DNA Polymerase from New England Biolabs (NEB Canada) was employed. Reaction mixtures were set up as follows: 1x Phusion HF buffer, 200 µM of each dNTP, 0.5 µM of forward and reverse primers, 0.02 U/µl Phusion DNA polymerase, and approximately 10 ng of template DNA in a total volume of 50 µl. The thermocycling conditions typically commenced with an initial denaturation at 98°C for 30 seconds, followed by 30 cycles of denaturation at 98°C for 10 seconds, annealing (temperature dependent on the primers used) for 30 seconds, and extension at 72°C (time dependent on the expected amplicon size). A final extension step at 72°C for 10 minutes was included to ensure complete amplification.

For colony PCR, a single bacterial or yeast colony was picked using a sterile pipette tip and resuspended in 20 µl of sterile distilled water. This suspension was then boiled for 10 minutes to lyse the cells and release the DNA. After a brief centrifugation, 2 µl of the supernatant was used as a template for the PCR, with the aforementioned Phusion™ High-Fidelity DNA Polymerase protocol. This method allowed for rapid screening of bacterial colonies for the presence of the desired plasmid constructs.

For PCR and gel clean-ups, the QIAquick PCR & Gel Cleanup Kit (Qiagen) was utilized. Following PCR amplification and confirmation of products via agarose gel electrophoresis, the PCR products were mixed with Buffer PB (5 volumes to 1 volume of PCR sample) and applied to a QIAquick spin column for centrifugation. Post-centrifugation, the flow-through was discarded,

and the column was washed with Buffer PE. For gel extractions, DNA bands were excised from the agarose gel, dissolved in Buffer QG with isopropanol, and then subjected to the same column-based purification process. The DNA was then eluted from the column with Buffer EB or water, and its concentration and purity were assessed using spectrophotometric methods. This streamlined process ensured efficient purification of PCR products and gel-extracted DNA, suitable for various downstream molecular biology applications.

3.2.6 Plasmid construction

For the overexpression of the *FBP1* gene, the integrative pYLEX1 plasmid, sourced from Yeastern Biotech, was employed. This plasmid, specifically chosen for its compatibility with the *Y. lipolytica* Po1g strain, operates under the control of a strong hybrid hp4d promoter. The initial step in the construction process involved the double digestion of this plasmid using PmII and KpnI restriction enzymes. Concurrently, the *FBP1* gene was PCR-amplified from the genomic DNA of the Po1g strain. This amplification used Phusion™ High-Fidelity DNA Polymerase from NEB, Canada, and was facilitated by two specially designed primers: the forward primer Y_FBP1_F1 (5'- GCGATCCACGTG gccgccaccATGGAAGCCAACCCCGAA-3') and the reverse primer Y_FBP1_R1 (5'- CTACGCGGTACC CGTCTCTTGGCCTCTGGTTC-3'), which included the respective PmII and KpnI enzyme recognition sites. Following amplification, the PCR product and the digested plasmid were ligated using the Quick Ligation™ Kit (NEB, Canada). The resultant plasmid was then introduced into *E. coli* HI-Control™ 10G chemically competent cells (Lucigen; WI) through heat shock transformation method.

For the knockout of the *FBP1* gene, a different approach was taken using the pCRISPRyl plasmid from Addgene (<https://www.addgene.org/70007/>). This foundational plasmid is equipped

with a codon-optimized Cas9 and a LEU marker for *Y. lipolytica*. It also features Pol III-tRNA hybrid promoters that drive sgRNA expression. A 20-nucleotide guide RNA sequence targeting the *FBPI* gene (FBP1gRNA297: 5' GGTGGTGTCCGAGGAGCAGG-3') was designed using the Chop-Chop online tool (<https://chopchop.cbu.uib.no>). The pCRISPRy1 vector was first linearized using the AvrII restriction enzyme. The gRNA sequences, along with the necessary homology sequences for cloning, were annealed and assembled into the linearized vector using the NEBuilder® HiFi DNA Assembly Master Mix. The assembled plasmid was transformed into *E. coli* HI-Control™ 10G chemically competent cells, and following transformation, the plasmids were purified and subjected to sequencing for validation of the constructs. Upon confirmation of the correct sequence, the Po1g strain was transformed with the plasmid to achieve the knockout of the *FBPI* gene. The transformed cells were then plated on SD-LEU plates to select for successful transformants, leading to the development of colonies that had the *FBPI* gene successfully knocked out.

3.2.7 Shake flask fermentation

In our shake flask cultivation method, the initial overnight culturing of Po1g strain was performed in 5 ml of YPG medium. The flasks were incubated at 30°C with continuous shaking at 200 rpm to ensure optimal growth conditions. Subsequently, 1% of this overnight culture was inoculated into fresh 150 ml of YPG medium. This seed culture was maintained under the same shaking conditions until the optical density at 600 nm (OD₆₀₀) reached between 0.7 and 0.9, indicating an appropriate cell density for subsequent experiments. Upon reaching this density, cells were harvested through centrifugation at 8000 rpm for 5 minutes. The collected cells were then equally divided into two parts to create duplicate samples for consistent data analysis. Each of these

samples was inoculated into a 10 ml rich medium, distinctively supplemented with one of the following carbon sources: 30g/L glucose, 30g/L glycerol, 30 g/L acetate, or 30g/L soybean oil. This step was essential for investigating the metabolic versatility of the Po1g strain. The cultivation was then continued under shaking conditions at 200 rpm, but at varied fermentation temperatures of 30°C, 34°C, and 37°C, to assess the temperature-dependent growth and metabolic profiles. The duration of this fermentation phase was set to 40 hours, allowing sufficient time for the cells to metabolize the respective substrates and exhibit discernible growth and production characteristics.

3.2.8 Analytical methods: HPLC and NMR

To accurately determine mannitol levels, culture samples were first diluted with a 0.15 M saline solution and their cell density measured at OD₆₀₀ using a Beckman Coulter DU520 spectrophotometer. The samples were then centrifuged at 8,000×g for 10 minutes and filtered through a 0.2µm syringe filter to obtain a cell-free medium. Mannitol and other extracellular metabolites were quantified using High-Performance Liquid Chromatography (HPLC), employing a Shimadzu LC-10AT system with an Aminex HPX-87H column from Bio-Rad Laboratories, optimized for organic acids. The HPLC system maintained the column at a steady 35°C and used a mobile phase of 5 mM H₂SO₄ at a flow rate of 0.6 mL/min. Mannitol was detected with a Refractive Index Detector (RID-10A, Shimadzu), suitable for non-UV reactive compounds. Concentrations were determined against a calibration curve created from known mannitol standards, with data acquisition and analysis conducted using Clarity Lite software from DataApex.

For the NMR-based determination of mannitol, amino acids, and organic acids, cell-free media derived from shake flask cultures of *Y. lipolytica* were used. Samples were first centrifuged

at 8,000×g for 10 minutes, followed by filtration through a 0.2 µm syringe filter to remove any remaining particulates. The procedure, in line with Sokolenko *et al.*, (2014), involved enriching 630 µL of the supernatant with 70 µL of an internal NMR standard containing 99.9% D₂O, 5 mM DSS, and 0.2% w/v sodium azide, sourced from Chenomx Inc., Edmonton, Canada. The mixture was thoroughly vortexed and transferred to a 5 mm NMR tube for analysis. NMR spectra were captured using a Bruker Avance 600.13 MHz spectrometer with a triple resonance probe, employing a NOESY pulse sequence with a 1s pre-saturation pulse, 100ms mixing time, and a 4s acquisition duration (Sokolenko *et al.*, 2014). Spectral processing and compound quantification were performed in the Chenomx NMR Suite 8.4, involving manual phase and baseline corrections, line asymmetry correction, and quantification against the 600 MHz library using DSS as the internal standard. Additional information on this targeted profiling is available on Chenomx's website (<http://www.chenomx.com/>).

3.2.9 Spectrophotometric sulfo-phospho-vanillin (SPV) lipid quantification

Spectrophotometric methods have been widely employed for lipid quantification due to their rapidity and precision. In this study, lipid quantification in samples was achieved using the sulfo-phospho-vanillin (SPV) reaction, which involves the formation of a chromogenic complex between lipids and vanillin in the presence of sulfuric acid. Briefly, lipid extracts were mixed with concentrated sulfuric acid and incubated at 100°C for 10 minutes. After cooling to room temperature, vanillin reagent was added, and the mixture was incubated for an additional 5 minutes. The absorbance of the resulting pink-colored complex was measured spectrophotometrically at 530 nm. The lipid content was then determined by comparing the absorbance values to a standard curve generated using known concentrations of a reference lipid.

This SPV-based method offers a reliable and reproducible means to quantify lipids in diverse samples (Mishra et al., 2014). For lipid quantification using this method, *Y. lipolytica* cells were cultivated in duplicates in 30 mL YPG at 30 °C, 34 °C and 37°C and 200 rpm until they reached the exponential growth phase (0.8OD₆₀₀). Post incubation, cells were harvested by centrifugation 8,000×g for 10 minutes and subjected to SPV assay.

3.2.10 RNA extraction

For RNA extraction, *Y. lipolytica* cells were cultivated in triplicate in 30 mL YPG at 30 °C, 34 °C and 37°C and 200 rpm until they reached the exponential growth phase (0.8OD₆₀₀). Post incubation, cells were harvested and subjected to RNA isolation using the High Pure RNA Isolation Kit from Roche Diagnostics, Basel, Switzerland. Adhering to the manufacturer's guidelines, cells were first lysed using the provided lysis buffer, ensuring complete disruption. This was followed by the addition of a binding buffer, which facilitated the binding of RNA to the silica membrane of the column provided in the kit. Any potential contaminants, including proteins and genomic DNA, were efficiently washed away using the wash buffers. Finally, RNA was eluted in a low salt elution buffer, ensuring the recovery of high-quality, intact RNA. The concentration and purity of the extracted RNA were determined using a NanoDrop spectrophotometer, while the integrity was assessed using an Agilent 2100 Bioanalyzer. RNA sequencing was then performed using these samples by Novogene.

3.2.11 Differential expression analysis

For RNA sequencing and differential expression (DE) analysis, raw sequence reads, as provided by the Novogene service, were subjected to quality control measures. The cutadapt program (Martin, 2011) was employed to trim and filter these reads, utilizing its default settings. Subsequently, the processed reads were aligned to the reference genome of *Y. lipolytica* CLIB122 (NCBI Assembly ID GCF_000002525.2) using the HISAT2 tool, adhering to its standard parameters (Kim et al., 2015). To obtain raw counts for the annotated genes, the featureCounts software was utilized (Liao et al., 2014). These counts were then channeled into the DESeq2 platform for differential expression analysis, again employing default settings (Love et al., 2014). For visualization purposes, z-scores were derived from the regularized log-transformed expression counts generated by DESeq2, facilitating a comprehensive representation of the data across samples. Genes with an adjusted p-value < 0.05 and a log₂ fold change > 1 or < -1 were deemed differentially expressed.

3.2.12 Gene Ontology (GO) enrichment analysis

For the *Y. lipolytica* CLIB122 genome, GO annotations were sourced from the QuickGO database hosted by EMBL-EBI, referencing the data as of October 27, 2018 (Binns et al., 2009). These annotations facilitated the identification of gene sets associated with specific GO terms. Utilizing the piano R package (Våremo et al., 2013), we pinpointed GO term sets, each encompassing a minimum of five genes, that exhibited significant enrichment among the top-ranking upregulated and downregulated genes. This determination was based on the FDR-adjusted P-values and log₂ fold-changes derived from the DESeq2 analysis. To rank the GO sets, we employed the median consensus score from gene set analyses, incorporating methods such as 'mean', 'fisher', 'stouffer',

'reporter', and 'tailStrength'. The analysis primarily highlights the top 50 GO term sets for each evaluated growth condition.

3.2.13 Data visualization

Data visualization aids in the interpretation and communication of complex datasets. For this study, various R packages were employed. The pheatmap package was used to generate heatmaps of differentially expressed genes, providing a visual representation of gene expression patterns across samples. Volcano plots and MA plots, created using ggplot2, offered a graphical view of the significance versus fold-change of the expressed genes. Additionally, Principal Component Analysis (PCA) was conducted to visualize the overall variance between samples, ensuring that temperature treatments were the primary source of variation.

3.3 Results

3.3.1 *Y. lipolytica* growth: a temperature and feedstock analysis

Exploring microbial growth dynamics is crucial in both academic research and industrial applications, as it can enhance production methods, improving productivity and efficiency. Yeasts typically grow best around 30°C but understanding the growth variations of specific strains like *Y. lipolytica* under different temperatures is vital for biomanufacturing. Our research focused on the effects of cultivating *Y. lipolytica* at varied temperatures (30°C, 34°C, and 37°C) using different feedstocks. We adhered to shake flask fermentation protocols established in our lab, starting with an optical density (OD₆₀₀) of 5.8 and recording data at 20 and 40-hour intervals to ensure accurate and consistent results.

Glycerol, commonly a byproduct in various industrial processes, serves as an intriguing carbon source for studying *Y. lipolytica's* growth. When grown on 30 g/L glycerol at different temperatures, distinct growth patterns emerged (Figure 3.1A). Over 40 hours, the yeast showed a consistent increase in cell density at 30°C, peaking at an OD₆₀₀ of 29.29 ± 1.42 , indicating favorable growth conditions. In contrast, at 34°C, growth was more modest, with OD₆₀₀ values reaching only 19.57 ± 0.69 . At 37°C, the growth was significantly less, with OD₆₀₀ readings of just 11.32 ± 0.51 , suggesting this temperature is suboptimal for *Y. lipolytica's* growth on glycerol.

When cultivated on glucose (30 g/L) as a carbon source, *Y. lipolytica* exhibited distinct growth patterns at different temperatures (Figure 3.1B). At 30°C, there was a consistent upward trend in growth, with cell density reaching an OD₆₀₀ of 29.45 ± 1.34 after 40 hours, matching typical yeast growth on glucose. However, at 34°C, growth dynamics altered, with OD₆₀₀ values indicating moderate growth at 19.92 ± 1.22 . The challenging conditions at 37°C impacted growth

even with glucose as the feedstock, resulting in significantly lower OD₆₀₀ values of just 11.21 ± 1.11.

Using 30 g/L acetate as a feedstock for *Y. lipolytica* yielded different growth results (Figure 3.1C). At 30°C, the yeast showed rapid growth in the initial 20 hours, reaching an OD₆₀₀ of 19.10 ± 1.13, but then the growth rate plateaued. At higher temperatures of 34°C and 37°C, the growth patterns were somewhat similar, displaying modest early growth but stabilizing at OD₆₀₀ values of 11.55 ± 0.35 and 9.99 ± 0.54, respectively. This suggests that while *Y. lipolytica* can effectively utilize acetate at the optimal temperature of 30°C, its metabolic efficiency is challenged at elevated temperatures with acetate as the carbon source.

In the examination of 30 g/L soybean oil as a carbon source for *Y. lipolytica*, distinct growth behaviors were observed (Figure 3.1D). At 30°C, the yeast exhibited vigorous growth, with a rapid increase in cell density peaking at an OD₆₀₀ of 34.62 ± 1.17 midway through the observation period. At 34°C, growth was steady, albeit slower, resulting in an OD₆₀₀ of 27.52 ± 2.02. Notably, at 37°C, after a slow start, a significant rise in OD₆₀₀ to 24.68 ± 0.94 was observed within 20 hours, indicating a possible metabolic adaptation by *Y. lipolytica* to assimilate soybean oil at this higher temperature.

This analysis of *Y. lipolytica*'s growth across various carbon sources and temperatures underscores the yeast's remarkable adaptability, highlighting the need to tailor growth conditions for enhanced bioprocessing yields. The data offer valuable quantitative insights into the yeast's physiological behavior, enhancing our understanding of its responses. This research significantly contributes to the broader knowledge of microbial growth dynamics and is particularly relevant for those in the field focusing on *Y. lipolytica*, a yeast of considerable industrial importance.

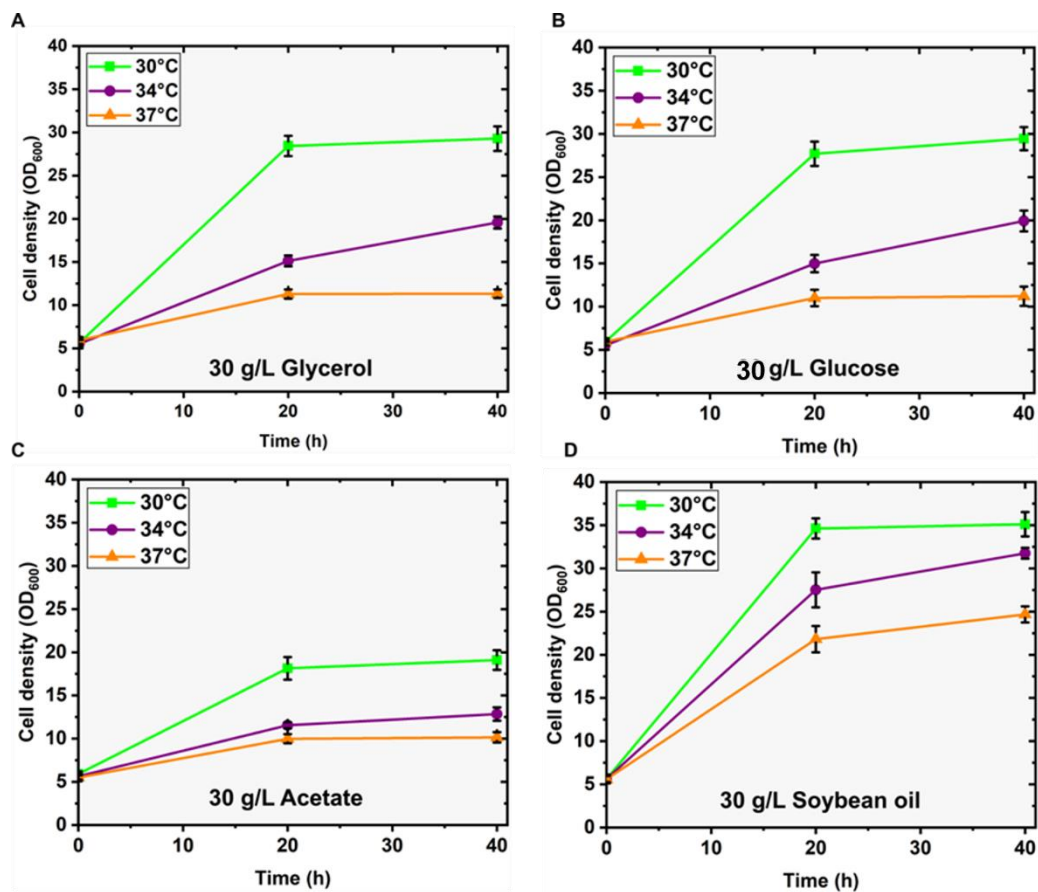


Figure 3.1 Detailed evaluation of the influence of varying temperatures on *Y. lipolytica* growth across distinct feedstocks. This figure depicts the progression of cell growth over time at three specific temperatures: 30°C, 34°C, and 37°C. Growth was monitored in shake-flask cultures supplemented with rich media containing the following feedstocks: (A) 30 g/L of glycerol, (B) 30 g/L of glucose, (C) 30 g/L of acetate, and (D) 30 g/L of soybean oil. The error bars present in the graph represent the standard deviations of duplicate experiments.

3.3.2 *Y. lipolytica*'s metabolic responses to temperature variations

Y. lipolytica's metabolic flexibility, particularly in regulating organic acids and lipids synthesis in response to pH variations, is well-documented. This prompted an exploration into the influence of temperature on its metabolic pathways. The experimental approach involved exposing *Y. lipolytica* cultures to temperatures of 30°C, 34°C, and 37°C, each eliciting distinct growth patterns. The variance from near-ambient 30°C to the higher thresholds of 34°C and 37°C provided insights into the organism's adaptability. Such knowledge is crucial for leveraging *Y. lipolytica*'s potential in industrial biotechnological applications, particularly in optimizing processes across different temperature ranges.

In our investigation, the initial use of HPLC offered a preliminary view of the metabolic changes in *Y. lipolytica* at various temperatures. To build on these insights, NMR was then employed, aiming to uncover shifts in carbon flux among primary metabolites under different temperature and substrate conditions. A notable observation emerged when analyzing the yeast's metabolic response to glycerol and soybean oil. Glycerol as a carbon source induced significant metabolic changes, especially at higher temperatures, while soybean oil-fed cultures showed minimal alterations under similar conditions (data not shown). This highlights *Y. lipolytica*'s metabolic pathway versatility and adaptability.

NMR results offered a deeper understanding of *Y. lipolytica*'s metabolic shifts when cultivated on glycerol at varying temperatures (Figure 3.2A). At elevated temperatures of 34°C and 37°C, a significant metabolic shift was observed, with over 60% and 77% of available carbon redirected towards the production of primary metabolites like amino acids, organic acids, and sugars, respectively. The detailed list of metabolites is presented in appendix 1. This contrasted with the base temperature of 30°C, where the yeast consumed these metabolites, as indicated by

the negative values in the graphical representation. Furthermore, considering *Y. lipolytica's* well-known lipid-accumulating behavior, we also investigated the impact of temperature on lipid production. Lipid content was determined using the reliable sulfo-phospho-vanillin (SPV) method, revealing a decrease in lipid accumulation with rising temperatures. The highest lipid content recorded was $4.98 \pm 0.25 \mu\text{g/ml}$ at 30°C , decreasing to $4.12 \pm 0.28 \mu\text{g/ml}$ at 34°C , and further to $3.19 \pm 0.18 \mu\text{g/ml}$ at 37°C (Figure 3.2B). These findings collectively illustrate how temperature significantly influences *Y. lipolytica's* metabolic behavior. While higher temperatures facilitate the synthesis of certain primary metabolites, they concurrently impede lipid accumulation. This demonstrates *Y. lipolytica's* complex metabolic networks and provides a promising basis for future industrial applications where optimizing metabolic pathways based on temperature could be crucial.

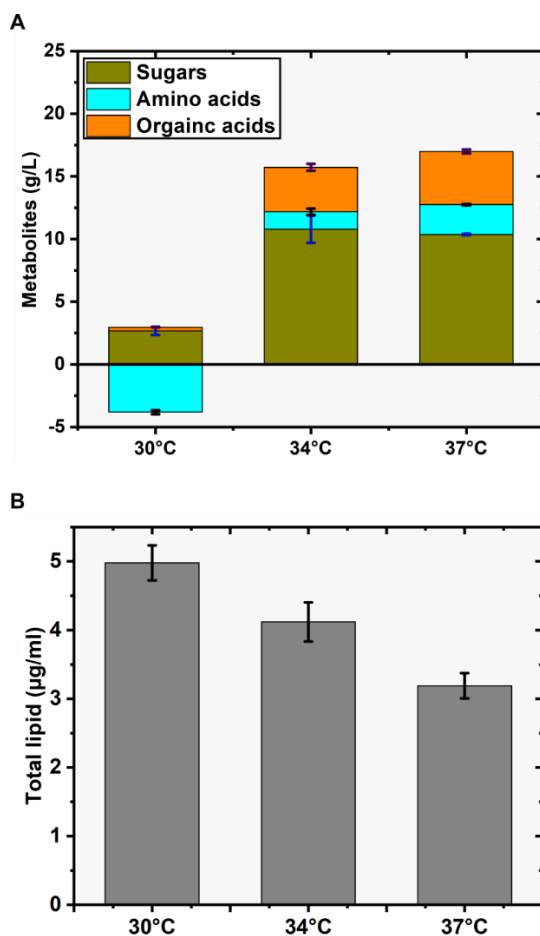


Figure 3.2 Temperature-dependent variations in metabolite production and lipid accumulation in *Y. lipolytica*. (A) Highlights the accumulation of three major metabolites- sugars, amino acids and organic acids across three different temperatures: 30°C, 34°C, and 37°C. (B) Portrays *Y. lipolytica* total lipid content under the same temperature conditions. These observations were made during a 20-hour cultivation period in shake-flasks. NMR was employed for detailed metabolite profiling, and the Sulfo-Phospho-Vanillin (SPV) assay was utilized to gauge the total lipid content. For consistency, 0.1 OD₆₀₀ cells from each culture were sampled at specific time intervals. The experimental medium was enriched with a concentration of 30g/L glycerol. Error bars signify the standard deviations derived from two replicate measurements.

3.3.3 Temperature-induced pyruvate and its derivative production with *Y. lipolytica*

Our in-depth analysis of *Y. lipolytica*'s response to elevated temperatures uncovered key metabolic alterations, as detailed through NMR profiling. As reported in the previous section, this profiling demonstrated a notable increase in the synthesis of organic acids and amino acids at higher temperatures. We further explored this, and one significant observation was the increased pyruvate production when cultivation temperatures were raised, evident from the jump in pyruvate levels from 0.95 ± 0.30 g/L at 34°C to 2.50 ± 0.22 g/L at 37°C (Figure 3.3A). Pyruvate, a critical precursor in various metabolic pathways, including those leading to organic acids and amino acids (Figure 3.3B), suggests an enhanced synthesis of pyruvate in warmer conditions. However, a contrasting trend was seen in α -ketoglutarate production, which decreased from 2.82 ± 0.54 g/L at 34°C to 2.04 ± 0.11 g/L at 37°C (Figure 3.3A), despite its potential synthesis from pyruvate (Figure 3.3B). This contrast in production patterns could imply a shift in metabolic focus or routes at higher temperatures.

In examining the amino acid profile of *Y. lipolytica*, the effects of increased temperatures were evident. Amino acids linked to pyruvate synthesis exhibited elevated levels at higher temperatures. Intriguingly, there was a shift from production to consumption of these amino acids at optimal temperatures, as indicated by the negative values in Figure 3.3C. A closer analysis of specific amino acids revealed, for instance, a significant increase in alanine synthesis, a direct pyruvate derivative, from 0.18 ± 0.14 g/L at 34°C to 0.55 ± 0.09 g/L at 37°C (Figure 3.3D). However, glutamate production, potentially interchanging with alanine, remained relatively stable at the elevated temperatures, as shown by consistent levels around 0.99 ± 0.20 g/L at 34°C and 0.98 ± 0.30 g/L at 37°C (Figure 3.3D).

This detailed study sheds light on *Y. lipolytica*'s metabolic flexibility to temperature changes, revealing the organism's enhanced pyruvate synthesis and related metabolite production at elevated temperatures. These findings provide a new understanding of *Y. lipolytica*'s metabolic resilience and cellular responses, paving the way for potential industrial applications. This research not only deepens our knowledge of *Y. lipolytica*'s metabolic mechanisms but also opens promising avenues for the biomanufacturing of pyruvate-based chemicals.

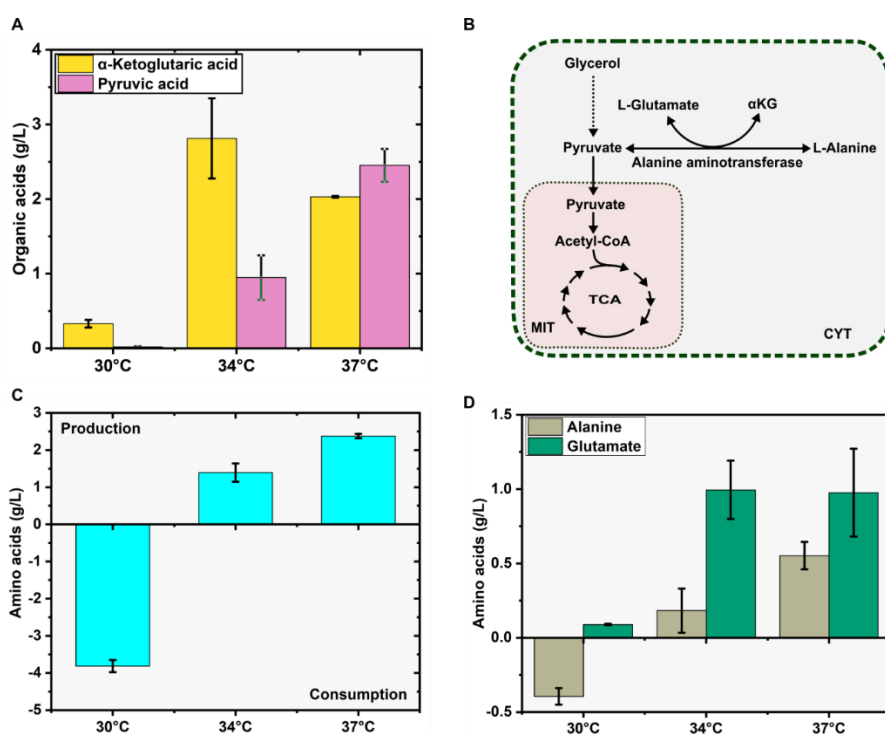


Figure 3.3 Variation in organic and amino acid production in *Y. lipolytica* under varying temperature conditions. The displayed data originates from NMR analysis following 20-hour shake-flask cultivations at temperatures of 30°C, 34°C, and 37°C. (A) Displays the production levels of pyruvic and α -ketoglutaric acids across the three temperatures. (B) Illustrates the metabolic pathways involved in the synthesis of glutamate, alanine, and α -ketoglutarate, indicating the conversion of glycerol to pyruvate and subsequently to other metabolites through various

enzymatic reactions. (C) Represents the overall content of amino acids at each temperature. (D) Highlights the primary amino acids, specifically alanine and glutamate, derived from pyruvate. To ascertain accurate production values, initial metabolite concentrations in the media were subtracted from the values observed at 20 hours. All experiments utilized a rich media supplemented with 30g/L glycerol. Error bars denote standard deviations from duplicate experiments.

3.3.4 Enhanced mannitol production using *Y. lipolytica* at elevated temperatures

Our NMR analysis provided us with crucial insights into the metabolic fate of glycerol. A deeper examination of the spectra revealed the transformation of glycerol primarily into sugars. Among the array of sugars detected, we found nominal amounts of arabinitol, erythritol, glucose, and trehalose (Appendix 1). Strikingly, the sugar alcohol, mannitol, emerged as the predominant product, accounting for an overwhelming 96% of total sugar content, especially when the experiments were conducted at elevated temperatures. To thoroughly investigate and potentially capitalize on this trend of dominant mannitol production, we initiated shake flask cultivations. Rich media supplemented with 30 g/L glycerol was used in these cultivations. Glycerol was chosen as the carbon source because it was found to be superior in driving mannitol production when compared with other potential carbon sources like glucose and acetate.

The dynamics of mannitol production were carefully tracked across various temperatures—30°C, 34°C, and 37°C. Our HPLC readings, as represented in Figure 3.4A, uncovered intriguing patterns. At an optimal temperature, *Y. lipolytica* pumped out 2.10 ± 0.44 g/L of mannitol within the first 20 hours of cultivation. However, a subsequent dip to 0.16 ± 0.01 g/L by the 40-hour mark was observed. The sharp drop is thought to be because the glycerol level dropped around the 20-hour mark, which may have caused *Y. lipolytica* to start using mannitol for its metabolic needs.

Raising the temperature of cultivation to 34°C produced different outcomes compared to 30°C. As illustrated in Figure 3.4B, mannitol titers soared to 10.62 ± 0.68 g/L within the span of 20 hours, with a yield of 0.45 ± 0.044 g/g. Extending the cultivation period to 40 hours revealed that mannitol titers plateaued around 11.02 ± 0.65 g/L, with a yield of 0.43 ± 0.04 g/g. This observation provided an essential insight: prolonging the cultivation duration beyond 20 hours may not significantly augment mannitol yields. Upon further elevating the temperature to 37°C, similar patterns were manifested as for 34°, as visualized in Figure 3.4C. The mannitol titer was recorded at 10.28 ± 0.65 g/L with a yield of 0.51 ± 0.03 g/g in the first 20 hours. Notably, a transition in temperature from 34°C to 37°C corresponded to an enhancement in mannitol yield (specifically, from 0.45 to 0.51 g/g). Yet, weighing in the unconsumed glycerol levels at these respective temperatures (6.65 ± 0.38 g/L at 34°C versus 9.73636 ± 0.38051 g/L at 37°C) and the growth tolerance of *Y. lipolytica* at these temperatures, 34°C emerges as the most conducive temperature for efficient bio-manufacturing of mannitol using *Y. lipolytica* in glycerol-fed media.

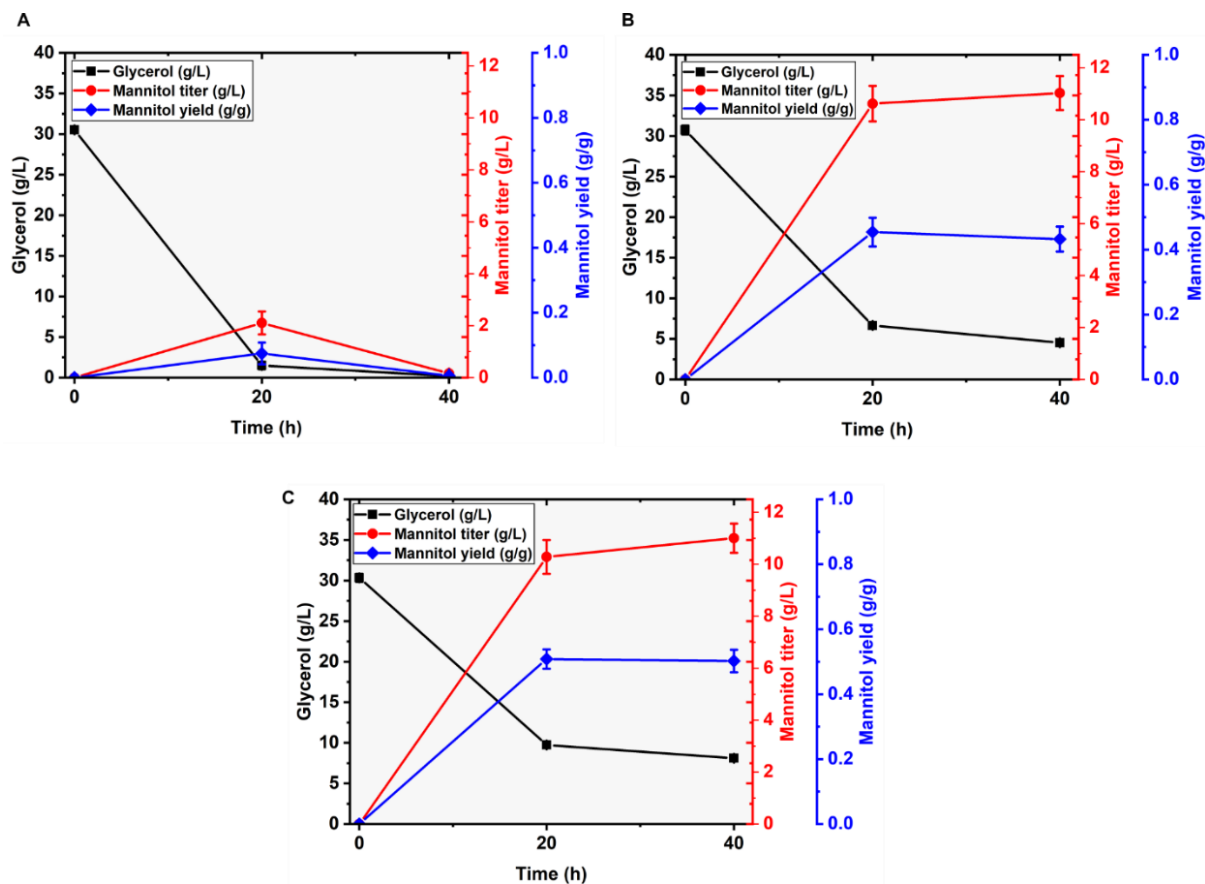


Figure 3.4 Temporal profile of mannitol production and glycerol consumption by *Y. lipolytica* in shake-flask experiments. The graph illustrates the dynamics of glycerol utilization and subsequent mannitol production across different time intervals and temperature conditions. (A) Glycerol utilization and mannitol production at 30°C, showcasing the decline in glycerol concentration (black line) and the corresponding increase in both mannitol titer (blue line) and yield (red line). Similarly, (B) captures these Glycerol utilization and mannitol production at 34°C, while (C) outlines the scenario at 37°C. For all experiments, a consistent initial glycerol concentration of 30 g/L was employed as the primary carbon source. Mannitol quantities were determined with HPLC. The error bars associated with each data point reflect the standard deviations from duplicate trials.

3.3.5 Modification of *FBP1* and its role in mannitol production

The quest to enhance the production of valuable compounds like mannitol has gathered momentum. Particularly, *Y. lipolytica* has emerged as an appealing candidate for its production. As demonstrated in the previous sections, *Y. lipolytica* exhibits an impressive capability to produce mannitol, especially when subjected to bioproduction strategies focused on growth temperature variations. In this section, we explored deeper into a genetic approach to investigate how manipulation of a specific gene can further boost mannitol production potential in *Y. lipolytica*.

The synthesis of mannitol involves a two-stage conversion process that originates from fructose-6-phosphate, as shown in Figure 3.5A. Specifically, this transformation is orchestrated by two essential enzymes: mannitol-1-P-dehydrogenase and mannitol-1-P-phosphatase. However, enhancing mannitol in *Y. lipolytica* through the manipulation of these genes becomes challenging as the genes responsible for these enzymes in *Y. lipolytica* remain unidentified. To circumvent this challenge, we focused on the gene encoding the enzyme fructose-1-6-bisphosphatase (*FBP1*). This enzyme is integral to the metabolic pathway, mediating the conversion of fructose-1-6-bisphosphate to fructose-6-phosphate and setting the stage for mannitol production. By overexpressing this gene using the robust hybrid promoter (hp4d) tailored for *Y. lipolytica* (Po1g), we aimed to bolster mannitol yields.

Overexpression of *FBP1* increased mannitol titers, achieving 13.50 ± 0.23 g/L and 11.34 ± 0.63 g/L when grown at 34°C and 37°C, respectively, over a 20-hour period. These results, translating to an impressive 35% and 10% surge in mannitol titers at the given temperatures compared to the baseline figures from the unaltered strains (Figure 4.5C). We also closely monitored glycerol assimilation to gain an in-depth understanding of the production process. At the end of a 20-hour growth period at 34°C, the wild-type strains did not consume 6.98 ± 0.40 g/L

of glycerol. Contrarily, the *FBPI* overexpressing strains demonstrated an aggressive consumption pattern, reducing residual glycerol levels to a mere 0.71 ± 0.06 g/L (Figure 3.5D). We further investigated the impact of *FBPI* on mannitol production by knocking this gene out using CRISPR/Cas9 gene-editing technology. By disrupting the native *FBPI* gene, we intended to understand its role in mannitol synthesis. The edited strains displayed reduced mannitol production compared to their wild-type counterparts, especially at elevated temperatures. This is evidenced by mannitol yields of 3.38 ± 0.10 g/L versus 10.05 ± 0.29 g/L and 3.37 ± 0.23 g/L versus 10.30 ± 0.38 g/L at 34°C and 37°C, respectively (Figure 3.5C). Interestingly, even with the *FBPI* gene disrupted, traces of mannitol synthesis persisted in the *Δfbp1* strain. This observation hints at the presence of alternative pathways, suggesting that other mechanisms might compensate, albeit minimally, for mannitol production. We also explored the implications of deleting or overexpressing the *FBP1* gene on the growth of *Y. lipolytica* and found that neither intervention disrupted its growth (Figure 3.5B)

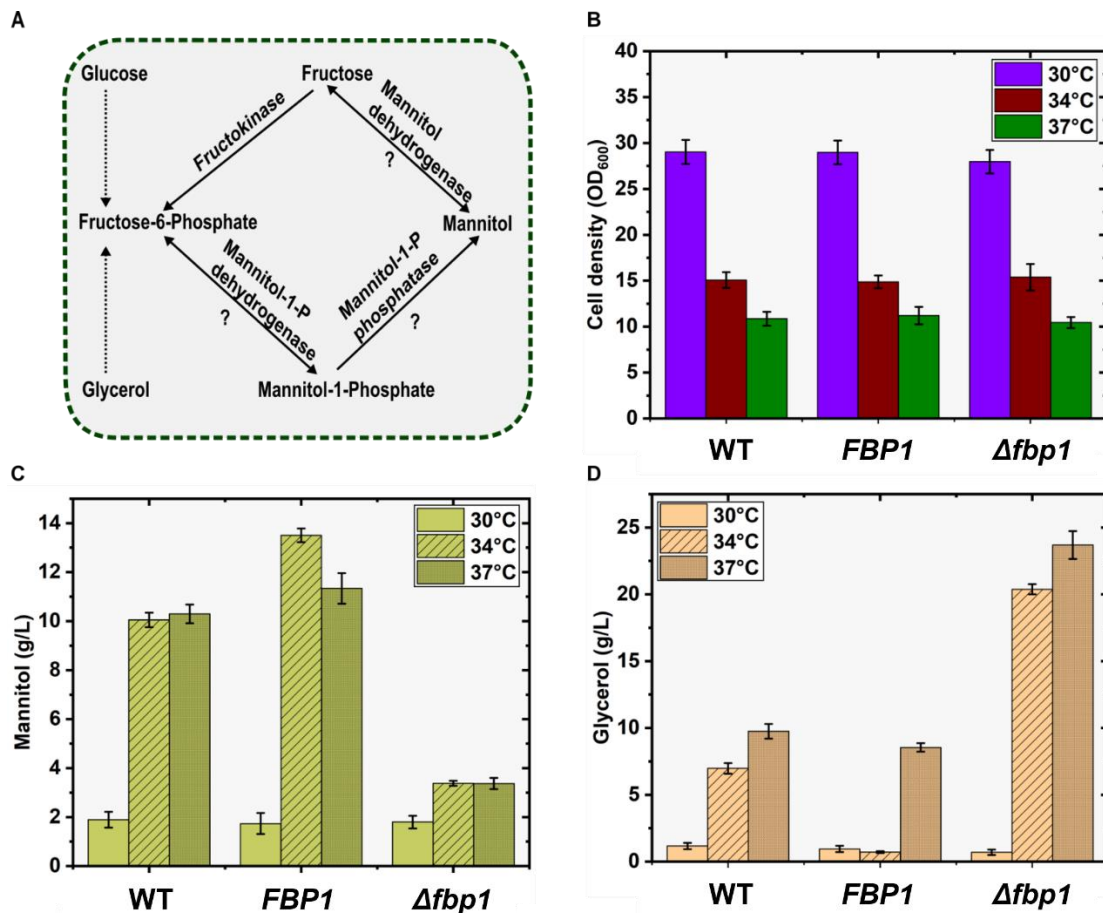


Figure 3.5 Comprehensive analysis of the effects of *FBP1* gene manipulation on mannitol synthesis in *Y. lipolytica*. (A) The primary mannitol synthesis pathways commonly found in fungi. Notably, question symbols signify the uncertainty surrounding the specific genes in *Y. lipolytica* responsible for the enzymes that catalyze these transformations. (B) Demonstrates the cell growth at varying temperatures—30°C, 34°C, and 37°C. (C) Mannitol production of the wild type, *FBP1* overexpressing, and $\Delta fbp1$ strains at the aforementioned temperatures (D) Represents glycerol consumption levels across the different strains and temperatures. HPLC was employed to quantify the glycerol and mannitol concentrations at the 20-hour mark. In the shake-flask experiments, an initial concentration of 30g/L glycerol was supplied as the primary feedstock. The data displayed is based on averages from duplicate experiments, with the accompanying standard deviations.

3.3.6 Transcriptional responses of *Y. lipolytica* to elevated temperatures

Y. lipolytica's response to elevated temperatures, as observed in previous sections, includes altered growth rates, reduced lipid content, and shifts in metabolite profiles. This sparked a curiosity about potential intrinsic changes at the gene transcription level, possibly linked to these phenomena or other related cellular processes. To unravel the underlying mechanisms dictating the cellular responses to temperature variations, we opted for a comprehensive approach, employing RNAseq to profile gene expression and conduct an unbiased whole transcriptome analysis. Our aim was not just to catalog these genetic changes but also to discern patterns, comprehend the functional implications, and decode the broader adaptive strategies employed by *Y. lipolytica* under thermal stress. Through a methodical examination of the transcriptomic data, supported by a robust bioinformatic framework, we sought to reveal the complex interplay between temperature fluctuations and cellular function.

To execute this analysis, total RNA was extracted from exponential-phase *Y. lipolytica* cultures grown in glycerol-rich media at 30°C, 34°C, and 37°C. The transcriptional changes due to temperature shifts were then quantified using RNAseq, with bioinformatics tools aiding in data interpretation. For RNAseq, reads were aligned to the well-annotated reference genome of *Y. lipolytica* CIB122, leveraging its comprehensive gene annotations and ontology information for accurate analysis.

In our study, we conducted a comprehensive differential gene expression analysis comparing conditions at 34°C and 37°C against the baseline of 30°C. Using stringent criteria of a Fold Change greater than 1.5 and an adjusted P-value below 0.05, we initially focused on quantifying the total number of significantly differentially expressed genes for each temperature comparison. This

study was designed to shed light on the broader patterns of gene expression in *Y. lipolytica*. As depicted in Figure 3.6D, from a total of 6447 genes, 1199 and 1756 genes were found to be significantly up-regulated, while 973 and 1567 genes were significantly down-regulated at 34°C and 37°C respectively. This distribution suggests that temperature does not exert a generalized effect on the gene expression of *Y. lipolytica*. We also conducted a gene-set enrichment analysis (GO) to scrutinize the differentially expressed genes, aiming to understand the systemic response of *Y. lipolytica* to the alterations in growth temperature. Employing the same cut-off values as before (Fold Change > 1.5 and adjusted P-value < 0.05), for both pairwise temperature conditions, we observed that genes predominantly associated with GO terms such as aerobic respiration, ATP biosynthetic processes, sterol biosynthetic processes, tricarboxylic acid cycle, and carboxylic acid metabolic processes were significantly down-regulated. In contrast, genes linked to carbohydrate: proton symporter activity and phospholipase activity, were predominantly up-regulated at both temperature conditions, as illustrated in Figure 3.6A. Interestingly, the genes implicated in lipid metabolic processes and oxidation-reduction processes exhibited a divided expression profile, showing differential gene expression relative to the optimal temperature (Figure 3.6A). Notably, genes with fatty acid beta-oxidation GO terms were predominantly up-regulated at 34°C (Figure 3.6B), whereas most of the genes related to gluconeogenesis and fatty acid metabolic processes were significantly down-regulated at 37°C (Figure 3.6C).

Considering the data on metabolite profiles, total lipid content, and growth rate changes under different temperatures and carbon sources, our focus shifted to exploring the correlation between these variations and gene expression levels. This analysis aimed to understand the impact of temperature on cellular changes. A detailed differential gene expression analysis was conducted, particularly on genes related to metabolic processes and transporters, as depicted in Figure 3.7.

The heatmaps in the figure are represented by Z-scores, providing a visual and statistical insight into the gene expression patterns relative to these physiological changes.

The transition in growth temperature from the optimal condition compelled *Y. lipolytica* to either expel the crucial biological precursor, pyruvate, from the cell or to convert it into α -Ketoglutarate and amino acids. This intriguing shift caught our attention, prompting us to explore the differential expression of genes associated with pyruvate transport and pyruvate metabolism to gain a clearer understanding of why the fate of pyruvate was altered under elevated temperature conditions. As illustrated in Figure 3.7 (heatmaps), we observed that the expression of *MPC1* (mitochondrial pyruvate carrier 1; YALI0_C03223g), a pivotal player in transporting pyruvate from the cytosol to the mitochondria, was significantly down-regulated at both 34°C and 37°C. The expression of *MPC2* (mitochondrial pyruvate carrier 2; YALI0_F00264g) also exhibited a slight down-regulation at these temperatures. These findings suggest that the transportation of pyruvate to the mitochondria was hindered, as the genes essential for this process were transcriptionally repressed due to the temperature impact. Despite this, we postulated that some amount of pyruvate might still be channeled into the mitochondria for acetyl-CoA synthesis. To explore this further, we examined the expression of *PDA1* (pyruvate dehydrogenase E1 component alpha chain; YALI0_F20702g) and *PDB1* (pyruvate dehydrogenase E1 component beta chain; YALI0_E27005g), aiming to understand the subsequent fate of pyruvate in this major downstream pathway. These genes were found to be significantly down-regulated as well (Figure 3.7). Additionally, pyruvate decarboxylase (*PDC1*; YALI0_D10131g), responsible for the conversion of pyruvate into acetaldehyde in the cytosol, was slightly downregulated at both elevated temperatures. Overall, these observations collectively imply that elevated temperatures have altered the normal metabolic pathway of pyruvate by compromising the expression of genes

involved in its downstream processing. However, it is crucial to note that the gene expression of pyruvate carboxylase 1 (*PYCI*; YALI0_C24101g) remained largely unaffected by the higher temperatures, as shown in Figure 3.7, indicating that the cell could utilize this as an alternative route to the TCA cycle to safeguard its growth.

A shift was also observed from lipid accumulation to an increased production of sugars, organic acids, and amino acids under elevated temperatures (Figure 3.2). While the impairment of pyruvate processing to the TCA cycle could partially contribute to this phenomenon, we conducted an exhaustive analysis of the gene expressions involved in the lipid biosynthetic pathway to identify any transcriptional changes that might be responsible for the observed reduction in lipid accumulation (Figure 3.7). Intriguingly, we detected a significant down-regulation in the expression of several key genes, including *ACCI* (Acetyl-CoA carboxylase; YALI0_C11407g), *FASI* (Fatty acid synthase subunit beta; YALI0_B15059g), *FAS2* (Fatty acid synthase subunit alpha; YALI0_B19382g), *ACLI* (ATP citrate lyase subunit 1; YALI0_E34793g), *ACL2* (ATP citrate lyase subunit 2; YALI0_B21540g), and *DGAI* (Diacylglycerol acyltransferase; YALI0_F10956g), indicating that the biosynthesis of fatty acids and their subsequent conversion into lipids was hampered. These findings are in line with our previous observations of reduced total lipid content at elevated temperatures, as shown in Figure 3.2. Additionally, the expression levels of genes involved in lipid catabolism, such as *FAAI* (long-chain-fatty-acid-CoA ligase; YALI0_B01298g), *POXI* (acyl-coenzyme A oxidase; YALI0_C12524g), and *MFEI* (multifunctional enzyme; YALI0_C21396g), remained relatively constant across the different temperature conditions (Figure 3.7).

To elucidate the mechanisms governing the transition in sugar and organic acid production more, we examined the gene expressions related to glycolysis and the pentose phosphate pathway.

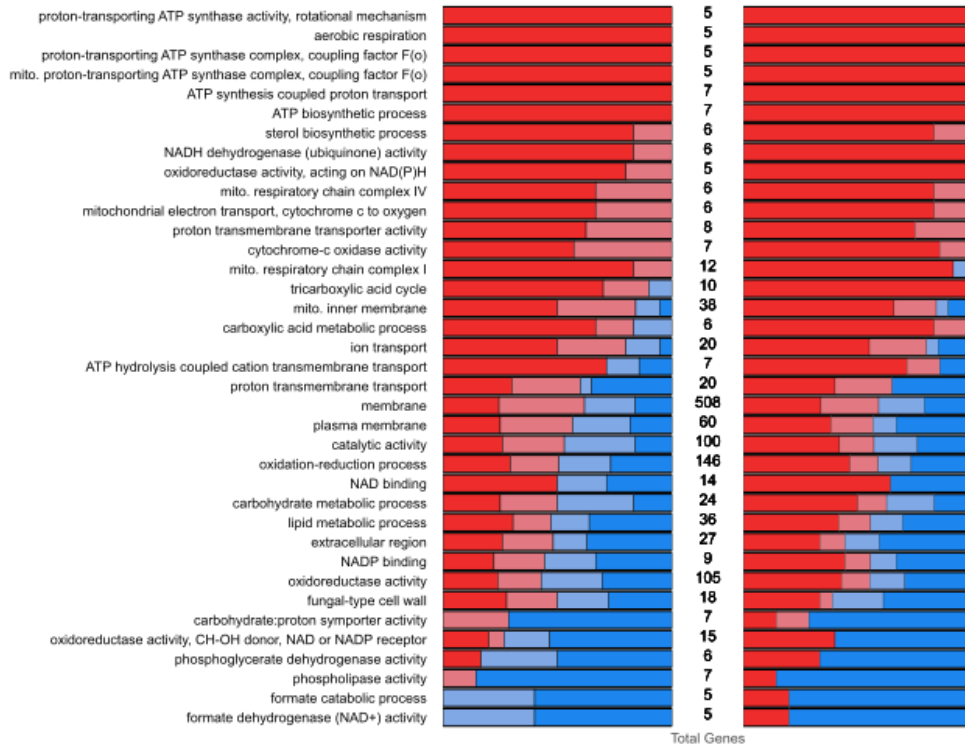
Here, we noted a substantial up-regulation of *PFK1* (6-phosphofructokinase; YALI0_B00339g) and *FBA1* (fructose-bisphosphate aldolase; YALI0_D14536g), genes imperative for glycolysis. Additionally, the expression of *ZWF1* (glucose-6-phosphate dehydrogenase; YALI0_C20298g), which participates in the pentose phosphate pathway, was markedly increased. These findings suggest that the cell reallocates resources under elevated temperature conditions, favoring pathways leading to the synthesis of sugars and organic acids. We also observed a significant up-regulation in the expression of genes associated with the glyoxylate cycle (*CIT2*, isocitrate lyase; YALI0_D07964g and *MLS1*, malate synthase; YALI0_D16876g), potentially contributing to the enhanced production of succinate under elevated temperature conditions. However, it is important to highlight those genes involved in amino acid biosynthesis exhibited a mixed expression profile, with some being up-regulated while others were down-regulated (Figure 3.7).

Sugars and amino acids are produced in high quantities at elevated growth temperatures, and they require transporters to leave the cell for the medium. So, we investigated how the expression of amino acid and sugar transporters changed when the temperature was changed in *Y. lipolytica*. This was crucial to understanding how the observed shifts in metabolite profiles, especially the increase in amino acids and sugars, correlated with changes at the transcriptional level. Amino acid transporters play a pivotal role in the uptake of amino acids from the external environment, and they can also be involved in intracellular amino acid trafficking. Analyzing the expression data, we noted a mixed response among amino acid transporters. Several genes encoding amino acid transporters were significantly up-regulated at elevated temperatures, suggesting an increased uptake or intracellular redistribution of amino acids. Specifically, the genes YALI0_E12345g and YALI0_F21032g, encoding general amino acid permeases, showed a notable increase in expression at 34°C and 37°C. This is in line with the increased amino acid

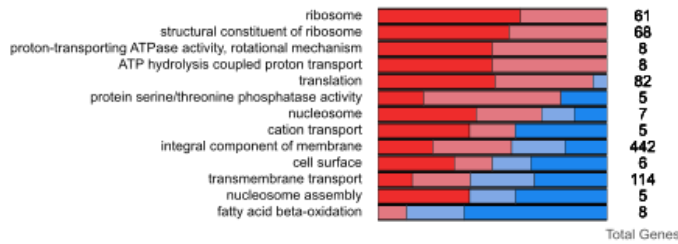
levels observed in the metabolite profile (Figure 3.2). On the other hand, some specific amino acid transporter genes were down-regulated, indicating a complex and varied regulation of amino acid transport in response to temperature changes. Sugar transporters are critical for the uptake of external sugars and their intracellular distribution, and their expression levels can directly impact the cellular metabolism of sugars. Upon analyzing the RNAseq data, we discovered a significant up-regulation of genes encoding sugar transporters at elevated temperatures. In particular, the expression of YALI0_C12345g and YALI0_D54321g, which encode high-affinity glucose transporters, was markedly increased at 34°C and 37°C. This suggests an enhanced capability of *Y. lipolytica* to uptake and metabolize glucose under thermal stress, correlating with the observed increase in sugar production in the metabolite profile. Additionally, the expression of genes encoding transporters for other sugars, such as fructose and mannose, also exhibited an up-regulation trend. The transcriptional up-regulation of these amino acid and sugar transporter genes underlines their potential role in facilitating the metabolic shifts observed in *Y. lipolytica* under elevated temperatures. These shifts are likely adaptive responses aimed at maintaining cellular homeostasis and ensuring survival under thermal stress conditions. Importantly, these findings offer valuable targets for genetic engineering to enhance the thermotolerance and metabolic performance of *Y. lipolytica*, potentially leading to improved yields in industrial bioproduction applications. By integrating these insights on transporter gene expression with our previously discussed findings on metabolic pathways and lipid biosynthesis, we were able to paint a more holistic picture of the cellular adaptations of *Y. lipolytica* to elevated temperatures. This comprehensive understanding is vital for devising strategies to harness and manipulate these adaptive responses, driving forward the fields of metabolic engineering and synthetic biology.

Our RNAseq analysis has shed light on the complex transcriptomic landscape of *Y. lipolytica* under varying temperature conditions, offering critical insights into the cellular strategies employed by this yeast to navigate and adapt to thermal stress. The evident transcriptional repression of genes involved in lipid biosynthesis and the concomitant up-regulation of genes linked to sugar and organic acid production, combined with the dysregulated expression of genes crucial for pyruvate processing, sketch a comprehensive portrait of the cellular reprogramming that ensues in response to elevated temperatures. These findings are instrumental in putting together the biological puzzle, allowing us to understand the complex interplay between temperature and cellular metabolism in *Y. lipolytica*, which holds profound implications for industrial biotechnology applications.

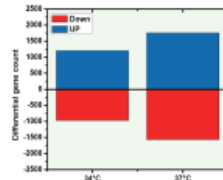
A



B



D



C

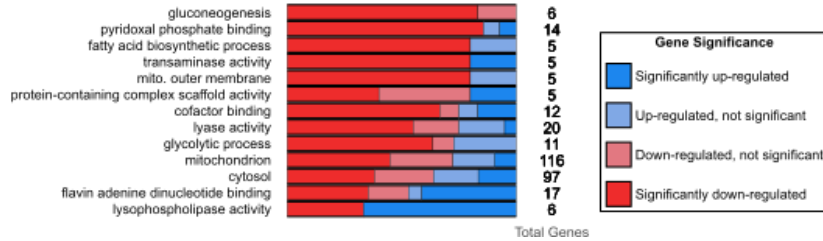


Figure 3.6 Comprehensive analysis of differentially expressed genes at elevated temperatures.

This figure delves into the gene set analysis of differentially expressed genes when subjected to temperatures of 34°C and 37°C, benchmarked against the control temperature of 30°C. Genes were methodically categorized based on Gene Ontology (GO) terms. Displayed are the top 50 GO term

gene sets that have a significant representation of exceptionally upregulated and downregulated genes under both temperature conditions. (A) Highlights the prominent GO term gene sets commonly identified for both the 34°C (on the left) and 37°C (on the right) conditions. (B) Underscores the GO term gene sets exclusively discerned for the 34°C in comparison to the 30°C condition. (C) Emphasizes the GO term gene sets that were unique to the 37°C compared to the 30°C setting. (D) Provides a visual representation of the total count of genes with significant differential expression relative to the 30°C baseline for each of the elevated temperature conditions. The spectrum of gene expression significance is demarcated by distinct color codes. Notably, genes with significant differential regulation are characterized by a Log2FoldChange greater than 1.5 and an FDR-adjusted P-value less than 0.05 when set against the 30°C control.

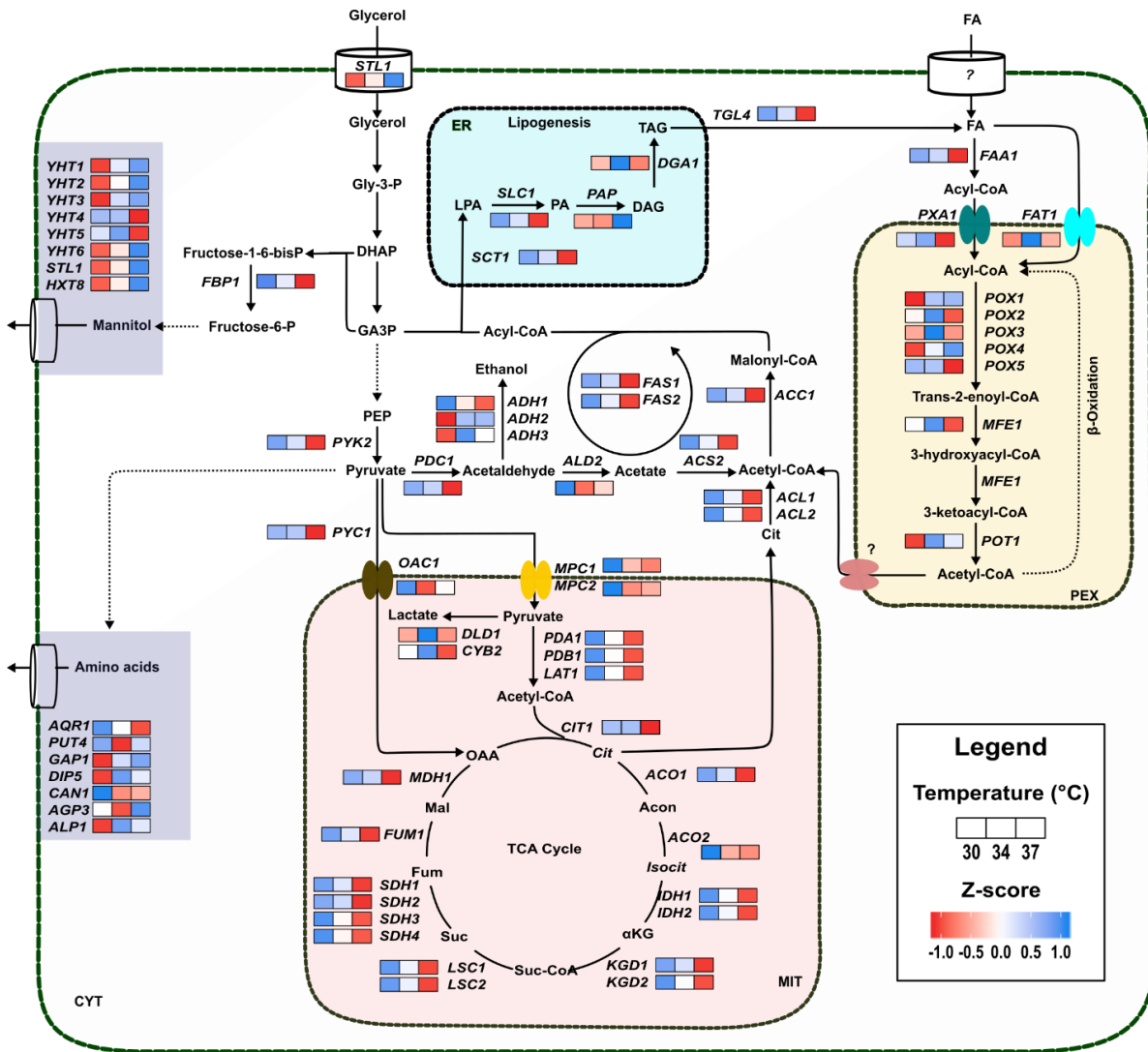


Figure 3.7 Detailed analysis of *Y. lipolytica* metabolic pathways and transporters in response to varied temperature conditions. This schematic representation, augmented by RNAseq heatmaps, offers an in-depth visual insight into the dynamic regulation of metabolic pathways and transporters under different thermal environments. The heatmaps chart the endogenous expression trends of pivotal catalytic enzymes and transporters, presenting them as Z-scores derived from the regularized logarithm transformation of the gene expression counts. Such a transformation ensures normalization in terms of library size, facilitating a comparative evaluation of gene expression

alterations across distinct samples and genes. Broken arrows symbolize processes that encompass multiple steps. Comprehensive gene annotations can be referenced in supplementary table 2, which catalogues the genes depicted here along with their respective differential Log₂FoldChange values. The presence of question marks denotes uncharted regions where further gene annotations are necessary for understanding the complete orchestration of these metabolic processes.

3.4 Discussion

3.4.1 *Y. lipolytica* growth: a temperature and feedstock analysis

Our investigation into *Y. lipolytica*'s response to different temperatures and carbon sources has provided a thorough understanding of its developmental dynamics. This research offers crucial insights for optimizing cultivation methods, enhancing its application in various fields. By correlating transcriptional and gene function data with physiological changes, we've developed a comprehensive framework to understand its complex behaviors. This contributes significantly to scientific literature and opens doors for future research and biotechnological advancements. The discussion ahead aims to thoroughly analyze these findings, placing them in a wider scientific context and underscoring their potential for both academic and practical advancements.

Y. lipolytica, an obligate aerobic yeast, optimally grows at moderate temperatures between 25 to 30°C and exhibits significant adaptability across various pH levels (Madzak, 2021). It can assimilate a wide range of carbon sources, including glucose, glycerol, acetate, and fructose, as well as hydrophobic molecules and industrial byproducts like crude glycerol (Fickers et al., 2005; Liu et al., 2015; Madzak, 2021). Given its phylogenetic placement in the Hemiascomycete phylum and divergence from a common ancestral fungus with *Saccharomyces cerevisiae* (De Hertogh et al., 2006), we explored *Y. lipolytica*'s growth at elevated temperatures, expecting similarity with *S. cerevisiae*, which thrives between 37.5°C and 39.8°C (Walsh and Martin, 1977). However, at 37°C, particularly when utilizing glycerol, *Y. lipolytica*'s growth decreased notably, diverging from our initial assumption and highlighting the need for species-specific research. Our transcriptional analysis further revealed that numerous genes vital for aerobic respiration, ATP production, sterol synthesis, and carboxylic acids formation were down-regulated, along with those involved in gluconeogenesis. These genetic changes likely contributed to the observed growth reduction,

highlighting the need to understand the metabolic adjustments of *Y. lipolytica* under different environmental conditions.

In our exploration of *Y. lipolytica's* growth dynamics, we initially chose glycerol as the feedstock. Glycerol is a byproduct of biodiesel production and recognized as an economical and abundant carbon source frequently used in microbial cultivation (Da Silva et al., 2009). Given this effectiveness for microbial growth, *Y. lipolytica's* limited growth under elevated thermal conditions led us to consider other carbon sources. Therefore, we extended our research to include glucose, acetate, and soybean oil, each of which resulted in distinct growth responses from *Y. lipolytica* at the elevated temperature of 37°C. This comprehensive approach aimed to uncover how different carbon sources influence *Y. lipolytica's* growth and adaptability under specific environmental conditions.

Soybean oil emerged as a particularly effective carbon source for promoting *Y. lipolytica's* growth at an elevated cultivation temperature of 37°C. Its rich composition of triglycerides offers a diverse range of fatty acids, which are critical substrates for *Y. lipolytica's* metabolic processes (Zhu and Jackson, 2015). The assimilation of soybean oil in *Y. lipolytica* primarily involves β -oxidation, a metabolic pathway localized in the peroxisome (Beopoulos et al., 2011). Our transcriptional analysis at 37°C confirmed this mechanism, showing a marked up-regulation of genes related to fatty acid beta-oxidation, such as *FAAI*, *POXI*, and *MFEI*. These findings suggest that *Y. lipolytica* efficiently utilizes the complex fatty acids in soybean oil, indicating a metabolic preference or adaptation at higher temperatures. This understanding opens new avenues for metabolic engineering, particularly in scenarios where directing carbon flux away from the TCA cycle and towards lipid utilization is advantageous. Our study highlights the potential of soybean

oil as a feedstock for industrial processes involving *Y. lipolytica*, especially in high-temperature fermentations.

At elevated cultivation temperatures, *Y. lipolytica* also displayed a similar growth pattern when using glucose as a carbon source. In contrast, acetate serves as both a carbon source and a metabolic byproduct, and as a short-chain fatty acid, its accumulation can inhibit growth in various microbial species (Chen et al., 2021). When employing acetate at 37°C, *Y. lipolytica* exhibited growth patterns indicative of unique metabolic or regulatory challenges specific to this temperature. These observations underscore the importance of further exploration into how *Y. lipolytica* responds metabolically to different substrates, especially at higher temperatures. Such understanding could unveil metabolic bottlenecks or adaptive mechanisms employed by *Y. lipolytica*, providing critical insights for optimizing growth conditions and advancing biotechnological applications.

We found that 37°C was too high fermentation temperature and not conducive to the growth of *Y. lipolytica*. Our transcriptional analysis revealed that at this elevated temperature, there was a notable down-regulation of the two mitochondrial pyruvate carrier subunits, encoded by *Mpc1* and *Mpc2*. This down-regulation suggests a possible impediment to the transport of pyruvate into the mitochondria. To address this and optimize growth conditions for *Y. lipolytica*, we explored the effects of reducing the temperature to 34°C. Our rationale was that a slight decrease in temperature could alleviate the growth constraints we observed at 37°C. Remarkably, at the more moderate temperature of 34°C, *Y. lipolytica* demonstrated robust growth across all tested carbon sources, underlining its remarkable adaptability. This resilience could be partially attributed to the sustained functionality of pyruvate carboxylase (*Pyc1*), an enzyme essential for converting pyruvate into oxaloacetate. Notably, the expression of the *PYCI* gene remained relatively stable at 34°C (Figure

3.7). This stability likely plays a critical role in enabling *Y. lipolytica* to engage in alternative metabolic pathways, thereby feeding into the TCA cycle and maintaining growth under these more favorable conditions. This ability of *Y. lipolytica* to thrive at a slightly reduced temperature, regardless of the carbon source, is particularly relevant for metabolic engineering and industrial processes seeking cost-effective and sustainable feedstocks. Our findings indicate that adjusting cultivation temperatures can significantly enhance *Y. lipolytica's* utility in a range of biotechnological applications.

Our study on *Y. lipolytica's* growth dynamics under varied conditions has yielded insights with significant implications for research and practical applications. The yeast's robust growth with soybean oil at 37°C and its continued growth at 34°C are pivotal for optimizing metabolic engineering processes. This adaptability in temperature and carbon source selection broadens the potential uses of *Y. lipolytica* in biotechnology, including biofuel production and high-value chemical synthesis. By integrating transcriptional data, gene functions, and physiological observations, we have achieved a comprehensive understanding of *Y. lipolytica*, which is instrumental for its application in various biotechnological sectors. This foundation sets the stage for future research focused on unraveling the metabolic and regulatory mechanisms that influence *Y. lipolytica's* growth, thereby maximizing its industrial utility.

3.4.2 *Y. lipolytica's* metabolic responses to temperature variations

Y. lipolytica's metabolic flexibility, particularly its response to pH fluctuations (Egermeier et al., 2017), highlights its value in diverse industrial applications, ranging from biofuel production to bioremediation and the synthesis of high-value chemicals. Temperature plays a key role in microbial metabolism, influencing metabolic pathways and accelerating enzymatic reactions at

higher temperatures, which can lead to increased production. However, excessively high temperatures may cause protein denaturation and disrupt cellular membranes, illustrating temperature's complex impact on microbial metabolism (Noll et al., 2020). A key observation in our study is the substantial alteration in *Y. lipolytica's* metabolite profiles when cultivated on glycerol at elevated temperatures. This finding emphasizes temperature's critical influence on metabolic pathway regulation and has significant implications for optimizing bioproduction processes and advancing metabolic engineering techniques. Therefore, this section explores temperature's role as a metabolic regulator in *Y. lipolytica*, exploring its effects on transcription, its applications in metabolic engineering for synthesizing products, and its overall impact on the yeast's biological functions.

When using glycerol as a feedstock at elevated temperatures, we observed an increase in the production of amino acids, organic acids, and sugars by *Y. lipolytica*, compounds crucial to the food, pharmaceutical, and chemical industries. This finding demonstrates the potential of temperature as a key factor in enhancing the biosynthesis of these valuable substances, offering a promising avenue for bioproduction methods. Understanding the transcriptional mechanisms driving this temperature-induced metabolic shift in *Y. lipolytica* could further advance metabolic engineering strategies. In contrast, employing soybean oil as a feedstock resulted in negligible metabolic changes, raising questions about the specific temperature sensitivities of *Y. lipolytica's* metabolic pathways and the impact of different carbon sources on its complex regulatory systems. It is known that various feedstocks elicit different metabolic responses in microorganisms, suggesting the distinct reactions of *Y. lipolytica* to glycerol and soybean oil at higher temperatures may be due to unique metabolic pathways associated with their assimilation.

Our study employed NMR for metabolite profiling, revealing significant shifts in *Y. lipolytica*'s carbon flux at elevated temperatures, notably at 34°C and 37°C. We observed a strategic redirection of metabolic pathways towards the synthesis of amino acids, organic acids, and sugars. This pattern is a similar response seen in other microorganisms under stress conditions, where sugars and amino acids accumulate for osmoregulation and organic acids are often secreted during high-temperature fermentations (Guan et al., 2017). Intriguingly, our initial hypothesis linked the production of organic acids and mannitol in *Y. lipolytica* to a drop in pH, as low pH typically leads to their generation (Egermeier et al., 2017). To test this, we conducted fermentation in a bioreactor, maintaining a constant pH of 7. Results showed mannitol production at levels comparable to shake-flask fermentation, suggesting that these metabolites are indeed a response to high cultivation temperatures, not pH changes. Further, our transcriptional analysis supports this temperature effect: we noted a mixed response in amino acid transporter genes and a significant up-regulation in genes encoding sugar transporters at elevated temperatures. This transcriptional up-regulation aligns with the increased production of sugars and amino acids (Guan et al., 2017), supporting the notion that *Y. lipolytica* activates specific transporters under thermal stress for enhanced sugar and amino acid metabolism. These findings provide valuable insights into the metabolic adjustments *Y. lipolytica* undergoes in response to thermal stress, enhancing our understanding of its metabolic capabilities and potential applications in biotechnology.

The temperature-induced metabolic shift in *Y. lipolytica* is further reflected in its lipid accumulation dynamics. *Y. lipolytica*, recognized for its oleaginous properties, typically accumulates substantial lipid content (Liu et al., 2015; Park and Ledesma-Amaro, 2023; Zhu and Jackson, 2015). However, our findings indicate a significant decrease in lipid accumulation as temperatures rise. This reduction correlates with the low carbon flux we observed through the

tricarboxylic acid (TCA) cycle, which is essential for the organism's lipid synthesis capabilities. *Y. lipolytica* is capable at converting glycerol or sugars into fatty acids through the *de novo* fatty acid biosynthesis pathway, accumulating lipids up to more than 25% of its dry cell weight (DCW), primarily as triacylglycerol (Liu et al., 2015; Park and Ledesma-Amaro, 2023; Zhu and Jackson, 2015). To quantify this lipid content, we employed the sulfo-phospho-vanillin (SPV) method, a rapid and efficient technique offering superior accuracy compared to lipophilic fluorescent dyes like Nile Red or BODIPY and yielding results on par with gas chromatography (GC)-based detection methods (Mishra et al., 2014). Our analysis revealed a marked decrease in lipid content at 37°C, with a less pronounced but noticeable reduction at 34°C. This decline in lipid accumulation could be linked to the down-regulation of pivotal genes integral to fatty acid synthesis. These include citrate lyase (*ACLI* and *ACL2*), acetyl-CoA carboxylase (*ACCI*), diacylglycerol acyltransferase (*DGAI*) and the multi-enzyme fatty acid synthase complex (*FAS1* and *FAS2*). This transcriptional down-regulation suggests an impairment in lipid biosynthesis pathways at elevated temperatures. The observed reduction in lipid accumulation under thermal stress emphasizes the critical role of temperature in modulating the metabolic pathways of *Y. lipolytica*. This understanding is vital for tailoring biotechnological processes, particularly those involving lipid production, to optimize yields under varying temperature conditions. This finding provides a comprehensive view of the metabolic adjustments *Y. lipolytica* undergoes in response to temperature changes, offering valuable insights for future research and applications in fields such as biofuel production and bioremediation, where lipid synthesis is a key factor.

3.4.3 Temperature-induced pyruvate and its derivative production with *Y. lipolytica*

The metabolic complexities of *Y. lipolytica* under high-temperature conditions offer a compelling view into the organism's adaptability and resilience. A key finding from our study is the pronounced upregulation of pyruvate synthesis and its derivative amino acids, such as alanine and glutamate, at elevated temperatures. This positions pyruvate as a pivotal node in *Y. lipolytica*'s metabolic network when cultivated at higher temperatures using glycerol as feedstock. Pyruvate's role is multifaceted: it is a crucial intermediary poised to enter the tricarboxylic acid (TCA) cycle, can convert into lactate, or serve as a precursor for amino acid synthesis, underscoring its versatility (McCommis and Finck, 2015; Pronk et al., 1996; Stotz, 1945). Our observations indicate a strategic redirection of metabolic flux towards pyruvate synthesis in *Y. lipolytica*, marked by a reduction in TCA cycle metabolites and an increase in amino acids that are a single conversion step away from pyruvate. This observed metabolic shift in *Y. lipolytica* has a noteworthy correlation with more general biological trends. Similar patterns have been seen in *S. cerevisiae* during fermentations conducted at elevated temperatures (Martinez-Force and Benitez, 1995; Zhao et al., 2022), suggesting a universal adaptive mechanism across different yeasts.

In our investigation into *Y. lipolytica*'s cellular responses at elevated temperatures, we observed a pronounced excretion of pyruvate coupled with a marked reduction in tricarboxylic acid (TCA) cycle metabolite synthesis. This led us to examine deeper into the metabolic pathways involved at gene transcription level. At the end of glycolysis, the enzyme pyruvate kinase (Pyk1) catalyzes an irreversible reaction, leading to pyruvate formation. This irreversibility precludes pyruvate from re-entering the gluconeogenesis pathway, thus directing it towards alternative metabolic fates. Under normal conditions, pyruvate primarily enters the mitochondria, fueling *Y.*

lipolytica's active TCA cycle. However, at elevated temperatures, this pathway appears to be disrupted.

The transport of pyruvate into mitochondria is mediated by the mitochondrial pyruvate carrier, consisting of two subunits, Mpc1 and Mpc2. Within the mitochondria, pyruvate is converted into acetyl-CoA by the pyruvate dehydrogenase complex, which includes the E1 component (Pda1), E2 component (Pdb1), and E3 component (Pdc1). Our RNAseq heatmap (Figure 3.7) revealed a downregulation in the expressions of *MPC1*, *MPC2*, *PDA1*, *PDB1*, and *PDC1* at higher temperatures, indicating a potential disruption in pyruvate's mitochondrial transport and subsequent conversion to acetyl-CoA. These findings suggest that the interruption of pyruvate processing in mitochondria might be an early event leading to its secretion, altering the metabolic flux and impacting the TCA cycle. Despite these changes, the expression of *PYC1*, the gene encoding pyruvate carboxylase – an enzyme critical for converting pyruvate into oxaloacetate was barely affected at 34°C. This might contribute to *Y. lipolytica's* resilience and adaptability, allowing it to potentially engage alternative metabolic pathways to feed into the TCA cycle, thereby sustaining its growth at 34°C.

The destiny of excess pyruvate in *Y. lipolytica* extends beyond mitochondrial processing. It can be converted to lactate by lactate dehydrogenase (Ldh) or used as a precursor for amino acid synthesis. Our RNAseq data reveals a transcriptional downregulation of LDH under elevated temperatures, suggesting a reduced conversion of pyruvate to lactate. This reduction, coupled with the downregulation of mitochondrial pyruvate transport and metabolism, likely leads to intracellular pyruvate accumulation, potentially causing pH stress within the cell.

In response to this stress, *Y. lipolytica* seems to implement a multifaceted strategy for adaptation. One key approach is the active export of excess pyruvate from its cells. Additionally,

the yeast turns to mannitol synthesis, a known response to combat thermal stress, and ramps up amino acid production to efficiently utilize surplus pyruvate. These actions could collectively contribute to mitigating the potential pH stress caused by pyruvate accumulation. Intriguingly, we observed upregulation of various sugar and amino acid transporter genes, as shown in our heatmap (Figure 3.7). The increased expression of transporter genes suggests an active remodeling of membrane transport processes, enabling the yeast to effectively respond to and manage the internal metabolic changes induced by heat. This upregulation further indicates that *Y. lipolytica* is enhancing its transport capabilities, likely to facilitate the efflux of mannitol and various amino acids out of the cell. Such a mechanism would aid in maintaining intracellular homeostasis, especially under conditions of thermal stress.

Our in-depth analysis of cellular responses in *Y. lipolytica* has also provided valuable insights into amino acid metabolism, particularly in how synthesis and consumption patterns shift across different temperatures. Amino acids, vital for a multitude of cellular functions, act as key indicators of a cell's metabolic state. Notably, we observed an increase in the production of pyruvate-based amino acids at higher temperatures, a trend that contrasts with their consumption at more optimal temperatures. This pattern suggests a strategic metabolic shift, likely aimed at enhancing the cell's defenses against thermal stress. For instance, our data highlighted a significant rise in alanine levels, increasing from 0.18 ± 0.14 g/L at 34°C to 0.55 ± 0.09 g/L at 37°C. Alanine is known for its protective roles under thermal and osmotic stress in various microorganisms (Monselise et al., 2003; Shao et al., 2015; Song et al., 2019; Wiesenthal et al., 2019), suggesting its increased production in *Y. lipolytica* under elevated temperatures is an adaptive response. Furthermore, the production of glutamate was also enhanced at higher temperatures. Given glutamate's known role in protecting cells from thermal stress (Li et al., 2019; Qiu et al., 2020), its increased synthesis in

Y. lipolytica suggests it plays a crucial part in maintaining cellular homeostasis during high-temperature fermentation. These observations point to a complex and finely tuned metabolic response in *Y. lipolytica*, where specific amino acids are synthesized in greater quantities to counteract the effects of thermal stress.

All these responses to elevated temperatures reveal the metabolic flexibility of *Y. lipolytica*. This deepened understanding of how temperature influences metabolic adjustments opens new possibilities for optimizing industrial bioprocesses and improving fermentation strategies. It underscores the importance of temperature in yeast biology, providing insights that are vital for enhancing *Y. lipolytica*'s utility in varied industrial settings, particularly where temperature control is essential. The above findings from our research offer a blueprint for metabolic engineering strategies to boost *Y. lipolytica*'s performance and stability in industrial processes. The observed surge in pyruvate and amino acid synthesis at higher temperatures heralds new opportunities for developing microbial cell factories tailored for specific productions, such as bio-based chemicals and valuable amino acids. These advancements align with the goals of sustainable production and strain improvement, potentially reducing the reliance on stringent temperature controls and energy-intensive cooling systems. Overall, our findings highlight *Y. lipolytica*'s metabolic flexibility and adaptability, paving the way for future innovations in bioprocess efficiency and sustainability, and offering a foundation for further exploration in the field of biotechnology.

3.4.4 Enhanced mannitol production using *Y. lipolytica* at elevated temperatures

Our investigation into the metabolic responses of *Y. lipolytica* under elevated temperatures has revealed a significant enhancement in its ability to produce mannitol, a crucial sugar alcohol widely used in various industries. In the pharmaceutical industry, mannitol is indispensable as an

excipient and diluent due to its stability. It is equally popular in the food industry as a low-calorie sweetener, ideal for diabetic-friendly products. Additionally, its osmoprotective qualities make it valuable in cosmetics (Godswill, 2017; Shawkat et al., 2012; Song and Vieille, 2009). These diverse applications of mannitol have led to a substantial demand, traditionally met through chemical synthesis methods. However, these conventional methods, while efficient, encounter considerable sustainability and environmental issues, mainly due to their reliance on metal catalysts and fructose, a substrate subject to variability in agricultural output and market trends (Dai et al., 2017). These concerns indicate the necessity for more sustainable production techniques. In response, green chemistry initiatives have been exploring eco-friendly methods for mannitol synthesis that reduce harmful inputs and waste (Dai et al., 2017; Song and Vieille, 2009). Microbial fermentation, utilizing the metabolic capacities of various microorganisms, is emerging as a promising alternative. For example, *Lactobacillus intermedius* (Martínez-Miranda et al., 2022; Saha and Nakamura, 2003) can efficiently convert fructose to mannitol, and yeasts like *Candida magnoliae* (Savergave et al., 2013; Song et al., 2002) are noted for their robust mannitol production. Enzymatic methods, especially using mannitol dehydrogenase, offer scalable solutions that are in line with sustainability goals (Slatner et al., 1998). These biological methods mark a substantial advancement towards sustainable mannitol production.

In light of these challenges with traditional chemical synthesis, our research has pivoted to focus on *Y. lipolytica*, a microorganism showing great promise in mannitol production. By utilizing glycerol as a substrate, our findings not only demonstrate *Y. lipolytica's* efficiency in mannitol biosynthesis but also its remarkable adaptability to higher fermentation temperatures, a key factor in enhancing mannitol yield. Prior studies have emphasized the significance of low pH conditions in boosting mannitol synthesis in *Y. lipolytica* (Egermeier et al., 2017). However, our research

introduces another crucial aspect: the role of elevated fermentation temperatures. This insight was drawn from our comprehensive NMR and HPLC analyses, showing a substantial conversion of glycerol into mannitol under these conditions, thus reinforcing *Y. lipolytica's* capability as a bio-manufacturing platform for this essential sugar alcohol. This finding gains further importance considering *Y. lipolytica's* ability to transform lignocellulosic biomass into valuable products, a potential for industrial biotechnology and sustainable production practices (Niehus et al., 2018).

Building on these fundamental discoveries about *Y. lipolytica's* potential for mannitol production, our extensive experimental analysis explored the organism's response to varying temperatures, uncovering complex patterns crucial for optimizing mannitol biosynthesis. We observed a significant decrease in mannitol concentration around the 40-hour mark at 30°C, likely due to glycerol depletion in the medium. This suggests that *Y. lipolytica*, upon exhausting its primary substrate, glycerol, begins metabolizing the produced mannitol to meet its metabolic needs. Interestingly, an increase in mannitol yield was noted when temperatures rose from 34°C to 37°C, with production climbing from 0.45 to 0.51 g/g. However, after assessing the levels of remaining glycerol and *Y. lipolytica's* growth tolerance at these temperatures, we suggest that 34°C is the most effective temperature for maximizing mannitol production. This optimal temperature represents a balance between high mannitol yield and efficient glycerol utilization, making it the ideal condition for efficient and sustainable mannitol bio-manufacturing.

Our mannitol production with *Y. lipolytica* not only corroborate but also significantly surpass previous studies for this yeast in terms of yield (Egermeier et al., 2017). This achievement highlights *Y. lipolytica's* remarkable capacity for mannitol production, especially as it was achieved without genetic modification of the strain. The implications are profound: by strategically combining optimal fermentation conditions with advanced genetic engineering techniques, there

is potential to further boost mannitol yields. Such advancements could revolutionize current production methods, leading to more cost-effective, sustainable, and high-yield processes for mannitol production. Consequently, our findings offer promising prospects for the industrial production of mannitol, potentially transforming the economic and environmental dynamics of its production and making it more viable and environmentally responsible.

Our comprehensive transcriptional analysis of *Y. lipolytica* under various temperatures has unveiled significant shifts in metabolic pathways, particularly in pyruvate metabolism. Key genes in this pathway, such as *MPC1*, *MPC2*, *PDA1*, *PDB1*, and *PDC1*, showed reduced expression at 34°C and 37°C, suggesting limited pyruvate transport to mitochondria and potential cytosolic accumulation. Initially, we theorized that this accumulation might cause a decrease in cytosolic pH, inducing cellular stress and leading to mannitol production as a protective response. However, experiments in a controlled pH environment within a bioreactor contradicted this hypothesis, as mannitol production remained steady, indicating that its synthesis is more likely a response to thermal stress than to pH changes. Additionally, our research revealed a notable metabolic shift at higher temperatures, from lipid accumulation to increased sugar. This shift was marked by a down-regulation in key lipid biosynthesis genes (*ACC1*, *FAS1*, *FAS2*, *ACLI*, *ACL2*, *DGAI*), pointing to a redirection of metabolic resources towards sugar. Simultaneously, the up-regulation of glycolysis genes (*PFK1*, *FBP1*) indicates a strategic metabolic adaptation. Particularly noteworthy is the up-regulation of the *FBP1* gene, essential in mannitol synthesis, providing a molecular basis for the increased mannitol yields we observed. Furthermore, our analysis identified an up-regulation in sugar transporters, notably high-affinity glucose transporters (*YALI0_C12345g* and *YALI0_D54321g*), supporting enhanced mannitol production and secretion at higher temperatures. These findings are essential for understanding *Y. lipolytica's* metabolic dynamics

and provide critical insights for future metabolic engineering efforts aimed at optimizing sustainable mannitol production processes. By elucidating these complex genetic and metabolic interactions, our study lays the groundwork for developing more efficient and environmentally friendly approaches to mannitol biosynthesis.

In our quest to enhance mannitol production at elevated fermentation temperatures, we explored the genetic engineering of *Y. lipolytica*, with a particular emphasis on the *FBPI* gene. This gene encodes fructose-1-6-bisphosphatase, a key enzyme in the mannitol synthesis pathway, as it catalyzes the conversion of fructose-1-6-bisphosphate to fructose-6-phosphate. In bacteria, the synthesis of mannitol from the glycolysis intermediate, fructose-6-phosphate, involves a two-step enzymatic process, primarily facilitated by mannitol-1-P-dehydrogenase and mannitol-1 P-phosphatase (Ortiz et al., 2013). However, *Y. lipolytica* does not have annotated genes for these enzymes, presenting a unique challenge for mannitol production. The strategic focus on *FBPI*, considering its crucial role in mannitol metabolism, was insightful. Our transcriptome analysis revealed that the expression of the *FBPI* gene was not affected by elevated fermentation temperatures, leading us to manipulate this gene to understand its potential impact on mannitol synthesis.

This significant increase in mannitol production achieved through manipulating the *FBPI* gene sets the stage for exploring even more potent genetic engineering strategies. By considering the use of stronger promoter systems, we can potentially unlock further enhancements in mannitol yield. The overexpression of the native *FBPI* gene significantly boosted mannitol production, yielding 13.50 ± 0.23 g/L and 11.34 ± 0.63 g/L at 34°C and 37°C, respectively, over a 20-hour period. This translated to an impressive 35% and 10% increase in mannitol titers at these temperatures compared to the production levels of the unmodified strain. The enhanced mannitol

production was achieved by driving *FBPI* gene expression using the hybrid promoter, hp4d. However, there is potential for even further improvement. Employing more advanced and potent versions of the hp4d promoter, such as UAS1B16-32-TEF or UAS1B16-32-LEU, which are known to be eight times stronger (Blazeck et al., 2011), could potentially yield even higher mannitol production levels. This novel approach not only demonstrates the significant potential of genetic manipulation in *Y. lipolytica* but also opens new avenues for optimizing industrial-scale mannitol production using more potent promoter systems.

In addition, we employed the CRISPR/Cas9 technique to disrupt the *FBPI* gene, aiming to further elucidate the role of Fbp1 in mannitol production. The marked decrease in mannitol production following this gene disruption provided compelling evidence of *FBPI*'s integral role in the synthesis process. Intriguingly, the observation of residual mannitol synthesis post-disruption hints at the existence of alternative biosynthetic pathways, which requires a deeper exploration. The presence of such alternative pathways is a plausible scenario, considering that organisms often develop redundant systems to ensure survival and adaptability under various conditions (Louca et al., 2018; Whitacre, 2012). In case of *Y. lipolytica*, this redundancy might be attributed to its evolutionary history, which necessitated adaptation to diverse environmental challenges. Unraveling and understanding these alternate metabolic routes could open new doors for metabolic engineering, potentially leading to even more efficient and enhanced mannitol production. This approach could help in developing strategies that leverage these redundant pathways, thereby optimizing *Y. lipolytica*'s capability for mannitol synthesis and contributing to the broader goal of sustainable and high-yield biotechnological production.

Our research into *Y. lipolytica*'s response to elevated temperatures has crucially revealed its potential for high-yield mannitol production, a significant advancement for industrial use. The

effective manipulation of the *FBPI* gene has notably enhanced mannitol production, marking a key step in refining cultivation methods and paving the way for future metabolic engineering advancements. These findings extend beyond academic research, offering practical insights for the development of more cost-effective, efficient, and sustainable mannitol production processes. Looking ahead, leveraging advanced metabolic engineering techniques, and exploring diverse substrates and cultivation conditions could further improve mannitol yields. This research not only promises to deepen our understanding of microbial biosynthesis but also aims to revolutionize mannitol production in industry, aligning with the increasing demand for sustainable and economically viable biotechnological approaches.

Chapter 4

Development of a dual gRNA CRISPR tool kit for manipulation of

Y. lipolytica

4.1 Introduction

The advent of the CRISPR-Cas system has revolutionized synthetic biology, offering unprecedented precision in genome editing. This technology, however, presents unique challenges when applied to *Y. lipolytica*, a yeast species with distinct genetic repair mechanisms. *Y. lipolytica* predominantly relies on the non-homologous end joining (NHEJ) pathway for DNA repair, a mechanism known for its unpredictability and the propensity to introduce insertions or deletions (indels) (Gao et al., 2018; Gao et al., 2016; Schwartz et al., 2016). These indels often complicate precise genetic engineering, as NHEJ can result in gene knockouts that do not necessarily lead to a loss of function, particularly in the absence of a repair template (Kosicki et al., 2022).

An alternative to NHEJ, homologous recombination (HR), offers a potential solution. However, HR's effectiveness varies among organisms and is notably lower in *Y. lipolytica*. The preference of this yeast's cellular mechanisms for the NHEJ pathway over HR poses additional challenges for researchers aiming for targeted gene editing (Gao et al., 2018; Gao et al., 2016; Schwartz et al., 2016). Furthermore, the enhancement of HR efficiency often requires the deactivation of genes such as *KU70* and *KU80*, which are critical for telomere maintenance (Kosicki et al., 2022; Rampakakis et al., 2008). However, this deactivation may adversely impact cell growth, an essential factor in synthetic biology applications.

This chapter introduces a novel dual-gRNA CRISPR system, embodied in the pCRISPRYL2 plasmid, designed to overcome the challenges posed by *Y. lipolytica*'s DNA repair mechanisms.

The system aims to leverage the yeast's inherent NHEJ mechanism, providing an efficient alternative to HR techniques. The development of this system was facilitated by strategic genetic modifications, including the creation of a URA-deficient *Y. lipolytica* strain to resolve the complexities arising from the concurrent use of *LEU2* markers in both the target gene overexpression vector and the Cas9/gRNA expression vector. This initiative was crucial to ensuring precise and effective genome editing.

Our research explored the gene editing efficacy of this dual gRNA CRISPR system, initially focusing on the *TRP1* gene. The experimental findings highlight the variances in editing efficiencies depending on whether single or dual gRNAs are employed. Notably, the use of dual gRNAs, while reducing overall editing efficiency, significantly enhances the functional knockout efficiency of target genes. This outcome is a critical demonstration of the dual gRNA strategy's potential for improving gene editing results in *Y. lipolytica*. The system's performance is further contextualized through a comparative analysis with existing methodologies. For instance, Gao et al. (2016) reported a lower disruption efficiency for the *TRP1* gene using a different CRISPR system. In contrast, our approach, utilizing TRP1gRNA1 and TRP1gRNA2, achieved notably higher editing efficiencies, demonstrating the robustness and reliability of our system.

This chapter aims to enhance our understanding of *Y. lipolytica*'s potential for genetic manipulation and establish the dual-gRNA CRISPR system as a vital tool in metabolic engineering. The discussion includes the system's efficiency, adaptability, and capability for complex gene editing tasks. Additionally, the future research directions outlined focus on validating the system's precision, exploring gene integration through HR, and expanding its applications to more complex biological systems. This holistic approach aims to maintain the

system's forefront position in genetic engineering and further its contributions to the field of metabolic engineering.

The hypothesis and objectives of this chapter are:

Hypothesis: The primary hypothesis of this chapter is that the development and implementation of a dual-gRNA CRISPR system will significantly enhance the precision of genetic manipulations in *Y. lipolytica*. This system, integrated into a single plasmid framework, is hypothesized to overcome the limitations posed by the yeast's natural preference for NHEJ in DNA repair mechanisms. We anticipate that the dual gRNA strategy will not only streamline the gene editing process but also increase the specificity and functional knockout efficiency in *Y. lipolytica*, even in the presence of inherent challenges associated with NHEJ-induced insertions or deletions (indels).

Objectives:

1. To create and assess a dual-gRNA CRISPR system integrated into a single plasmid, specifically designed for the genetic manipulation of *Y. lipolytica*. This system aims to improve the precision of gene editing by overcoming the limitations of *Y. lipolytica*'s natural DNA repair mechanisms.
2. To evaluate the functional knockout efficiency of target genes in *Y. lipolytica* using the dual gRNA system, compare the outcomes with traditional single gRNA strategies to establish the advantages of the dual gRNA approach.
3. To test the dual gRNA CRISPR system on a variety of genes within *Y. lipolytica* to ascertain its versatility and adaptability for different genetic contexts. This objective includes examining the system's performance across multiple genes and assessing its applicability for multiplex gene editing.

4.2 Materials and methods

4.2.1 Chemicals and enzymes

Chemicals used in this study were obtained from Sigma-Aldrich unless otherwise stated. Phusion™ High-Fidelity DNA Polymerase and NEBuilder® HiFi DNA Assembly Master Mix were purchased from New England Biolabs (NEB, Canada). Plasmid mini-preps were performed using the EZ-10 Spin Column Plasmid DNA Miniprep Kit (Biobasics, Canada). PCR and gel clean-ups were performed using the QIAquick PCR & Gel Cleanup Kit (Qiagen). Oligonucleotides and guide RNA were purchased from either IDTDNA.

4.2.2 Strains

Pog1 strain of *Y. lipolytica*, a derived from wild-type strain W29 (ATCC 20460) was acquired from Yeastern Biotech. This strain underwent a series of genetic modifications from the original strain W29 and characterized by its genotype as *MatA*, *leu2-270*, *ura3-302::URA3*, *xpr2-332*, *axp-2*. The W29 strain was chosen due to its well-documented genetic background and its amenability to genetic manipulation. Over the years, W29 has been the subject of numerous studies, making it a reliable reference point for our experiments. Additionally, its genome has been fully sequenced, providing a comprehensive genetic map that aids in the design and verification of CRISPR targets. We derived a *URA3*-deficient strain Poh1 in our lab. Plasmid propagation was performed using *E. coli* HI-Control™ 10G chemically competent cells (Lucigen; WI).

4.2.3 Media and culture conditions

For the initial cultivation of *Y. lipolytica* strains, the Yeast Extract Peptone Glycerol (YPG) medium was employed, which comprises 1% yeast extract, 2% peptone, and 2% Glycerol. Synthetic Defined (SD) medium, containing 0.67% yeast nitrogen base without amino acids and 2% glycerol, was utilized for the selection and maintenance of transformants. For the selection of URA3 transformants, the Yeast Nitrogen Base (YNB) medium was used, which is devoid of uracil and contains 0.67% yeast nitrogen base, 2% glycerol, and appropriate drop-out supplements. Additionally, the Lysogeny Broth (LB) medium, containing 1% tryptone, 0.5% yeast extract, and 1% NaCl, was employed for cultivating *E. coli* strains that harbored the CRISPR plasmids. To prepare solid media, agar was incorporated at a concentration of 1.5%. For the selection of transformants, the media were supplemented with the appropriate antibiotics or selection markers at the recommended concentrations. Lastly, ensuring the correct pH and sterility was paramount. All media were adjusted to a pH of 6.5, either with HCl or NaOH, and sterility was maintained by autoclaving the media at 121°C for 20 minutes.

Regarding culture conditions, *Y. lipolytica* cultures were typically maintained at 30°C with an agitation rate of 200 rpm to ensure optimal growth and aeration. The inoculum was prepared by inoculating a single colony of *Y. lipolytica* from a freshly streaked plate into 5 mL of YPG medium, which was then grown overnight. This pre-culture served as the basis to inoculate larger volumes for subsequent experiments.

Counter-selective agents 5-Fluoroorotic Acid (5-FOA) and 5-fluoroanthranilic acid (FAA) were employed to isolate *URA3* and *TRP1* negative *Y. lipolytica* genetic backgrounds, respectively. Post-transformation, yeast cells were cultured on non-selective media for recovery. Subsequently, they are exposed to media containing 5-FOA or FAA. Strains with a functional *URA3* gene

metabolize 5-FOA into the toxic 5-fluorouracil, allowing only URA3-deficient mutants to survive. Similarly, strains possessing an active *TRP1* gene convert FAA into a toxic derivative, ensuring the survival of only TRP1-deficient mutants. Following incubation at 30°C, resistant colonies were isolated and subjected to molecular characterization to confirm genetic alterations.

4.2.4 gRNA design and plasmid construction

Detailed primers and guide RNAs utilized in this research are documented in Tables 4.1 and 4.2. The sgRNA sequences were meticulously designed via the Chop-Chop online tool (<https://chopchop.cbu.uib.no>), targeting specific gene sequences while considering their efficiency rankings. The foundational plasmid for our system, pCRISPRy1, was sourced from Addgene (<https://www.addgene.org/70007/>). As depicted in Figure 4.1, it comprises a codon-optimized Cas9, a LEU marker customized for *Y. lipolytica*, and Pol III-tRNA hybrid promoters that drive sgRNA expression. Using this plasmid, we created the advanced pCRISPRYL2 vector.

To make pCRISPRYL2 plasmid system, we linearized pCRISPRy1 with primers CRISPR2.FOR and CRISPR2.REV, situated upstream of the gRNA scaffold. The subsequent assembly, enabled by the NEBuilder® HiFi DNA Assembly Master Mix, incorporated the SCR1-tRNAGLY promoter from pCRISPRy1 (amplified via SCR1-tRNAGLY.FOR and SCR1-tRNAGLY.REV), the gRNA scaffold (amplified with gRNA_scaffold.FOR and gRNA_scaffold.REV), and the *URA3* gene from Pog1 (amplified using URA3_gib1.FOR and URA3_gib1.REV) as a substitute for the LEU marker. It's worth noting that the AvrII restriction enzyme site was designated for the initial gRNA in pCRISPRy1, while the MfeI enzyme site was introduced for the second gRNA. All these steps resulted in the successful creation of the pCRISPRYL2 vector.

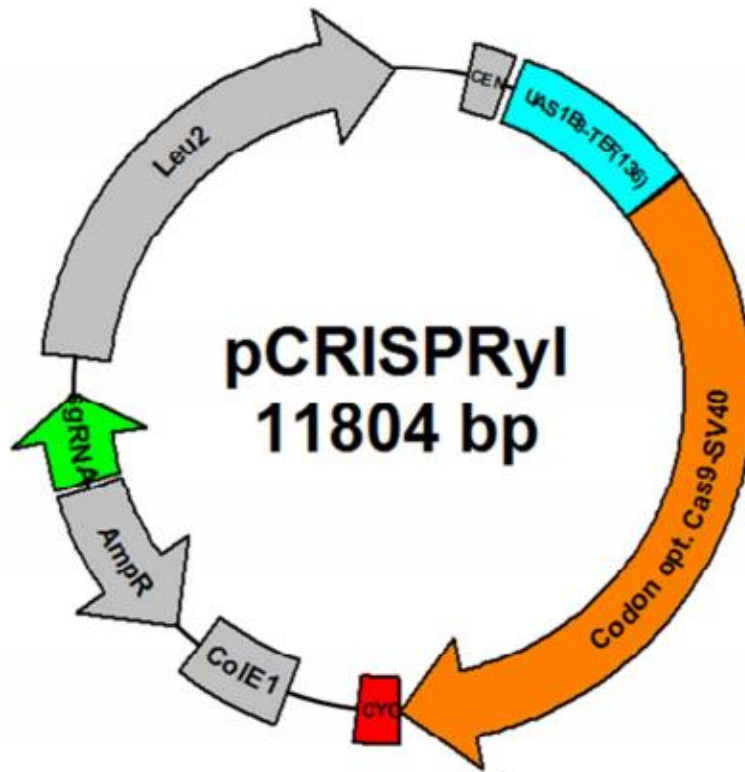


Figure 4.1 Detailed map of the parent pCRISPRyl vector designed for *Y. lipolytica* gene editing. It contains essential components such as the codon-optimized Cas9 (Codon opt. Cas9 SV40), sgRNA expression site, *LEU2* marker, and other integral elements including CEN, promoter (UAS1B8-TEF136), AmpR, ColE1, and CYC terminator.

Table 4.1 Primers used for developing a dual gRNA expression plasmid pCRISPRYL2.

Primer name	Sequence 5' to 3'	Target fragment/gene
SCR1-tRNAGLY.FOR	ATAGGCGTATCACGAGGCCCA CACATTTCCCCGAAAAG	SCR1-tRNAGLY promoter
SCR1-tRNAGLY.REV	GCTCTAAAACCAATTGTCAACC TGCGCCGAC	SCR1-tRNAGLY promoter
gRNA_scaffold.FOR	CGCAGGTTGACAATTGGTTTTA GAGCTAGAAATAGCAAG	gRNA scaffold
gRNA_scaffold.REV	GTACTCCAAAGGATATGATAT GGTGTCGAAGC	gRNA scaffold
URA3_gib1.FOR	CCATATCATATCCTTTGGAGTA CGACTCC	<i>URA3</i>
URA3_gib1.REV	AAACGCGCGAGACGAAAGGGC CACAAGTCAGCTTTCTTCAA	<i>URA3</i>
CRISPR2.FOR	GGCCCTTTCGTCTCGC	pCRISPRyl backbone
CRISPR2.REV	GGCCTTCGTGATACGC	pCRISPRyl backbone

Table 4.2 Guide RNA expressed with pCRISPRYL2 and their target genes.

gRNA name	Sequence 5' to 3'	Target gene
TRP1gRNA1	GGGTCGGCGCAGGTTGACGTACGCCGAGGA GTGGTACCGGGTTTTAGAGCTAGAAATAGC	<i>TRP1</i>
TRP1gRNA2	GGGTCGGCGCAGGTTGACGTTCCGGGCTTGTC TTTTTCGGAGGTTTTAGAGCTAGAAATAGC	<i>TRP1</i>
PEX10gRNA1	GGGTCGGCGCAGGTTGACGTGATAGGATATC TGCAACCCGGTTTTAGAGCTAGAAATAGC	<i>PEX10</i>
PEX10gRNA2	GGGTCGGCGCAGGTTGACGTTGCTGCATAGC AGTGCACAGGTTTTAGAGCTAGAAATAGC	<i>PEX10</i>
FAA1gRNA1	GGGTCGGCGCAGGTTGACGTATACAAGGAG GCCCTTAAGCGTTTTAGAGCTAGAAATAGC	<i>FAA1</i>
FAA1gRNA2	GGGTCGGCGCAGGTTGACGTAGATATGAAGA TCTACACCAGTTTTAGAGCTAGAAATAGC	<i>FAA1</i>

The plasmids constructed for gene editing purposes are presented in Table 3. Oligonucleotides, synthesized to encompass 20 nucleotide guide sequences, were flanked by sequences facilitating cloning at the AvrII and MfeI restriction sites. Initially, guide RNAs TRP1gRNA1, PEX10gRNA1, and FAA1gRNA1 were integrated at the AvrII site. Subsequently, to establish a dual guide RNA CRISPR editing framework, the corresponding TRP1gRNA2, PEX10gRNA2, and FAA1gRNA2 were integrated at the MfeI site. These oligonucleotides underwent annealing and were subsequently incorporated into the pCRISPRyl vector, leveraging

the precision of the NEBuilder® HiFi DNA Assembly Master Mix. This assembly technique ensured a streamlined and error-minimized cloning process. Post-assembly, the *E. coli* HI-Control™ 10G chemically competent cells were transformed with the resultant mixture utilizing the heat shock protocol. Following purification, the plasmids were subjected to sequencing to validate the integrity of the constructs.

Table 4.3 Plasmids used in this study.

Plasmid name	Source
pCRISPRyl	addgene
pCRISPRYL2	This study
pCRISPRYL2- TRP1gRNA1	This study
pCRISPRYL2- TRP1gRNA2	This study
pCRISPRYL2- TRP1gRNA1&2	This study
pCRISPRYL2- PEX10gRNA1	This study
pCRISPRYL2- PEX10gRNA2	This study
pCRISPRYL2- PEX10gRNA1&2	This study
pCRISPRYL2- FAA1gRNA1	This study
pCRISPRYL2- FAA1gRNA2	This study
pCRISPRYL2- FAA1gRNA1&2	This study

4.2.5 Colony PCR, plasmid extraction and PCR conditions

Plasmid DNA was extracted from bacterial cultures using the QIAquick PCR & Gel Cleanup Kit (Qiagen) according to the manufacturer's instructions. Briefly, bacterial colonies were inoculated into LB medium supplemented with the appropriate antibiotic and grown overnight at 37°C with shaking at 280 rpm. Following overnight growth, cells were harvested by centrifugation, and the pellet was resuspended in the provided buffer. The subsequent lysis and neutralization steps were performed as per the kit's protocol. The lysate was then applied to the QIAquick spin column, and after a series of washing steps, plasmid DNA was eluted in the provided elution buffer.

For PCR amplification, the Phusion™ High-Fidelity DNA Polymerase from New England Biolabs (NEB Canada) was employed. Reaction mixtures were set up as follows: 1x Phusion HF buffer, 200 µM of each dNTP, 0.5 µM of forward and reverse primers, 0.02 U/µl Phusion DNA polymerase, and approximately 10 ng of template DNA in a total volume of 50 µl. The thermocycling conditions typically commenced with an initial denaturation at 98°C for 30 seconds, followed by 30 cycles of denaturation at 98°C for 10 seconds, annealing (temperature dependent on the primers used) for 30 seconds, and extension at 72°C (time dependent on the expected amplicon size). A final extension step at 72°C for 10 minutes was included to ensure complete amplification.

For colony PCR, a single bacterial colony was picked using a sterile pipette tip and resuspended in 20 µl of sterile distilled water. This suspension was then boiled for 10 minutes to lyse the cells and release the DNA. After a brief centrifugation, 2 µl of the supernatant was used as a template for the PCR, with the aforementioned Phusion™ High-Fidelity DNA Polymerase protocol. This method allowed for rapid screening of bacterial colonies for the presence of the desired plasmid constructs.

4.2.6 Transformation of *E. coli* and *Y. lipolytica*

Transformation of *Escherichia coli* was executed using the *E. coli* HI-Control™ 10G chemically competent cells. Initially, plasmid DNA (typically 1-5 ng) was mixed with 50 µl of the competent cells in a pre-chilled microcentrifuge tube. This mixture was incubated on ice for 30 minutes, ensuring the DNA uptake by the cells. Following the incubation, a heat shock was applied by placing the tube in a 42°C water bath for exactly 45 seconds. The tube was then immediately transferred back to ice for a 2-minute incubation. Subsequently, 950 µl of pre-warmed LB medium was added to the cells, which were then incubated at 37°C with shaking at 280 rpm for 1 hour to allow recovery and expression of the antibiotic resistance marker. Post-recovery, the transformed cells were plated onto LB agar plates supplemented with the appropriate antibiotic and incubated overnight at 37°C for colony development.

For the transformation of *Y. lipolytica*, the Fast Yeast Transformation™ kit from G-Biosciences was employed. *Y. lipolytica* cells, grown to mid-log phase, were harvested and washed with the provided wash buffer. The cell pellet was then resuspended in the transformation buffer from the kit. To this suspension, 1 µg of the desired plasmid DNA was added along with the provided carrier DNA. The mixture was incubated at room temperature for 20 minutes. Following the incubation, the proprietary Fast Yeast Transformation Reagent™ was added, and the mixture was further incubated at room temperature for an additional 20 minutes. The cells were then heat-shocked at 42°C for 40 minutes. After the heat shock, cells were centrifuged, and the pellet was resuspended in YPD medium, allowing them to recover for 2 hours at 28°C with gentle shaking. Finally, the transformed *Y. lipolytica* cells were plated onto selective media plates and incubated at 28°C until colonies appeared, typically after 2-3 days.

4.2.7 Data Analysis

To assess the gene editing efficiency of the CRISPR/Cas9 system in *Y. lipolytica*, the *TRP1* gene was strategically targeted. Following transformation with the CRISPR/Cas9 construct designed for TRP1 disruption, colonies were initially selected on plates lacking uracil, leveraging the uracil auxotrophy for initial selection. Subsequently, these colonies were subjected to counter-selection on media supplemented with 5-fluoroanthranilic acid (5-FAA). In this context, cells retaining a functional *TRP1* gene would metabolize 5-FAA into a toxic derivative, inhibiting their growth. Thus, only colonies with a successful *TRP1* disruption, indicating a loss-of-function, would proliferate on the 5-FAA plates. The gene editing efficiency was then deduced by comparing the number of colonies that grew on the uracil-deficient plates with those that survived on the 5-FAA plates, offering a comprehensive measure of the precision and efficiency of the CRISPR/Cas9-mediated editing in *Y. lipolytica*. All experiments were conducted in duplicates to ensure reproducibility. Data were compiled and analyzed using OriginPro software.

4.3 Results

4.3.1 Development of the Poh1 strain

In this section, we detail the development and genetic engineering of the Poh1 strain, a derivative of the *Y. lipolytica* Po1g strain. The original Po1g strain, acquired from Yeastern Biotech, is characterized by a *LEU2* deficiency, with a unique genotype identified as *MatA*, *leu2-270*, *ura3-302::URA3*, *xpr2-332*, *axp-2*. Key to our modifications was the use of the integrative overexpression plasmid, pYLEX1, procured from Yeastern Biotech, and the parent plasmid pCRISPRy1, obtained from Addgene, both of which contain LEU markers. However, we recognized a potential issue with using LEU markers on both the overexpression vector for our target gene and the Cas9/gRNA expression vector from pCRISPRy1. This simultaneous application of *LEU2* markers could potentially impede effective genome manipulation in *Y. lipolytica*, as it might complicate the selection and integration processes. This realization necessitated a re-evaluation of our approach to ensure precise and efficient genome editing in this strain.

To overcome the challenge of using LEU markers on both the gene overexpression vector and the Cas9/gRNA expression vector in *Y. lipolytica* Po1g, we strategized the development of a URA-deficient strain. Our approach also involved modifying the Cas9/gRNA expression vector to carry a URA marker, thereby ensuring compatibility and enabling vector recycling through 5-FOA counter-selection. Utilizing the genetic framework of the Po1g strain, as depicted in Figure 4.2A, we initiated a homologous recombination process between a disrupted *URA3* site and an intact one, aiming to create a *URA3*-deficient variant. The subsequent plating on both YPG and YPG plus 5-FOA resulted in a significant number of colonies on the 5-FOA selection plates, as shown in Figure 4.2B. For additional verification, we cultured these colonies on both YPG and SG-Ura plates. The results were definitive: the colonies flourished on YPG plates, but showed no growth

on SG-Ura plates, confirming the successful elimination of *URA3* function with 100% efficiency, as illustrated in the right panel of Figure 4.2B. Further molecular confirmation was carried out through PCR analysis on six of the 5-FOA-positive strains. As Figure 4.2C reveals, unlike the wild-type Po1g strain with its intact 855 bp *URA3* gene, these six colonies did not exhibit the *URA3* gene in PCR tests. After thorough molecular validation, we designated these strains as Poh1 and selected them for our subsequent experimental endeavors. This approach not only resolved the marker incompatibility issue but also set the stage for more effective and precise genetic modifications in future experiments involving *Y. lipolytica*.

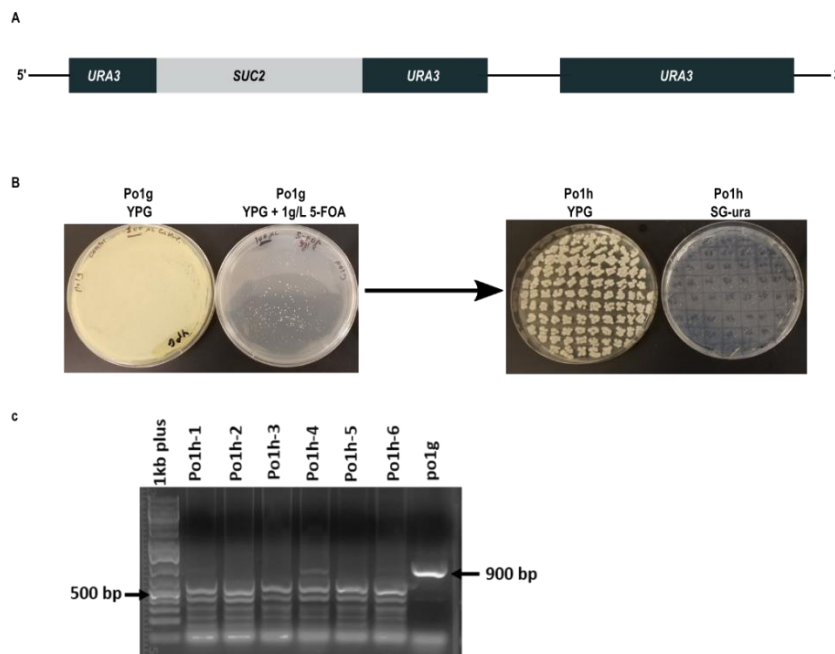


Figure 4.2 Po1h strain development from Po1g. A) Illustration of the disrupted and normal *URA3* gene in Po1g genome. B) Screening of *URA3* negative cells (Po1h) on YPG + 5-FOA plate (left) and confirmation of loss of *URA3* function on SG-Ura plate (right). C) *URA3* gene disruption confirmation by colony PCR. Primers targeted the *URA3* ORF.

4.3.2 Development of a Dual gRNA CRISPR Tool for *Y. lipolytica*

In *Y. lipolytica*, the dominant DNA repair mechanism is NHEJ, which poses significant challenges for CRISPR-based gene editing. The NHEJ pathway is prone to inducing insertions or deletions (indels), which may not always lead to effective gene disruption. This uncertainty in gene function disruption complicates precise genome editing. An alternative pathway, HR, does exist in *Y. lipolytica*, but its inherent efficiency is considerably lower. Enhancing HR often requires deactivating the *KU70* and *KU80* genes, which play critical roles in telomere maintenance. However, this deactivation can potentially impact cell growth – a factor of crucial importance in synthetic biology. The balance between achieving effective gene editing and maintaining robust cell growth presents a complex challenge in the use of *Y. lipolytica* for synthetic biology applications.

To tackle the challenges posed by the NHEJ mechanism in *Y. lipolytica*, we engineered the pCRISPRYL2 plasmid, implementing a novel dual-gRNA CRISPR system. This system enhances the natural efficiency of NHEJ within a single plasmid framework, circumventing the requirement for an HR repair template and setting it apart from existing CRISPR methodologies. The design and intended application of this plasmid, particularly for the knockout of the *TRP1* gene involved in tryptophan biosynthesis, are illustrated in Figure 4.3.

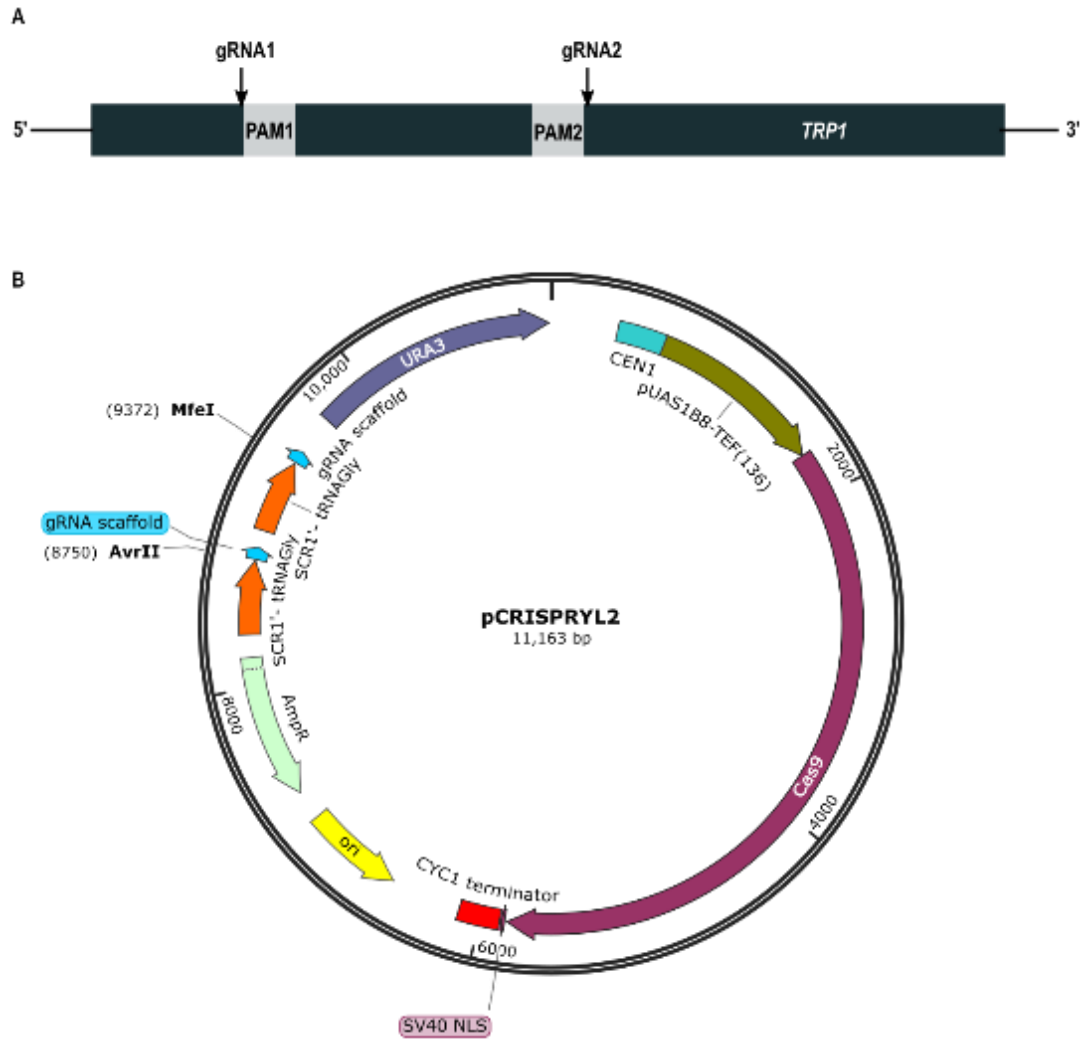


Figure 4.3 Dual gRNAs based gene editing system for *Y. lipolytica* using pCRISPRYL2 vector. A) *TRP1* gene editing with dual gRNAs (gRNA1: gRNA95 and gRNA2: gRNA441) B) Recyclable CRISPR vector for dual gRNAs cloning.

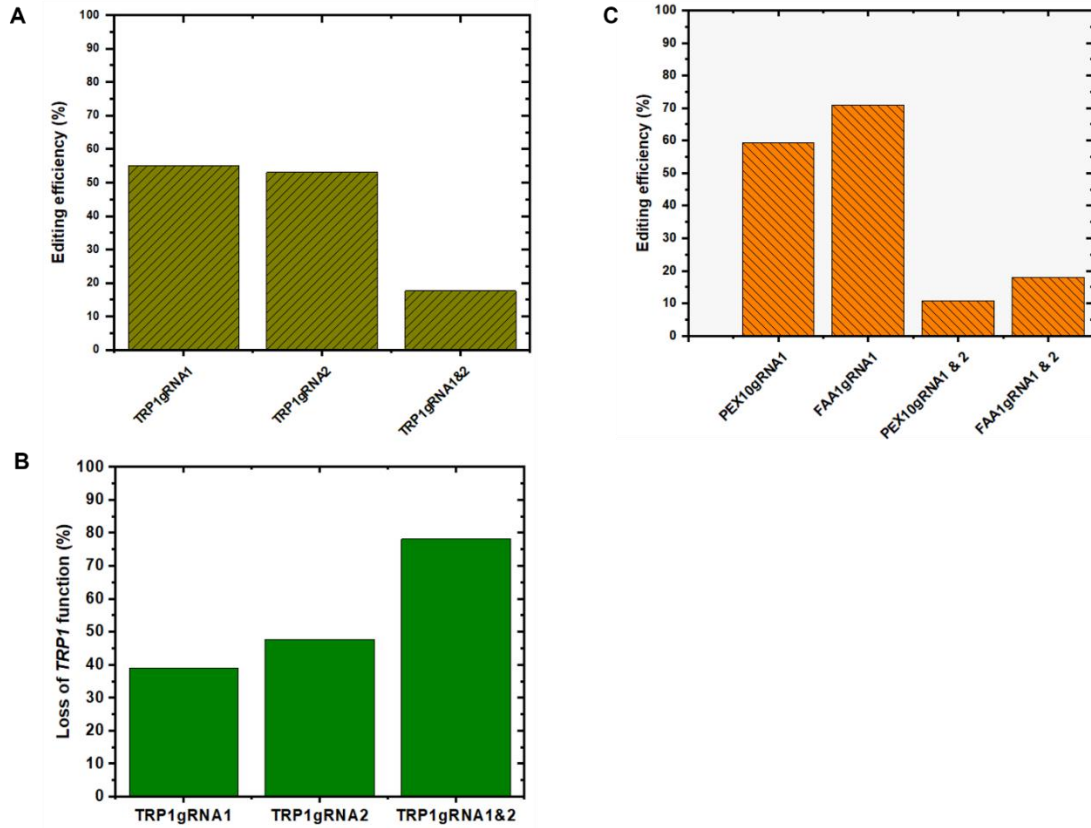


Figure 4.4 Gene editing efficiencies using pCRISPRYL2 vector. A) Editing efficiency for *TRP1* gene B) Percentage of colonies which lost Trp1 function from a total of 48 colonies plated on SG-Trp media. C) Editing efficiency for *PEX10* and *FAA1* genes. These experiments were performed only once.

Our research then progressed to a series of experiments aimed at assessing the gene editing efficacy of this dual gRNA CRISPR system, with an initial focus on the *TRP1* gene. When applied individually, TRP1gRNA1 and TRP1gRNA2 achieved editing efficiencies of 55.02% and 53.72%, respectively. However, when both were used together, a remarkable reduction in editing efficiency to 17.65% was observed (Figure 4.4A). Expanding our investigation to include the *PEX10* and

FAAI genes, we noted editing efficiencies of 59.42% and 70.87%, respectively, with the dual gRNA approach again showing lower efficiencies (Figure 4.4C). Interestingly, a deeper analysis into the functional impact of these edits revealed that the individual application of TRP1gRNA1 and TRP1gRNA2 led to a functional loss of the *TRP1* gene in 39.06% and 47.75% of the edited colonies, respectively. Notably, the combined use of these gRNAs significantly enhanced this loss of function, affecting 78.13% of the colonies (Figure 4.4B). This finding highlights the effectiveness of the dual-gRNA strategy in amplifying gene knockout results.

4.4 Discussion

The development of the Poh1 strain was the first step in our endeavor to create a dual-gRNA CRISPR system specifically designed for *Y. lipolytica*. Originating from the well-characterized Pog1 strain, Poh1 brought to the table a range of attributes, including a fully sequenced genome and established genetic properties (Pomraning and Baker, 2015). However, the path to genome manipulation of Po1g was not without its complexities, especially when introducing specific genetic tools like the pYLEX1 overexpression plasmid and the pCRISPRy1 plasmid, both of which carried a *LEU2* marker essential for gene manipulation in *Y. lipolytica*. This situation demanded a careful and strategic approach to overcome potential obstacles arising from the concurrent use of *LEU2* markers in both the target gene overexpression and Cas9/gRNA expression vectors. To address this, we engineered the Poh1 strain to lack *URA3*, thereby reserving the *LEU2* marker exclusively for gene expression. This adaptation not only facilitated the successful deployment of our dual gRNA CRISPR system but also optimized our use of *URA3* as a preferred marker. This modification streamlined the vector recycling process via counter-selection on 5-FOA, an essential step for the repeated application of the Cas9/gRNA expression plasmid.

The successful development of the URA-deficient Poh1 strain, in tandem with the modification of the Cas9/gRNA expression vector to incorporate a URA marker, resulted in an efficient and streamlined system for genetic engineering. The robust growth of colonies on YPG plates coupled with the absence of growth on SG-Ura plates, complemented by conclusive molecular evidence from PCR analyses, validated the total loss of *URA3* function. This achievement not only endorsed our strategic approach but also significantly enhanced the utility of our CRISPR toolkit. By dedicating the *LEU2* marker solely to gene overexpression experiments,

we effectively optimized our methodology for genetic manipulations in *Y. lipolytica*, paving the way for advanced research and applications in the field of synthetic biology.

To tackle the challenges presented by *Y. lipolytica*'s preference for NHEJ in DNA repair, we developed a solution through our dual gRNA CRISPR tool. Employing the pCRISPRYL2 plasmid and its dual-gRNA system, our aim was to enhance the natural efficiency of the NHEJ repair mechanism. Our experiments revealed that the editing efficiencies varied, influenced by both the target gene. Importantly, we observed a substantial increase in functional knockout efficiency when employing both TRP1gRNA1 and TRP1gRNA2 together. This finding is crucial as it demonstrates the effectiveness of the dual gRNA strategy in augmenting gene editing outcomes in *Y. lipolytica*, offering a promising approach to overcoming the inherent limitations of the organism's DNA repair preferences.

In our research, the dual gRNA CRISPR system we developed demonstrated superior efficiency and specificity when compared to other methods documented in the literature. For instance, Gao et al. (2016) reported a lower initial disruption efficiency of $12.5 \pm 7.4\%$ for the *TRP1* gene using the pCAS1yl system in wild-type (WT) *Y. lipolytica*, immediately following transformation. This efficiency notably increased to $85.6 \pm 7.1\%$ after allowing a four-day outgrowth period before plating. In contrast, our use of TRP1gRNA1 and TRP1gRNA2 individually yielded significantly higher editing efficiencies of 55.02% and 53.72%, respectively, under similar immediate plating conditions post-transformation. Even when using our dual gRNA configuration, the efficiency stood at 17.65%, surpassing the efficiency of Gao et al.'s single gRNA system for same-day plating. This enhanced performance in our system may stem from differences in gRNA design or the distinct attributes of our CRISPR system. Additionally, our method showed consistent efficiency across different genes: we observed editing efficiencies of 59.42% for *PEX10*

and 70.87% for *FAAI*. Notably, our *PEX10* editing efficiency was on par with the $62.5 \pm 21.4\%$ mutation efficiency reported by Gao et al. (2016) in the MYA-2613 strain. These findings demonstrate the robustness and reliability of our CRISPR system, establishing its efficacy in gene editing within *Y. lipolytica*.

While our method bears resemblance to the precision of dual gRNA-directed Cas9 cleavage, as detailed by Gao et al. (2018), it is distinct in its integration into a single plasmid system, diverging from the dual-plasmid approach adopted by Gao and colleagues. Although we have not directly tested our system for precise DNA fragment excision, its similarities to Gao et al.'s (2018) system imply its capability for not only accurate gene excisions but also gene integration via HR, thus offering a streamlined and efficient workflow, particularly beneficial for applications involving multiple gene edits.

One notable aspect of our system is the observed decrease in gene editing efficiency when employing dual gRNAs. This trade-off is, however, counterbalanced by a significant rise in functional knockout efficiency, offering a solution that is both comprehensive and dependable. The dual gRNA strategy enhances specificity and guarantees the functional knockout of target genes, affirming the system's role as a precision genetic tool. Furthermore, consolidating the dual gRNA CRISPR system into a single plasmid not only simplifies sequential gene knockouts but also eases vector recycling via 5-FOA counter-selection. This integration sets our system apart in terms of efficiency and practicality compared to the two-plasmid system used by Gao et al. (2018), presenting a more streamlined and effective approach for precision genetics in various applications.

Chapter 5

Optimizing 5-aminolevulinic acid production via cell-free metabolic engineering (CFME)

5.1 Introduction

5-Aminolevulinic Acid (5-ALA) is emerging as a molecule of significant biological and commercial importance. As a non-proteinogenic amino acid, it acts as a precursor to key tetrapyrrole compounds such as heme, porphyrin, chlorophyll, and vitamin B12, crucial for a myriad of biological functions in both prokaryotic and eukaryotic organisms. These functions include essential processes like oxygen transport, photosynthesis, and various enzymatic activities, highlighting the indispensable role of 5-ALA in life (Jiang et al., 2022; Kang et al., 2017). Beyond its biochemical relevance, 5-ALA's versatility extends to a broad spectrum of applications. In the medical field, it is instrumental in photodynamic therapy, offering a novel treatment avenue for various cancers (Gold and Goldman, 2004). In agriculture, its role as a biostimulant is pivotal, where it enhances plant growth and productivity by aiding chlorophyll synthesis (Rhaman et al., 2021). Furthermore, 5-ALA's utility in livestock management as a dietary supplement is gaining recognition for its ability to improve animal health and overall productivity (Hendawy et al., 2019).

The growing demand for 5-ALA, fueled by its expanding applications, is reshaping its market dynamics, with projections estimating the global market value to surge from US\$ 101.5 million in 2021 to a remarkable US\$ 145.7 million by 2028 (Wu et al., 2023). However, this growing demand also brings to light the critical need for augmented production capabilities. The current state of 5-ALA production faces challenges, primarily due to the complexities and inefficiencies of the traditional chemical synthesis methods. These conventional approaches,

characterized by low yields and high costs (Kang et al., 2017), significantly impede the widespread adoption and accessibility of 5-ALA. Consequently, there is an urgent need to innovate and develop more efficient, sustainable, and cost-effective strategies for its production, addressing these fundamental challenges to meet the increasing global demand.

In the pursuit of more effective production methods for 5-ALA, microbial fermentation has risen as a formidable and advantageous alternative to traditional chemical synthesis. This biotechnological approach, distinguished by its potential for higher yields and cost-effectiveness, has demonstrated its efficacy with engineered microbial strains. Notably, *E. coli* and *C. glutamicum* have achieved substantial 5-ALA titers of 6.93 g/L and 5.6 g/L, respectively (Ge et al., 2021; Miscevic et al., 2021). However, the route of cell-based bioproduction comes with inherent challenges, including complexities associated with cell growth, nutrient demands, and by-product generation. These factors often complicate process optimization and scalability (Garcia et al., 2021; Lim and Kim, 2019; Rasor et al., 2021). To circumvent these hurdles, Cell-Free Metabolic Engineering (CFME), especially leveraging lysates from *E. coli*, presents a groundbreaking approach for 5-ALA production. This innovative strategy overcomes the limitations linked to cell growth and maintenance, offering a controlled production environment. It enables accelerated reaction rates, facilitates easy scalability, and allows for real-time modulation of reaction parameters (Garcia et al., 2021; Grubbe et al., 2020; Lim and Kim, 2019; Rasor et al., 2021).

This chapter explores into optimizing 5-ALA production through CFME. Our research pioneers this approach in 5-ALA production, focusing on enhancing production parameters to achieve higher titers efficiently and cost-effectively. By leveraging the unique capabilities of cell-

free systems, we aim to revolutionize the production process for 5-ALA, setting a new standard in the field and paving the way for more sustainable, economical, and efficient production methods.

The hypothesis and objective of this chapter are:

Hypothesis and objective of this chapter:

Hypothesis: The hypothesis of this chapter is that the production of 5-ALA can be significantly improved through cell-free metabolic engineering (CFME), leveraging strategic genetic modifications, including the overexpression of *hemA* and repression of *hemB* in *E. Coli*. This study hypothesizes that these genetic and biochemical interventions in CFME will lead to a more efficient and scalable production process for 5-ALA compared to traditional whole-cell systems. Additionally, the hypothesis extends to the assertion that environmental factors, notably temperature and glycine concentration, play a critical role in optimizing the synthesis of 5-ALA in a cell-free setup, with the potential to achieve greater scalability and efficiency in production.

Objectives:

1. To optimize 5-ALA production through CFME. This involves exploring various parameters, particularly focusing on the genetic modifications of *E. coli* strains used for cell lysate preparation. The aim is to assess the impact of these modifications on 5-ALA yield.
2. To compare a cell-free system with traditional whole-cell systems. Analyzing the efficiency, resource utilization, and time consumption of CFME versus traditional whole-cell systems to establish the advantages of adopting a cell-free approach in biotechnological applications.

3. To investigate the role of cofactors. Studying the influence of ATP and CoA on the production of 5-ALA in CFME setups and identifying optimal conditions for maximum production
4. To determine the optimal temperature for 5-ALA production. Conducting experiments at different temperatures to find the most effective condition for 5-ALA synthesis using cell lysate.
5. To assess the effect of glycine concentration. Exploring how varying concentrations of glycine, in conjunction with succinate, influence 5-ALA synthesis in a CFME setup.
6. To evaluate the scalability of cell-free 5-ALA synthesis. Conducting experiments with different concentrations of cell lysate and substrates to understand the scalability potential of CFME for 5-ALA production and setting the groundwork for future optimization and industrial scaling.

5.2 Materials and methods

5.2.1 Strains and plasmids

The BL21 strain of *E.coli* was selected for the preparation of lysates in our 5-ALA cell-free synthesis study, leveraging its protease deficiency for enhanced protein stability. Recognized for its robust protein production capabilities and compatibility with a wide array of plasmids, BL21 ensures efficient and high-yield protein expression. Using BL21, we developed the three strains (hemA, L4 and L4 hemA) listed below for this study:

1. WT: This is a BL21 strain served as the control strain.
2. *hemA*: This strain was engineered for the overexpression of *hemA* from *Rhodobacter sphaeroides* DSM 158. The *hemA* gene was amplified through PCR and cloned into the pk184 plasmid, resulting in the pK-*hemA* plasmid. BL21 cells were then transformed with this plasmid, and colonies were selected on LB agar plates supplemented with 50 µg/mL kanamycin.
3. L4: This strain was engineered to repress *hemB* using CRISPR interference (CRISPRi). BL21 cells were co-transformed with pdcas9-bacteria and pgRNA-L4 plasmids, and colonies were selected on LB agar plates supplemented with 100 µg/mL ampicillin and 34 µg/mL chloramphenicol.
4. L4 *hemA*: This strain was a combination of the *hemA* overexpression and *hemB* repression modifications. BL21 cells were transformed with pdcas9-bacteria, pgRNA-L4, and pK-*hemA* plasmids, and colonies were selected on LB agar plates supplemented with 100 µg/mL ampicillin, 34 µg/mL chloramphenicol, and 50 µg/mL kanamycin.

5.2.2 Shake flask cultivation

To facilitate the preparation of cell lysates from BL21 strains of *E. coli*, we followed a modified shake flask protocol that we traditionally employed for product synthesis in *E. coli*, with specific adjustments made to the cultivation medium. The four strains delineated in Section 5.2.1 were initially cultured in 5 ml of LB broth, each supplemented with the required antibiotics to ensure plasmid stability, as previously detailed. These starter cultures were incubated at 37°C, with continuous shaking at 280 rpm in a rotary shaker (New Brunswick Scientific, NJ, USA), allowing for optimal growth conditions overnight. Subsequently, 2 ml of each pre-culture were transferred into 50 ml of Terrific Broth (TB), supplemented with the necessary antibiotics. Concurrently, protein expression was induced: 1 mM of isopropyl β -D-1-thiogalactopyranoside (IPTG) was added for the *hemA* strain, 200 ng/ml of anhydrotetracycline for the L4 strain, and a combination of IPTG and anhydrotetracycline for the L4 *hemA* strain. This strategic addition of inducers directly to the TB medium facilitated a seamless transition to the protein production phase. The cultures were then allowed to proliferate for an additional 4-6 hours at 37°C, maintaining a consistent agitation speed of 280 rpm. This protocol leveraged the nutrient-rich conditions of TB, ensuring vigorous cell growth and high-efficiency protein expression. Following this expression period, cells were collected via centrifugation at 5,000 \times g for 10 minutes at 4°C. This process yielded a cell pellet, suitably prepared for the subsequent steps of lysate preparation.

5.2.3 Cell lysis and extract preparation

To prepare the cell-free extract for our study, the Microson Ultrasonic Cell Disruptor (Misonix, NY, USA) was employed, operating at power level 4 and maintaining a temperature of 4°C, to optimize the balance between efficient cell lysis and the preservation of enzyme integrity. The

bacterial cells, suspended in S30 buffer—consisting of 10 mM Tris-acetate (pH 8.2), 14 mM magnesium acetate, 60 mM potassium acetate, and 1 mM dithiothreitol—created an ideal environment to maintain protein stability throughout the process. We conducted five 10-second sonication bursts, followed by a 30-second cooling on ice. This was done to maximize cell wall disruption while minimizing the potential thermal degradation of sensitive biomolecules. Following the sonication, a centrifugation step at 10,000×g for 10 minutes at 4°C was employed to separate the cellular debris from the supernatant, which was rich in soluble proteins and essential enzymes. To further refine the quality of our extract, the supernatant was filtered through a 0.22 µm membrane filter. At this stage, the extracts were used immediately for cell-free reactions or stored at -80°C to ensure the preservation of enzyme activity for subsequent uses.

5.2.4 Reaction setup for 5-ALA production

To facilitate the cell-free production of 5-ALA, a reaction mixture comprising 2 g/L succinate, 4 g/L glycine, and 400 µl of a pre-arranged cell-free extract was prepared for batch reactions. In contrast, fed-batch reactions involved a staggered addition of 0.5 g/L succinate every hour over four hours, totaling 2 g/L, along with an initial inclusion of 4 g/L glycine and 400 µl of cell-free extract. To investigate the role of co-factors in 5-ALA production, 1 mM ATP and 1 mM CoA were selectively added to certain reactions. Consistent incubation conditions were maintained for all reactions at 30°C with constant agitation at 140 rpm for a duration of four hours, except for experiments specifically aimed at assessing temperature effects on cell-free 5-ALA synthesis. The experiment also entailed varying the amounts of cell lysate and precursor concentrations to deepen our understanding of their impacts on 5-ALA synthesis.

5.2.5 Quantification of 5-ALA

To quantify 5-ALA in the cell-free medium, we prepared a modified Ehrlich's reagent, comprising 4-dimethylaminobenzaldehyde (DMAB) dissolved in a combination of glacial acetic acid and HCl. Given the reagent's sensitivity to light, we stored it in amber glass bottles to ensure its stability and consistent performance in assays. For the quantification procedure, we mixed 0.4 mL of the cell-free reactions with 0.5 mL of the modified Ehrlich's reagent, incubated the mixture at 65°C for 10 minutes, and then allowed it to cool to room temperature. Using a UV-visible spectrophotometer (DU520, Beckman Coulter, Fullerton, CA), we measured the absorbance at 553 nm. A standard curve, created with known concentrations of 5-ALA, facilitated the accurate determination of 5-ALA levels in our samples, with results expressed in milligrams per liter (mg/L). This spectrophotometric method, leveraging the specific interaction between 5-ALA and DMAB in an acidic environment, results in a chromophore with a distinct absorbance peak at 553 nm, ensuring reliable and reproducible quantification for our cell-free reactions.

5.3 Results

5.3.1 Production of 5-ALA through CFME

To optimize 5-ALA production through CFME, we thoroughly examined various parameters in this study, particularly focusing on the genetic modifications of the strains used for cell lysate preparation. Four distinct strains were selected for our experiments: the wild-type BL21 (WT), the L4 strain with *HemB* repression via CRISPRi, the BL21 strain with overexpressed *hemA* from *Rhodobacter sphaeroides* DSM 158, and an L4 strain featuring both *hemB* repression and *hemA* overexpression. We tested the lysates from each strain across different reaction setups, including batch and fed-batch types, under a range of conditions with varying levels of ATP and CoA (Figure 5.1). Simultaneously, we conducted a thorough comparison between the cell-free approach and traditional whole-cell systems to evaluate their efficiency in terms of time and resource utilization (Table 5.1). This analysis aimed to provide a comprehensive understanding of the factors that influence 5-ALA production and to illustrate the benefits of adopting the cell-free approach in biotechnological applications.

Under specific batch reaction conditions (2 g/L succinate and 4 g/L glycine, without ATP and CoA supplementation), the wild-type BL21 (WT) strain produced 0.1 g/L of 5-ALA, while the *hemB*-repressed L4 strain yielded slightly less at 0.07 ± 0.01 g/L (Figure 5.1). Overexpression of *hemA* in BL21 cells markedly increased 5-ALA production, with the *hemA* and *hemA* L4 strains generating 0.42 ± 0.03 g/L and 0.69 ± 0.08 g/L, respectively (Figure 5.1). Supplementing ATP and CoA in batch reactions led to slight increases in 5-ALA production for the WT (0.12 ± 0.01 g/L) and *hemA* (0.45 ± 0.05 g/L) strains, while the *hemA* L4 strain exhibited a substantial increase, reaching 0.81 ± 0.06 g/L of 5-ALA. The L4 strain's performance remained relatively constant, producing 0.07 ± 0.01 g/L, similar to its output without supplements. In fed-batch reactions, where

0.5 g/L succinate was added every hour along with an initial 4 g/L glycine, the WT and L4 strains showed slight increases in 5-ALA production (0.11 ± 0.01 g/L and 0.07 ± 0.01 g/L respectively), while the *hemA* strain increased its production to 0.48 ± 0.04 g/L. Notably, the *hemA* L4 strain achieved the highest 5-ALA yield of 0.95 ± 0.11 g/L under these conditions (Figure 5.1), continuing the trend observed in batch reactions and emphasizing the strain's enhanced production capabilities.

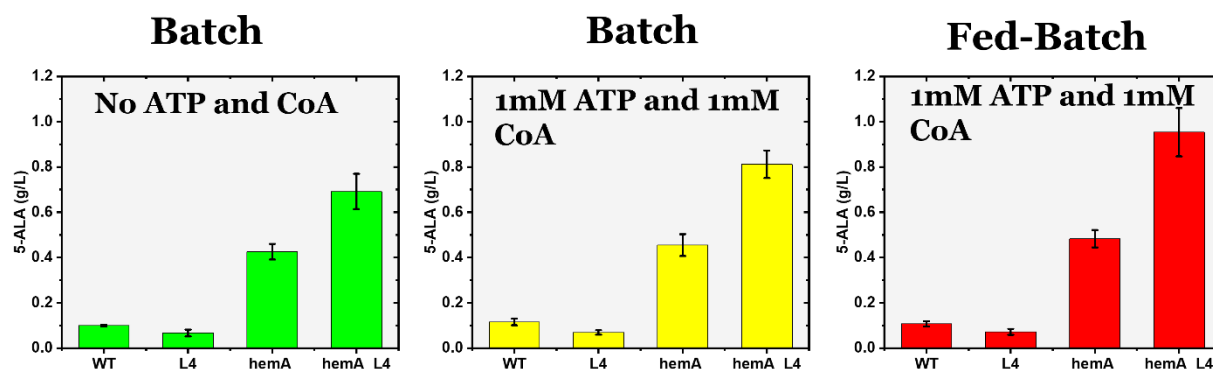


Figure 5.1 5-ALA synthesis via CFME A) Batch reaction with no ATP and CoA addition B) Batch reaction with 1mM ATP and CoA addition C) Fed-Batch reaction with 1mM ATP and CoA addition. 0.5g/L succinate added every hour in the fed-batch reaction whereas 2g/L succinate added in the batch reactions. Glycine concentration was kept at 4g/L in all reactions and added at the start of the reactions. The error bars associated with each data point reflect the standard deviations from duplicate trials.

Simultaneously, we evaluated the operational efficiency and practicality of the CFME approach compared to the traditional whole-cell system (Table 5.1). Both methods required an initial overnight culture and a 4–6-hour seed culture, but the cell-free method distinctly outperformed in synthesis time, completing the process in just 4 hours versus the whole-cell

system's 48 hours. This significant reduction in time not only enhances production efficiency but also opens avenues for cost savings, energy conservation, and optimized resource utilization in facilities. Moreover, the cell-free system demonstrated markedly reduced cell number (3.5 OD₆₀₀), indicating a lesser need for biological materials, which could lead to cost-effective and simpler biomass generation processes. These advantages are crucial for the feasibility and efficiency of large-scale industrial applications, demonstrating the 40-hour time advantage of the CFME approach as highly significant.

Table 5.1 Comparison of whole cell and cell free metabolic engineering efficiency

Parameter	CFME	WCME
Time	<ul style="list-style-type: none"> ▪ Overnight culture (12 h) ▪ 4-6 h Seed culture ▪ 1-2 h Lysate processing ▪ 1 h cultivation set up ▪ <u>4 h synthesis</u> <p>Total= 22-24 h</p>	<ul style="list-style-type: none"> ▪ Overnight culture (12 h) ▪ 4-6 h Seed culture ▪ 1-2 h cultivation set up ▪ <u>48 h synthesis</u> <p>Total= 65-67 h</p>
OD units	3.4 OD₆₀₀ units per reaction	150 OD₆₀₀ units per shake flask culture

Our comprehensive study demonstrates the crucial role of genetic modifications, particularly the overexpression of *hemA* and repression of *hemB*, in enhancing 5-ALA production. We observed modest increases in titer with the addition of ATP and CoA, highlighting these cofactors' roles in cell-free 5-ALA synthesis. Their impact is especially pronounced in genetically optimized strains, such as the *hemA* L4 strain. Furthermore, fed-batch reactions have demonstrated efficacy in 5-ALA production, especially with genetically modified strains. The *hemA* L4 strain consistently outperformed all others across various conditions, suggesting a synergistic effect of

hemB repression and *hemA* overexpression in maximizing 5-ALA yield in a cell-free system. This indicates the potential of cell-free metabolic engineering as a powerful, versatile platform for synthesizing valuable compounds like 5-ALA, setting the stage for more sustainable and cost-effective industrial applications.

5.3.2 Effect of temperature on 5-ALA synthesis

Temperature is a crucial parameter in optimizing cell-free synthesis processes. To determine the optimal temperature for 5-ALA production via CFME using *hemA* L4 strain's cell lysate, we conducted a series of standardized experiments. Each trial, performed at 22°C, 30°C, and 37°C, maintained a consistent 400µl lysate volume and underwent 4 hours of incubation with constant agitation at 140 rpm (Figure 5.2). This approach ensured a uniform experimental setup across all temperature conditions.

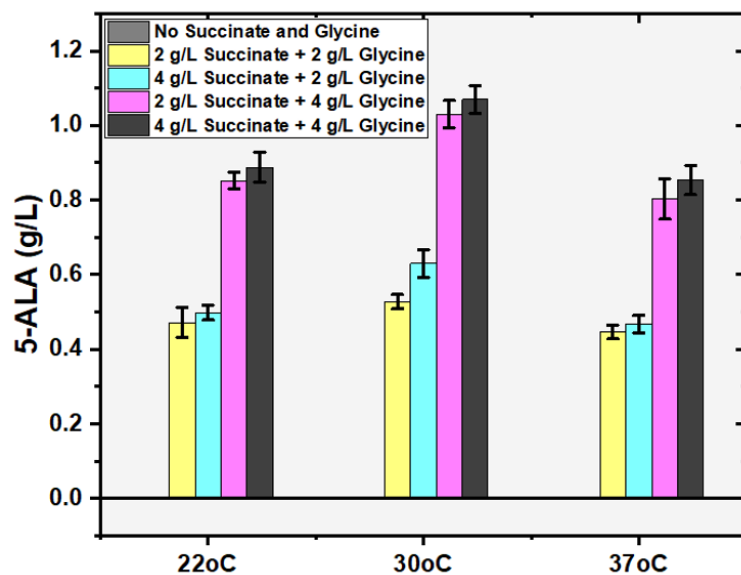


Figure 5.2 Effect of temperature of reaction on CFME based 5-ALA production. The error bars associated with each data point reflect the standard deviations from duplicate trials.

At 22°C, as shown in Figure 5.2, we observed an absence of 5-ALA production in conditions devoid of succinate and glycine. Supplementing the reaction with 2 g/L each of succinate and glycine marked the onset of production, achieving a level of 0.47 ± 0.04 g/L. Increasing the succinate concentration to 4 g/L, while glycine remained at 2 g/L, yielded a modest increase in the 5-ALA titer, registering at 0.50 ± 0.02 g/L. A substantial enhancement was noted with the combination of 2 g/L succinate and 4 g/L glycine, resulting in a titer of 0.85 ± 0.02 g/L. The optimal production at this temperature, 0.89 ± 0.04 g/L, was attained when both succinate and glycine were present at a concentration of 4 g/L. At 30°C, the absence of both reagents once again resulted in a non-detectable level of 5-ALA synthesis. A blend of 2 g/L succinate and 2 g/L glycine marked an improvement in production, yielding a value of 0.53 ± 0.02 g/L. This production level was further elevated to 0.63 ± 0.04 g/L when the succinate concentration was increased to 4 g/L, with glycine fixed at 2 g/L. A substantial increase in 5-ALA production was achieved with 2 g/L succinate and 4 g/L glycine, reaching a titer of 1.03 ± 0.04 g/L. The most favorable condition at this temperature, featuring both succinate and glycine at 4 g/L, led to a peak titer of 1.07 ± 0.06 g/L. At 37°C, the absence of both succinate and glycine still resulted in no 5-ALA production. The utilization of 2 g/L for both reagents culminated in a production value of 0.45 ± 0.02 g/L, while a combination of 4 g/L succinate and 2 g/L glycine saw a slight increase to 0.47 ± 0.02 g/L. The mixture of 2 g/L succinate and 4 g/L glycine led to a production of 0.80 ± 0.05 g/L. Finally, a 4 g/L concentration for both succinate and glycine yielded a titer of 0.85 ± 0.04 g/L.

From these results, it becomes unequivocally clear that the absence of succinate and glycine led to non-detectable 5-ALA levels across all temperatures. Notably, the temperature of 30°C stands out as the optimal condition for 5-ALA synthesis using the *hemA* L4 strain cell lysate. Moreover, the combination of 4 g/L succinate and 4 g/L glycine at this optimal temperature has

proven to be the most efficacious for 5-ALA production (Figure 5.2), underscoring the profound impact of substrate concentrations and temperature in maximizing yield within cell-free metabolic engineering frameworks.

5.3.3 Effect of glycine concentration on 5-ALA synthesis

To elucidate the impact of glycine concentration on 5-ALA synthesis in a cell-free system, we conducted a detailed experiment using cell lysate derived from the *hemA* L4 strain (Figure 5.3). For each trial, we maintained a volume of 400 μ l of cell lysate, ensuring standardized conditions across all tests. The experiment was conducted at a temperature of 30°C with a 4-hour incubation period and a constant agitation rate of 140 rpm, aiming to provide a stable environment for the cell-free synthesis process.

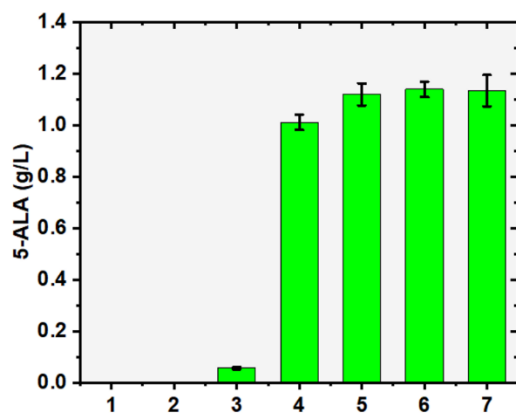


Figure 5.3 Effect of glycine concentration on CFME based 5-ALA production. 1-No Succinate and glycine 2-2 g/L Succinate + No Glycine 3-No Succinate + 4 g/L Glycine 4-2 g/L Succinate + 4 g/L Glycine 5-2 g/L Succinate + 6 g/L Glycine 6-2 g/L Succinate + 8 g/L Glycine 7-2 g/L Succinate + 10 g/L Glycine. The error bars associated with each data point reflect the standard deviations from duplicate trials.

In the absence of both succinate and glycine, 5-ALA production was nonexistent. Similarly, when 2 g/L of succinate was introduced without any glycine, 5-ALA production remained undetectable, highlighting the necessity of glycine for initiating the synthesis process in this cell-free system. Introducing glycine into the system brought about notable changes. In the absence of succinate, but with 4 g/L of glycine present, we observed a modest production of 5-ALA, yielding a titer of 0.06 ± 0.00 g/L. This outcome demonstrates that glycine alone can contribute to 5-ALA synthesis, albeit at a relatively low level. When we combined 2 g/L of succinate with varying concentrations of glycine, a significant increase in 5-ALA production was observed. With 4 g/L of glycine, the production dramatically increased to 1.01 ± 0.03 g/L. Further increases in glycine concentration to 6 g/L and 8 g/L resulted in even higher 5-ALA titers, measuring at 1.12 ± 0.04 g/L and 1.14 ± 0.03 g/L, respectively (Figure 5.3). Interestingly, when the glycine concentration was increased to 10 g/L, in the presence of 2 g/L succinate, the 5-ALA production slightly decreased to 1.13 ± 0.06 g/L.

These results collectively underline the crucial role glycine plays in boosting 5-ALA synthesis within a cell-free setup, particularly when combined with succinate. The data suggest that the optimal glycine concentration for maximizing 5-ALA production lies around 8 g/L, in conjunction with 2 g/L of succinate. This finding is pivotal for refining substrate concentrations in cell-free metabolic engineering, aiming to enhance production yields and efficiency.

5.3.4 Scalability of cell-free 5-ALA synthesis

In our exploration to understand the scalability of cell-free 5-ALA synthesis, we orchestrated a series of experiments employing the cell lysate prepared from the *hemA* L4 strain (Figure 5.4). All trials were conducted at a steady temperature of 30°C, ensuring a consistent environment for the

synthesis process. The incubation period was set at 4 hours with an agitation rate of 140 rpm, aiming to provide optimal conditions for the reaction.

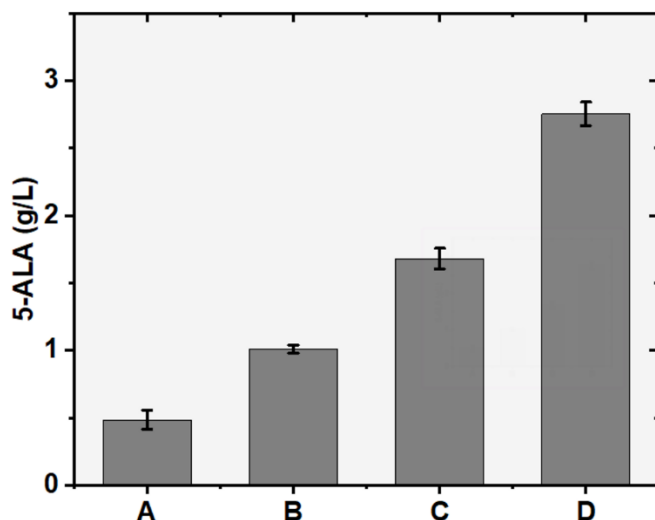


Figure 5.4 Scalability of CFME based 5-ALA production. A=1.75 OD Units plus 1 g/L Succinate + 2 g/L Glycine, B=3.5 OD Units plus 2 g/L Succinate + 4 g/L Glycine, C=7 OD Units plus 4g/L Succinate + 6 g/L Glycine, D=10.5 OD Units plus 6 g/L Succinate + 8 g/L Glycine. The error bars associated with each data point reflect the standard deviations from duplicate trials.

Our initial condition A is comprised of 1.75 OD units of cell lysate, supplemented with 1 g/L succinate and 2 g/L glycine. This setup resulted in a 5-ALA production of 0.48 ± 0.07 g/L, establishing a baseline for our scalability investigation. This modest yield indicates that while 5-ALA synthesis is achievable under these conditions, there is potential for enhancement through the adjustment of cell lysate concentration and substrate availability. We increased the cell lysate concentration to 3.5 OD units and adjusted the substrate concentrations to 2 g/L succinate and 4 g/L glycine in condition B. This alteration led to a notable increase in 5-ALA production, reaching a titer of 1.01 ± 0.03 g/L. This result demonstrates the positive impact of higher cell lysate

concentrations and substrate availability on 5-ALA synthesis, hinting at the scalability of the cell-free system. In condition C, we further increased the cell lysate concentration to 7 OD units, accompanied by an increase in substrate concentrations to 4 g/L succinate and 6 g/L glycine. This setup yielded a 5-ALA production of 1.68 ± 0.08 g/L, illustrating a significant enhancement in synthesis capabilities. This trend of increasing yields with higher cell lysate and substrate concentrations continues to affirm the scalability of the cell-free synthesis process. Reaching our final condition D, we maximized the cell lysate concentration to 10.5 OD units while also increasing the substrate concentrations to 6 g/L succinate and 8 g/L glycine. This combination resulted in an impressive 5-ALA production of 2.75 ± 0.09 g/L, the highest yield observed in our experiment (Figure 5.4). This result solidly demonstrates the scalable nature of cell-free 5-ALA synthesis, highlighting the potential for substantial production increases with the appropriate adjustments to cell lysate and substrate concentrations.

Our comprehensive analysis into the scalability of cell-free 5-ALA synthesis offers crucial insights, particularly highlighting the pronounced increase in 5-ALA production in response to elevated concentrations of cell lysate and substrate. This trend highlights the significant potential of cell-free synthesis, marking a pivotal step towards future optimization and scaling up in this domain. These findings not only affirm the viability of this innovative approach but also open avenues for advancements in CFME, propelling us towards fully harnessing its capabilities for efficient 5-ALA production.

5.4 Discussion

In the preceding results section of this dissertation, we have presented a comprehensive analysis focusing on the optimization of 5-ALA production through CFME. We carefully investigated the effects of various genetic modifications and reaction conditions on the synthesis of 5-ALA. We explored four genetically distinct strains: the wild-type BL21 (WT), the L4 strain with *hemB* repression via CRISPRi, the BL21 strain with overexpressed *hemA* from *R. sphaeroides* DSM 158, and an L4 strain featuring both *hemB* repression and *hemA* overexpression. Our experiments spanned different reaction setups, including batch and fed-batch types, under diverse conditions with varying levels of ATP and CoA. We also compared the cell-free approach with traditional whole-cell systems, evaluating their efficiency in terms of time and resource utilization. Our findings highlighted the significant role of genetic modifications in enhancing 5-ALA yield, the impact of temperature and glycine concentration on synthesis efficiency, and the scalable nature of CFME for 5-ALA production.

The purpose of this discussion is to dive deeper into the implications, significance, and broader context of these findings. We aim to interpret the results in light of existing literature, examine the practical applications and limitations of our study, and suggest directions for future research. This discussion seeks to bridge the gap between our experimental findings and their potential impact on the field of biotechnology, particularly in the synthesis and industrial application of 5-ALA. Through this, we intend to contribute to the ongoing advancements in metabolic engineering and demonstrate the value of CFME as a potent tool in biotechnological innovations.

A key aspect of our study was the investigation into how specific genetic modifications, namely the overexpression of *hemA* and the repression of *hemB*, influence the production of 5-

ALA in CFME systems. Our findings clearly demonstrated that these genetic alterations play a crucial role in enhancing 5-ALA synthesis. The overexpression of *hemA*, a gene integral to the biosynthetic pathway of 5-ALA, resulted in a marked increase in production levels, as evidenced in both the *hemA* and *hemA* L4 strains. This increase was particularly pronounced in the *hemA* L4 strain, which combined *hemA* overexpression with *hemB* repression, underscoring the synergistic effect of these genetic modifications.

In contrast, the wild-type BL21 (WT) strain, lacking these specific genetic enhancements, exhibited relatively lower production levels of 5-ALA. This baseline performance provided a critical reference point for assessing the impact of genetic modifications. The L4 strain, with only *hemB* repression, also showed a distinct production profile, further highlighting the individual contributions of these genetic alterations. When comparing across different reaction conditions, such as batch and fed-batch setups with varying ATP and CoA levels, the modified strains consistently outperformed the WT, with the *hemA* L4 strain often achieving the highest titer. This comparative analysis not only emphasizes the efficacy of targeted genetic modifications in CFME but also offers insights into optimizing strain selection for enhanced 5-ALA production in various operational contexts. Through these findings, our study contributes to a deeper understanding of the genetic determinants in cell-free systems and paves the way for more effective biotechnological applications involving 5-ALA.

The impact of reaction conditions on 5-ALA production was a significant focus of our research, particularly examining the differences between batch and fed-batch setups and the role of ATP and CoA supplementation. In batch reactions, where substrates were added at the beginning without further supplementation, we observed a baseline production of 5-ALA across all strains. However, when we switched to fed-batch reactions, which involve the continuous or

periodic addition of substrates, there was a noticeable increase in 5-ALA production. This increase was most pronounced in the genetically modified strains, especially the *hemA* L4 strain, highlighting the efficiency of fed-batch processes in sustaining and enhancing metabolic activities in CFME systems.

The supplementation of ATP and CoA, key cofactors in metabolic pathways, also played a critical role in modulating 5-ALA production. Our results indicated that the addition of these cofactors led to increased 5-ALA yields in both batch and fed-batch setups. The impact of ATP and CoA was particularly evident in the genetically modified strains, where the provision of these cofactors facilitated more efficient biosynthetic processes. Interestingly, the extent of the increase varied among different strains, suggesting a complex interaction between genetic factors and the availability of metabolic cofactors. This aspect of our study not only sheds light on the optimization of reaction conditions for enhanced 5-ALA production but also points out the complex interplay between genetic modifications and reaction environments in CFME. By analyzing these factors, our research provides valuable insights into the development of more efficient and productive CFME processes, particularly for the synthesis of valuable compounds like 5-ALA.

In our exploration of optimizing 5-ALA synthesis, a critical focus was also placed on understanding the effects of temperature and glycine concentration, two key factors that significantly influence metabolic reactions. Our study systematically examined 5-ALA production at various temperatures (22°C, 30°C, and 37°C) and glycine concentrations. We discovered that the synthesis of 5-ALA was dependent on these parameters. At 30°C, a notable peak in 5-ALA production was observed, indicating this temperature as the optimal condition for the *hemA* L4 strain's cell lysate activity. This finding indicates the importance of maintaining an ideal thermal environment for enzymatic and metabolic stability in CFME systems. Furthermore, the

concentration of glycine, a critical precursor in the 5-ALA biosynthetic pathway, markedly influenced production levels. Our results revealed a direct correlation between increased glycine concentrations and enhanced 5-ALA titers, with an optimal concentration of around 8 g/L, in conjunction with 2 g/L of succinate. However, it was also observed that beyond this concentration, the production rate plateaued and even slightly decreased, suggesting a limit to the beneficial effects of glycine supplementation. These findings on temperature and glycine concentration provide crucial insights for optimizing cell-free synthesis processes. Identifying these optimal conditions is paramount for maximizing 5-ALA yield, offering a valuable guideline for future endeavors in metabolic engineering and biotechnological production of 5-ALA and similar compounds. This part of our study not only contributes to the fundamental understanding of cell-free system parameters but also has significant practical implications for enhancing the efficiency and effectiveness of industrial-scale 5-ALA production.

Another vital aspect of our research involved assessing the scalability and operational efficiency of the CFME process for 5-ALA production. Scalability, a crucial factor for industrial application, was evaluated through a series of experiments that varied the concentrations of cell lysate and substrates. Our findings demonstrated a positive correlation between increased concentrations of cell lysate and substrates and 5-ALA titer, signifying the CFME system's capacity for scaling. Particularly, the significant increase in 5-ALA production with higher cell lysate concentrations, from 1.75 OD₆₀₀ units to 10.5 OD₆₀₀ units, alongside the escalated substrate levels, exemplified the system's scalability. This trend highlights the CFME's adaptability to varying scales of operation, a key attribute for its application in large-scale industrial processes. In terms of operational efficiency, our study compared CFME with traditional whole-cell systems. The CFME approach exhibited a remarkable reduction in synthesis time, completing the process

in just 4 hours compared to the 48 hours required by whole-cell systems. This substantial time efficiency is a critical advantage in industrial settings where time equates to cost and resource allocation. Moreover, the cell-free system required a markedly reduced cell number, indicating a lower demand for biological materials and potentially simpler biomass handling processes. This aspect of CFME not only suggests a more cost-effective approach but also aligns with sustainable practices by minimizing resource consumption. Our analysis of scalability and operational efficiency firmly establishes CFME as a superior method for synthesizing 5-ALA, offering a viable and more efficient alternative to traditional methods. This advancement in CFME technology represents a significant progress in biotechnological production for 5-ALA and other biochemicals, setting the stage for more sustainable, efficient, and scalable industrial applications.

In contextualizing our findings within the broader scientific landscape, a comparative analysis with existing literature was conducted to discern the novelty and implications of our research on 5-ALA production via CFME. Our study's emphasis on the synergistic effects of genetic modifications in CFME, particularly the overexpression of *hemA* and repression of *hemB*, presented novel insights. Previous studies have individually explored the roles of these genetic factors, but often within whole-cell systems (Miscевич et al., 2021; Su et al., 2019). Our research extends this understanding by demonstrating their amplified impact in a cell-free context, which has not been documented before. The scalability and efficiency of CFME demonstrated in our research also mark a significant contribution to the field. While earlier studies have acknowledged the potential of CFME (Grubbe et al., 2020; Perez et al., 2016), our findings provide concrete evidence of its superiority over traditional whole-cell systems in terms of time efficiency and scalability. This not only corroborates but also extends existing knowledge by offering a quantifiable assessment of the advantages of CFME.

The findings from our study on optimizing 5-ALA production through CFME hold substantial practical implications and potential applications in various industrial and biotechnological domains. The enhanced production rates achieved through genetic modifications and optimal reaction conditions, particularly the overexpression of *hemA* and repression of *hemB*, open avenues for more efficient 5-ALA synthesis in large-scale manufacturing. In industrial settings, the ability to produce 5-ALA efficiently is crucial, given its widespread applications in agriculture as a plant growth enhancer, in medicine for photodynamic therapy and cancer treatment, and as a precursor in the synthesis of various biologically active compounds.

The operational efficiency and scalability of CFME, demonstrated in our research, are particularly relevant for industrial applications. The reduced synthesis time and lower biological material requirements compared to traditional whole-cell systems not only ensure cost-effectiveness but also align with sustainable manufacturing practices. Industries focusing on bio-production can leverage these advantages to scale up their production processes, meeting the growing demand for 5-ALA in a cost-effective and environmentally friendly manner.

Furthermore, our study's elucidation of optimal conditions for 5-ALA production, especially concerning temperature and substrate concentration, provides a valuable framework for industrial setups. By tailoring these conditions, industries can maximize their yield, reduce resource waste, and optimize process efficiency. The versatility and adaptability of CFME highlighted in our study suggest its potential application in synthesizing other valuable compounds, expanding the horizons of biotechnological innovations. In summary, our findings not only enhance the current understanding of CFME but also offer practical strategies for its implementation in industrial and biotechnological applications, potentially revolutionizing the way biochemicals like 5-ALA are produced on a commercial scale.

While our study provides significant insights into optimizing 5-ALA production via CFME, it is important to acknowledge certain limitations and challenges encountered during the research process. One notable limitation was the scale of our experimental setup, which, while sufficient for laboratory-scale analysis, may not fully replicate the complexities and variables present in large-scale industrial processes. This gap suggests the need for further research to validate our findings in a larger production environment. Additionally, while we explored a range of genetic modifications, temperature, and substrate concentrations, other potentially influential parameters, such as pH levels and ionic strength, were not extensively examined. These unexplored parameters could play a significant role in optimizing CFME for 5-ALA production and warrant further investigation. Another challenge was the precision of quantifying the effects of genetic modifications in a cell-free context. The interaction between various genetic and environmental factors is highly complex and dissecting these interactions to precisely attribute improvements in 5-ALA yield posed a considerable challenge. Moreover, the comparative analysis of CFME with traditional whole-cell systems, while comprehensive, could benefit from a broader range of comparative metrics to fully encapsulate the efficiency and scalability advantages of CFME.

Chapter 6

Production of heme and heme derived pigments using engineered

E. coli

6.1 Introduction

Heme, an iron-containing molecule, is fundamental to various biological functions, including oxygen transport in hemoglobin and catalysis of enzymatic reactions, illustrating its critical role in sustaining life processes (Choi et al., 2022; Frankenberg et al., 2003). Its importance broadens beyond biological functions to diverse industrial applications, such as the development of therapeutic agents and diagnostic tools in medicine and replicating the sensory attributes of traditional meats in the expanding plant-based meat industry, offering sustainable and ethical alternatives (Di Pierro and Granata, 2020; Fontanellas et al., 2016; Ko et al., 2021; Yang et al., 2023). Traditional methods of heme production, primarily reliant on natural extraction, confront challenges regarding sustainability and scalability (Ko et al., 2021; Yang et al., 2023). In response, advancements in metabolic engineering have shifted towards efficient microbial synthesis using *E. coli*. This approach not only enhances production efficiency but also supports environmental sustainability, presenting a scalable, eco-friendly solution that aligns with global sustainability goals while addressing increasing market demands methods (Choi et al., 2022; Ko et al., 2021; Su et al., 2023; Yang et al., 2023).

Building on these developments, heme derivatives such as biliverdin, Phycocyanobilin (PCB), and Phycoerythrobilin (PEB) are garnering attention for their therapeutic, diagnostic, and coloring roles. The growing demand for these derivatives is indicative of a global trend toward sustainable and natural products, particularly in the food and cosmetic industries (Eriksen, 2013;

Joshi et al., 2018; Morone et al., 2019; Mourelle et al., 2017). While biotechnological advancements, notably in *E. coli* metabolic engineering, have shown promise in the production of these pigments, challenges persist in terms of scalability and cost-effectiveness. Overcoming these challenges is essential for enhancing their commercial viability and expanding their accessibility in various industries.

Our research employs advanced synthetic biology and enzyme screening to overcome natural regulatory barriers and metabolic bottlenecks, facilitating scalable and sustainable production of these high-value compounds. This attempt is not just about fulfilling existing market demands; it represents a forward-looking approach to exploring new applications and markets for heme derivatives (Eriksen, 2013; Joshi et al., 2018; Morone et al., 2019; Mourelle et al., 2017). The growing market for heme and its derivatives, driven by the increasing demand for natural colorants and the therapeutic potential of these pigments, indicates the need to refine biomanufacturing processes to meet diverse industry requirements for quality, safety, and volume.

This last chapter of the dissertation asserts that through advanced genetic and cell-free metabolic engineering, *E. coli* can be optimized for the efficient biosynthesis of heme and its derivatives. Key objectives include developing a precise HPLC analytical method, implementing an innovative C-4 heme synthesis pathway via overexpression of the *hemA* gene, exploiting cell-free systems to transcend the production limits of in vivo processes, and identifying optimal enzymes for converting heme into its derivatives. These strategic initiatives are aimed at meeting the burgeoning industrial demand for these compounds with an innovative, efficient, and sustainable production methodology.

Hypothesis and objectives of this chapter are:

Hypothesis: Utilizing genetically engineered *E. coli* strains and applying cell-free metabolic engineering techniques can enhance the production of heme and its derivatives, including biliverdin, Phycocyanobilin (PCB), and Phycoerythrobilin (PEB). This hypothesis is based on the observation that specific genetic modifications in *E. coli*, particularly the overexpression of the *hemA*, *hemB*, *hemG*, and *hemH* genes, coupled with the application of cell-free systems, can overcome typical challenges faced in whole-cell systems, such as feedback inhibition and cofactor imbalances. We anticipate that these combined approaches will result in increased yields and improved process efficiency in the biosynthesis of heme, leading to more effective and sustainable production methods suitable for industrial applications. The rationale behind this hypothesis is grounded in the demonstrated potential of *E. coli* as a robust host for metabolic engineering and the advantages of cell-free systems in offering greater control and flexibility over biosynthetic processes.

Objectives:

1. To establish a robust and high-throughput analytical platform using HPLC that can accurately separate and quantify heme, biliverdin, and PCB, thereby providing a foundational tool for monitoring and optimizing the production process.

2. To implement and evaluate the efficiency of a novel C-4 heme synthesis pathway in *E. coli* by overexpressing the *hemA* gene from *R. sphaeroides*, with the aim of increasing the production yield and simplifying the regulatory landscape of heme biosynthesis.
3. To leverage cell-free metabolic engineering techniques to enhance heme production, determining the optimal conditions and cofactor requirements that lead to improved yields beyond what is achievable with *in vivo* systems.
4. To screen for and identify the most effective enzymes from a diverse set of organisms for each step in the conversion of heme to biliverdin, and subsequently to PCB and PEB, thereby optimizing the enzymatic transformation processes within *E. coli*.
5. To optimize the expression and activity of selected enzymes in *E. coli* for increased production of biliverdin, PCB, and PEB, using visual color assessment as a preliminary indicator of synthesis efficiency and proceeding to detailed quantitative analyses.

6.2 Materials and methods

6.2.1 Chemicals and enzymes

Chemical reagents for this research were primarily procured from Sigma-Aldrich Co. (St. Louis, MO, USA), apart from yeast extract and tryptone, which were supplied by BD Diagnostic Systems (Franklin Lakes, NJ, USA). Analytical standards for heme and biliverdin were obtained from Toronto Research Chemicals (TRC, Toronto, Canada), and Phycocyanobilin (PCB) was sourced from Frontier Specialty Chemicals (Logan, Utah, USA). Molecular biology enzymes, including Phusion™ High-Fidelity DNA Polymerase and NEBuilder® HiFi DNA Assembly Master Mix, were purchased from New England Biolabs (NEB, Ipswich, MA, USA). Plasmid purification was conducted using the EZ-10 Spin Column Plasmid DNA Miniprep Kit from Bio Basic Inc. (Markham, ON, Canada), while the QIAquick PCR & Gel Cleanup Kit from Qiagen was utilized for the purification of PCR amplifications and gel extractions. Oligonucleotides and synthetic gene sequences were acquired from Integrated DNA Technologies (IDT, Coralville, IA, USA).

6.2.2 Bacterial strains and plasmids

We utilized *E. coli* HI-Control™ 10G chemically competent cells (from Lucigen, Wisconsin, USA) for plasmid propagation and cloning. For applications involving whole-cell metabolic engineering, we used the Sbm *E. coli* strain, a genetically modified variant of the parent BW25113 strain. BL21 cells were employed for cell-free metabolic engineering experiments. The specifics of the bacterial strains, plasmids, and primers we used are detailed in Table 6.1 and Table 6.2.

Our engineering efforts were primarily focused on incorporating the C4 heme synthesis pathway into the Sbm and BL21 production strains. This involved the heterologous expression of

the *hemA* gene, which we sourced from *Rhodobacter sphaeroides*. We cloned this gene into the pK184 vector to create the pK184-*hemA* construct, thereby transforming the *E. coli* strains to facilitate *hemA* production. To develop strains overexpressing both *hemA* and *hemB*, we amplified the *hemB* gene from the genomic DNA of BL21 cells using the primers hemB-hemA.FOR and hemB-pk184.REV. We then integrated this gene into a linearized pK184-*hemA* plasmid, which we had prepared via PCR with the primers pK18:hemA-hemB.FOR and pk184:hemA-hemB.REV. The resulting construct, pK184-*hemA-hemB*, was assembled using the NEBuilder® HiFi DNA Assembly Master Mix. We then extended our work to create strains that could also express *hemG*, termed hemABG strains. The *hemG* gene was PCR-amplified from BL21 genomic DNA using the primer set hemG-hemB.FOR/hemG-pk184.REV. We inserted this product into the pre-linearized pK184-*hemA-hemB* vector using the primer sets pK184-*hemG.FOR/hemB-hemG.REV*. Following a similar method, we created hemABGH strains by amplifying the *hemH* gene with the primers hemH-hemG.FOR/hemH-pK184.REV. This gene was then cloned into the pK184-*hemA-hemB-hemG* plasmid, which had been linearized using the primer pair pK184-*hemH.FOR/hemG-hemH.REV*. In all cloning steps, we included ribosomal binding sites (RBS) between each gene to support efficient translation. This careful cloning approach arranged the *hemA*, *hemB*, *hemG*, and *hemH* genes in tandem within the pK184 vector.

Table 6.1 List of primers used for exploring heme and its derivatives production

Primers	Sequence (5'-3')
hemB-hemA.FOR	CCTGAATTCACACAGGAAACAGACCATGACAG ACTTAATCCAACGCC
hemB-pk184.REV	AATTCGTAATCATTAAACGCAGAATCTTCTTCTC AGC
pK18:hemA-hemB.FOR	ATTCTGCGTTAAATGATTACGAATTCGAGCTCGG
pk184:hemA-hemB.REV	GTCATGGTCTGTTTCCTGTGTGAAATTCAGGCAA CGACCTCGG
hemG-hemB.FOR	CGTTAAATTCACACAGGAAACAGACCGTGAAA ACATTAATTCTTTTCTCAACAAGG
hemG-pk184.REV	AATTCGTAATCATTTATTTACAGCGTCGGTTTGTCG
pK184-hemG.FOR	ACGCTGAAATAAATGATTACGAATTCGAGCTCG G
hemB-hemG.REV	GTTTTACGGTCTGTTTCCTGTGTGAAATTTAACG CAGAATCTTCTTCTCAGC
hemH-hemG.FOR	GCTGAAATAAATTTACACAGGAAACAGACCAT GCGTCAGACTAAAACCGG
hemH-pK184.REV	AATTCGTAATCATTTAGCGATACGCGGCAACAA
pK184-hemH.FOR	GCGTATCGCTAAATGATTACGAATTCGAGCTCGG
hemG-hemH.REV	TAGTCTGACGCATGGTCTGTTTCCTGTGTGAAAT TTATTTACGCGTCGGTTTGTCG
pTrc99a-HO2582 optm.FOR	ACGTGAAGTATTTGCGGGATCTTGAGAATTCGAG CTCGGTACCCG
pTrc99a-HO2582 optm.REV	GTAAAGGGGAATGTAACGGCAGTCATGGTCTGT TTCCTGTGTGAAATTGT
2308opt_2582opt.FOR	GCGGGATCTTGAATTTACACAGGAAACAGACC ATGAGTTTACGCCAACATCAACATCC
2308opt_pTrc99a.REV	CGAGCTCGAATTCCTAAACGGGGGGGACATCAA AAAG
pTrc99a_2308opt.FOR	CCCCCGTTTAGGAATTCGAGCTCGGTACCCG
2502opt_2308opt.REV	GGCGTAAACTCATGGTCTGTTTCCTGTGTGAAAT TCAAGATCCCGCAAATACTTCACGTAAT
PSSM2 opt_2582 opt.FOR	GCGGGATCTTGAATTTACACAGGAAACAGACC ATGACTAAGAATCCGCGCAATAACAAAC
PSSM2opt_2582opt.REV	CGAGCTCGAATTCCTCATTTATAAGAAAAAAGGA AGTCGTTTACGAACGC
2582opt_PSSMopt.FOR	TCTTATAAATGAGAATTCGAGCTCGGTACCC
2582opt_PSSM2opt.REV	GATTCTTAGTCATGGTCTGTTTCCTGTGTGAAAT CAAGATCCCGCAAATACTTCACGTAAT

Table 6.2 List of plasmids used for exploring heme and its derivatives production.

Plasmid name	Overexpressed genes	Source
pK184-hemA	<i>hemA</i>	(76)
pK184-hemA-hemB	<i>hemA</i> and <i>hemB</i>	This study
pK184-hemA-hemB-hemG	<i>hemA</i> , <i>hemB</i> and <i>hemG</i>	This study
pK184-hemA-hemB-hemG-hemH	<i>hemA</i> , <i>hemB</i> , <i>hemG</i> and <i>hemH</i>	This study
pTrc99a-HO2582 optm	HO	This study
pTrc99a-HO2582opt- pcyAtII2308otp	HO and <i>pcyA</i>	This study
pTrc99a-HO2582(opt)-pebS (PSSM2 opt)	HO and <i>pebS</i>	This study
Strains name		This study
Sbm-hemA	<i>hemA</i>	This study
Sbm-hemAB	<i>hemA</i> and <i>hemB</i>	This study
Sbm-hemABG	<i>hemA</i> , <i>hemB</i> and <i>hemG</i>	This study
Sbm-hemABGH	<i>hemA</i> , <i>hemB</i> , <i>hemG</i> and <i>hemH</i>	This study
BL21-hemA	<i>hemA</i>	This study
BL21-hemAB	<i>hemA</i> and <i>hemB</i>	This study
BL21-hemABG	<i>hemA</i> , <i>hemB</i> and <i>hemG</i>	This study
BL21-hemABGH	<i>hemA</i> , <i>hemB</i> , <i>hemG</i> and <i>hemH</i>	This study
HO	HO	This study
HO-pcyA	HO and <i>pcyA</i>	This study
HO-pebS	HO and <i>pebS</i>	This study

We also developed *E. coli* strains for the synthesis of biliverdin, phycocyanobilin (PCB), and phycoerythrobilin (PEB) through the construction of specific plasmids. The pTrc99a-HO2582 optm plasmid for biliverdin production was assembled by PCR linearization of the pTrc99a vector using the primer set pTrc99a-HO2582 optm.FOR and pTrc99a-HO2582 optm.REV, followed by the integration of an optimized synthetic heme oxygenase gene from *Pseudomonas putida*. This plasmid was introduced into the Sbm *E. coli* strain to create the HO strain. For PCB, the pTrc99a-

HO2582opt-*pcyAtII2308otp* plasmid was synthesized by amplifying the optimized *pcyA* gene from *Thermosynechococcus elongatus* BP-1 using the primer 2308opt_2582opt.FOR and combining it with the linearized pTrc99a-HO2582 optm vector, previously linearized with primers pTrc99a_2308opt.FOR and 2502opt_2308opt.REV. The pTrc99a-HO2582opt-*pcyAtII2308otp* construct was then introduced into the Sbm *E. coli* strain, generating the HO-*pcyA* strain for PCB production. In the case of PEB production, the codon-optimized *pebS* gene from *Prochlorococcus phage* P-SSM2 was PCR-amplified using the primers PSSM2_opt_2582_opt.FOR and PSSM2_opt_2582_opt.REV. This gene was subsequently integrated into a pre-linearized pTrc99a-HO2582 optm vector using the primers 2582_opt_PSSMopt.FOR and 2582_opt_PSSM2opt.REV to form the pTrc99a-HO2582(opt)-*pebS* (PSSM2_opt) plasmid. The transformation of this plasmid into the Sbm *E. coli* strain led to the establishment of the HO-*pebS* strain. All plasmid assemblies were conducted using NEBuilder® HiFi DNA Assembly Master Mix, with ribosomal binding sites (RBS) strategically introduced between genes to optimize translational efficiency, and detailed sequences of these codon-optimized genes are presented in Appendix 2.

6.2.3 Media and cultivation conditions

For the cultivation of *E. coli* strains, we maintained glycerol stock cultures at -80°C. These stocks were plated on lysogeny broth (LB) agar containing 10 g/L tryptone, 5 g/L yeast extract, and 5 g/L NaCl, augmented with specific antibiotics: 100 mg/L ampicillin, 50 mg/L kanamycin, and 25 mg/L chloramphenicol. The plates were incubated at 37°C for 14-16 hours to facilitate bacterial growth. Following this, we initiated shake-flask cultivation by transferring single colonies from the LB agar plates into 30 mL LB medium in 125 mL conical flasks. These flasks were then incubated in a rotary shaker (New Brunswick Scientific, NJ, USA) at 37°C with an agitation speed of 280 rpm

to develop seed cultures. For larger volume cultivation, 1% (v/v) of these seed cultures were used to inoculate 220 mL of LB medium supplemented with the appropriate antibiotics in 1 L conical flasks. These cultures were also incubated in the rotary shaker under the same conditions until the optical density at 600 nm (OD_{600}) reached 0.80. At this point, the cells were harvested via centrifugation at $9,000\times g$ for 10 minutes at $20^{\circ}C$ and resuspended in 30 mL of modified M9 production medium. The modified M9 medium consisted of 25 g glycerol, 5 g yeast extract, 10 mM $NaHCO_3$, 1 mM $MgCl_2$, and 200 mL M9 salts mix per liter. The M9 salts mix comprised 33.9 g Na_2HPO_4 , 15 g KH_2PO_4 , 5 g NH_4Cl , and 2.5 g $NaCl$. Additionally, the medium included a 1 ml/L dilution of Trace Metal Mix A5, supplying essential trace elements: 2.86 g/L H_3BO_3 , 1.81 g/L $MnCl_2\cdot 4H_2O$, 0.222 g/L $ZnSO_4\cdot 7H_2O$, 0.39 g/L $Na_2MoO_4\cdot 2H_2O$, 79 $\mu g/L$ $CuSO_4\cdot 5H_2O$, and 49.4 $\mu g/L$ $Co(NO_3)_2\cdot 6H_2O$. For inducing protein expression, 0.1 mM isopropyl β -D-1-thiogalactopyranoside (IPTG) was also added to the medium.

For bioreactor cultivation, we adopted a protocol paralleling the shake-flask method but utilized super broth (SB) medium instead. This medium, with its enhanced nutrient profile, contains 32 g/L tryptone and 20 g/L yeast extract, offering a richer environment for bacterial growth. The inoculation was carried out in 125 mL conical flasks, followed by overnight incubation at $37^{\circ}C$ and 280 rpm. After this incubation, the cells were harvested and resuspended in fresh LB medium. This suspension served as the inoculum for a 1 L stirred tank bioreactor (CelliGen 115, Eppendorf AG, Hamburg, Germany), which is equipped with two Rushton radial flow disks to ensure effective mixing. The production medium in the bioreactor was a semi-defined formulation, comprising 30 g/L glycerol, 0.23 g/L K_2HPO_4 , 0.51 g/L NH_4Cl , 49.8 mg/L $MgCl_2$, 48.1 mg/L K_2SO_4 , 1.52 mg/L $FeSO_4$, 0.055 mg/L $CaCl_2$, 2.93 g/L $NaCl$, 0.72 g/L tricine, and 10 g/L yeast extract. It also included 10 mM $NaHCO_3$ and the same trace elements solution as used

in the shake-flask method, supplemented with isopropyl β -D-1-thiogalactopyranoside (IPTG) to induce protein expression. During the cultivation process within the bioreactor, we maintained aerobic conditions by purging air at a rate of 1 volume of air per volume of culture per minute (vvm). The pH of the medium was consistently monitored and controlled at 7.0 ± 0.1 . Adjustments were made using 30% (v/v) NH_4OH for increasing alkalinity and 15% (v/v) H_3PO_4 for acidification, optimizing conditions for bacterial growth and production. This controlled environment in the bioreactor was pivotal for ensuring optimal bacterial growth and efficient production processes.

6.2.4 PCR amplification and plasmid isolation protocols

Plasmid DNA was extracted from bacterial cultures using the QIAquick PCR & Gel Cleanup Kit (Qiagen) according to the manufacturer's instructions. Briefly, bacterial colonies were inoculated into LB medium supplemented with the appropriate antibiotic and grown overnight at 37°C with shaking at 280 rpm. Following overnight growth, cells were harvested by centrifugation, and the pellet was resuspended in the provided buffer. The subsequent lysis and neutralization steps were performed as per the kit's protocol. The lysate was then applied to the QIAquick spin column, and after a series of washing steps, plasmid DNA was eluted in the provided elution buffer.

For PCR amplification, the PhusionTM High-Fidelity DNA Polymerase from New England Biolabs (NEB Canada) was employed. Reaction mixtures were set up as follows: 1x Phusion HF buffer, 200 μM of each dNTP, 0.5 μM of forward and reverse primers, 0.02 U/ μl Phusion DNA polymerase, and approximately 10 ng of template DNA in a total volume of 50 μl . The thermocycling conditions typically commenced with an initial denaturation at 98°C for 30 seconds, followed by 30 cycles of denaturation at 98°C for 10 seconds, annealing (temperature dependent

on the primers used) for 30 seconds, and extension at 72°C (time dependent on the expected amplicon size). A final extension step at 72°C for 10 minutes was included to ensure complete amplification.

For colony PCR, a single bacterial colony was picked using a sterile pipette tip and resuspended in 20 µl of sterile distilled water. This suspension was then boiled for 10 minutes to lyse the cells and release the DNA. After a brief centrifugation, 2 µl of the supernatant was used as a template for the PCR, with the aforementioned Phusion™ High-Fidelity DNA Polymerase protocol. This method allowed for rapid screening of bacterial colonies for the presence of the desired plasmid constructs.

6.2.5 Transformation of *E. coli*

Transformation of *Escherichia coli* was executed using the *E. coli* HI-Control™ 10G chemically competent cells. Initially, plasmid DNA (typically 1-5 ng) was mixed with 50 µl of the competent cells in a pre-chilled microcentrifuge tube. This mixture was incubated on ice for 30 minutes, ensuring the DNA uptake by the cells. Following the incubation, a heat shock was applied by placing the tube in a 42°C water bath for exactly 45 seconds. The tube was then immediately transferred back to ice for a 2-minute incubation. Subsequently, 950 µl of pre-warmed LB medium was added to the cells, which were then incubated at 37°C with shaking at 280 rpm for 1 hour to allow recovery and expression of the antibiotic resistance marker. Post-recovery, the transformed cells were plated onto LB agar plates supplemented with the appropriate antibiotic and incubated overnight at 37°C for colony development.

6.2.6 Cell lysis and extract preparation

To prepare the cell-free extract for our study, the Microson Ultrasonic Cell Disruptor (Misonix, NY, USA) was employed, operating at power level 4 and maintaining a temperature of 4°C, to optimize the balance between efficient cell lysis and the preservation of enzyme integrity. The bacterial cells, suspended in S30 buffer—consisting of 10 mM Tris-acetate (pH 8.2), 14 mM magnesium acetate, 60 mM potassium acetate, and 1 mM dithiothreitol—created an ideal environment to maintain protein stability throughout the process. We conducted five 10-second sonication bursts, followed by a 30-second cooling on ice. This was done to maximize cell wall disruption while minimizing the potential thermal degradation of sensitive biomolecules. Following the sonication, a centrifugation step at 10,000×g for 10 minutes at 4°C was employed to separate the cellular debris from the supernatant, which was rich in soluble proteins and essential enzymes. To further refine the quality of our extract, the supernatant was filtered through a 0.22 µm membrane filter. At this stage, the extracts were used immediately for cell-free reactions or stored at -80°C to ensure the preservation of enzyme activity for subsequent uses.

6.2.7 Reaction setup for heme production

For the investigation of cell-free heme biosynthesis, reaction vials were systematically labeled to correspond to each bacterial strain under examination as well as to the distinct experimental conditions, encompassing both experimental samples and necessary controls. To each vial, 500 µL of cell-free extract—derived from either BL21 or BL21 hemABGH strains—was carefully aliquoted. The biosynthetic pathway was initiated by the addition of 1 g/L 5-aminolevulinic acid (5-ALA), serving as the substrate for the enzymatic cascade leading to heme production. In a subset of reactions, 500 µM Ammonium iron (III) citrate was included to supply iron, an essential

cofactor in the heme assembly process. The vials were then placed in an incubator set at a stable temperature of 30°C, with a constant agitation speed of 140 rpm, to maintain an environment conducive to the enzymatic reactions required for heme generation. This incubation setup was upheld for a duration of 24 hours.

6.2.8 Heme and heme-derivatives extraction

Heme and its derivatives were extracted using a two-phase separation method. Samples were treated with a 20% hydrochloric acid (HCl) and 80% chloroform mixture, incubated at 50°C for 1 hour with intermittent vortexing to ensure complete mixing. After cooling to ambient temperature, 3 mL of deionized water was added to each sample to facilitate phase separation. The mixture was then centrifuged at 4000 rpm for 15 minutes. The lower chloroform phase containing heme was carefully collected. To prepare for analysis, the chloroform was evaporated and heme and its derivatives were reconstituted in an appropriate solvent for HPLC based assessment.

6.2.9 Analytical method for simultaneous separation and quantification of heme, biliverdin and PCB

For the simultaneous separation of heme and bilins, a reverse phase HPLC method was employed using The Waters HPLC system equipped with The Waters 2998 photodiode array detector. The detector was set to perform a full scan from 200-800nm. The chromatographic separation was achieved on a Luna C(18)2 Phenomenex column. Samples were prepared in a mixture of 90% methanol and 10% DMSO and were injected at a volume of 10µL. The flow rate was maintained at 1.2 ml/min. The mobile phase consisted of solvent A (1:9 Methanol: Acetonitrile) and solvent

B (0.5% TFA at pH 2.6). The HPLC method followed a linear gradient over 20 minutes. Initially, at time 0, the mobile phase composition was set at 60% A and 40% B. By 20 minutes, it shifted to 100% A and 0% B, maintaining this composition until 30 minutes. At 31 minutes, the composition reverted to 60% A and 40% B and remained constant until 40 minutes.

6.3 Result

6.3.1 Efficient HPLC method for simultaneous separation of heme, biliverdin and PCB

In our study, we faced a challenge of analyzing the biochemical transformations from heme to biliverdin and further to Phycocyanobilin (PCB). This sequence of transformations demanded a methodological approach capable of precise separation and identification of these distinct compounds. To address this need, we meticulously developed an advanced High-Performance Liquid Chromatography (HPLC) method. This technique is specifically tailored to efficiently separate and concurrently analyze heme, biliverdin, and PCB. The HPLC method's robustness and precision are pivotal in providing clear, distinct chromatographic profiles for each compound, thereby ensuring accurate qualitative and quantitative assessment of their transformation processes. This analytical advancement not only enhances the reliability of our biochemical analyses but also contributes significantly to the understanding of these complex metabolic pathways.

We utilized Waters HPLC system in conjunction with a Waters 2998 photodiode array detector. This setup was pivotal in enabling an extensive spectral scanning range from 200 to 800 nm, which is crucial for accurately discerning the unique spectral profiles of heme, biliverdin, and Phycocyanobilin (PCB). For chromatographic separation, we opted for a Luna C(18)2 Phenomenex column, renowned for its superior efficacy in differentiating a broad array of substances. The methodological precision of our approach was further enhanced by our carefully formulated sample matrix, consisting of 90% methanol and 10% Dimethyl Sulfoxide (DMSO). We consistently injected a sample volume of 10 μ L into the system. Additionally, we calibrated the flow rate at 1.2 ml/min, ensuring optimal conditions for effective separation. This tailored

HPLC method represents a step forward in our ability to separate and analyze these pigments with high accuracy.

For the effective separation of heme, biliverdin, and Phycocyanobilin (PCB) in our study, we made the mobile phase composition, which was instrumental in achieving successful chromatographic separation. The mobile phase comprised two solvents: Solvent A, a blend of Methanol and Acetonitrile in a 1:9 ratio, and Solvent B, consisting of 0.5% Trifluoroacetic Acid with a pH adjusted to 2.6. This combination was chosen for its efficiency in separating these complex molecules (Seok et al., 2019). Our method employed a carefully programmed linear gradient over a span of 20 minutes modified from Seok et al. (2019) work. This commenced with a 10-minute equilibration phase at 60% Solvent A and 40% Solvent B, followed by a transition to a composition of 100% Solvent A. This specific composition was then maintained for an additional 10 minutes to ensure thorough separation. Our chromatographic profile, as detailed in Figure 6.1A, validated the method's effectiveness, where heme, biliverdin, and PCB were distinctly eluted at 22.25, 4.11, and 4.78 minutes, respectively. Complementing the chromatographic analysis, the spectral data from the photodiode array detector were instrumental in confirming the separation results. This data provided detailed spectral signatures for each pigment. Heme was identified by its Soret band at 400 nm and Q-bands at 503, 536, 573, and 628 nm. Biliverdin displayed a Soret band at 375 nm and a prominent Q-band at 673 nm, while PCB was characterized by spectral peaks at 369 nm and 687 nm, as shown in Figure 6.1B. These spectral characteristics were pivotal in ensuring the precise identification of each compound, demonstrating the robustness and reliability of our HPLC method.

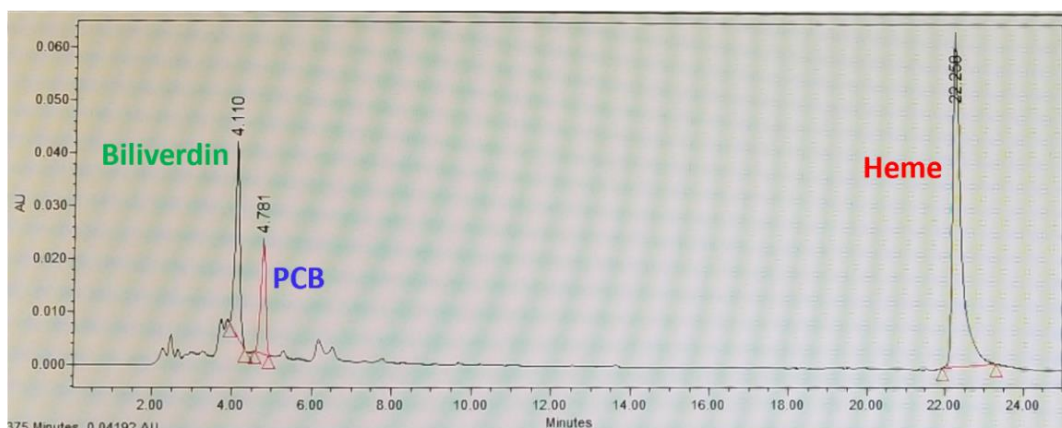
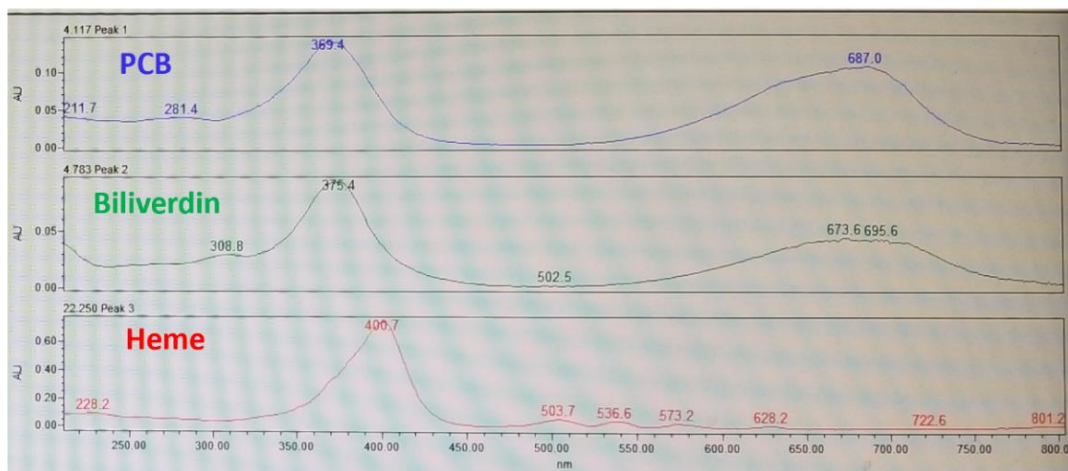
A**B**

Figure 6.1 Simultaneous separation of heme and bilins with reverse phase HPLC A) representative peaks of heme, biliverdin and PCB. B) Full scan for the corresponding peaks with their Soret peak and Q-bands.

6.3.2 Heme production with engineered *E. coli* and cell free metabolic engineering

In our quest to optimize heme production, we implemented a comprehensive strategy that combined genetic engineering with cell-free metabolic engineering techniques. We focused on modifying an *E. coli* strain, Sbm, to enhance its heme synthesis capabilities. Central to this strategy

was the genetic modification to overexpress the *hemA* gene from *R. sphaeroides*, thereby introducing the C-4 heme synthesis pathway into *E. coli*. This pathway was selected for its efficiency compared to the native *E. coli* C-5 pathway, which is characterized by its regulatory complexity and lower productivity (Figure 6.2). To complement the overexpression of *hemA*, we simultaneously upregulated several native *E. coli* genes integral to the heme synthesis process, including *hemB*, *hemG*, and *hemH* (Figure 6.2). This approach was designed to create a synergistic effect, bolstering the overall efficiency of the heme biosynthesis pathway in the modified strain. The upregulation of these genes aimed to enhance the entire pathway, both in terms of catalyzing the biosynthetic steps ('push') and ensuring efficient conversion and utilization of the intermediates ('pull'), thereby optimizing the metabolic flux towards heme production. The performance of the genetically engineered strains was thoroughly evaluated under shake-flask cultivation conditions, utilizing 30 g/L glycerol as the primary carbon source. The decision to use glycerol was based on its efficacy as a carbon source in promoting the growth of *E. coli* and facilitating the biosynthesis of heme. The strain that overexpressed the entire set of genes (*hemA*, *hemB*, *hemG*, and *hemH*) demonstrated a notable heme synthesis, confirming the effectiveness of our multifaceted approach (Figure 6.3A).

During the cultivation of our genetically modified *E. coli* strains, we encountered intriguing variations in the pigmentation of the cultures. Notably, the strain that overexpressed the *hemA*, *hemB*, and *hemG* genes exhibited a distinct red pigmentation in the supernatant, as seen in Figure 6.3B. This observation was in contrast to the intracellular pigment concentration, which was markedly lower within the same strain. Conversely, the strain with overexpression of all four genes (*hemA*, *hemB*, *hemG*, and *hemH*) displayed a prominent red pigmentation within the cells, with only minimal pigment detected extracellularly (Figure 6.3C, upper panel). This pattern suggested

an efficient accumulation of heme within the cells, highlighting the effectiveness of our genetic engineering strategy in enhancing intracellular heme biosynthesis.

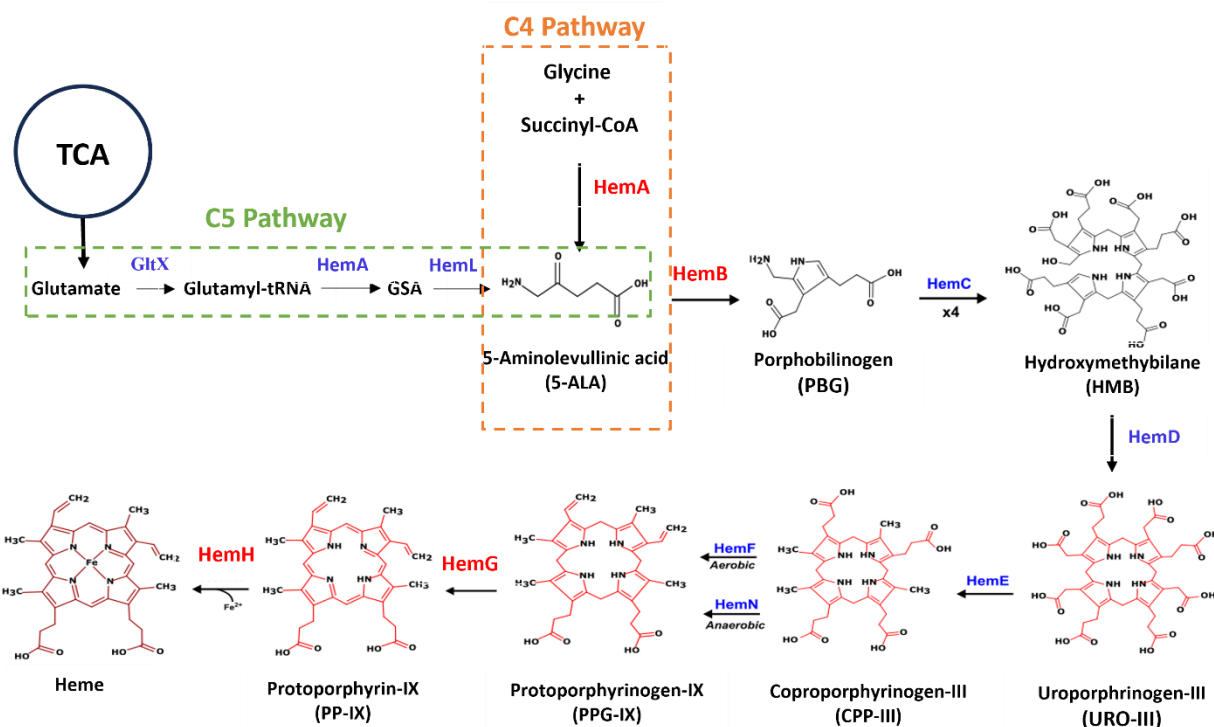


Figure 6.2 C4 and C5 heme biosynthesis pathway. C-4 pathway was introduced into *E. coli* by overexpressing *hemA* from *R. sphaeroides*. Native genes (*hemB*, *hemH* and *hemG*) were overexpressed via medium copy plasmid. The genes highlighted in blue are native and not overexpressed.

Further analysis was conducted through phase separation experiments on the culture filtrate from the strain overexpressing *hemA*, *hemB*, and *hemG*. Contrary to our initial expectations, the red pigment predominantly resided in the water phase rather than the chloroform phase. This unexpected finding indicated either an altered solubility profile of the pigment or the synthesis of an alternative water-soluble red pigment (Figure 6.3B). On the other hand, the pigment extracted

from the cell pellet of the strain with quadruple gene overexpression was clearly concentrated in the chloroform phase, aligning with the expected solubility characteristics of heme. We employed our HPLC method, and the analysis revealed that this strain produced heme at a concentration of 8.5 mg/L (Figure 6.3C, lower panel). This quantification not only affirmed the success of our genetic modifications in boosting heme production but also provided valuable insights into the intracellular accumulation and extracellular release dynamics of heme in our genetically engineered *E. coli* strains.

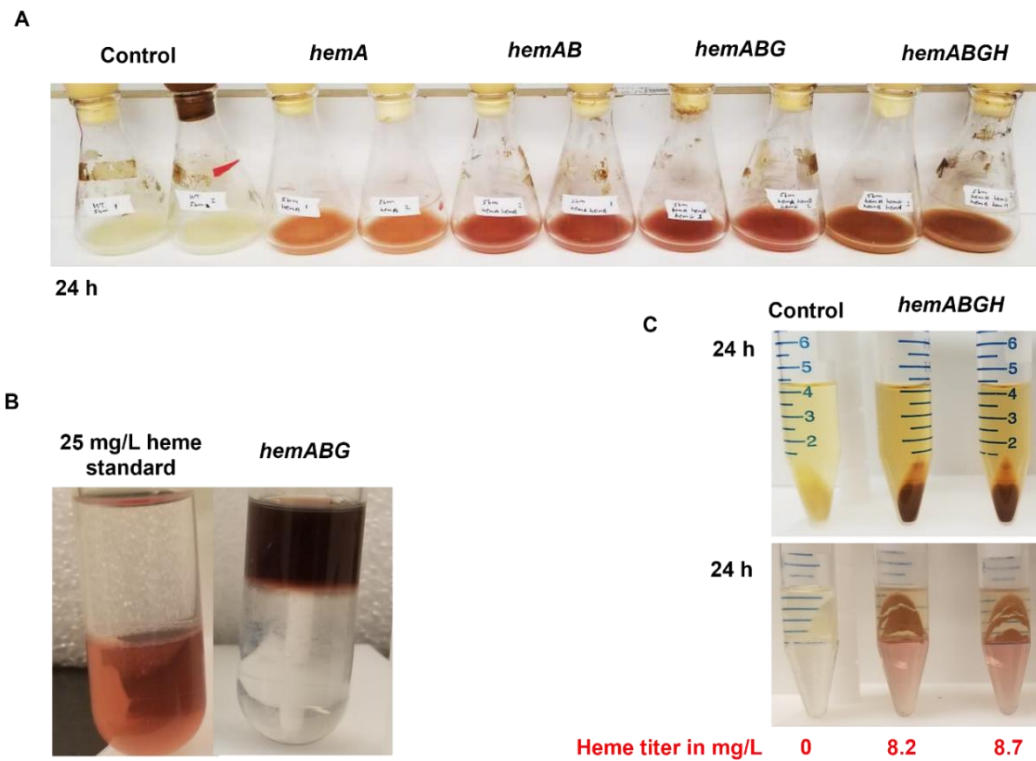


Figure 6.3 Heme production with engineered *E. coli*. A) Shake flasks cultivations after 24 hours B) Phase separation of heme standard and hemABG C) Phase separation for hemABGH sample.

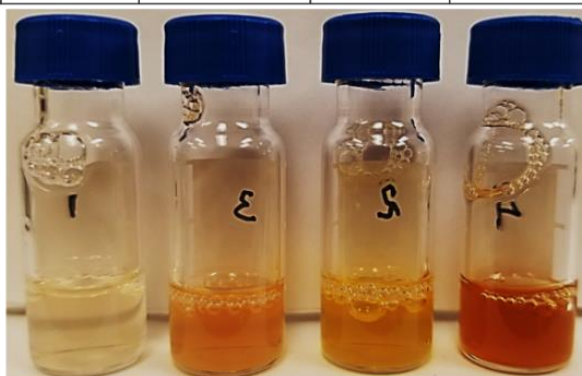
Considering the modest production titers achieved through the above traditional methods, we pivoted our focus towards cell-free metabolic engineering, leveraging the protease-deficient *E. coli* strain BL21. This strain was specifically engineered to overexpress the four genes central to the heme biosynthetic pathway (*hemA*, *hemB*, *hemG*, and *hemH*). From this strain, we prepared cell extracts to facilitate cell-free heme synthesis, aiming to capitalize on the potential advantages of this innovative approach.

Our experiments with the cell-free system yielded encouraging results. We observed a notable enhancement in heme production, which peaked 24 hours after initiating the reaction. The cell extract from the BL21 hemABGH strain exhibited a substantial increase in heme biosynthesis capabilities. When the reaction mixture was supplemented solely with 5-Aminolevulinic Acid (5-ALA), a precursor in the heme synthesis pathway, heme production attained a level of 3.5 mg/L (Figure 6.4, 24h). The most enhancement in heme production was observed when we further supplemented the reaction mixture with Ammonium iron (III) citrate in addition to 5-ALA. Under these conditions, the heme production in the BL21 hemABGH extract surged to 11.3 mg/L within the same 24-hour period (Figure 6.4, 24h). This marked increase indicates the vital role of iron in the heme biosynthesis pathway, highlighting how its availability can significantly amplify production yields.

These findings not only demonstrate the efficacy of cell-free metabolic engineering as a viable alternative to traditional cultivation-based methods but also emphasize the importance of key substrates and cofactors in optimizing biosynthetic pathways. The success in enhancing heme production through cell-free techniques represents a significant progress in our ongoing efforts to develop more efficient, scalable, and sustainable methods for heme and its derivatives' production.

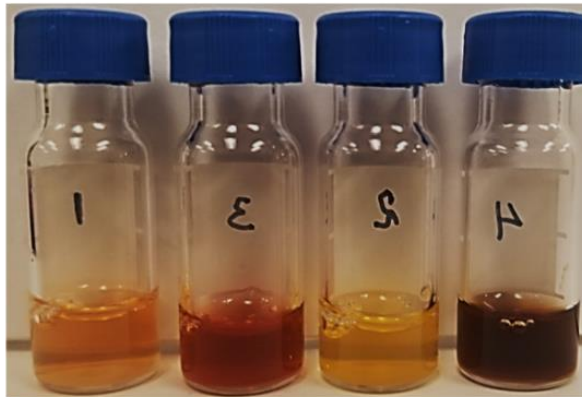
500 μ l Cell lysate:	BL21	BL21 heme ABGH	BL21	BL21 heme ABGH
500 μ M Ammonium iron (III) citrate :	-	-	+	+
1g/L 5-ALA :	+	+	+	+

4h



Heme titer in mg/L 0.11 0.21 0.17 2.7

24h



Heme titer in mg/L 0.23 3.5 0.22 11.3

Figure 6.4 Heme production via cell free metabolic engineering. The cell free extracts were prepared from BL21 and BL21 overexpressing the four heme biosynthesis pathway genes (hemA, hemB, hemG, and hemH), hemABGH strain.

6.3.3 Biliverdin PCB and PEB production with engineered *E. coli*

In our endeavor to exploit the genetic engineering potential of *E. coli*, we focused on converting heme into economically valuable pigments, namely biliverdin, Phycocyanobilin (PCB), and Phycoerythrobilin (PEB). These pigments, known for their vibrant colors, hold significant applications in food, cosmetics, and healthcare industries. Building on our established techniques for heme production, we ventured into the biosynthesis of these pigments, a process detailed in Figure 6.5. The transformation of heme into biliverdin, the initial step in our pigment production pathway, is executed by the enzyme heme oxygenase (HO) in a single-step reaction. Biliverdin then serves as a precursor for further conversion into the blue pigment PCB, a process catalyzed by Phycocyanobilin:ferredoxin oxidoreductase (PcyA). Additionally, biliverdin undergoes a separate transformation pathway to produce the pink pigment PEB. This process can follow two distinct routes: either a two-step enzymatic reaction involving PebA and PebB enzymes or a more streamlined single-step synthesis facilitated by Phycoerythrobilin synthase (PebS).

For efficient pigment production, a meticulous screening and selection process of enzymes was paramount. Thus, we embarked on a systematic approach, codon-optimizing various enzymes for *E. coli* expression to enhance production efficiency. Our comprehensive screening encompassed seven enzymes for biliverdin synthesis, four for PCB, and two for PEB production, as detailed in Table 6.3. The enzymes screened were sourced from a diverse range of organisms, including *Pseudomonas* species, Cyanobacteria, and specific Bacteriophages, showcasing the breadth of our enzymatic library. The initial phase of screening involved shake flask cultivations, which served as an effective platform for qualitative assessment. In this phase, the visual intensity of the pigment produced was our primary metric for evaluating enzymatic efficiency. This

approach enabled us to discern the most effective enzymes, based on the vibrancy and richness of the color produced.

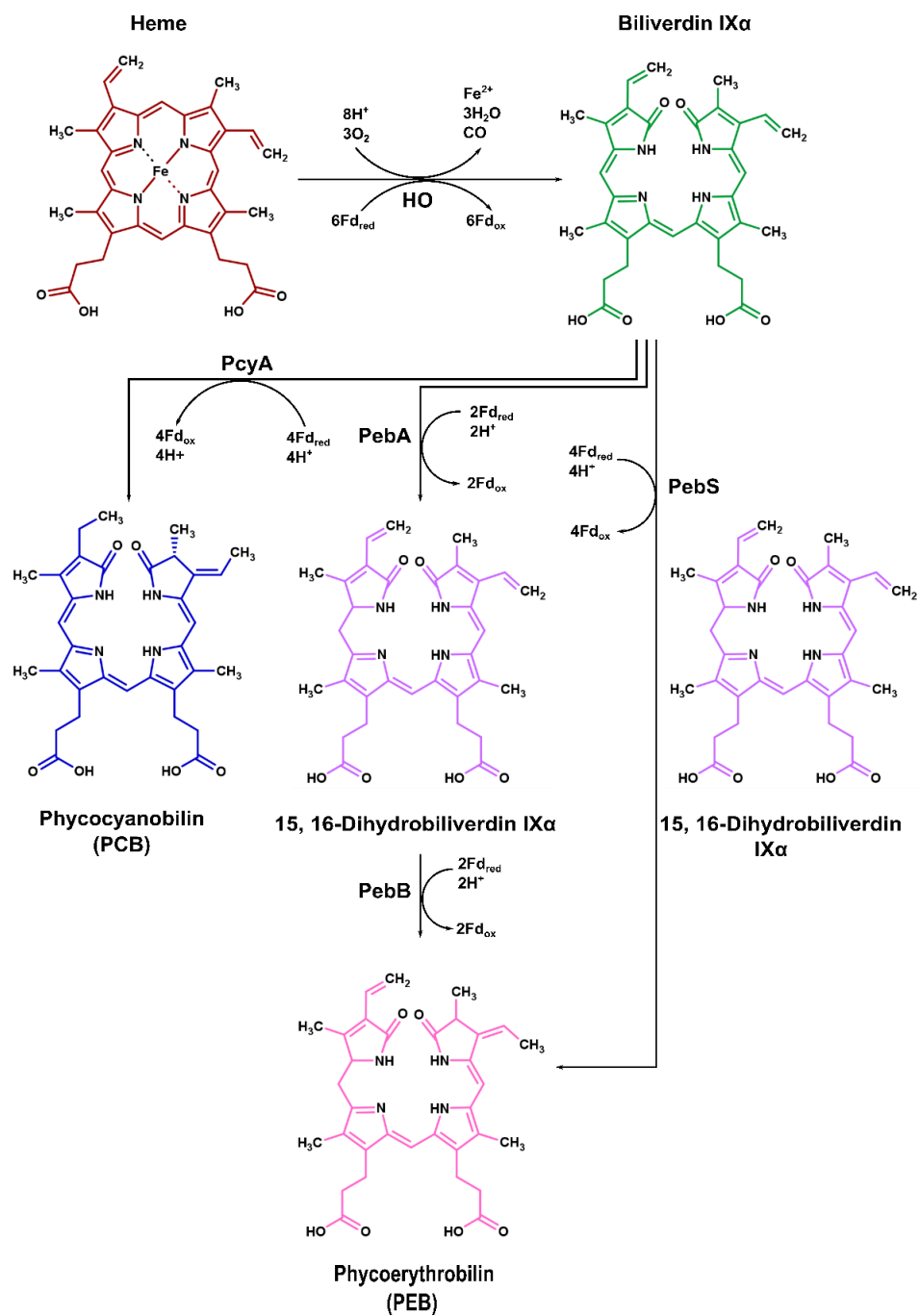


Figure 6.5 Structure of heme derivatives and their biosynthesis pathways.

Table 6.3 Enzymes screened to produce biliverdin, PCB and PEB and their sources

Product	Gene	Function	Source	Codon optimization
Biliverdin Blue green	<i>HO2582</i>	Heme oxygenase	<i>Pseudomonas putida</i> KT2440	Yes
	<i>HO5199</i>	Heme oxygenase	<i>Pseudomonas fluorescence</i> Pf-5	Yes
	<i>bphO</i>	Heme oxygenase	<i>Pseudomonas aeruginosa</i>	Yes
	<i>hemO</i>	Heme oxygenase	<i>Nisseria meningitidis</i>	Yes
	<i>hmuO</i>	Heme oxygenase	<i>Corynebacterium diphtheriae</i>	Yes
	<i>ho1</i>	Heme oxygenase	<i>Gloeobacter violaceus</i> (Cyanobacteria)	Yes
	<i>ho1</i>	Heme oxygenase	<i>Prochlorococcus phage P-SSM2</i> (Cyanophage)	Yes
Phycocyanobilin (PCB) Blue	<i>pcyA</i>	Phycocyanobilin:ferredoxin oxidoreductase	<i>Synechocystis sp.</i> PCC 6803	Yes
	<i>MAE_RS02905</i>	Phycocyanobilin:ferredoxin oxidoreductase	<i>Microcystis aeruginosa</i> NIES-843 (Cyanobacteria)	Yes
	<i>pcyA</i>	Phycocyanobilin:ferredoxin oxidoreductase	Cyanophage P-TIM40 (Cyanophage)	Yes
	<i>tII2308</i>	Phycocyanobilin:ferredoxin oxidoreductase	<i>Thermosynechococcus elongatus</i> BP-1 (Cyanobacteria)	Yes
Phycoerythrobilin (PEB) Pink	<i>CPXG_00107</i>	Phycoerythrobilin synthase	Cyanophage P-RSM6 (Cyanophage)	Yes
	<i>PSSM2_058</i>	Phycoerythrobilin synthase	<i>Prochlorococcus phage P-SSM2</i> (Cyanophage)	Yes

Following this qualitative assessment, we identified the optimal enzymes for each pigment. For biliverdin synthesis, the enzyme HO (HO2582) from *Pseudomonas putida* KT2440 was selected due to its superior performance. In the case of PCB production, the enzyme PcyA from *Thermosynechococcus elongatus* BP-1 emerged as the most efficient. Finally, for PEB production, the enzyme PebS from *Prochlorococcus phage* P-SSM2 was determined to be the most effective. These selections represent a significant milestone in our research, marking a step forward in the optimized production of these valuable pigments.

With successful overexpression of heme oxygenase (HO) enzyme HO2582 in *E. coli*, our initial observation of biliverdin synthesis occurred in shake flask cultivations, as depicted in Figure 6.6A. We then scaled up this process in a 1L batch bioreactor, which resulted in a culture filtrate displaying a distinct vibrant green color, a clear indication of biliverdin presence (Figure 6.6B and C). The purification of biliverdin from this filtrate and its subsequent quantification using HPLC revealed a promising titer of 6.3 mg/L. Furthermore, the overexpression of both the HO2582 and the selected *pcyA* genes in *E. coli* facilitated the production of PCB. This co-expression system, initially tested in shake flask cultivation, showed encouraging results (Figure 6.7A). Scaling up to a 1L batch bioreactor further substantiated our findings, as illustrated in Figure 6.7C. Upon purification, the quantification of PCB from this system yielded a titer of 3.1 mg/L, demonstrating the efficacy of our engineered approach. Our final set of experiments focused on the transformation of biliverdin into PEB using the PebS enzyme derived from *Prochlorococcus phage* P-SSM2. The results of shake flask cultivation revealed a noticeable pink coloration in the culture (Figure 6.8), indicating the successful production of PEB. However, a significant challenge was encountered: the absence of a PEB standard. This lack of a standard reference material for PEB hindered our ability to conduct a quantitative analysis, posing a limitation to the study.

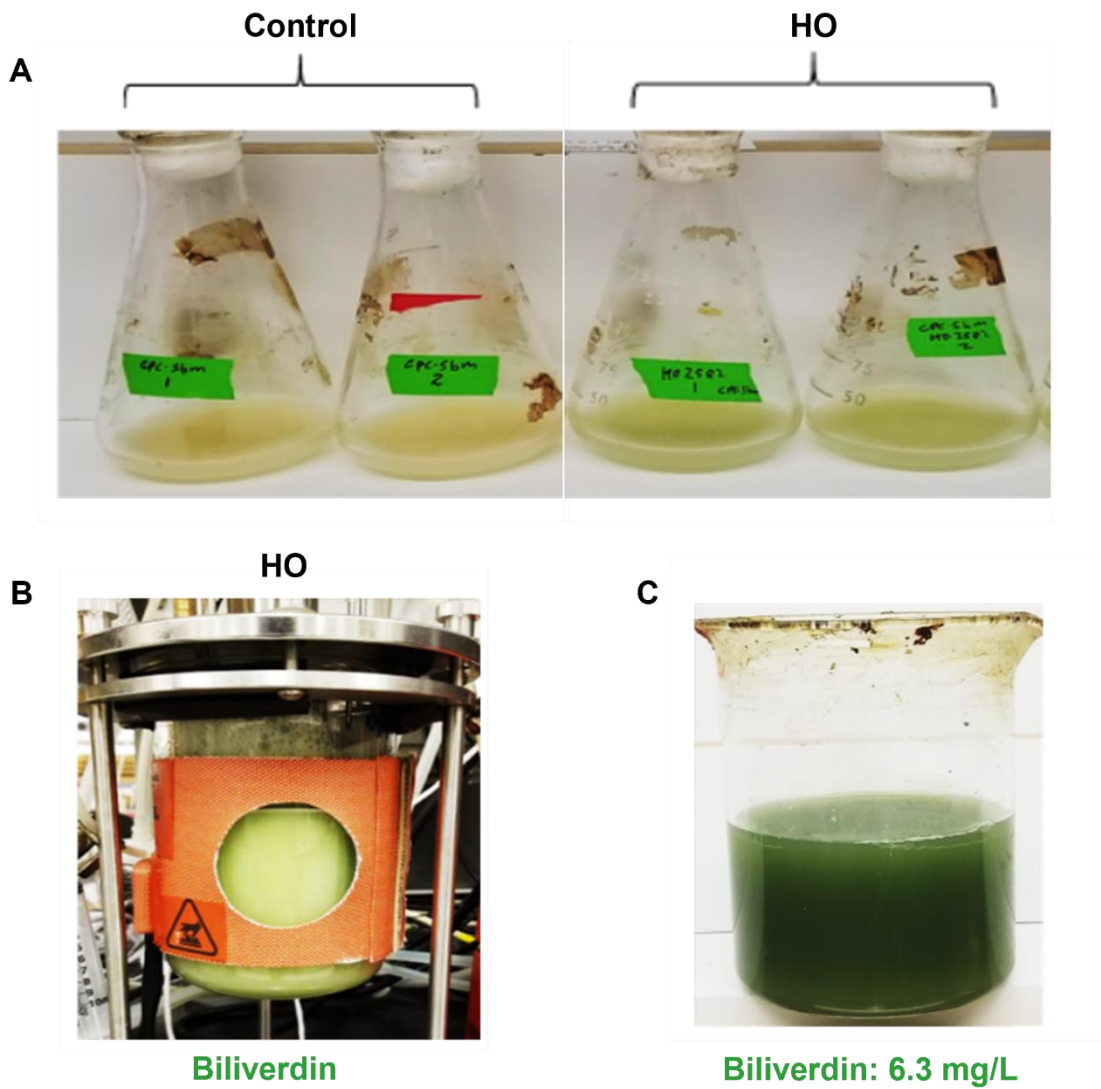


Figure 6.6 Biliverdin synthesis using engineered *E. coli*. (A) biliverdin production in 8h shake-flask cultivations (B) biliverdin synthesis in 16h bioreactor cultivation and (C) biliverdin collected from foam generated in bioreactor. The heme oxygenase (HO) was from *Pseudomonas putida*.

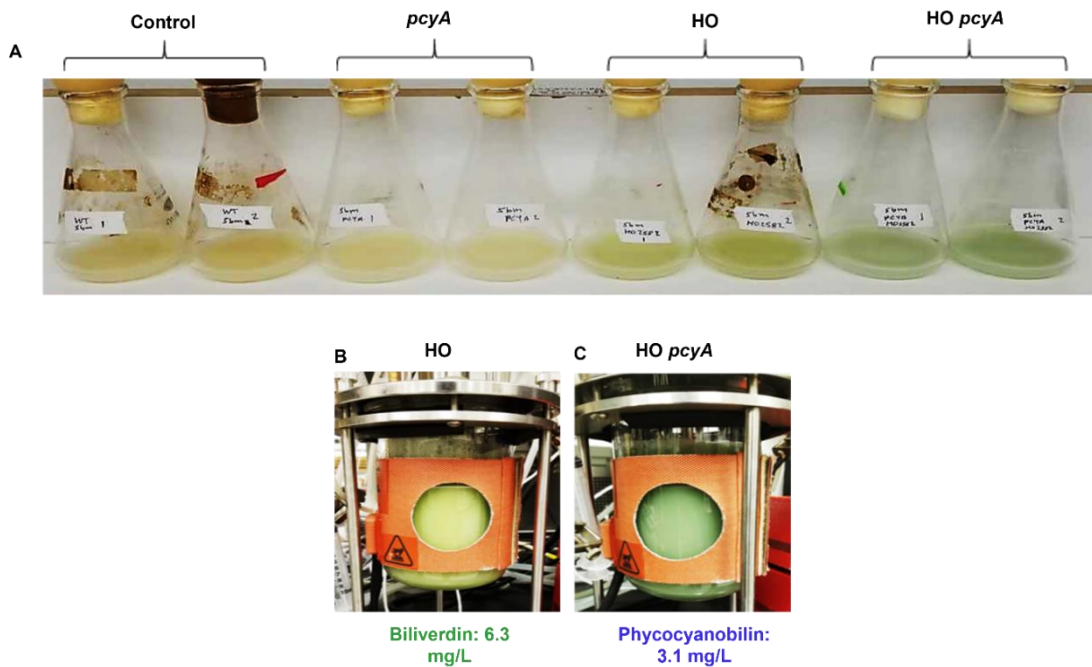


Figure 6.7 Phycocyanobilin (PCB) synthesis using engineered *E. coli*. (A) phycocyanobilin production in 6h shake-flask cultivations and (B) Color comparison of biliverdin (green) and (C) phycocyanobilin (blue) in 16h bioreactor cultivations. The heme oxygenase (HO) and phycocyanobilin:ferredoxin oxidoreductase (pcyA) are from *Pseudomonas putida* and *Thermosynechococcus elongatus* BP-1, respectively.

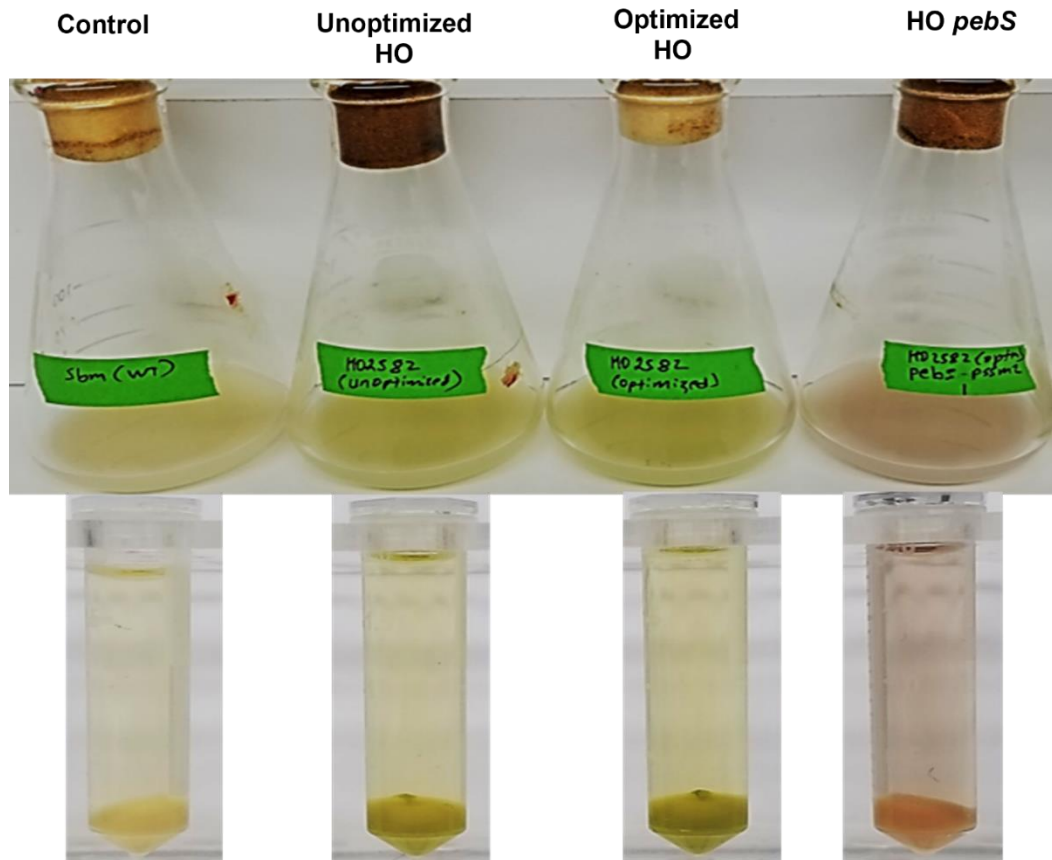


Figure 6.8 Phycoerythrobilin (PEB) synthesis using engineered *E. coli*. The shake- flasks were from 8h cultivations. Biliverdin is the green pigment while the pink pigment is PEB. The heme oxygenase (HO) and phycoerythrobilin synthase (pebS) are from *Pseudomonas putida* and *Prochlorococcus phage P-SSM2* (Cyanophage), respectively.

6.4 Discussion

Heme, a complex molecule with an iron atom at its center, plays a pivotal role in various biological processes, including oxygen transport, electron transfer, and the catalysis of diverse biochemical reactions. Its commercial value is highlighted by its application in the food and healthcare industries, where it's used as an additive for plant-based meats and as a prosthetic group in pharmaceuticals (Ko et al., 2021; Zhao et al., 2018). As the demand for sustainable and natural products increases, bioproduction of heme has come to the forefront, offering a promising alternative to traditional methods, which are often costly and environmentally unfriendly.

Heme biosynthesis in microbial systems offers a spectrum of challenges along with unique opportunities for scientific advancement. *E. coli* naturally orchestrates heme production through its intrinsic C-5 pathway. This endogenous process is subjected to stringent regulation, rendering it suboptimal for industrial-scale heme production due to inherent feedback inhibition mechanisms that limit production potential. In contrast, the C-4 pathway, with its simpler regulatory landscape, has been shown to facilitate a more robust metabolic flux towards heme synthesis (Ko et al., 2021; Yang et al., 2023). Our strategic approach involves the genetic enhancement of the *E. coli* strain to overexpress the *hemA* gene sourced from *R. sphaeroides*. This gene is responsible for the production of 5-aminolevulinate synthase, the key enzyme initiating the C-4 heme biosynthetic route. By leveraging this inherently less constrained C-4 pathway from *R. sphaeroides*, we aimed to circumvent the natural regulatory bottlenecks and substantially augment heme biosynthesis. Moreover, our research investigates the synergistic potential of combining genetic and cell-free metabolic engineering strategies. Traditional genetic engineering has been instrumental in refining microbial metabolic pathways; however, cell-free metabolic engineering emerges as a groundbreaking technique that promises to overcome cellular limitations. Freed from the

constraints of the cell, this approach allows for a more customized and precise manipulation of the biosynthetic processes (Garcia et al., 2021; Grubbe et al., 2020; Lim and Kim, 2019; Rasor et al., 2021). Our goal was to harness this synergy to unlock new frontiers for significantly elevating heme production yields.

In our research, we focused on a genetically engineered *E. coli* strain, overexpressing *hemA*, *hemB*, *hemG*, and *hemH* genes, which resulted in a significant increase in intracellular heme accumulation. This enhancement was visually confirmed by the pronounced red coloration within the bacterial cells, a clear indication of active heme synthesis. Interestingly, the supernatant showed a lower concentration of this red pigment, implying efficient intracellular retention of heme (Choi et al., 2022). The heme production achieved by this strain, quantified at 8.5 mg/L, is noteworthy but still modest compared to the highest known production in *E. coli*, recorded at 1.03 g/L in a 6.6 L fed-batch fermenter. This peak production was attained through comprehensive microbial engineering strategies, including optimized cell density, continuous iron supplementation, and abundant nutrient supply (Choi et al., 2022). This comparison suggests ample room for further enhancement of our strain, potentially by adopting similar bioreactor-based strategies for nutrient optimization and metabolic adjustment.

Moreover, the field has seen remarkable advancements, such as the work by Ko et al. (2021) on *C. glutamicum*, which achieved high heme production and significant extracellular secretion, thanks to a combination of system metabolic engineering and membrane modifications, reaching a yield of 309.18 mg/L. Similarly, Ishchuk et al. (2022) demonstrated the potential of *S. cerevisiae* in tripling heme synthesis through genome-scale metabolic modeling and targeted genetic alterations. These developments, along with contributions from Yang et al. (2023) and Zhao et al. (2018) in engineering *B. subtilis* and *E. coli* for enhanced heme production, underscore the

potential of sophisticated engineering techniques. They offer valuable insights into optimizing heme biosynthesis, paving the way for our *E. coli*-based system to adopt and benefit from these diverse and innovative strategies. These collective advancements in microbial engineering not only enrich our understanding but also provide a framework for furthering our *E. coli*-based heme production strategy, aligning with the goal of achieving high-yield and industrially scalable biosynthesis.

To develop an efficient heme production strategy, we explored a cell-free metabolic engineering approach using extracts from a protease-deficient *E. coli* BL21 strain, specifically engineered to overexpress the *hemA*, *hemB*, *hemG*, and *hemH* genes. The protease-deficiency in these extracts played a pivotal role in preserving enzyme integrity, thereby enhancing the biosynthesis process. This strategic approach led to a significant increase in heme production, peaking at 11.3 mg/L upon supplementation with ammonium iron (III) citrate and 5-aminolevulinic acid (5-ALA). This finding demonstrates the essential role of iron in the heme biosynthetic pathway. Iron, being a core component of heme, directly influences the pathway's efficiency, with its availability being crucial for optimal productivity. Our results align with those of Choi et al. (2022), indicating that iron supplementation is key to maximizing heme production. The synergy between a protease-deficient host and precise nutrient supplementation in a cell-free system not only yields higher heme concentrations but also offers a scalable and flexible alternative to traditional whole-cell methods. Looking forward, the potential of cell-free systems in industrial-scale heme production is promising, especially if future research focuses on fine-tuning conditions like, reaction temperature, pH, amount of cell extracts, precursor, and iron concentrations to enhance the process's economic viability.

We also explored the use of heme as a precursor in the biosynthesis of commercially valuable pigments like biliverdin, PCB, and PEB in genetically engineered *E. coli*. These pigments, with their extensive industrial applications, were produced by employing a novel set of enzymes, representing a shift towards more sustainable and cost-effective production methods compared to traditional chemical synthesis. Our bio-based approach, utilizing microbial cell factories, offers a significant advancement over conventional low-yield biliverdin synthesis methods. Notably, while an *E. coli* system expressing cyanobacterial HO1 achieved a biliverdin yield of 23.5 mg/L (Chen et al., 2012), and *C. glutamicum* recorded up to 68.74 ± 4.97 mg/L (Seok et al., 2019), our research is unique in its use of a codon-optimized heme oxygenase enzyme from *Pseudomonas putida* KT2440, which has never been explored for its potential in making biliverdin. This approach led to a promising biliverdin yield of 6.3 mg/L from a 1L batch bioreactor fermentation, even without extensive engineering and process optimization. This result indicates significant potential for further development and enhancement of production yields, marking an important step forward in the field of microbial pigment biosynthesis.

The traditional commercial production of PCB has predominantly depended on extracting it from *Spirulina* species, a method faced with challenges due to the organism's complex cell wall and risk of contamination (Mysliwa-Kurdziel and Solymosi, 2017). As a result, there's been a shift towards using heterologous hosts like *E. coli*, with recorded titers reaching up to 6.64 mg/L (Ge et al., 2018). With our approach, we introduced Phycocyanobilin:ferredoxin oxidoreductase (PcyA) from *Thermosynechococcus elongatus* BP-1 into *E. coli*, achieving a PCB production titer of 3.1 mg/L. While this yield is currently below the highest reported, it establishes a solid basis for future improvements, particularly considering the preliminary stage of our process development. Additionally, we've ventured into the production of PEB, typically more challenging to synthesize.

By employing Phycoerythrobilin synthase (PebS) from *Prochlorococcus phage P-SSM2* in *E. coli*, we achieved visible PEB production, a significant milestone given the absence of commercial quantitative benchmarks. To our knowledge, this is the first time these specific enzymes have been used for synthesizing PCB and PEB in *E. coli*, representing a significant advancement in the field of microbial pigment production and offering enzymes for sustainable and efficient pigment biosynthesis.

Our study has demonstrated the capability of selected enzymes to facilitate efficient pigment production in *E. coli*. While the current production rates are below the highest yields reported in the literature, they are noteworthy considering the minimal optimizations undertaken in our experiments. This indicates a strong inherent potential of these enzymes for industrial-scale pigment production. The results achieved with only basic adjustments highlight the possibility of greatly enhancing these yields through more focused genetic engineering and process optimization. This research establishes a foundational strategy for microbial pigment production using *E. coli*, employing a distinctive set of enzymes.

Chapter 7

Conclusions and future directions

7.1 Conclusions

Our comprehensive investigation into the growth dynamics of *Y. lipolytica* under various environmental conditions, particularly focusing on different temperatures and carbon sources, has significantly advanced our understanding of its metabolic behavior. This yeast shows optimal growth at moderate temperatures, between 25 to 30°C, and exhibits remarkable adaptability to a range of carbon sources, including glucose, glycerol, acetate, and soybean oil. The results of our study are pivotal, highlighting the organism's potential in diverse biotechnological applications and demonstrating the importance of species-specific research in optimizing bioprocesses. Particularly noteworthy is *Y. lipolytica's* continued growth at a slightly reduced temperature of 34°C, across all tested carbon sources, indicating its remarkable adaptability and resilience, which are essential for metabolic engineering and industrial processes seeking cost-effective and sustainable feedstocks.

The metabolic flexibility of *Y. lipolytica*, especially in response to temperature fluctuations, further emphasizes its value in industrial applications. Our study revealed significant alterations in the yeast's metabolite profiles when cultivated on different feedstocks at elevated temperatures, indicating the critical role of temperature in metabolic pathway regulation. This has profound implications for bioproduction processes, as understanding these metabolic shifts can lead to advances in metabolic engineering. The pronounced upregulation of pyruvate synthesis and its derivative amino acids at higher temperatures positions pyruvate as a central node in *Y. lipolytica's* metabolic network at elevated fermentation temperatures. This insight into the yeast's metabolic

responses, combined with our findings on mannitol production, presents a blueprint for future research in optimizing biotechnological applications.

Examining deeper into *Y. lipolytica*'s metabolic responses, our research revealed a significant enhancement in its ability to produce mannitol at elevated temperatures. This finding is particularly relevant given the wide range of industrial applications of mannitol and the environmental concerns associated with its traditional chemical synthesis methods. Our successful manipulation of the *FBPI* gene, a key player in mannitol metabolism, has opened up new possibilities for advanced genetic engineering strategies. This, coupled with the potential existence of alternative biosynthetic pathways for mannitol synthesis indicated by our study, underscores the versatility and adaptability of *Y. lipolytica*. These findings highlight the organism's potential as a bio-manufacturing platform and lay the groundwork for optimizing its industrial utility, particularly in the fields of biofuel production, high-value chemical synthesis, and beyond.

The development of the Poh1 strain from the established Pog1 strain, combined with our dual-gRNA CRISPR system, represents a significant advancement in the genetic engineering of *Y. lipolytica*. This approach navigates the challenges of natural DNA repair mechanisms in *Y. lipolytica*, setting a better benchmark for genetic manipulations. Our comprehensive analysis demonstrates the system's efficiency, adaptability, and capability for complex gene editing. Despite a slight decrease in editing efficiency with dual gRNAs, our method offers higher specificity. The integration of this system into a single plasmid streamlines gene knockout processes and simplifies vector recycling, offering significant practical advantages over similar approaches. This research not only enhances our understanding of *Y. lipolytica*'s biotechnological potential but also positions our system as a key tool in advancing metabolic engineering.

Our research on optimizing 5-ALA production via CFME represents a substantial advancement in the field of metabolic engineering. We have demonstrated the potential of genetic modifications and the optimization of reaction conditions to improve the efficiency and scalability of 5-ALA synthesis. These findings are not only significant for the theoretical understanding of CFME but also have practical implications for its application in industrial biotechnology. As we look to the future, our study lays the groundwork for further research and development in this area, with the potential to change the production of biochemically important compounds and contribute to more sustainable and efficient industrial processes.

Our exploration of heme and heme-derived pigment production using genetically engineered *E. coli* represents a significant progress in biotechnological advancement. Heme, as a vital molecule in biological systems and a valuable commodity in the food and healthcare sectors, has traditionally not been produced through environmentally friendly methods. Our study demonstrates a viable, sustainable alternative by optimizing microbial biosynthetic pathways, notably by employing the less regulated C-4 pathway from *R. sphaeroides*. This approach allowed us to circumvent natural regulatory mechanisms, leading to a notable increase in intracellular heme accumulation, though the yields suggest further enhancement is possible.

The integration of genetic and cell-free metabolic engineering has been pivotal in our research, with the latter offering an unprecedented level of precision and customization in the biosynthesis of heme. The protease-deficient *E. coli* strain BL21 and the subsequent cell-free system, supplemented with key nutrients like ammonium iron (III) citrate and 5-aminolevulinic acid (5-ALA), led to a peak heme production of 11.3 mg/L. This not only underscores the potential of our metabolic engineering approach but also marks a promising leap towards scalable and efficient industrial biosynthesis.

Moreover, we examined the production of valuable pigments, utilizing heme as a precursor. We have made significant progress in synthesizing biliverdin, PCB, and PEB. Notably, our pioneering use of a codon-optimized heme oxygenase from *Pseudomonas putida* KT2440 and the introduction of unique enzymes like PcyA and PebS into *E. coli* demonstrate our innovative edge, despite our current titers being lower than the highest reported. These initial productions are especially promising as they were achieved with minimal optimization, implying that with targeted genetic and process refinements, there is a strong potential to significantly elevate production.

Our research not only adds to the growing body of knowledge in microbial biosynthesis but also sets a new benchmark for future studies. The successful production of these pigments in *E. coli* opens the door to more sustainable and cost-effective industrial practices. As we continue to refine these biosynthetic pathways, there is an optimistic prospect of meeting and exceeding the needs of industries reliant on these pigments. The implications of our findings are profound, indicating that with further optimization, microbial cell factories like *E. coli* can become cornerstone technologies for environmentally friendly and economically viable pigment production on a commercial scale.

7.2 Future directions

Our research on *Y. lipolytica*'s growth and metabolic responses at elevated temperatures, while insightful, was limited to certain feedstocks and temperature ranges. Future studies should expand the types of feedstocks, particularly focusing on lignocellulosic biomass and other industrial byproducts. These alternative feedstocks align with the principles of a circular economy and environmental sustainability, offering cheaper and more eco-friendly options for industrial bioprocesses. Additionally, refining our understanding of the optimal fermentation temperatures

for different bioprocesses and product syntheses is crucial. Expanding the temperature range beyond 30°C, 34°C, and 37°C could fine-tune the conditions for optimal microbial activity and product yield.

Moreover, our study was conducted using the Po1g strain of *Y. lipolytica*, which may not fully represent the growth dynamics and metabolic capabilities of other laboratory or wild-type strains. Future research should include a broader spectrum of *Y. lipolytica* strains to evaluate their growth and metabolic flexibility under various environmental conditions, including elevated temperatures and diverse feedstocks. This would enable more comprehensive conclusions about the organism's capabilities and potential applications.

In our investigation, rich media supplemented with different carbon sources were used. Considering the cost implications for large-scale production, particularly in the context of mannitol production, exploring more economical alternatives, such as M9 salt minimum media, is recommended. This approach would not only make the process more cost-effective but also more appealing for industrial-scale applications.

Additionally, while our study focused on the *FBP1* gene, there are other genes that exhibited differential expression under thermal stress and may play significant roles in mannitol, pyruvate, and amino acid synthesis. Investigating these genes could provide valuable insights for developing strategies to enhance the production of these key metabolites. Employing bioinformatics tools to identify and manipulate genes directly involved in mannitol synthesis, such as mannitol-1-P-dehydrogenase and mannitol-1 P-phosphatase, could further improve mannitol yields. This approach would also complement our current transcriptome analysis by providing a more complete picture of the expression of genes involved in mannitol synthesis at elevated fermentation temperatures.

Our findings also suggest that fermentation temperature can act as a switch for different chemical syntheses. With *Y. lipolytica* known for producing valuable lipids and accumulating substantial lipid content, investigating the production of high-value lipids using cheaper oils as feedstocks is a promising avenue. By exploiting the reduced flux through the TCA cycle and lipid synthesis at higher temperatures, these cheaper feedstocks could be converted into valuable lipids more efficiently. Such a strategy could be extended to other bioprocesses that leverage slow TCA and reduced lipid synthesis for enhanced production of various chemicals using oil and fat feedstocks.

These future directions offer a roadmap for broader and more impactful research on *Y. lipolytica*. By exploring these avenues, we can unlock the full potential of this versatile organism for a range of industrial applications, contributing to the development of more sustainable and cost-effective biotechnological processes.

Our dual gRNA CRISPR system presents several exciting research opportunities to enhance and expand its functionalities. Key among these is the direct testing for precise DNA fragment excision, a critical step to establish the system's effectiveness and accuracy in gene editing. Investigating gene integration through homologous recombination will further elucidate its efficiency and reliability in various genetic settings. Expanding the application of our system to higher organisms offers an avenue to explore its adaptability and effectiveness in more complex biological systems. Additionally, a detailed analysis of the indels produced by the NHEJ mechanism, along with targeting a broader spectrum of genes, will enrich our understanding of the gene editing process and assess the versatility of our system. Ongoing comparative studies and refinement are essential to maintain the system's status as a forefront technology in genetic engineering, ensuring it continues to be a powerful tool for metabolic engineering of *Y. lipolytica*.

Our study on optimizing 5-ALA production through CFME opens several avenues for future research. One promising area is the exploration of additional genetic modifications to enhance yields. This includes the identification of potential bottlenecks in the metabolic pathway that were not addressed in this study and the exploration of alternative pathways that could improve the efficiency of 5-ALA production. For instance, the introduction of mutations that increase the activity or stability of enzymes involved in the synthesis of 5-ALA could be valuable. The role of cofactors and reaction conditions in CFME has proven significant. Future studies should consider a broader range of cofactors, such as different energy carriers or enzyme coactivators, which may further enhance 5-ALA production. Additionally, the optimization of reaction conditions, including pH, temperature, and ionic strength, could provide a more holistic understanding of the optimal conditions for CFME processes. Scaling up the experimental setup to more closely mimic industrial-scale production is another crucial area, offering insights into the practical application and scalability of CFME for commercial purposes. The versatility of the CFME platform suggests that it could be effectively utilized to produce other valuable compounds. Future research should explore the applicability of CFME for the synthesis of pharmaceuticals, biofuels, and fine chemicals, potentially revolutionizing multiple sectors within the biotech industry.

The pursuit of enhancing heme production in microbial systems begins with a focus on the availability of key precursors: serine, glycine, and succinyl-CoA. These compounds play essential roles in the heme biosynthetic pathway, and their abundance can significantly influence the overall yield. Engineering efforts, such as the overexpression of serine hydroxymethyltransferase and glycine dehydrogenase in *E. coli*, could lead to increased concentrations of these crucial amino acids, thereby facilitating the synthesis of 5-ALA, the initial precursor in heme biosynthesis. Moreover, the redirection of carbon flux within central metabolic pathways presents an

opportunity to channel more resources towards heme production. This approach has been validated in yeast by Ishchuk et al. (2022), who successfully increased heme output by diverting fluxes from ethanol production. Similarly, in *C. glutamicum*, the work of Ko et al. (2021) highlights the possibility of boosting succinyl-CoA levels, thereby enhancing the production of the target compounds. These genetic and metabolic engineering strategies demonstrate the potential to augment the biosynthesis of heme significantly.

The composition of the growth medium and the supplementation with essential nutrients are recognized as critical factors in microbial heme production. For instance, the addition of iron, a central component of the heme molecule, can markedly improve production rates. This was shown by Choi et al. (2022), whose research on *E. coli* revealed that the strategic variation of iron levels and carbon sources could improve heme synthesis. Additionally, the careful management of process parameters, such as pH, temperature, and oxygen levels, can create optimal conditions for microbial growth and product formation. Zhao et al. (2018) demonstrated the benefits of such meticulous control by engineering *E. coli* to export heme directly into the growth medium, thereby simplifying the purification process and offering a potential reduction in production costs. This integrated approach to media composition and process optimization is poised to play a significant role in the future of heme biosynthesis at scale.

The development of robust heme exporters in microbial systems could enhance extracellular heme concentrations, thereby easing the challenges associated with downstream processing. The pioneering work by Zhao et al. (2018) highlighted the advantages of engineering *E. coli* to secrete heme, avoiding the complexities of cell lysis and intracellular product purification. Furthermore, in cell-free systems, the stability of key enzymes like 5-aminolevulinate synthase (ALAS) is a critical factor for sustained productivity. Advances in protein engineering could lead to versions

of ALAS with increased stability and activity, extending the productive lifespan of heme biosynthesis processes and allowing for continuous production over extended periods. Such innovations in both living and cell-free systems represent a transformative step towards more efficient and scalable heme production technologies.

The economic feasibility of heme production on an industrial scale is a significant consideration. The preference for cost-effective substrates such as glucose, due to its affordability and efficacy in microbial fermentation, stands in contrast to more expensive alternatives like 5-ALA. Lee & Kim (2022) have highlighted the necessity for economically viable substrates to ensure the sustainability of industrial heme production. Furthermore, the exploration of alternative microbial hosts for heme production, like *Bacillus subtilis*, expands the potential for metabolic engineering. The application of genome-scale metabolic models, as demonstrated by the successful use of the Yeast8 model in *S. cerevisiae*, could provide invaluable insights into metabolic bottlenecks and inform targeted genetic modifications to optimize production, as posited by Yang *et al.* (2023).

Production of heme-derivatives could benefit from the above suggested strategies for enhancing heme production. The implications for heme-derived pigments, such as biliverdin, PCB, and PEB, are particularly profound, where the optimization of production processes and the standardization of quantification methods are critical steps toward industrial application. Our initial work in the cell-free synthesis of heme sets a precedent for the application of similar methodologies to pigment production. The cell-free approach, which has demonstrated potential in heme synthesis, could be extended to the production of biliverdin, PCB, and PEB. This technique would allow for the precise control of the biosynthetic pathway, reducing the complexity associated with whole-cell systems and potentially leading to more efficient and higher-yield

production of these valuable pigments. The cell-free platform offers a versatile and customizable approach, enabling rapid screening and optimization of the enzymatic steps required for pigment biosynthesis.

For heme derivatives' production, the use of heme oxygenases from cyanobacteria has been a conventional strategy in engineered *E. coli*. Nonetheless, their current production rates remain suboptimal. Exploring the diverse range of bacterial heme oxygenases presents an opportunity to enhance these rates significantly. By conducting a comprehensive screening of these enzymes, it is possible to identify the most efficient ones to be used in *E. coli* for elevated biliverdin production, which is the precursor to other critical pigments. This strategy holds the potential to vastly improve the efficiency and output of pigment production processes.

Furthermore, redox and cofactor engineering are key in boosting the production of heme-derivatives. The synthesis of bilins is dependent on the action of heme oxygenases and Ferredoxin-NADPH Reductase, necessitating cofactors such as NADPH and ferredoxin to maintain cellular redox balance. By coupling alterations in carbon metabolism with cofactor and redox engineering strategies, we can optimize the conversion of heme to heme-derivatives. Techniques like enhancing NADPH availability through overexpression of specific enzymes, increasing ferredoxin availability via FDX gene overexpression, and introducing efficient Ferredoxin-NADPH Reductase from a variety of bacterial sources are all strategies that could have a significant impact on the bioproduction of pigments. These redox changes, alongside strategic enzyme overexpression, are designed to sustain redox balance and increase pigment bioproduction, setting the stage for a transformative era in microbial pigment production.

References

- Abbasi, A.R., Liu, J., Wang, Z., Zhao, A., Ying, H., Qu, L., Alam, M.A., Xiong, W., Xu, J., and Lv, Y. (2021). Recent advances in producing sugar alcohols and functional sugars by engineering *Yarrowia lipolytica*. *Frontiers in Bioengineering and Biotechnology* 9, 648382.
- Abdel-Mawgoud, A., and Stephanopoulos, G. (2020). Improving CRISPR/Cas9-mediated genome editing efficiency in *Yarrowia lipolytica* using direct tRNA-sgRNA fusions. *Metabolic Engineering* 62, 106-115.
- Ajioka, R.S., Phillips, J.D., and Kushner, J.P. (2006). Biosynthesis of heme in mammals. *Biochimica et Biophysica Acta (BBA)-Molecular Cell Research* 1763, 723-736.
- Anzaldi, L.L., and Skaar, E.P. (2010). Overcoming the Heme Paradox: Heme Toxicity and Tolerance in Bacterial Pathogens. *Infection and Immunity* 78, 4977-4989.
- Bai, B., Liu, Y., You, Y., Li, Y., and Ma, L. (2015). Intraperitoneally administered biliverdin protects against UVB-induced skin photo-damage in hairless mice. *Journal of Photochemistry and Photobiology B: Biology* 144, 35-41.
- Baisya, D., Ramesh, A., Schwartz, C., Lonardi, S., and Wheeldon, I. (2022). Genome-wide functional screens enable the prediction of high activity CRISPR-Cas9 and-Cas12a guides in *Yarrowia lipolytica*. *Nature communications* 13, 922.
- Baylor, J.L., and Butler, M.W. (2019). Immune challenge-induced oxidative damage may be mitigated by biliverdin. *The Journal of Experimental Biology* 222, jeb200055.
- Beopoulos, A., Cescut, J., Haddouche, R., Uribelarrea, J.-L., Molina-Jouve, C., and Nicaud, J.-M. (2009). *Yarrowia lipolytica* as a model for bio-oil production. *Progress in lipid research* 48, 375-387.

- Beopoulos, A., Nicaud, J.-M., and Gaillardin, C. (2011). An overview of lipid metabolism in yeasts and its impact on biotechnological processes. *Applied microbiology and biotechnology* 90, 1193-1206.
- Bermejo Román, R., Álvarez-Pez, J.M., Acién Fernández, F.G., and Molina Grima, E. (2002). Recovery of pure B-phycoerythrin from the microalga *Porphyridium cruentum*. *Journal of Biotechnology* 93, 73-85.
- Bilal, M., Xu, S., Iqbal, H.M., and Cheng, H. (2021). *Yarrowia lipolytica* as an emerging biotechnological chassis for functional sugars biosynthesis. *Critical Reviews in Food Science and Nutrition* 61, 535-552.
- Binns, D., Dimmer, E., Huntley, R., Barrell, D., O'donovan, C., and Apweiler, R. (2009). QuickGO: a web-based tool for Gene Ontology searching. *Bioinformatics* 25, 3045-3046.
- Blazeck, J., Hill, A., Jamoussi, M., Pan, A., Miller, J., and Alper, H.S. (2015). Metabolic engineering of *Yarrowia lipolytica* for itaconic acid production. *Metabolic engineering* 32, 66-73.
- Blazeck, J., Hill, A., Liu, L., Knight, R., Miller, J., Pan, A., Otoupal, P., and Alper, H.S. (2014). Harnessing *Yarrowia lipolytica* lipogenesis to create a platform for lipid and biofuel production. *Nature communications* 5, 3131.
- Blazeck, J., Liu, L., Redden, H., and Alper, H. (2011). Tuning gene expression in *Yarrowia lipolytica* by a hybrid promoter approach. *Applied and environmental microbiology* 77, 7905-7914.
- Brabender, M., Hussain, M.S., Rodriguez, G., and Blenner, M.A. (2018). Urea and urine are a viable and cost-effective nitrogen source for *Yarrowia lipolytica* biomass and lipid accumulation. *Applied microbiology and biotechnology* 102, 2313-2322.

- Braga, A., and Belo, I. (2015). Production of γ -decalactone by *Yarrowia lipolytica*: insights into experimental conditions and operating mode optimization. *Journal of Chemical Technology & Biotechnology* *90*, 559-565.
- Bredeweg, E.L., Pomraning, K.R., Dai, Z., Nielsen, J., Kerkhoven, E.J., and Baker, S.E. (2017). A molecular genetic toolbox for *Yarrowia lipolytica*. *Biotechnology for Biofuels* *10*, 2.
- Brígida, A.I., Amaral, P.F., Coelho, M.A., and Goncalves, L.R. (2014). Lipase from *Yarrowia lipolytica*: Production, characterization and application as an industrial biocatalyst. *Journal of Molecular Catalysis B: Enzymatic* *101*, 148-158.
- Busch, A.W., Reijerse, E.J., Lubitz, W., Frankenberg-Dinkel, N., and Hofmann, E. (2011). Structural and mechanistic insight into the ferredoxin-mediated two-electron reduction of bilins. *Biochemical Journal* *439*, 257-264.
- Cao, X., Wei, L.-J., Lin, J.-Y., and Hua, Q. (2017). Enhancing linalool production by engineering oleaginous yeast *Yarrowia lipolytica*. *Bioresource Technology* *245*, 1641-1644.
- Carlson, E.D., Gan, R., Hodgman, C.E., and Jewett, M.C. (2012). Cell-free protein synthesis: applications come of age. *Biotechnology advances* *30*, 1185-1194.
- Cavallo, E., Charreau, H., Cerrutti, P., and Foresti, M.L. (2017). *Yarrowia lipolytica*: a model yeast for citric acid production. *FEMS yeast research* *17*, fox084.
- Celis, A.I., and DuBois, J.L. (2019). Making and breaking heme. *Current Opinion in Structural Biology* *59*, 19-28.
- Chakdar, H., and Pabbi, S. (2016). Cyanobacterial phycobilins: production, purification, and regulation. In *Frontier Discoveries and Innovations in Interdisciplinary Microbiology* (Springer), pp. 45-69.

- Chen, D., Brown, J.D., Kawasaki, Y., Bommer, J., and Takemoto, J.Y. (2012). Scalable production of biliverdin IX α by *Escherichia coli*. *BMC Biotechnology* *12*, 89.
- Chen, L., Yan, W., Qian, X., Chen, M., Zhang, X., Xin, F., Zhang, W., Jiang, M., and Ochsenreither, K. (2021). Increased lipid production in *Yarrowia lipolytica* from acetate through metabolic engineering and Cosubstrate fermentation. *ACS synthetic biology* *10*, 3129-3138.
- Choi, K.R., Yu, H.E., Lee, H., and Lee, S.Y. (2022). Improved production of heme using metabolically engineered *Escherichia coli*. *Biotechnology and Bioengineering* *119*, 3178-3193.
- Claassens, N.J., Burgener, S., Vögeli, B., Erb, T.J., and Bar-Even, A. (2019). A critical comparison of cellular and cell-free bioproduction systems. *Current opinion in biotechnology* *60*, 221-229.
- Cornejo, J., Beale, S., Terry, M., and Lagarias, J. (1992). Phytochrome assembly. The structure and biological activity of 2 (R), 3 (E)-phytychromobilin derived from phycobiliproteins. *Journal of Biological Chemistry* *267*, 14790-14798.
- Cornejo, J., Willows, R.D., and Beale, S.I. (1998). Phytobilin biosynthesis: cloning and expression of a gene encoding soluble ferredoxin-dependent heme oxygenase from *Synechocystis* sp. PCC 6803. *The Plant Journal* *15*, 99-107.
- Cui, Z., Zheng, H., Jiang, Z., Wang, Z., Hou, J., Wang, Q., Liang, Q., and Qi, Q. (2021a). Identification and characterization of the mitochondrial replication origin for stable and episomal expression in *Yarrowia lipolytica*. *ACS Synthetic Biology* *10*, 826-835.
- Cui, Z., Zheng, H., Zhang, J., Jiang, Z., Zhu, Z., Liu, X., Qi, Q., and Hou, J. (2021b). A CRISPR/Cas9-mediated, homology-independent tool developed for targeted genome

- integration in *Yarrowia lipolytica*. *Applied and Environmental Microbiology* 87, e02666-02620.
- Curran, K.A., Morse, N.J., Markham, K.A., Wagman, A.M., Gupta, A., and Alper, H.S. (2015). Short synthetic terminators for improved heterologous gene expression in yeast. *ACS synthetic biology* 4, 824-832.
- Da Silva, G.P., Mack, M., and Contiero, J. (2009). Glycerol: a promising and abundant carbon source for industrial microbiology. *Biotechnology advances* 27, 30-39.
- da Silva, J.L., Sales, M.B., de Castro Bizerra, V., Nobre, M.M.R., de Sousa Braz, A.K., da Silva Sousa, P., Cavalcante, A.L., Melo, R.L., Gonçalves De Sousa Junior, P., and Neto, F.S. (2023). Lipase from *Yarrowia lipolytica*: Prospects as an Industrial Biocatalyst for Biotechnological Applications. *Fermentation* 9, 581.
- Dai, Y., Meng, Q., Mu, W., and Zhang, T. (2017). Recent advances in the applications and biotechnological production of mannitol. *Journal of Functional Foods* 36, 404-409.
- Dailey, H.A., Dailey, T.A., Gerdes, S., Jahn, D., Jahn, M., O'Brian, M.R., and Warren, M.J. (2017). Prokaryotic heme biosynthesis: multiple pathways to a common essential product. *Microbiology and Molecular Biology Reviews* 81, 10.1128/mmbr.00048-00016.
- Darvishi, F., Fathi, Z., Ariana, M., and Moradi, H. (2017). *Yarrowia lipolytica* as a workhorse for biofuel production. *Biochemical engineering journal* 127, 87-96.
- De Hertogh, B.t., Hancy, F.d.r., Goffeau, A., and Baret, P.V. (2006). Emergence of Species-Specific Transporters During Evolution of the Hemiascomycete Phylum. *Genetics* 172, 771-781.
- Di Pierro, E., and Granata, F. (2020). Nutrients and porphyria: An intriguing crosstalk. *International Journal of Molecular Sciences* 21, 3462.

- Dils, R., and Popják, G. (1962). Biosynthesis of fatty acids in cell-free preparations. 5. Synthesis of fatty acids from acetate in extracts of lactating-rat mammary gland. *Biochemical Journal* 83, 41.
- Ding, Z.K., and Xu, Y.Q. (2002). Purification and Characterization of Biliverdin IX α from Atlantic Salmon (*Salmo salar*) Bile. *Biochemistry (Moscow)* 67, 927-932.
- Dujon, B., Sherman, D., Fischer, G., Durrens, P., Casaregola, S., Lafontaine, I., De Montigny, J., Marck, C., Neuvéglise, C., and Talla, E. (2004). Genome evolution in yeasts. *Nature* 430, 35-44.
- Egermeier, M., Russmayer, H., Sauer, M., and Marx, H. (2017). Metabolic flexibility of *Yarrowia lipolytica* growing on glycerol. *Frontiers in microbiology* 8, 49.
- Eriksen, N.T. (2013). Pigments from microalgae: a new perspective with emphasis on phycocyanin. Paper presented at: 7 th International Congress on Pigments in Food.
- Ferraro, N., Barbarite, E., Albert, T.R., Berchmans, E., Shah, A.H., Bregy, A., Ivan, M.E., Brown, T., and Komotar, R.J. (2016). The role of 5-aminolevulinic acid in brain tumor surgery: a systematic review. *Neurosurgical review* 39, 545-555.
- Fickers, P., Benetti, P.-H., Waché, Y., Marty, A., Mauersberger, S., Smit, M., and Nicaud, J.-M. (2005). Hydrophobic substrate utilisation by the yeast *Yarrowia lipolytica*, and its potential applications. *FEMS yeast research* 5, 527-543.
- Filonov, G.S., Piatkevich, K.D., Ting, L.-M., Zhang, J., Kim, K., and Verkhusha, V.V. (2011). Bright and stable near-infrared fluorescent protein for in vivo imaging. *Nature Biotechnology* 29, 757.
- Fontanellas, A., Ávila, M.A., and Berraondo, P. (2016). Emerging therapies for acute intermittent porphyria. *Expert reviews in molecular medicine* 18, e17.

- Fournier, P., Abbas, A., Chasles, M., Kudla, B., Ogrydziak, D.M., Yaver, D., Xuan, J.W., Peito, A., Ribet, A.M., Feynerol, C., *et al.* (1993). Colocalization of centromeric and replicative functions on autonomously replicating sequences isolated from the yeast *Yarrowia lipolytica*. *Proceedings of the National Academy of Sciences of the United States of America* *90*, 4912-4916.
- Frankenberg-Dinkel, N. (2004). Bacterial Heme Oxygenases. *Antioxidants & Redox Signaling* *6*, 825-834.
- Frankenberg, N., Moser, J., and Jahn, D. (2003). Bacterial heme biosynthesis and its biotechnological application. *Applied microbiology and biotechnology* *63*, 115-127.
- Gao, C., Qi, Q., Madzak, C., and Lin, C.S.K. (2015). Exploring medium-chain-length polyhydroxyalkanoates production in the engineered yeast *Yarrowia lipolytica*. *Journal of Industrial Microbiology and Biotechnology* *42*, 1255-1262.
- Gao, D., Smith, S., Spagnuolo, M., Rodriguez, G., and Blenner, M. (2018). Dual CRISPR-Cas9 cleavage mediated gene excision and targeted integration in *Yarrowia lipolytica*. *Biotechnology journal* *13*, 1700590.
- Gao, S., Tong, Y., Wen, Z., Zhu, L., Ge, M., Chen, D., Jiang, Y., and Yang, S. (2016). Multiplex gene editing of the *Yarrowia lipolytica* genome using the CRISPR-Cas9 system. *Journal of Industrial Microbiology and Biotechnology* *43*, 1085-1093.
- Gao, Y., Wang, F., Li, X., Mao, G., Xie, H., Song, A., dos Santos, J.C., and Zhang, Z. (2022a). Tailored production of citric acid and mannitol by *Yarrowia lipolytica* from corn stover pretreated by glycerol-assisted instant catapult steam explosion. *Industrial Crops and Products* *189*, 115820.

- Gao, Y., Wang, F., Li, X., Mao, G., Xie, H., Song, A., Santos, J.C.d., and Zhang, Z. (2022b). Tailored production of citric acid and mannitol by *Yarrowia lipolytica* from corn stover pretreated by glycerol-assisted instant catapult steam explosion. *Industrial Crops and Products* *189*, 115820.
- Garcia, D.C., Dinglasan, J.L.N., Shrestha, H., Abraham, P.E., Hettich, R.L., and Doktycz, M.J. (2021). A lysate proteome engineering strategy for enhancing cell-free metabolite production. *Metabolic Engineering Communications* *12*, e00162.
- Ge, B., Chen, Y., Yu, Q., Lin, X., Li, J., and Qin, S. (2018). Regulation of the heme biosynthetic pathway for combinational biosynthesis of phycocyanobilin in *Escherichia coli*. *Process Biochemistry* *71*, 23-30.
- Ge, B., Li, Y., Sun, H., Zhang, S., Hu, P., Qin, S., and Huang, F. (2013). Combinational biosynthesis of phycocyanobilin using genetically-engineered *Escherichia coli*. *Biotechnology Letters* *35*, 689-693.
- Ge, F., Li, X., Ge, Q., Zhu, D., Li, W., Shi, F., and Chen, H. (2021). Modular control of multiple pathways of *Corynebacterium glutamicum* for 5-aminolevulinic acid production. *AMB Express* *11*, 1-12.
- Geisberg, J.V., Moqtaderi, Z., Fan, X., Ozsolak, F., and Struhl, K. (2014). Global analysis of mRNA isoform half-lives reveals stabilizing and destabilizing elements in yeast. *Cell* *156*, 812-824.
- Gemperlein, K., Dietrich, D., Kohlstedt, M., Zipf, G., Bernauer, H.S., Wittmann, C., Wenzel, S.C., and Müller, R. (2019). Polyunsaturated fatty acid production by *Yarrowia lipolytica* employing designed myxobacterial PUFA synthases. *Nature communications* *10*, 4055.

- Geng, Z., Ge, J., Cui, W., Zhou, H., Deng, J., and Xu, B. (2022). Efficient De Novo Biosynthesis of Heme by Membrane Engineering in *Escherichia coli*. *International Journal of Molecular Sciences* *23*, 15524.
- Georgiadis, I., Tsiligkaki, C., Patavou, V., Orfanidou, M., Tsourekis, A., Andreadelli, A., Theodosiou, E., and Makris, A.M. (2023). Identification and Construction of Strong Promoters in *Yarrowia lipolytica* Suitable for Glycerol-Based Bioprocesses. *Microorganisms* *11*, 1152.
- Ghoreishi, S., and Shahrestani, R.G. (2009). Innovative strategies for engineering mannitol production. *Trends in food science & technology* *20*, 263-270.
- Godswill, A.C. (2017). Sugar alcohols: chemistry, production, health concerns and nutritional importance of mannitol, sorbitol, xylitol, and erythritol. *Int J Adv Acad Res* *3*, 31-66.
- Gold, M.H., and Goldman, M.P. (2004). 5-aminolevulinic acid photodynamic therapy: where we have been and where we are going. *Dermatologic surgery* *30*, 1077-1084.
- Grubbe, W.S., Rasor, B.J., Krüger, A., Jewett, M.C., and Karim, A.S. (2020). Cell-free styrene biosynthesis at high titers. *Metabolic Engineering* *61*, 89-95.
- Gu, Y., Ma, J., Zhu, Y., Ding, X., and Xu, P. (2020). Engineering *Yarrowia lipolytica* as a chassis for de novo synthesis of five aromatic-derived natural products and chemicals. *ACS synthetic biology* *9*, 2096-2106.
- Guan, N., Li, J., Shin, H.-d., Du, G., Chen, J., and Liu, L. (2017). Microbial response to environmental stresses: from fundamental mechanisms to practical applications. *Applied Microbiology and Biotechnology* *101*, 3991+.

- Gutiérrez-Grobe, Y., Vitek, L., Tiribelli, C., Kobashi-Margáin, R.A., Uribe, M., and Méndez-Sánchez, N. (2016). Biliverdin and heme oxygenase antiviral activity against hepatitis C virus. *Annals of hepatology* *10*, 105-107.
- Hackenschmidt, S., Bracharz, F., Daniel, R., Thürmer, A., Bruder, S., and Kabisch, J. (2019). Effects of a high-cultivation temperature on the physiology of three different *Yarrowia lipolytica* strains. *FEMS Yeast Research* *19*, foz068.
- Hashemi, A. (2020). CRISPR–Cas9/CRISPRi tools for cell factory construction in *E. coli*. *World Journal of Microbiology and Biotechnology* *36*, 96.
- Hendawy, A., Shirai, M., Takeya, H., Sugimura, S., Miyanari, S., Taniguchi, S., and Sato, K. (2019). Effects of 5-aminolevulinic acid supplementation on milk production, iron status, and immune response of dairy cows. *Journal of Dairy Science* *102*, 11009-11015.
- Hoagland, M.B. (1960). The relationship of nucleic acid and protein synthesis as revealed by studies in cell-free systems. *The nucleic acids* *3*, 349-408.
- Holkenbrink, C., Dam, M.I., Kildegaard, K.R., Beder, J., Dahlin, J., Doménech Belda, D., and Borodina, I. (2018). EasyCloneYALI: CRISPR/Cas9-based synthetic toolbox for engineering of the yeast *Yarrowia lipolytica*. *Biotechnology journal* *13*, 1700543.
- Hong, S.P., Seip, J., Walters-Pollak, D., Rupert, R., Jackson, R., Xue, Z., and Zhu, Q. (2012). Engineering *Yarrowia lipolytica* to express secretory invertase with strong FBA1IN promoter. *Yeast (Chichester, England)* *29*, 59-72.
- Ishchuk, O.P., Domenzain, I., Sánchez, B.J., Muñoz-Paredes, F., Martínez, J.L., Nielsen, J., and Petranovic, D. (2022). Genome-scale modeling drives 70-fold improvement of intracellular heme production in *Saccharomyces cerevisiae*. *Proceedings of the National Academy of Sciences* *119*, e2108245119.

- Jagtap, S.S., Bedekar, A.A., Singh, V., Jin, Y.-S., and Rao, C.V. (2021). Metabolic engineering of the oleaginous yeast *Yarrowia lipolytica* PO1f for production of erythritol from glycerol. *Biotechnology for Biofuels* *14*, 1-17.
- Jiang, M., Hong, K., Mao, Y., Ma, H., Chen, T., and Wang, Z. (2022). Natural 5-aminolevulinic acid: Sources, biosynthesis, detection and applications. *Frontiers in Bioengineering and Biotechnology* *10*, 841443.
- Joshi, S., Kumari, R., and Upasani, V.N. (2018). Applications of algae in cosmetics: An overview. *Int J Innov Res Sci Eng Technol* *7*, 1269-1278.
- Juretzek, T., Wang, H.-J., Nicaud, J.-M., Mauersberger, S., and Barth, G. (2000). Comparison of promoters suitable for regulated overexpression of β -galactosidase in the alkane-utilizing yeast *Yarrowia lipolytica*. *Biotechnology and Bioprocess Engineering* *5*, 320-326.
- Juszczak, P., Rywińska, A., Kosicka, J., Tomaszewska-Hetman, L., and Rymowicz, W. (2023). Sugar Alcohol Sweetener Production by *Yarrowia lipolytica* Grown in Media Containing Glycerol. *Molecules* *28*, 6594.
- Kang, Z., Ding, W., Gong, X., Liu, Q., Du, G., and Chen, J. (2017). Recent advances in production of 5-aminolevulinic acid using biological strategies. *World Journal of Microbiology and Biotechnology* *33*, 1-7.
- Kang, Z., Wang, Y., Gu, P., Wang, Q., and Qi, Q. (2011). Engineering *Escherichia coli* for efficient production of 5-aminolevulinic acid from glucose. *Metabolic engineering* *13*, 492-498.
- Kim, D., Langmead, B., and Salzberg, S.L. (2015). HISAT: a fast spliced aligner with low memory requirements. *Nature methods* *12*, 357-360.
- Ko, Y.J., Kim, M., You, S.K., Shin, S.K., Chang, J., Choi, H.J., Jeong, W.-Y., Lee, M.-E., Hwang, D.-H., and Han, S.O. (2021). Animal-free heme production for artificial meat in

- Corynebacterium glutamicum* via systems metabolic and membrane engineering. *Metabolic Engineering* 66, 217-228.
- Koch, M., Faulon, J.-L., and Borkowski, O. (2018). Models for cell-free synthetic biology: make prototyping easier, better, and faster. *Frontiers in bioengineering and biotechnology* 6, 182.
- Kosaka, J., Morimatsu, H., Takahashi, T., Shimizu, H., Kawanishi, S., Omori, E., Endo, Y., Tamaki, N., Morita, M., and Morita, K. (2013). Effects of biliverdin administration on acute lung injury induced by hemorrhagic shock and resuscitation in rats. *PLoS One* 8, e63606.
- Kosicki, M., Allen, F., Steward, F., Tomberg, K., Pan, Y., and Bradley, A. (2022). Cas9-induced large deletions and small indels are controlled in a convergent fashion. *Nature communications* 13, 3422.
- Kumar, S., and Bandyopadhyay, U. (2005). Free heme toxicity and its detoxification systems in human. *Toxicology Letters* 157, 175-188.
- Lajus, S., Dusséaux, S., Verbeke, J., Rigouin, C., Guo, Z., Fatarova, M., Bellvert, F., Borsenberger, V., Bressy, M., and Nicaud, J.-M. (2020). Engineering the yeast *Yarrowia lipolytica* for production of polylactic acid homopolymer. *Frontiers in bioengineering and biotechnology* 8, 954.
- LaMattina, J.W., Nix, D.B., and Lanzilotta, W.N. (2016). Radical new paradigm for heme degradation in *Escherichia coli* O157:H7. *Proceedings of the National Academy of Sciences of the United States of America* 113, 12138-12143.
- Larroude, M., Celinska, E., Back, A., Thomas, S., Nicaud, J.M., and Ledesma-Amaro, R. (2018). A synthetic biology approach to transform *Yarrowia lipolytica* into a competitive biotechnological producer of β -carotene. *Biotechnology and bioengineering* 115, 464-472.

- Larroude, M., Nicaud, J.M., and Rossignol, T. (2021). *Yarrowia lipolytica* chassis strains engineered to produce aromatic amino acids via the shikimate pathway. *Microbial Biotechnology* *14*, 2420-2434.
- Larroude, M., Trabelsi, H., Nicaud, J.-M., and Rossignol, T. (2020). A set of *Yarrowia lipolytica* CRISPR/Cas9 vectors for exploiting wild-type strain diversity. *Biotechnology letters* *42*, 773-785.
- Lehmann, E., El-Tantawy, W.H., Ocker, M., Bartenschlager, R., Lohmann, V., Hashemolhosseini, S., Tiegs, G., and Sass, G. (2010). The heme oxygenase 1 product biliverdin interferes with hepatitis C virus replication by increasing antiviral interferon response. *Hepatology* *51*, 398-404.
- Li, J., Ma, Y., Liu, N., Eser, B.E., Guo, Z., Jensen, P.R., and Stephanopoulos, G. (2020). Synthesis of high-titer alkaloids in *Yarrowia lipolytica* is enabled by a discovered mechanism. *Nature Communications* *11*, 6198.
- Li, Z.-G., Ye, X.-Y., and Qiu, X.-M. (2019). Glutamate signaling enhances the heat tolerance of maize seedlings by plant glutamate receptor-like channels-mediated calcium signaling. *Protoplasma* *256*, 1165-1169.
- Liao, Y., Smyth, G.K., and Shi, W. (2014). featureCounts: an efficient general purpose program for assigning sequence reads to genomic features. *Bioinformatics* *30*, 923-930.
- Lim, H.J., and Kim, D.-M. (2019). Cell-free metabolic engineering: recent developments and future prospects. *Methods and protocols* *2*, 33.
- Liu, H.-H., Ji, X.-J., and Huang, H. (2015). Biotechnological applications of *Yarrowia lipolytica*: past, present and future. *Biotechnology Advances* *33*, 1522-1546.

- Liu, J., Hu, Y., Gu, W., Lan, H., Zhang, Z., Jiang, L., and Xu, X. (2023). Research progress on the application of cell-free synthesis systems for enzymatic processes. *Critical Reviews in Biotechnology* 43, 938-955.
- Liu, L., Otoupal, P., Pan, A., and Alper, H.S. (2014). Increasing expression level and copy number of a *Yarrowia lipolytica* plasmid through regulated centromere function. *FEMS Yeast Research* 14, 1124-1127.
- Louca, S., Polz, M.F., Mazel, F., Albright, M.B., Huber, J.A., O'Connor, M.I., Ackermann, M., Hahn, A.S., Srivastava, D.S., and Crowe, S.A. (2018). Function and functional redundancy in microbial systems. *Nature ecology & evolution* 2, 936-943.
- Love, M.I., Huber, W., and Anders, S. (2014). Moderated estimation of fold change and dispersion for RNA-seq data with DESeq2. *Genome biology* 15, 1-21.
- Lyles, K.V., and Eichenbaum, Z. (2018). From Host Heme To Iron: The Expanding Spectrum of Heme Degrading Enzymes Used by Pathogenic Bacteria. *Frontiers in Cellular and Infection Microbiology* 8.
- Madzak, C. (2015). *Yarrowia lipolytica*: recent achievements in heterologous protein expression and pathway engineering. *Applied microbiology and biotechnology* 99, 4559-4577.
- Madzak, C. (2018). Engineering *Yarrowia lipolytica* for Use in Biotechnological Applications: A Review of Major Achievements and Recent Innovations. *Molecular Biotechnology* 60, 621-635.
- Madzak, C. (2021). *Yarrowia lipolytica* Strains and Their Biotechnological Applications: How Natural Biodiversity and Metabolic Engineering Could Contribute to Cell Factories Improvement. *Journal of fungi (Basel, Switzerland)* 7.

- Madzak, C., Tréton, B., and Blanchin-Roland, S. (2000). Strong hybrid promoters and integrative expression/secretion vectors for quasi-constitutive expression of heterologous proteins in the yeast *Yarrowia lipolytica*. *Journal of molecular microbiology and biotechnology* *2*, 207-216.
- Makkee, M., Kieboom, A., and Van Bekkum, H. (1985). Production methods of d-mannitol. *Starch-Stärke* *37*, 136-141.
- Markham, K.A., and Alper, H.S. (2018). Synthetic biology expands the industrial potential of *Yarrowia lipolytica*. *Trends in biotechnology* *36*, 1085-1095.
- Martin, M. (2011). Cutadapt removes adapter sequences from high-throughput sequencing reads. *EMBnet journal* *17*, 10-12.
- Martinez-Force, E., and Benitez, T. (1995). Effects of varying media, temperature, and growth rates on the intracellular concentrations of yeast amino acids. *Biotechnology progress* *11*, 386-392.
- Martínez-Miranda, J.G., Chairez, I., and Durán-Páramo, E. (2022). Mannitol production by heterofermentative lactic acid bacteria: A review. *Applied Biochemistry and Biotechnology* *194*, 2762-2795.
- McCarty, M.F. (2007). Clinical potential of *Spirulina* as a source of phycocyanobilin. *Journal of medicinal food* *10*, 566-570.
- McCarty, M.F., Barroso-Aranda, J., and Contreras, F. (2010). Oral phycocyanobilin may diminish the pathogenicity of activated brain microglia in neurodegenerative disorders. *Medical hypotheses* *74*, 601-605.
- McCommis, K.S., and Finck, B.N. (2015). Mitochondrial pyruvate transport: a historical perspective and future research directions. *Biochemical journal* *466*, 443-454.

- McDonagh, A.F. (2005). Biliverdin, immune-mediated liver injury, and the Gigo effect. *Hepatology* *41*, 680-681.
- McDonagh, A.F., and Palma, L.A. (1980). Preparation and properties of crystalline biliverdin IX α . Simple methods for preparing isomerically homogeneous biliverdin and [¹⁴C]biliverdin by using 2,3-dichloro-5,6-dicyanobenzoquinone. *Biochemical Journal* *189*, 193-208.
- Miscevic, D., Mao, J.-Y., Kefale, T., Abedi, D., Moo-Young, M., and Perry Chou, C. (2021). Strain engineering for high-level 5-aminolevulinic acid production in *Escherichia coli*. *Biotechnology and Bioengineering* *118*, 30-42.
- Mishra, S.K., Suh, W.I., Farooq, W., Moon, M., Shrivastav, A., Park, M.S., and Yang, J.-W. (2014). Rapid quantification of microalgal lipids in aqueous medium by a simple colorimetric method. *Bioresource Technology* *155*, 330-333.
- Monselise, E.B.-I., Parola, A.H., and Kost, D. (2003). Low-frequency electromagnetic fields induce a stress effect upon higher plants, as evident by the universal stress signal, alanine. *Biochemical and Biophysical Research Communications* *302*, 427-434.
- Moore, S.J., MacDonald, J.T., and Freemont, P.S. (2017). Cell-free synthetic biology for in vitro prototype engineering. *Biochemical Society Transactions* *45*, 785-791.
- Morone, J., Alfeus, A., Vasconcelos, V., and Martins, R. (2019). Revealing the potential of cyanobacteria in cosmetics and cosmeceuticals—A new bioactive approach. *Algal Research* *41*, 101541.
- Mourelle, M., Gómez, C., and Legido, J. (2017). The potential use of marine microalgae and cyanobacteria in cosmetics and thalassotherapy. *Cosmetics* *4*, 46.

- Mukougawa, K., Kanamoto, H., Kobayashi, T., Yokota, A., and Kohchi, T. (2006). Metabolic engineering to produce phytochromes with phytochromobilin, phycocyanobilin, or phycoerythrobilin chromophore in *Escherichia coli*. *FEBS Letters* *580*, 1333-1338.
- Müller, K., Engesser, R., Timmer, J., Nagy, F., Zurbriggen, M.D., and Weber, W. (2013). Synthesis of phycocyanobilin in mammalian cells. *Chemical communications* *49*, 8970-8972.
- Mumberg, D., Müller, R., and Funk, M. (1995). Yeast vectors for the controlled expression of heterologous proteins in different genetic backgrounds. *Gene* *156*, 119-122.
- Mysliwa-Kurdziel, B., and Solymosi, K. (2017). Phycobilins and phycobiliproteins used in food industry and medicine. *Mini reviews in medicinal chemistry* *17*, 1173-1193.
- Nambu, S., Matsui, T., Goulding, C.W., Takahashi, S., and Ikeda-Saito, M. (2013). A new way to degrade heme the *Mycobacterium tuberculosis* enzyme MhuD catalyzes heme degradation without generating CO. *Journal of Biological Chemistry* *288*, 10101-10109.
- Nicaud, J.-M., Madzak, C., van den Broek, P., Gysler, C., Duboc, P., Niederberger, P., and Gaillardin, C. (2002). Protein expression and secretion in the yeast *Yarrowia lipolytica*. *FEMS yeast research* *2*, 371-379.
- Nicaud, J.M. (2012). *Yarrowia lipolytica*. *Yeast (Chichester, England)* *29*, 409-418.
- Niehus, X., Crutz-Le Coq, A.-M., Sandoval, G., Nicaud, J.-M., and Ledesma-Amaro, R. (2018). Engineering *Yarrowia lipolytica* to enhance lipid production from lignocellulosic materials. *Biotechnology for Biofuels* *11*, 1-10.
- Nielsen, J. (2001). Metabolic engineering. *Applied microbiology and biotechnology* *55*, 263-283.

- Nirenberg, M.W., and Matthaei, J.H. (1961). The dependence of cell-free protein synthesis in *E. coli* upon naturally occurring or synthetic polyribonucleotides. *Proceedings of the National Academy of Sciences* 47, 1588-1602.
- Nishida, K., and Kondo, A. (2021). CRISPR-derived genome editing technologies for metabolic engineering. *Metabolic Engineering* 63, 141-147.
- Noll, P., Lilge, L., Hausmann, R., and Henkel, M. (2020). Modeling and exploiting microbial temperature response. *Processes* 8, 121.
- Nurwono, G., O’Keeffe, S., Liu, N., and Park, J.O. (2023). Sustainable metabolic engineering requires a perfect trifecta. *Current Opinion in Biotechnology* 83, 102983.
- Ó’carra, P., and Colleran, E. (1970). Separation and identification of biliverdin isomers and isomer analysis of phycobilins and bilirubin. *Journal of Chromatography A* 50, 458-468.
- Ortiz, M.E., Bleckwedel, J., Raya, R.R., and Mozzi, F. (2013). Biotechnological and in situ food production of polyols by lactic acid bacteria. *Applied microbiology and biotechnology* 97, 4713-4726.
- Overhaus, M., Moore, B.A., Barbato, J.E., Behrendt, F.F., Doering, J.G., and Bauer, A.J. (2006). Biliverdin protects against polymicrobial sepsis by modulating inflammatory mediators. *American Journal of Physiology-Gastrointestinal and Liver Physiology* 290, G695-G703.
- Papanikolaou, S., Chevalot, I., Komaitis, M., Marc, I., and Aggelis, G. (2002a). Single cell oil production by *Yarrowia lipolytica* growing on an industrial derivative of animal fat in batch cultures. *Applied microbiology and biotechnology* 58, 308-312.
- Papanikolaou, S., Muniglia, L., Chevalot, I., Aggelis, G., and Marc, I. (2002b). *Yarrowia lipolytica* as a potential producer of citric acid from raw glycerol. *Journal of applied microbiology* 92, 737-744.

- Papanikolaou, S., Muniglia, L., Chevalot, I., Aggelis, G., and Marc, I. (2003). Accumulation of a cocoa-butter-like lipid by *Yarrowia lipolytica* cultivated on agro-industrial residues. *Current Microbiology* *46*, 0124-0130.
- Park, G., Kim, Y.C., Jang, M., Park, H., Lee, H.-W., Jeon, W., Kim, B.-G., Choi, K.-Y., and Ahn, J. (2023). Biosynthesis of aliphatic plastic monomers with amino residues in *Yarrowia lipolytica*. *Frontiers in Bioengineering and Biotechnology* *10*, 825576.
- Park, Y.-K., and Ledesma-Amaro, R. (2023). What makes *Yarrowia lipolytica* well suited for industry? *Trends in Biotechnology* *41*, 242-254.
- Pendrak, M.L., and Roberts, D.D. (2013). Methods for the production of biliverdin (Google Patents).
- Pentón-Rol, G., Marín-Prida, J., and Pentón-Arias, E. (2016). Cytoprotection in Multiple Sclerosis and Ischemic Stroke with C-Phycocyanin and Phycocyanobilin. *J Neurol Neurol Sci Disord* *2*, 017-021.
- Perez, J.G., Stark, J.C., and Jewett, M.C. (2016). Cell-free synthetic biology: engineering beyond the cell. *Cold Spring Harbor perspectives in biology* *8*, a023853.
- Piatkevich, K.D., Subach, F.V., and Verkhusha, V.V. (2013). Far-red light photoactivatable near-infrared fluorescent proteins engineered from a bacterial phytochrome. *Nature Communications* *4*, 2153.
- Pomraning, K.R., and Baker, S.E. (2015). Draft genome sequence of the dimorphic yeast *Yarrowia lipolytica* strain W29. *Genome announcements* *3*, 10.1128/genomea.01211-01215.
- Pontrelli, S., Chiu, T.-Y., Lan, E.I., Chen, F.Y.-H., Chang, P., and Liao, J.C. (2018). *Escherichia coli* as a host for metabolic engineering. *Metabolic engineering* *50*, 16-46.

- Pronk, J.T., Yde Steensma, H., and Van Dijken, J.P. (1996). Pyruvate metabolism in *Saccharomyces cerevisiae*. *Yeast (Chichester, England)* *12*, 1607-1633.
- Pu, W., Chen, J., Zhou, Y., Qiu, H., Shi, T., Zhou, W., Guo, X., Cai, N., Tan, Z., and Liu, J. (2023). Systems metabolic engineering of *Escherichia coli* for hyper-production of 5-aminolevulinic acid. *Biotechnology for Biofuels and Bioproducts* *16*, 31.
- Qiao, K., Abidi, S.H.I., Liu, H., Zhang, H., Chakraborty, S., Watson, N., Ajikumar, P.K., and Stephanopoulos, G. (2015). Engineering lipid overproduction in the oleaginous yeast *Yarrowia lipolytica*. *Metabolic engineering* *29*, 56-65.
- Qiu, X.-M., Sun, Y.-Y., Ye, X.-Y., and Li, Z.-G. (2020). Signaling role of glutamate in plants. *Frontiers in Plant Science* *10*, 1743.
- Rampakakis, E., Di Paola, D., and Zannis-Hadjopoulos, M. (2008). Ku is involved in cell growth, DNA replication and G1-S transition. *Journal of cell science* *121*, 590-600.
- Rasor, B.J., Vögeli, B., Landwehr, G.M., Bogart, J.W., Karim, A.S., and Jewett, M.C. (2021). Toward sustainable, cell-free biomanufacturing. *Current Opinion in Biotechnology* *69*, 136-144.
- Rather, L.J., Mir, S.S., Ganie, S.A., Islam, S.-u., and Li, Q. (2022). Research progress, challenges, and perspectives in microbial pigment production for industrial applications-A review. *Dyes and Pigments*, 110989.
- Reed, R., Davison, I., Chudek, J., and Foster, R. (1985). The osmotic role of mannitol in the Phaeophyta: an appraisal. *Phycologia* *24*, 35-47.
- Rhaman, M.S., Imran, S., Karim, M.M., Chakraborty, J., Mahamud, M.A., Sarker, P., Tahjib-Ul-Arif, M., Robin, A.H.K., Ye, W., and Murata, Y. (2021). 5-aminolevulinic acid-mediated plant adaptive responses to abiotic stress. *Plant Cell Reports* *40*, 1451-1469.

- Rigouin, C., Lajus, S., Ocando, C., Borsenberger, V., Nicaud, J.M., Marty, A., Avérous, L., and Bordes, F. (2019). Production and characterization of two medium-chain-length polyhydroxyalkanoates by engineered strains of *Yarrowia lipolytica*. *Microbial Cell Factories* *18*, 1-9.
- Rodriguez, E.A., Tran, G.N., Gross, L.A., Crisp, J.L., Shu, X., Lin, J.Y., and Tsien, R.Y. (2016). A far-red fluorescent protein evolved from a cyanobacterial phycobiliprotein. *Nature methods* *13*, 763.
- Saha, B.C. (2003). Production of mannitol by fermentation. Paper presented at: ACS Symposium Series (Washington, DC; American Chemical Society; 1999).
- Saha, B.C., and Nakamura, L.K. (2003). Production of mannitol and lactic acid by fermentation with *Lactobacillus intermedius* NRRL B-3693. *Biotechnology and bioengineering* *82*, 864-871.
- Sarria, S., Kruyer, N.S., and Peralta-Yahya, P. (2017). Microbial synthesis of medium-chain chemicals from renewables. *Nature Biotechnology* *35*, 1158-1166.
- Sassa, S. (2004). Why Heme Needs to Be Degraded to Iron, Biliverdin IX α , and Carbon Monoxide? *Antioxidants & Redox Signaling* *6*, 819-824.
- Savergave, L.S., Gadre, R.V., Vaidya, B.K., and Jogdand, V.V. (2013). Two-stage fermentation process for enhanced mannitol production using *Candida magnoliae* mutant R9. *Bioprocess and biosystems engineering* *36*, 193-203.
- Schmitt, M.P. (1997). Utilization of host iron sources by *Corynebacterium diphtheriae*: identification of a gene whose product is homologous to eukaryotic heme oxygenases and is required for acquisition of iron from heme and hemoglobin. *Journal of Bacteriology* *179*, 838-845.

- Schwartz, C., Cheng, J.-F., Evans, R., Schwartz, C.A., Wagner, J.M., Anglin, S., Beitz, A., Pan, W., Lonardi, S., and Blenner, M. (2019). Validating genome-wide CRISPR-Cas9 function improves screening in the oleaginous yeast *Yarrowia lipolytica*. *Metabolic engineering* 55, 102-110.
- Schwartz, C., Frogue, K., Ramesh, A., Misa, J., and Wheeldon, I. (2017a). CRISPRi repression of nonhomologous end-joining for enhanced genome engineering via homologous recombination in *Yarrowia lipolytica*. *Biotechnology and bioengineering* 114, 2896-2906.
- Schwartz, C., Shabbir-Hussain, M., Frogue, K., Blenner, M., and Wheeldon, I. (2017b). Standardized markerless gene integration for pathway engineering in *Yarrowia lipolytica*. *ACS synthetic biology* 6, 402-409.
- Schwartz, C., and Wheeldon, I. (2018). CRISPR-Cas9-mediated genome editing and transcriptional control in *Yarrowia lipolytica*. *Synthetic Biology: Methods and Protocols*, 327-345.
- Schwartz, C.M., Hussain, M.S., Blenner, M., and Wheeldon, I. (2016). Synthetic RNA polymerase III promoters facilitate high-efficiency CRISPR–Cas9-mediated genome editing in *Yarrowia lipolytica*. *ACS synthetic biology* 5, 356-359.
- Schweet, R., Lamfrom, H., and Allen, E. (1958). The synthesis of hemoglobin in a cell-free system. *Proceedings of the National Academy of Sciences* 44, 1029-1035.
- Seok, J., Ko, Y.J., Lee, M.-E., Hyeon, J.E., and Han, S.O. (2019). Systems metabolic engineering of *Corynebacterium glutamicum* for the bioproduction of biliverdin via protoporphyrin independent pathway. *J Biol Eng* 13, 28-28.

- Shabbir Hussain, M., Wheeldon, I., and Blenner, M.A. (2017). A strong hybrid fatty acid inducible transcriptional sensor built from *Yarrowia lipolytica* upstream activating and regulatory sequences. *Biotechnology Journal* *12*, 1700248.
- Shao, Y., Li, C., Chen, X., Zhang, P., Li, Y., Li, T., and Jiang, J. (2015). Metabolomic responses of sea cucumber *Apostichopus japonicus* to thermal stresses. *Aquaculture* *435*, 390-397.
- Shawkat, H., Westwood, M.-M., and Mortimer, A. (2012). Mannitol: a review of its clinical uses. *Continuing Education in Anaesthesia, Critical Care & Pain* *12*, 82-85.
- Shcherbakova, D.M., Baloban, M., and Verkhusha, V.V. (2015). Near-infrared fluorescent proteins engineered from bacterial phytochromes. *Current Opinion in Chemical Biology* *27*, 52-63.
- Shcherbakova, D.M., and Verkhusha, V.V. (2013). Near-infrared fluorescent proteins for multicolor in vivo imaging. *Nature Methods* *10*, 751.
- Skaar, E.P., Gaspar, A.H., and Schneewind, O. (2004). IsdG and IsdI, heme-degrading enzymes in the cytoplasm of *Staphylococcus aureus*. *Journal of Biological Chemistry* *279*, 436-443.
- Slatner, M., Nagl, G., Haltrich, D., Kulbe, K.D., and Nidetzky, B. (1998). Enzymatic production of pure D-mannitol at high productivity. *Biocatalysis and Biotransformation* *16*, 351-363.
- Sokolenko, S., Blondeel, E.J., Azlah, N., George, B., Schulze, S., Chang, D., and Aucoin, M.G. (2014). Profiling convoluted single-dimension proton NMR spectra: a Plackett–Burman approach for assessing quantification error of metabolites in complex mixtures with application to cell culture. *Analytical chemistry* *86*, 3330-3337.
- Sonani, R.R., Rastogi, R.P., Patel, R., and Madamwar, D. (2016). Recent advances in production, purification and applications of phycobiliproteins. *World J Biol Chem* *7*, 100-109.

- Song, K.-H., Lee, J.-K., Song, J.-Y., Hong, S.-G., Baek, H., Kim, S.-Y., and Hyun, H.-H. (2002). Production of mannitol by a novel strain of *Candida magnoliae*. *Biotechnology letters* 24, 9-12.
- Song, M., Zhao, J., Wen, H.-S., Li, Y., Li, J.-F., Li, L.-M., and Tao, Y.-X. (2019). The impact of acute thermal stress on the metabolome of the black rockfish (*Sebastes schlegelii*). *PloS one* 14, e0217133.
- Song, S.H., and Vieille, C. (2009). Recent advances in the biological production of mannitol. *Applied microbiology and biotechnology* 84, 55-62.
- Spagnuolo, M., Yaguchi, A., and Blenner, M. (2019). Oleaginous yeast for biofuel and oleochemical production. *Current Opinion in Biotechnology* 57, 73-81.
- Stanic-Vucinic, D., Minic, S., Nikolic, M.R., and Velickovic, T.C. (2018). Spirulina Phycobiliproteins as Food Components and Complements. *Microalgal Biotechnology*, 1st ed; Jacob-Lopes, E, Queiroz Zepka, L, Queiroz, MI, Eds, 129-149.
- Stephanopoulos, G. (1999). Metabolic Fluxes and Metabolic Engineering. *Metabolic Engineering* 1, 1-11.
- Stiefelmaier, J., Ledermann, B., Sorg, M., Banek, A., Geib, D., Ulber, R., and Frankenberg-Dinkel, N. (2018). Pink bacteria—Production of the pink chromophore phycoerythrobilin with *Escherichia coli*. *Journal of Biotechnology* 274, 47-53.
- Stoop, J.M., Williamson, J.D., and Pharr, D.M. (1996). Mannitol metabolism in plants: a method for coping with stress. *Trends in Plant Science* 1, 139-144.
- Stotz, E. (1945). Pyruvate metabolism. *Advances in Enzymology and Related Areas of Molecular Biology* 5, 129-164.

- Su, H., Chen, X., Chen, S., Guo, M., and Liu, H. (2023). Applications of the Whole-Cell System in the Efficient Biosynthesis of Heme. *International Journal of Molecular Sciences* *24*, 8384.
- Su, T., Guo, Q., Zheng, Y., Liang, Q., Wang, Q., and Qi, Q. (2019). Fine-tuning of hemB using CRISPRi for increasing 5-aminolevulinic acid production in *Escherichia coli*. *Frontiers in Microbiology* *10*, 1731.
- Sugimoto, R., Tanaka, Y., Noda, K., Kawamura, T., Toyoda, Y., Billiar, T.R., McCurry, K.R., and Nakao, A. (2012). Preservation solution supplemented with biliverdin prevents lung cold ischaemia/reperfusion injury. *European journal of cardio-thoracic surgery* *42*, 1035-1041.
- Tai, M., and Stephanopoulos, G. (2013). Engineering the push and pull of lipid biosynthesis in oleaginous yeast *Yarrowia lipolytica* for biofuel production. *Metabolic engineering* *15*, 1-9.
- Takemoto, J.Y., Chang, C.-W.T., Chen, D., and Hinton, G. (2019). Heme-Derived Bilins. *Israel Journal of Chemistry* *59*, 378-386.
- Takemoto, J.Y., and Chen, D. (2017). Recombinant non-animal cell for making biliverdin (Google Patents).
- Tan, M.-J., Chen, X., Wang, Y.-K., Liu, G.-L., and Chi, Z.-M. (2016). Enhanced citric acid production by a yeast *Yarrowia lipolytica* over-expressing a pyruvate carboxylase gene. *Bioprocess and biosystems engineering* *39*, 1289-1296.
- Tian, W.-F., Weng, P., Sheng, Q., Chen, J.-L., Zhang, P., Zhang, J.-R., Du, B., Wu, M.-C., Pang, Q.-F., and Chu, J.-J. (2017). Biliverdin protects the isolated rat lungs from ischemia-reperfusion injury via antioxidative, anti-inflammatory and anti-apoptotic effects. *Chinese medical journal* *130*, 859.

- Tietz, A. (1961). Fat synthesis in cell-free preparations of the locust fat-body. *Journal of lipid research* 2, 182-187.
- Ting, W.W., and Ng, I.S. (2023). Effective 5-aminolevulinic acid production via T7 RNA polymerase and RuBisCO equipped *Escherichia coli* W3110. *Biotechnology and Bioengineering* 120, 583-592.
- Tomaszewska, L., Rywińska, A., and Gładkowski, W. (2012). Production of erythritol and mannitol by *Yarrowia lipolytica* yeast in media containing glycerol. *Journal of Industrial Microbiology and Biotechnology* 39, 1333-1343.
- Tooley, A.J., Cai, Y.A., and Glazer, A.N. (2001). Biosynthesis of a fluorescent cyanobacterial C-phycoyanin holo- α subunit in a heterologous host. *Proceedings of the National Academy of Sciences* 98, 10560-10565.
- Trassaert, M., Vandermies, M., Carly, F., Denies, O., Thomas, S., Fickers, P., and Nicaud, J.-M. (2017). New inducible promoter for gene expression and synthetic biology in *Yarrowia lipolytica*. *Microbial Cell Factories* 16, 1-17.
- Tyndall, S.M., Maloney, G.R., Cole, M.B., Hazell, N.G., and Augustin, M.A. (2022). Critical food and nutrition science challenges for plant-based meat alternative products. *Critical Reviews in Food Science and Nutrition*, 1-16.
- Uda, Y., Goto, Y., Oda, S., Kohchi, T., Matsuda, M., and Aoki, K. (2017). Efficient synthesis of phycocyanobilin in mammalian cells for optogenetic control of cell signaling. *Proceedings of the National Academy of Sciences* 114, 11962-11967.
- Väremo, L., Nielsen, J., and Nookaew, I. (2013). Enriching the gene set analysis of genome-wide data by incorporating directionality of gene expression and combining statistical hypotheses and methods. *Nucleic acids research* 41, 4378-4391.

- Walsh, R.M., and Martin, P.A. (1977). Growth of *Saccharomyces cerevisiae* and *saccharomyces uvarum* in a temperature gradient incubator *Journal of the Institute of Brewing* 83, 169-172.
- Wang, H., Mu, X., Yang, J., Liang, Y., Zhang, X.-D., and Ming, D. (2019). Brain imaging with near-infrared fluorophores. *Coordination Chemistry Reviews* 380, 550-571.
- Wang, J., Zhou, H.-C., Pan, P., Zhang, N., and Li, W.-Z. (2010). Exogenous biliverdin improves the function of lung grafts from brain dead donors in rats. Paper presented at: Transplantation proceedings (Elsevier).
- Wang, K., Shi, T.-Q., Lin, L., Wei, P., Ledesma-Amaro, R., and Ji, X.-J. (2022). Engineering *Yarrowia lipolytica* to produce tailored chain-length fatty acids and their derivatives. *ACS Synthetic Biology* 11, 2564-2577.
- Weymarn, F.N.W.v., Kiviharju, K.J., Jääskeläinen, S.T., and Leisola, M.S. (2003). Scale-up of a New Bacterial Mannitol Production Process. *Biotechnology progress* 19, 815-821.
- Whitacre, J.M. (2012). Biological robustness: paradigms, mechanisms, and systems principles. *Frontiers in genetics* 3, 67.
- Wiesenthal, A.A., Müller, C., Harder, K., and Hildebrandt, J.-P. (2019). Alanine, proline and urea are major organic osmolytes in the snail *Theodoxus fluviatilis* under hyperosmotic stress. *Journal of Experimental Biology* 222, jeb193557.
- Wilding, K.M., Schinn, S.-M., Long, E.A., and Bundy, B.C. (2018). The emerging impact of cell-free chemical biosynthesis. *Current opinion in biotechnology* 53, 115-121.
- Wilks, A., and Heinzl, G. (2014). Heme oxygenation and the widening paradigm of heme degradation. *Archives of biochemistry and biophysics* 544, 87-95.

- Wong, L., Engel, J., Jin, E., Holdridge, B., and Xu, P. (2017). YaliBricks, a versatile genetic toolkit for streamlined and rapid pathway engineering in *Yarrowia lipolytica*. *Metabolic engineering communications* 5, 68-77.
- Wong, L., Holdridge, B., Engel, J., and Xu, P. (2019). Genetic Tools for Streamlined and Accelerated Pathway Engineering in *Yarrowia lipolytica*. In *Microbial Metabolic Engineering: Methods and Protocols*, C.N.S. Santos, and P.K. Ajikumar, eds. (New York, NY: Springer New York), pp. 155-177.
- Wu, J., Jiang, M., Kong, S., Hong, K., Zhao, J., Sun, X., Cui, Z., Chen, T., and Wang, Z. (2023). Unveiling the Effect of NCgl0580 Gene Deletion on 5-Aminolevulinic Acid Biosynthesis in *Corynebacterium glutamicum*. *Fermentation* 9, 213.
- Wu, M.-Y., Sung, L.-Y., Li, H., Huang, C.-H., and Hu, Y.-C. (2017). Combining CRISPR and CRISPRi systems for metabolic engineering of *E. coli* and 1, 4-BDO biosynthesis. *ACS Synthetic Biology* 6, 2350-2361.
- Xie, D., Jackson, E.N., and Zhu, Q. (2015). Sustainable source of omega-3 eicosapentaenoic acid from metabolically engineered *Yarrowia lipolytica*: from fundamental research to commercial production. *Applied microbiology and biotechnology* 99, 1599-1610.
- Xing, R., Zou, Q., Yuan, C., Zhao, L., Chang, R., and Yan, X. (2019). Self-Assembling Endogenous Biliverdin as a Versatile Near-Infrared Photothermal Nanoagent for Cancer Theranostics. *Advanced Materials* 31, 1900822.
- Xiong, X., and Chen, S. (2020). Expanding toolbox for genes expression of *Yarrowia lipolytica* to include novel inducible, repressible, and hybrid promoters. *ACS synthetic biology* 9, 2208-2213.

- Xu, P., Qiao, K., and Stephanopoulos, G. (2017). Engineering oxidative stress defense pathways to build a robust lipid production platform in *Yarrowia lipolytica*. *Biotechnology and bioengineering* *114*, 1521-1530.
- Xue, Z., Sharpe, P.L., Hong, S.-P., Yadav, N.S., Xie, D., Short, D.R., Damude, H.G., Rupert, R.A., Seip, J.E., and Wang, J. (2013). Production of omega-3 eicosapentaenoic acid by metabolic engineering of *Yarrowia lipolytica*. *Nature biotechnology* *31*, 734-740.
- Yang, D., Park, S.Y., Park, Y.S., Eun, H., and Lee, S.Y. (2020). Metabolic engineering of *Escherichia coli* for natural product biosynthesis. *Trends in Biotechnology* *38*, 745-765.
- Yang, S., Wang, A., Li, J., Shao, Y., Sun, F., Li, S., Cao, K., Liu, H., Xiong, P., and Gao, Z. (2023). Improved biosynthesis of heme in *Bacillus subtilis* through metabolic engineering assisted fed-batch fermentation. *Microbial Cell Factories* *22*, 1-12.
- Yao, C.K., Tan, H.L., Van Langenberg, D., Barrett, J.S., Rose, R., Liels, K., Gibson, P.R., and Muir, J.G. (2014). Dietary sorbitol and mannitol: food content and distinct absorption patterns between healthy individuals and patients with irritable bowel syndrome. *Journal of Human Nutrition and Dietetics* *27*, 263-275.
- Yu, A., Zhao, Y., Pang, Y., Hu, Z., Zhang, C., Xiao, D., Chang, M.W., and Leong, S.S.J. (2018). An oleaginous yeast platform for renewable 1-butanol synthesis based on a heterologous CoA-dependent pathway and an endogenous pathway. *Microbial Cell Factories* *17*, 1-10.
- Zeng, S.Y., Liu, H.H., Shi, T.Q., Song, P., Ren, L.J., Huang, H., and Ji, X.J. (2018). Recent advances in metabolic engineering of *Yarrowia lipolytica* for lipid overproduction. *European Journal of Lipid Science and Technology* *120*, 1700352.

- Zhang, P., Wenping, W., Ying, Z., and Bangece, Y. (2021). Construction of a light-controlled expression system and its application in *Yarrowia lipolytica*. *Synthetic Biology Journal* 2, 778.
- Zhao, X.R., Choi, K.R., and Lee, S.Y. (2018). Metabolic engineering of *Escherichia coli* for secretory production of free haem. *Nature Catalysis* 1, 720-728.
- Zhao, Y., Liu, S., Han, X., Zhou, Z., and Mao, J. (2022). Combined effects of fermentation temperature and *Saccharomyces cerevisiae* strains on free amino acids, flavor substances, and undesirable secondary metabolites in huangjiu fermentation. *Food Microbiology* 108, 104091.
- Zheng, J., Inoguchi, T., Sasaki, S., Maeda, Y., McCarty, M.F., Fujii, M., Ikeda, N., Kobayashi, K., Sonoda, N., and Takayanagi, R. (2012). Phycocyanin and phycocyanobilin from *Spirulina platensis* protect against diabetic nephropathy by inhibiting oxidative stress. *American Journal of Physiology-Regulatory, Integrative and Comparative Physiology* 304, R110-R120.
- Zhou, H., Qian, H., Liu, J., Zhu, D., Ding, W., Pan, P., Jin, D., Wang, J., and Li, W. (2011). Protection against lung graft injury from brain-dead donors with carbon monoxide, biliverdin, or both. *The Journal of Heart and Lung Transplantation* 30, 460-466.
- Zhu, Q., and Jackson, E.N. (2015). Metabolic engineering of *Yarrowia lipolytica* for industrial applications. *Current opinion in biotechnology* 36, 65-72.
- Zhu, W., Wilks, A., and Stojiljkovic, I. (2000). Degradation of heme in gram-negative bacteria: the product of the hemO gene of *Neisseriae* is a heme oxygenase. *Journal of bacteriology* 182, 6783-6790.

Zhu, Z., Wilson, A.T., Luxon, B.A., Brown, K.E., Mathahs, M.M., Bandyopadhyay, S., McCaffrey, A.P., and Schmidt, W.N. (2010). Biliverdin inhibits hepatitis C virus nonstructural 3/4A protease activity: mechanism for the antiviral effects of heme oxygenase? *Hepatology* 52, 1897-1905.

Appendices

Appendix 1. Metabolite profile in the culture filtrate of a *Y. lipolytica* strain Po1g cultivated at 37°C for 20 hours.

Metabolites	Molecular Weight	Titer in g/L
Total		20.19534516
Mannitol	182.1718	8.265579875
Pyruvate	88.0621	3.987011578
Glutamate	147.1293	1.501863199
Alanine	89.0932	0.761548875
Lysine	146.1876	0.650762223
Serine	105.0926	0.533274883
Glucose	180.1559	0.523332872
Phenylalanine	165.1891	0.435805554
Threonine	119.1192	0.422806983
sn-Glycero-3-phosphocholine	258.2292	0.300607481
Asparagine	132.1179	0.279458718
Pyroglutamate	129.114	0.27013518
Valine	117.1463	0.258997453
Arginine	174.201	0.247888023
Fumarate	116.0722	0.176004146
Glutamine	146.1445	0.167757648
2-Oxoisocaproate	130.1418	0.163009835
Histidine	155.1546	0.13732906
Lactate	90.0779	0.124127346
2-Hydroxybutyrate	104.1045	0.120425772
Tryptophan	204.2252	0.102657201
Acetate	60.052	0.0960832
Butyrate	88.1051	0.08306353
Formate	46.0254	0.075369149
Isoleucine	131.1729	0.073617146
Trehalose	342.2965	0.073099319
Uracil	112.0868	0.063540762
Glycocholate	465.6227	0.059910121
Isobutyrate	88.1051	0.041928238
Adenine	135.1267	0.035147956
Guanosine	283.2407	0.034995962
Cholate	408.5714	0.034773966

2-Oxobutyrate	102.0886	0.029605694
Uridine	244.2014	0.028327362
Tyrosine	181.1885	0.026534049
Betaine	117.1463	0.00497221
Ethanol	46.0684	0.003992595

Appendix 2. Codon optimized synthetic genes used to make heme derivatives.

HO (HO2582) from *Pseudomonas putida* KT2440

ATGACTGCCGTTACATTCCCCTTTACCGAGCCCTCGCGTTGTAAACGTTTGAAAGCCG
CATCGTCCC GCGACCATGACAGTGTGATCAACTTGTCATGGCAGCCCGCCCCTTCGA
GTCTCGTGAGCGCTATGGTCGTTTTCTTCAGGTACAGCACCGTTTCCACGGCAGCCTT
TTAGCGCTGTATCAAGACGAACAGCTTAACCAGCAATTGCCCGGATTGGCTGCATTGT
CCCGCTTTGCAGCAGTGGAAGCGGATCTTCGTGACTTAGGTCTGCCTTTGCCAACGC
CAACACAGCCGGTACGTGTTTCATCAGCACAGGCCTTGGGCTGGCTGTACTGCAGTG
AGGGCAGTAACCTGGGTGCCGCCTTTTTGTACAAACACACACAACGCCTTGGACTGG
AAGGAGATAATGGGGCACGCCATCTTGCTCCCCATCCAGATGGCCGCGCGCTTCATTG
GCGTGAGTTCGTTGCACGTCTGGATTCACTGGTATTGGGTGAACAAGAGGAAGCCGA
GGTCGTAGCTGGAGCAATTGCCGCGTTTGACTCCTACCGCGTTCATTTACGTGAAGTA
TTTGCGGGATCTTGA

PcyA from *Thermosynechococcus elongatus* BP-1

ATGAGTTTACGCCAACATCAACATCCATTGATCCAGCGTCTTGCCGATCGTATCGAAG
CGATCTGGCAAGCCTTTTTTCCCTTAGCTCCTTACGCATTGCCGGAGGATCTGGGGTAT
GTGGAGGGAAAGTTAGAGGGCGAACGTTTAACAATCGAGAACCATTGCTACCAAGCT
CCGCCTTTTCGCAAACCTGCACCTTGAGCTTGCGCGTGTTGGAGAATCGTTAGATATT
TACACTGCGTGATGTTTCCCGAGCCCCGCTATGACCTGCCTATGTTCCGGATGTGATCTG
GTCGGTGGGCGCGGTCAAATTCAGCGGCCATTGTAGACTTGTCACCGGTGACGGGC
CAGTTACCTGCTGCTTATACCTGTGCACTTAATGCTTTACCGAAATTGACATTCCGTCA
ACCTCGTGAACCTCCACCCTGGGGGCACATTTTTTCCCCTTTCTGCATCTTTATCCGCC
CCCAGGGGGAGGCAGAAGAACAACAATTCCTTGATCGCATTGGAGAGTACCTTACGC
TGCACTGTCAGTTAAGTCAACAAGCAGTACCCACCGATCATCCCCAAGCCGTCATTGC
TGGTCAGCGCCAATACTGTCAACAGCAGCAACAAAATGATAAGACTCGCCGCGTATT
AGAAAAGGCCTTCGGGGTGCCCTGGGCGGAACGTTATATGACGACAGTGCTTTTTGA
TGTCACCCCGTTTAG

PebS from *Prochlorococcus phage P-SSM2*

ATGACTAAGAATCCGCGCAATAACAAACCGAAAAAATCTTAGATAGCAGCTACAAG
AGTAAGACAATCTGGCAGAACTATATTGATGCATTATTTGAGACTTTCCCGCAATTGGA
GATCAGTGAGGTTTGGGCTAAATGGGATGGCGGCAACGTGACAAAGGACGGTGGGG
ATGCAAAGCTGACTGCGAACATCCGTACGGGTGAGCATTTTTTGAAAGCCCGTGAGG
CCCATATTGTGGACCCCAACTCGGATATTTACAACACTATTTTATATCCGAAGACGGGG
GCTGATTTACCGTGTTTTGGTATGGACCTTATGAAGTTCAGCGACAAAAAAGTTATCA
TTGTTTTTCGATTTCCAGCATCCACGCGAGAAATACCTGTTTAGCGTAGATGGCTTACCA
GAAGACGATGGAAAATATCGCTTTTTTCGAGATGGGCAATCACTTTAGTAAGAATATCT
TCGTGCGTTATTGCAAACCTGACGAGGTCGATCAGTATTTGGACACTTTCAAGTTATA
CTTGACCAAATACAAGGAGATGATTGATAATAACAAGCCAGTTGGAGAAGACACTAC
GGTTTACTCGGACTTCGACACCTATATGACTGAATTAGACCCAGTGCGCGGATATATGA
AAAACAAATTTGGAGAGGGTCGCTCCGAAGCGTTCGTAAACGACTTCCTTTTTTCTTA
TAAATGA